SEM (JMS-5800 LV, JEOL) was used for study of the morphology of cross-sectional sample at an accelerating voltage of 6 kV. After fracturing a specimen under liquid N<sub>2</sub>, its cross-sectional area was coated with platinum under a 12 Pa vacuum. The storage modulus and  $\tan \delta$  of the polymer composite were examined by dynamic mechanical thermal analysis (DMTA V) in tension mode at 10 Hz, 0.05% strain and different temperatures. The physical testing of polymer composite was analyzed by universal testing machine (LR10K, Lloy Intruments) based on ASTM D 412 at 500 mm/min using 5 dumbbell test pieces. Its hardness was measured according to ASTM D 2240 while an Impacts-15 resilience test pendulum impact tester (Yasdu, No. 258-D) was applied for determination of impact resistance at 25-28°C

# 3. Results and discussion\

# 3.1 Analysis of polymer composite

Before mixing the masticated NRG dispersed in toluene with PSF waste solution and MA, the size and size distribution of NRG suspension are measured by a particle size analyzer and the data are shown in Fig. 1.

# Figure 1

Result indicated that 75% of the dispersed NRG were in the size ranging from 250 to 500 micron. ATR-FTIR was then used for analysis of the chemical structures of the NRG/PSF blend in the presence of 10% MA and of the NRG/PSF blended with 10% MA and 5% cellulose or polymer composite. Fig. 2 shows the spectra of NRG/ PSF blended with 10% MA (a) before and (b) after immersion in toluene and those of polymer composite having 50/50 NRG/PSF blended with 10% MA and 5% cellulose (c) before and (d) after immersion in toluene.

5 Figure 2 8 The characteristic peaks at 3025 (C-H aromatic), 1610 (C-C aromatic), 2920 and 2849 (CH<sub>2</sub>CH<sub>2</sub>), 1490 and 1450 (C<sub>6</sub>H<sub>5</sub>), 905 and 697 (C-H aromatic) cm<sup>-1</sup> of PS appeared in Fig. 2 (a)-(d). The bands at 1076 and 1664 cm<sup>-1</sup> attributed, respectively, to the symmetric C-S-C stretching vibrations and C=C of NRG were also noticed. The grafted MA in the blend was deduced from the absorbance ratio of peaks at 1780-1784 cm<sup>-1</sup> to 1835-1854 cm<sup>-1</sup> (CH stretching on C=C of cis-1,4-polyisoprene) in (b) (Zhang et al., 2010). The characteristic 25 peaks at 3200-3400 cm<sup>-1</sup> due to OH from cellulose fiber were observed in (c) and (d). A shoulder at 1745 cm<sup>-1</sup> confirmed that the small amount of ester groups remained in side chains of the polymer composite. After adding cellulose in NRG/PSF blend, the intensity of peak at 3400 cm<sup>-1</sup> of polymer composite decreased. In addition, the increase of bands at 1745 and 1270 cm<sup>-1</sup> due to ester C=O and C-O-C of cellulose in polymer composite was detected. The peaks at 821, 896, 1046, 1382 and 2926 corresponding to the out of plane deformation of COOH, C-H deformation, C-O-C from \(\beta-1.4\)—glycosidic, OH bending and C-H stretching, respectively, also appeared. 3.2 Gel content The influence of NRG/PSF ratio on the gel content of the polymer blend containing 10% MA without cellulose is presented in Fig. 3 (a). 56 174 Figure 3 

51 198

56 200 

Results showed that the gel content of polymer blend having NRG/PSF of 30/70 was similar to that of 50/50 which was greatly lower than that of 70/30. It was believed that the high NRG content whose molecules were still partially crosslinked with sulphur was responsible for the high gel content. As expected, the gel contents of all NRG/PSF blends strongly increased with adding cellulose fiber as shown in Fig. 3(b). The gel contents of polymer composites containing 3, 5 and 12% were 58, 60 and 63%, respectively. It was possibly caused from the adsorption of macromolecular chains at the filler/matrix interface, filler/filler interactions and the chemical reaction between MA and polymer matrix as previously reported in the case of NR filled with cellulose (Bendahou et al., 2010).

The optical micrographs of PSF blended with 5% cellulose and various amounts of MA (0, 5, 10 and 15%) after immersion in toluene are displayed in Fig. 4.

Figure 4 

The good dimensional stability of PSF/cellulose added with MA especially of 15% was observed in Fig. 4 (d). This result indicated the occurrence of chemical interaction between PSF and MA or between cellulose and MA during blending process.

# 3.3 SEM morphology

The morphology affecting the physical properties of polymer composite was investigated. SEM micrographs in Fig. 5 show PSF blended with 5% cellulose in the presence of (a) 0, (b) 5, (c) 10, (d) 15% w/w of MA and those of polymer composite containing 50/50 NRG/PSF, 5% cellulose and (e) 0, (f) 10% w/w of MA.

In Fig. 5 (a), it seemed that the polar cellulose fibers were hard to disperse in nonpolar PSF and NRG/PSF matrix due to the difference in the surface energy of each

component (Zhange et al., 2008). The strong adhesion between PSF and cellulose was observed after addition of MA in Fig. 5 (b)-(d). A large number of voids were observed on the fracture surface of all PSF samples. When NRG was added in PSF/cellulose in the absence of MA in Fig.5 (e), the voids were also noticed due to poor interface interaction. After adding MA, the strong adhesion or chemical bond between cellulose fiber and polymer matrix occurred in Fig. 5 (f) which would affected the mechanical strength of the polymer composite. Figure 5 

3.4 Mechanical strength

51 223

56 225 

Fig. 6 (a)-(d) show the effects of cellulose contents (0, 3, 5 and 12%) on tensile strength of the polymer composites having NRG/PSF of 0/100, 30/70, 50/50 and 70/30.

Figure 6 

It was observed that the tensile strength of PSF was 2 MPa and that of polymer blend without cellulose in Fig. 6 (a) decreased from 3.4, 1.4 to 0.7 MPa when NRG/PSF were 30/70, 50/50 and 70/30, respectively. After addition of 3, 5 and 12% cellulose in the 30/70 NRG/PSF, the tensile strength of the polymer composites in Fig. 6 (b)-(d) increased from 5.2, 5.8 to 6.2 MPa, respectively. The results agreed well with those of NR filled cellulose previously reported (Bras, 2010). The drop in the tensile properties of the polymer composites when increasing NRG content was reasonably due to poor interaction between cellulose and the NRG/PSF matrix. Moreover, the poor dispersion and/or agglomeration of

51 248

 the filler in the matrix led to the in-homogeneity of phase morphology which became the dominant process in the mixing. This effect was more pronounced with increasing filler content.

At low cellulose content of 3% w/w, the polymer composite exhibited an elastic nonlinear behavior which is typical for amorphous polymer at temperature greater than glass transition temperature (Tg). At high filler content of 12%, the mechanical behavior of NRG/PSF waste was high because a considerable amount of fibers allowed the transfer of the applied load between them. The higher compatibility between cellulose fiber and the hydrophobic polymer matrix by adding MA which ensued higher filler/matrix adhesion was also responsible for this difference (Bendahou et al., 2010).

The effect of MA content on the hardness of polymer composite containing 50/50 NRG/PSF and 5% cellulose is shown in Fig. 7.

Figure 7

The presence of 5% MA significantly increased the hardness of the polymer composites from 46 to 65 shore A. With 10 and 15% of MA, the hardness values were constant, i.e., 64 and 62 shore A, respectively. The change in hardness was possibly caused from the chemical reaction between MA and NRG/PSF matrix which efficiently facilitated energy transfer process and, hence, toughened the composite (Chong et al., 2010). The influence of the both cellulose and polymer blend ratio on the hardness of the polymer blend is presented in Fig. 8 I.

56 250 Figure 8

Results showed that the hardness of the polymer composites decreased from 94 to 62 shore A when varying NRG/PSF from 30/70 to 50/50. Further increase in NRG content, the hardness of the polymer composites having 50/50 and 70/30 NRG/PSF were constant. This was due to the fact that the cellulose fiber sheet was in the center of specimen. It was confirmed by the insignificantly change of hardness of the polymer composites when changing the cellulose contents.

The data of impact strength of the polymer composites containing 30/70, 50/50 and 70/30 NRG/PSF plotted with cellulose contents are presented in Fig. 8 II.

The increase in impact strength when increasing the amount of NRG was explained from the ductile fracture initiated by the shear yielding mechanism [Mathew et al., 2001c]. Due to the low Tg of NR (-78°C), the NRG chains easily moved at room temperature and played the role of toughening agent. The dual phase continuity and phase interpenetration might also enhance the impact resistance. It was reported that the co-continuous interpenetrating polymer network (IPN) structure exhibited high impact strength of polymer composite because the uniform rubbery phase allowed the energy to be dissipated into the whole sample (Mathew et al., 2001). This effective dissipation of energy was the principal role of rubbery phase in impact resistant materials.

The effect of cellulose content on the impact strength of the polymer composites was also displayed in Fig. 8 II. At 50/50 NRG/PSF, the impact strength values of the polymer composites with 0, 3, 5 and 12% cellulose were 7, 12, 21 and 23.5 J/m<sup>2</sup>, respectively. The reinforcement might be because a polymer chain could interact with several units of the fibers. If this chain breaks due to the impact energy, the load is transferred to many other chains providing the increase in impact strength of the material (Megiatto Jr et al., 2010).

277	4.Conclusions
278	The pol

51 298

The polymer composite was developed from the blend of NRG and PSF wastes with addition of MA and cellulose from sugar can leave. Their mechanical properties were better than those of PSF due to the chemical reaction between PSF/cellulose and MA which were confirmed by gel content and ATR-FTIR. The highest tensile strength of sample was found in 30/70 NRG/PSF blended with 10% MA and 12% cellulose. This observation was supported by SEM, toluene resistance, impact strength and hardness. The polymer composite would potentially be used in artificial wood.

# Acknowledgements

The authors would like to thank The Thailand Research Fund (TRF)/ Commission on Higher Education for the research grant. P.T. is TRF Senior Researcher.

## References

Berekaa, M.M., Linos A., Reichelt, R., Keller, U., Steinbüchel, A. 2000. Effect of pretreatment of rubber material on its biodegradability by various rubber degrading bacteria FEMS. Microbiology Letters 184, 199-206.

Bendahou, A., Kaddami, H., Alain Dufresne, A. 2010. Investigation on the effect of cellulosic nanoparticles' morphology on the properties of natural rubber based nanocomposites. European Polymer Journal 46, 609-620.

Beach, M.W., Rondan, N.G., Froese, R.D., Gerhart, B.B., John G. Green, Bill G. Stobby, Andrey G. Shmakov, Vladimir M. Shvartsberg, Oleg P. Korobeinichev. 2008. Studies of degradation enhancement of polystyrene by flame retardant additives. Polymer Degradation and Stability 93, 1664-1673

1	300	Bhutta, M.A.R., Ohama, Y., Tsuruta, K. 2011. Strength properties of polymer mortar panels
1 2 3	301	using methyl methacrylate solution of waste expanded polystyrene as binder.
4 5	302	Construction and Building Materials 25, 779-784
6 7 8	303	Chong, E.L., Ahmad, I., Dahlan, H.M., Abdullah, I. 2010. Reinforcement of natural
9	304	rubber/high density polyethylene blends with electron beam irradiated liquid natural
11 12 13	305	rubber-coated rice husk. Radiation Physics and Chemistry 79, 906-911.
14 15	306	Chuayjuljit, S., Boonmahitthisud, A. 2010. Natural rubber nanocomposites using
16 17 18	307	polystyrene-encapsulated nanosilica prepared by differential microemulsion
19	308	polymerization. Applied Surface Science 256, 7211-7216.
<ul><li>21</li><li>22</li><li>23</li></ul>	309	Conrardy, J., Hillanbrand, M., Myers, S., Nussbaum, G.F. 2010. Reducing medical waste .
<ul><li>23</li><li>24</li><li>25</li></ul>	310	AORN 91, 711-721.
26 27	311	Dong, D., Tasaka S., Inagaki, N. 2001. Thermal degradation of monodisperse polystyrene in
28 29 30	312	bean oil. Polymer Degradation and Stability 72, 345-351
31 32	313	Hall, W.J., Zakaria, N., Williams, P.T. 2009. Pyrolysis of latex gloves in the presence of Y-
33 34 35	314	zeolite. Waste Management 29, 797-803.
36 37	315	Hourston, D.J., Schäfer, F.U., Gradwell, M.H.S., Song, M. 1998.TMXDI-based poly(ether
38 39 40	316	urethane)/polystyrene interpenetrating polymer networks: 2. Tg behaviour, mechanical
41 42	317	properties and modulus-composition studies. Polymer, 39, 5609-5617.
43 44 45	318	Hsu, P.C., Foster, K.G., Ford, T.D., Wallman, P.H., Watkins, B.E., Pruneda, C.O., Adamson,
46 47	319	M.G. 2000. Treatment of solid waste with molten salt oxidation. Waste Management
48 49	320	20, 363-368.
50 51 52	321	Long, C., Li, Q., Li, Y., Liu, Y., Li, A., Zhang Q. 2010. Adsorption characteristics of
53 54	322	benzene-chlorobenzene vapor on hypercrosslinked polystyrene adsorbent and a pilot-
<ul><li>55</li><li>56</li><li>57</li></ul>	323	scale application study. Chemical Engineering Journal 160, 723-72
58 59		
60		

1	324	Mathew, A.P., Packirisamy, S., Thomas, S. 2001. Studies on the thermal stability of natural
2	325	rubber/polystyrene interpenetrating polymer networks: thermogravimetric analysis.
4 5 6	326	Polymer Degradation and Stability 72, 423-439.
7 8	327	Mathew, A.P., Packirisamy, S., Radusch, H.J., Thomas, S.b. 2001. Effect of initiating system,
	328	blend ratio and crosslink density on the mechanical properties and failure topography of
11 12 13	329	nano-structured full-interpenetrating polymer networks from natural rubber and
14 15	330	polystyrene. European Polymer Journal 37, 1921-1934.
16 17 18	331	Mathew, A.P., and Thomas, S. 2001. Izod impact behavior of natural rubber/polystyrene
19 20	332	interpenetrating polymer networks. Materials Letters 5, 154-163.
21 22 23	333	Mathew, A.P., Packirisamy, S., Stephen R., Thomas, S. 2002. Transport of aromatic solvents
25	334	through natural rubber/polystyrene (NR/PS) interpenetrating polymer network
26 27 28	335	membranes. Journal of Membrane Science 201, 213-227.
29 30	336	Madorsky, S.L., Straus, S., Thompson, D., Williamson L. 1949. Pyrolysis of polyisobutene
31 32	337	(vistanex), polyisoprene, polybutadiene, GR-S and polyethylene in a high vacuum.
33 34 35	338	Journal of Research of the National Institute of Standards and Technology 42, 499–514.
36	339	Megiatto, Jr., Jackson, D., Ramires, E.C., Frollini, E. 2010. Phenolic matrices and sisal fibers
38 39 40	340	modified with hydroxy terminated. polybutadiene rubber: Impact strength, water
<del>1</del> ∠	341	absorption, and morphological aspects of thermosets and composites. Industrial Crops
43 44 45	342	and Products 31, 178-184
46 47	343	Rajan, V.V., Dierkes, W.K., Joseph, R., Noordermeer, J.W.M. 2006. Science and technology of
48 49 50	344	rubber reclamation with special attention to NR-based waste latex products. Progress in
	345	Polymer Science 31, 811-834.
53 54 55	346	Riyajan, S., Sakdapipanich, J.T., Yasuyuki, T. 2003. Controlled Degradation of Cured
56 57	347	Natural Rubber by Encapsulated Benzophenone as a Photosensitizer. Journal of
58 59	348	Applied Polymer Science 90, 297-305.
60		

1	349	Riyajan, S., Chaiponban, S. 2009. Activation Energy and Thermal Behaviors of
2	350	Thermoplastic Elastomer Based on Natural Rubber and Polyvinyl Alcohol. KGK-
4 5 6	351	Kaustschuk Gummi Kunststoffe 63, 28-33.
7	352	Wang, S.,Liu, Q., Luo, Z., Wen, L.,Cen K. 2007. Mechanism study on cellulose pyrolysis
9	353	using thermogravimetric analysis coupled with infrared spectroscopy. Front Energy
11 12 13	354	Power Eng China 1, 413–419.
14 15	355	Wiesław, W., Agnieszka, S., Barbara, W., Wioletta. S., Bajdur, M., Sułkowska, A. 2005.
16 17 18	356	Preparation and properties of flocculants derived from polystyrene waste.
19 20	357	pyrolysis of representative medical waste. Polymer Degradation and Stability 90, 272-280
<ul><li>21</li><li>22</li><li>23</li></ul>	358	Zhang, Y.F., Wang, Y. 2008. Thermogravimetric analysis and kinetic study pyrolysis of
24 25	359	representative medical waste composition. Waste Management 28,1572-1580
26 27 28	360	Zhang, H., Datta, R.N., Talma, A.G., Noordermeer, J.W.M. 2010. Maleic-anhydride grafted
	361	EPM as compatibilising agent in NR/BR/EPDM blends. European Polymer Journal 46,
31	362	754-766.
33 34 35	363	Zhang, W., Zhang, X., Liang, M., Lu, C. 2008. Mechanochemical preparation of surface-
36 37	364	acetylated cellulose powder to enhance mechanical properties of cellulose-filler-
38 39 40	365	reinforced NR vulcanizates. Composites Science and Technology 68, 2479-2484.
41 42	366	Zhang, H., Datta, R.N., Talma, A.G., Noordermeer, J.W.M. 2010. Maleic-anhydride grafted
43 44 45	367	EPM as compatibilising agent in NR/BR/EPDM blends. European Polymer Journal 46,
	368	754-766.
48	369	
50 51	370	
52 53	5 / 1	Figure caption
54	372	
55 56	373 374	Figure 1 Size of NRG dispersed in toluene measured by particle size analyzer
57	374	Figure 2 ATR-FTIR spectra of NRG/PSF blended with 10% MA (a) before and (b) after
58	376	immersion in toluene and polymer composite containing 50/50 NRG/PSF, 10% MA and 5%
59 60	277	cellulose (c) before and (d) after immersion in toluene

	16
378 1 379	Figure 3 Effect of NRG/PSF on gel content of polymer blend
$\frac{2}{3}$ 380	
381 5 382 6 383	<b>Figure 4</b> Photographs of PSF in the presence of 5% cellulose and (a) 0, (b) 5, (c) 10 and 15% of MA after toluene resistant test
7 384 8 385 9 386 11 387	<b>Figure 5</b> SEM micrographs of PSF blended with 5% cellulose in the presence of (a) 0, (b) 5, (c) 10, (d) 15% w/w of MA and those of polymer composite containing 50/50 NRG/PSF, 5% cellulose and (e) 0, (f) 10% w/w of MA.
12 <b>388</b> 13 <b>389</b>	<b>Figure 6</b> Effect of cellulose contents of (a) 0, (b) 3, (c) 5 and (d) 12%w/w on tensile strength of PSF and polymer composite containing NRG/PSF of 0/100, 30/70, 50/50 and 70/30
15 390 16 391 17 392	Figure 7 Hardness of 50/50 NRG/PSF blended with different MA contents
18 393 19 394 20 395 21 396	<b>Figure 8</b> (I) Effects of cellulose contents of (a) 0, (b) 3, (c) 5 and (d) 12 % on hardness of polymer composite containing 50/50 NRG/PSF and (II)Effects of cellulose contents on impact strength of polymer composites having NRG/PSF of (a) 30/70, (b) 50/50 and (c) 70/30
23 <b>397</b> 24	
<sup>25</sup> <sub>26</sub> <sup>398</sup>	
27	
29 30	
31 32	
33 34	
35 36	
37 38	
39	
40 41	
42 43	
44 45	
4 6 4 7	
48	
49 50	
51 52	
53 54	
55 56	
57	
58 59	
60	

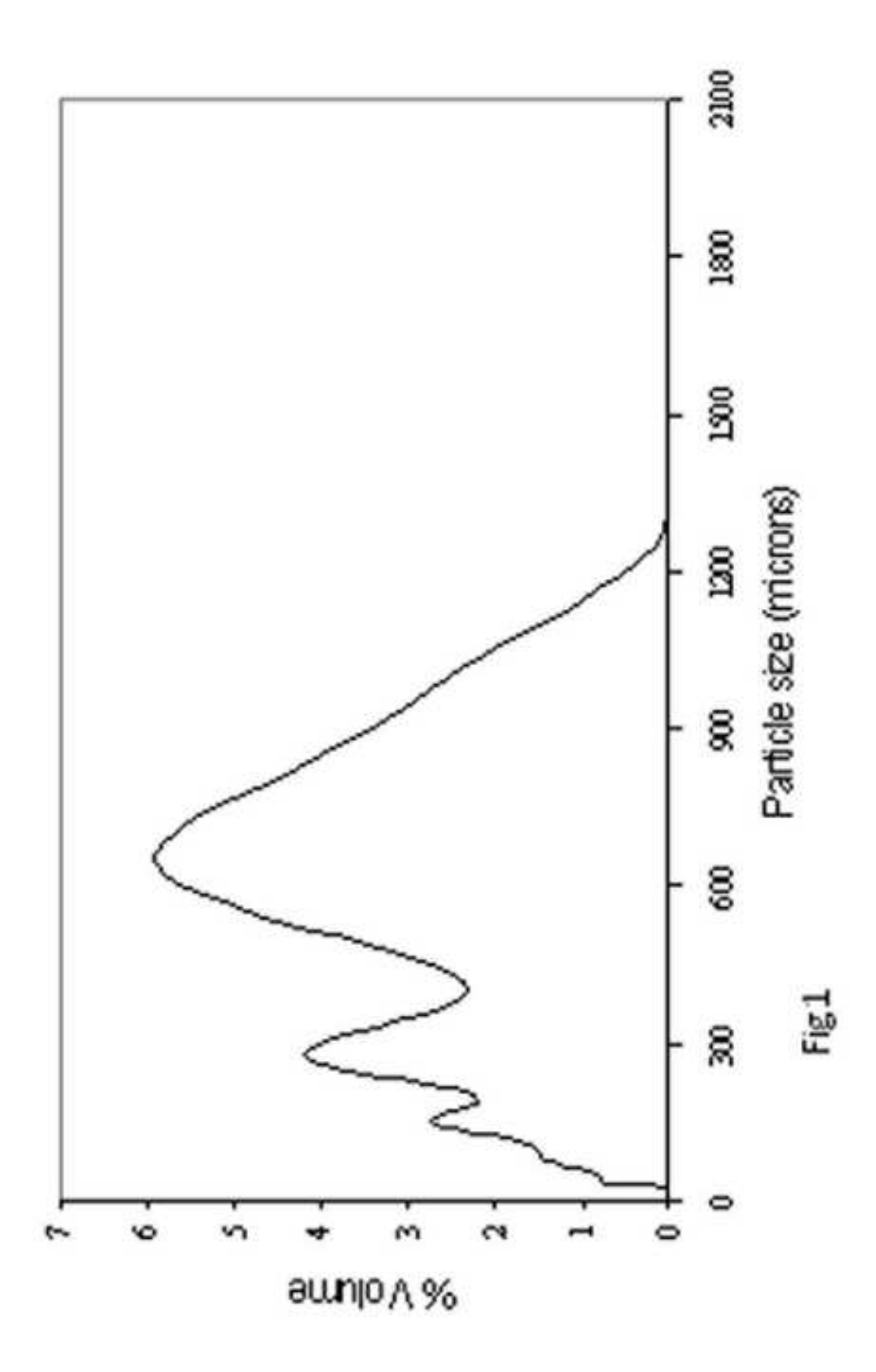
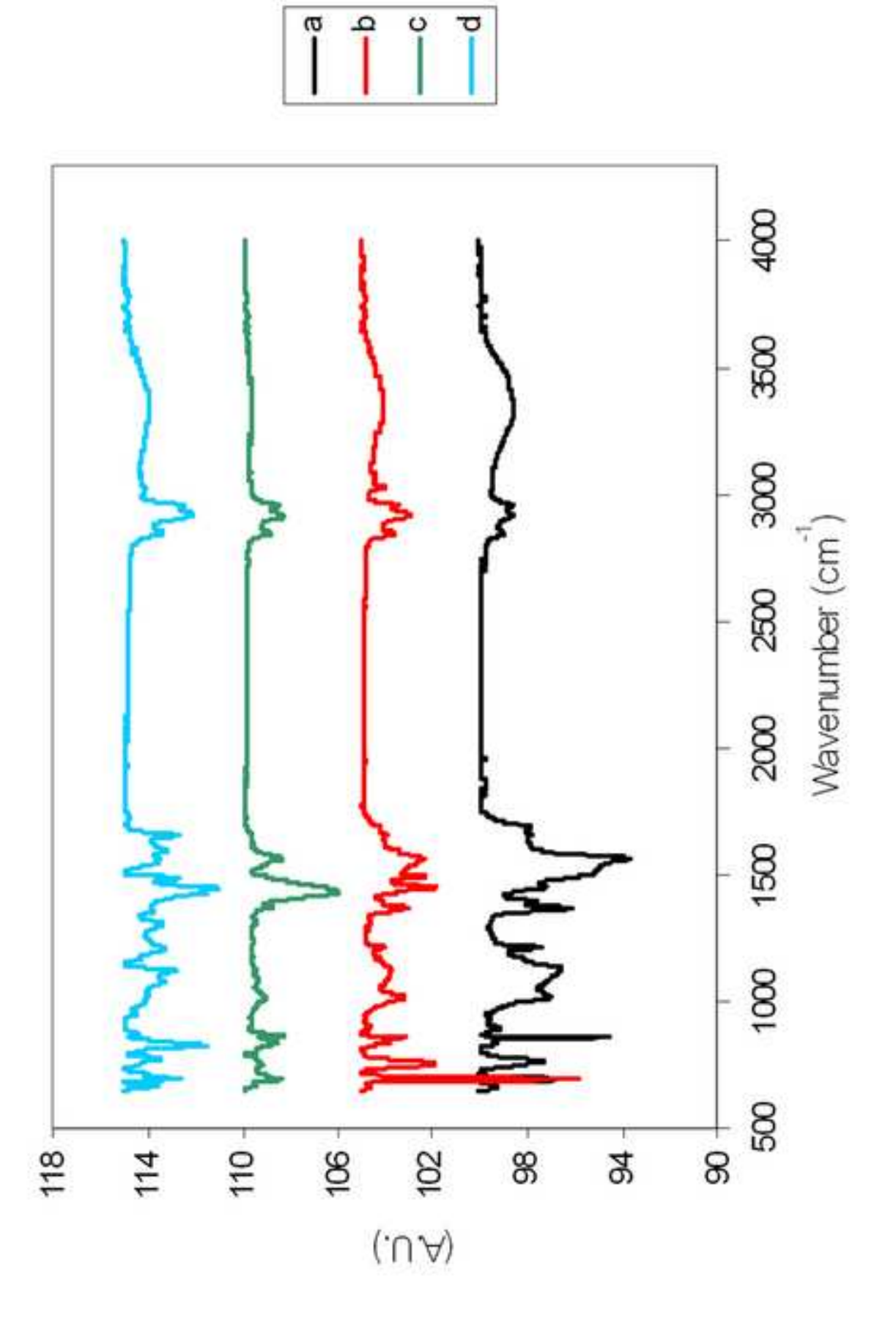


Figure2 Click here to download high resolution image



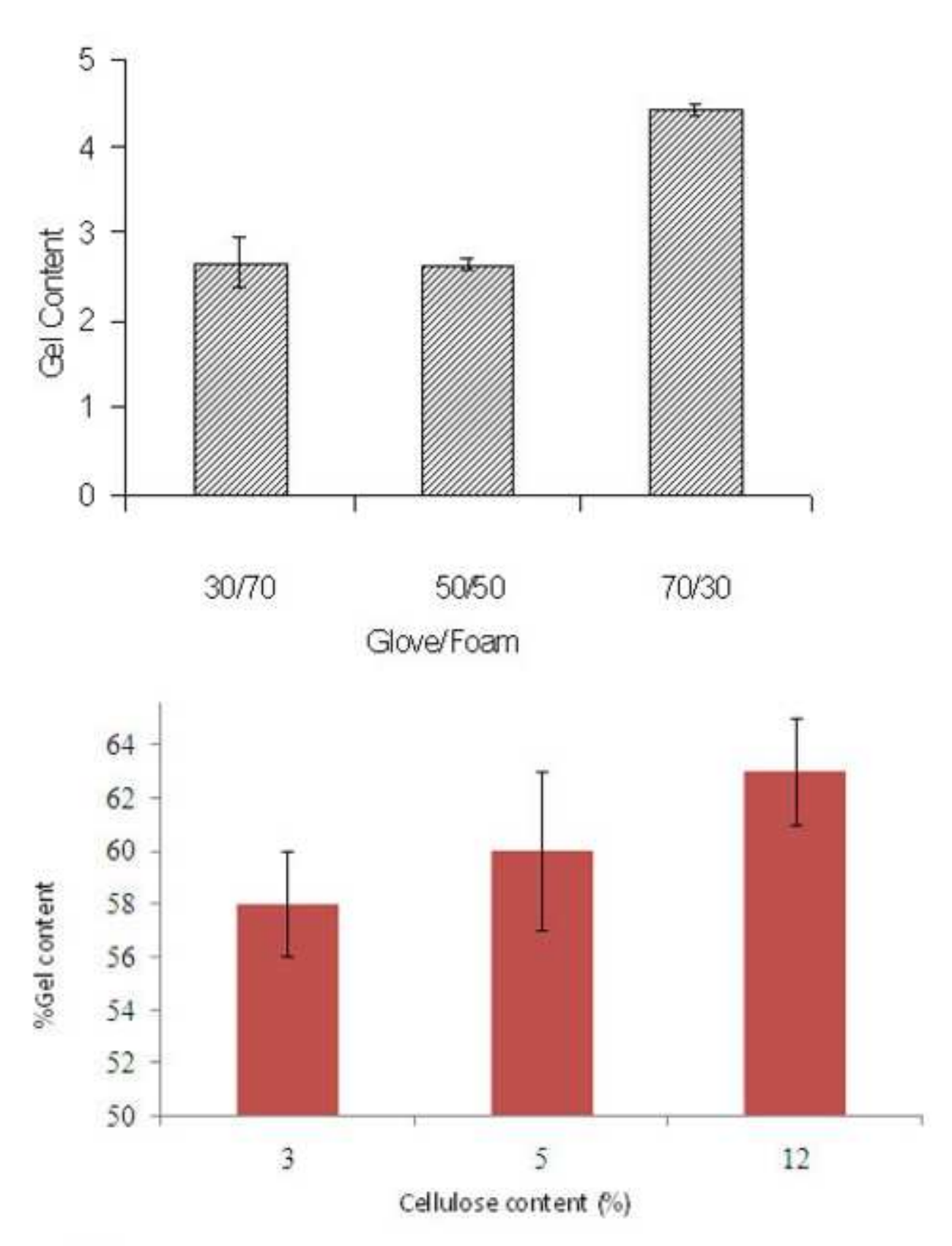


Fig.3.

Figure4
Click here to download high resolution image

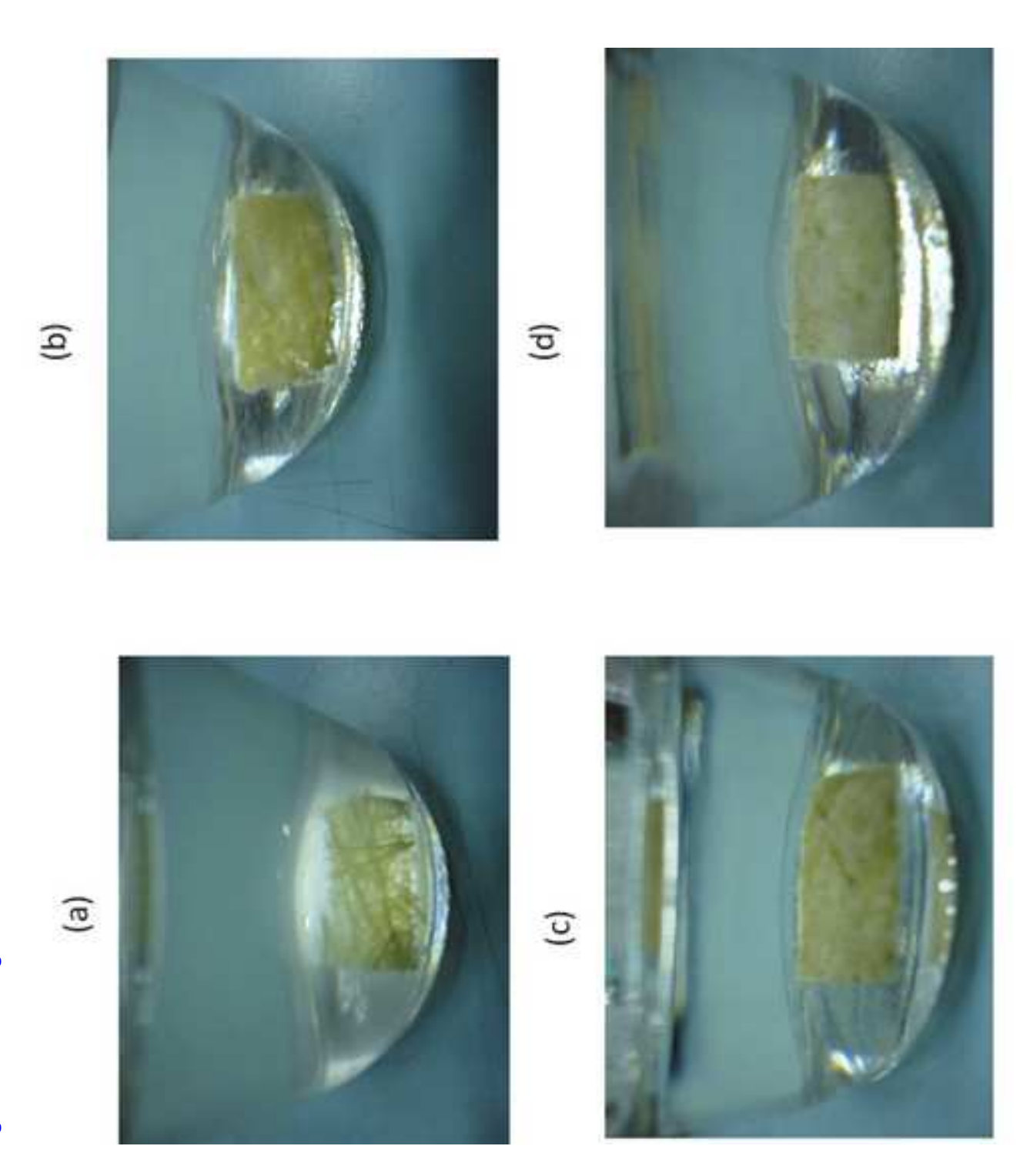


Fig.4

Figure5 Click here to download high resolution image

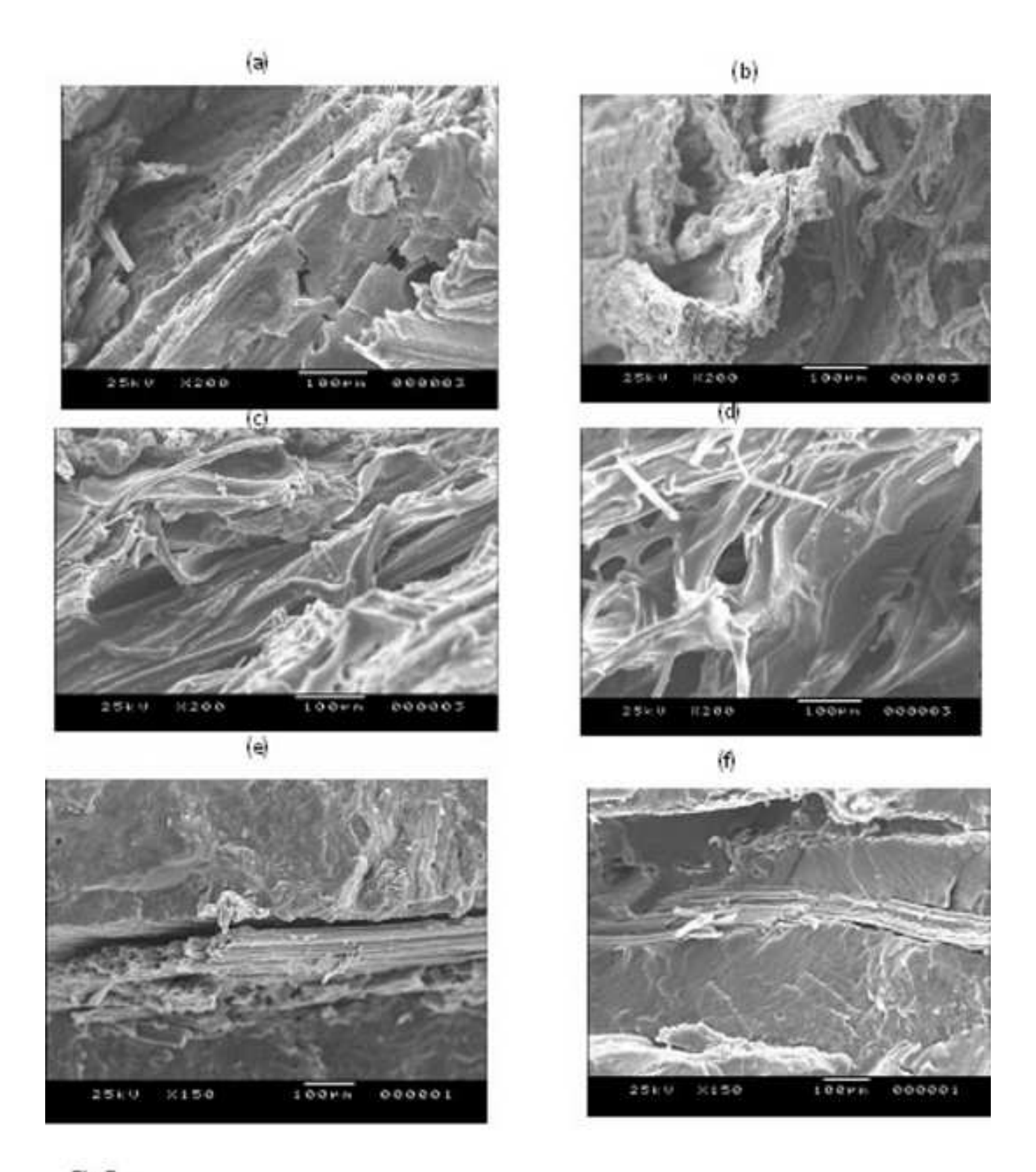
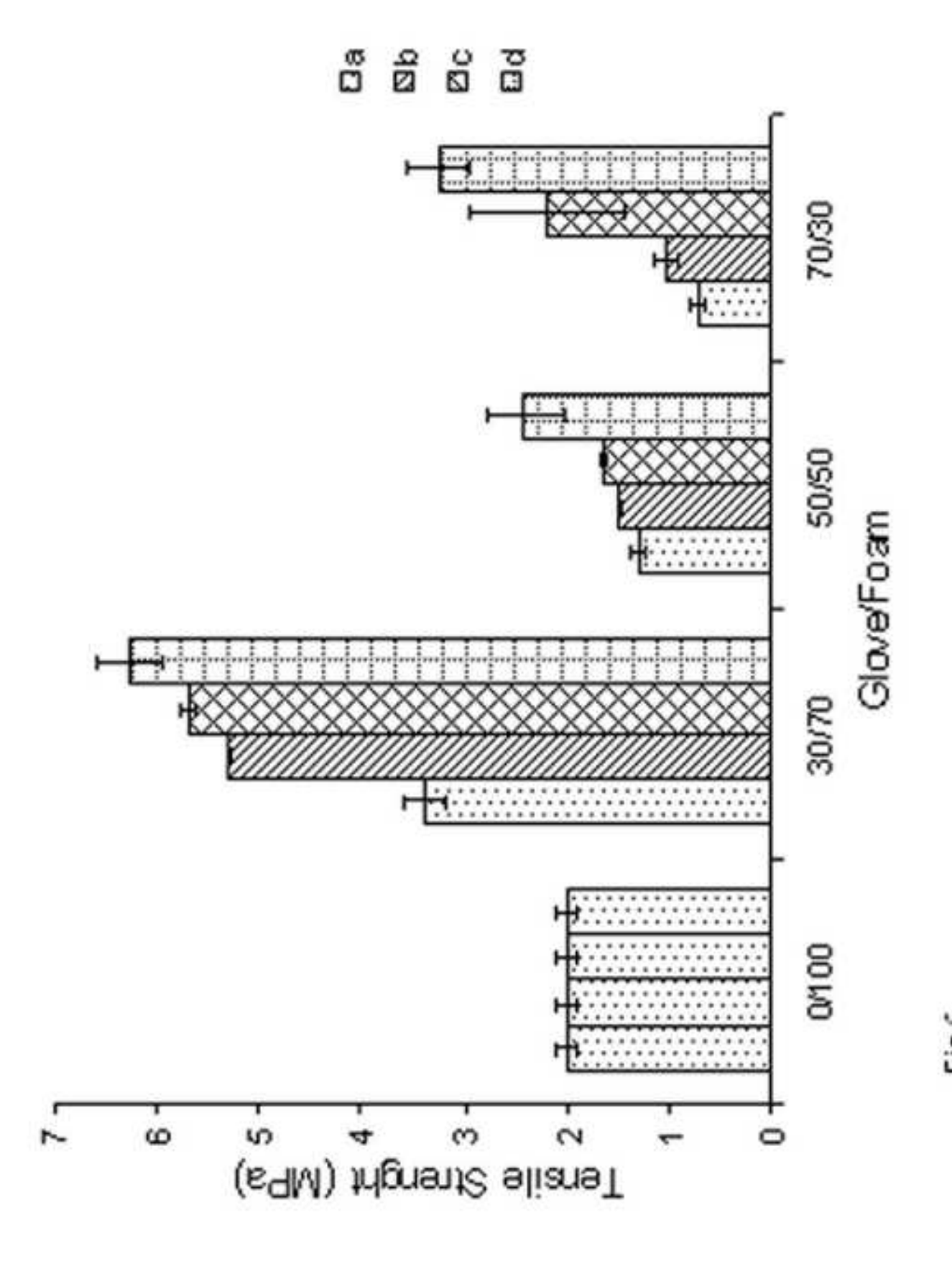


Fig 5.



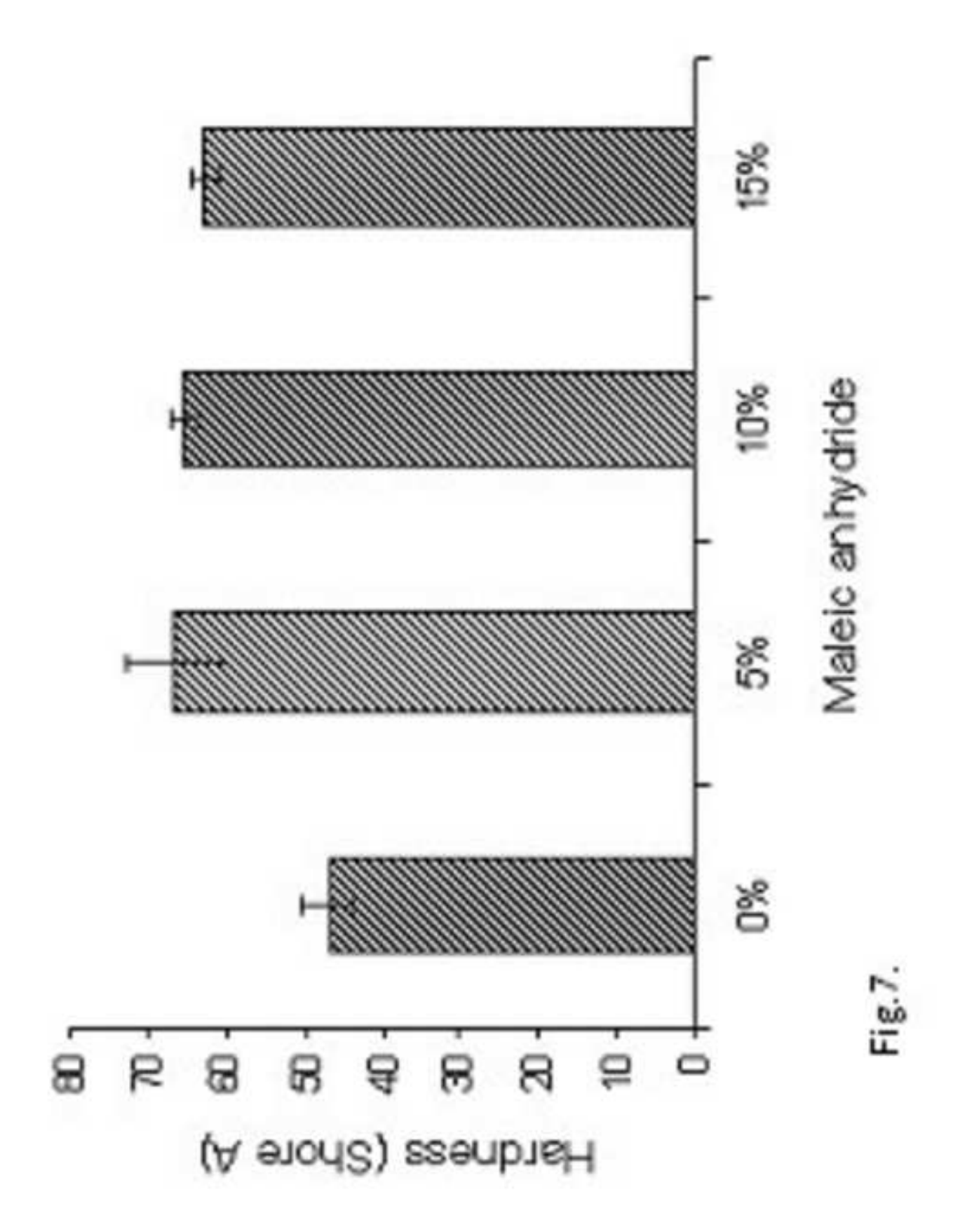


Figure8 Click here to download high resolution image

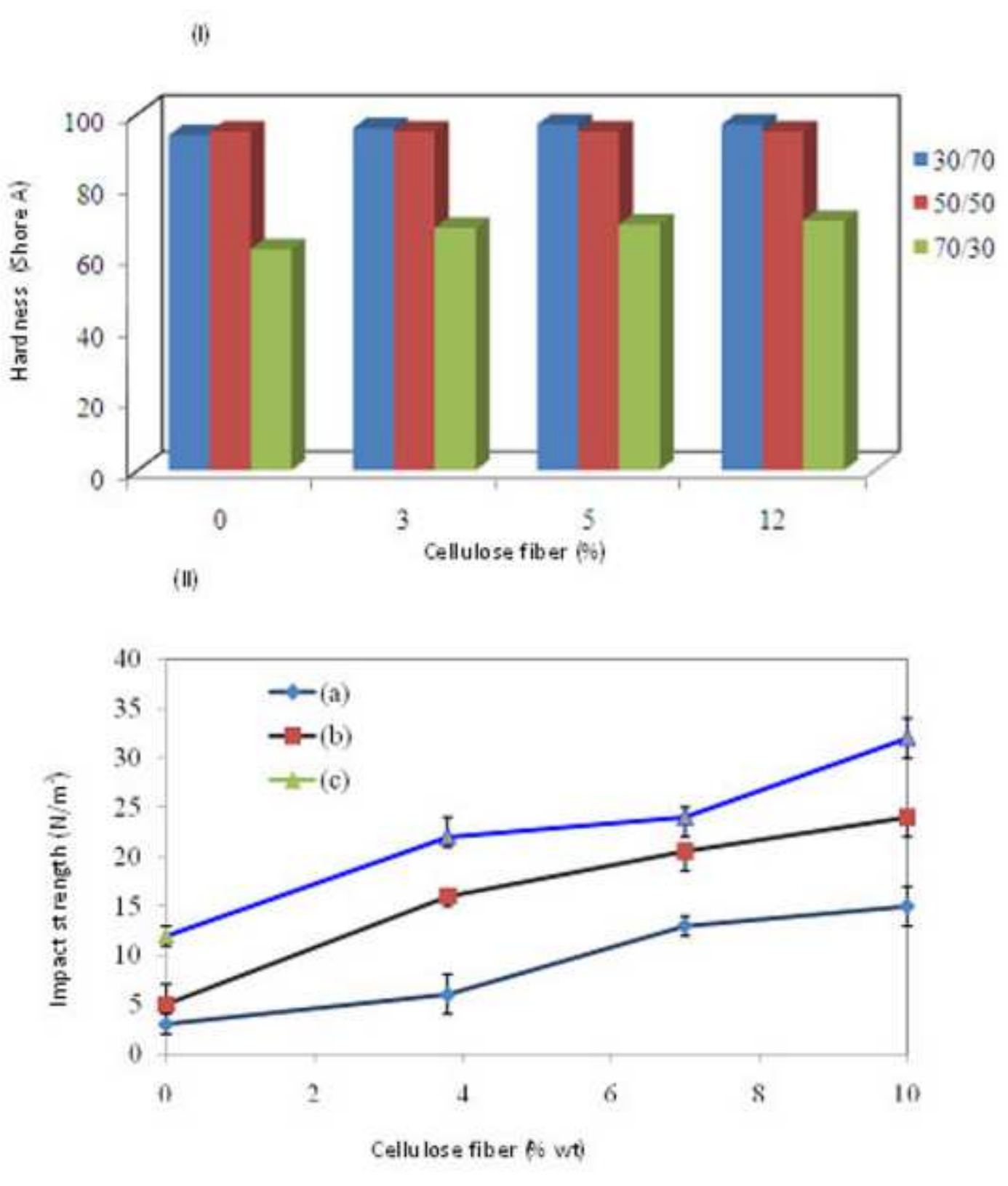


Fig 8

# Backing-required Properties of Films based on Natural Rubber for Transdermal Patch Application

S. Wirasate<sup>1,2,3\*</sup>, C. Chokbunpiam<sup>1,2</sup>, R. Thonggoom<sup>1,2</sup> and P. Tangboriboonrat<sup>1</sup>

<sup>1</sup>Department of Chemistry, Faculty of Science, Mahidol University, Bangkok10400, Thailand

<sup>2</sup>Center for Surface Science and Engineering, Faculty of Science, Mahidol University, Salaya, Nakhorn Pathom73170, Thailand

<sup>3</sup>Center for Rubber Research and Technology, Faculty of Science, Mahidol University, Salava, Nakhorn Pathom73170, Thailand

#### **Abstract**

The backing required properties, including oxygen transmission rate (OTR), water vapor transmission rate (WVTR) and Young's modulus, of natural rubber based films were investigated. Both NR and epoxidized NR (ENR) latexes with mole % epoxide ranging from 10 to 39 % were prevulcanized using *tert*-butyl hydroperoxide/fructose system. The surface of peroxide prevulcanized (PP) NR was grafted with acrylamide (PPNR-g-AAm) by dipping the PPNR strip treated with O<sub>2</sub> plasma into an aqueous solution of acrylamide monomer. The OTR of PPNR and PPENR films decreased with increasing theirs glass transition temperature. The WVTR of PPENR was directly proportional to mole % epoxide and the WVTR of PPENR film having 39 mole % epoxide was closed to 100 g/m²/day. Both the OTR and WVTR of PPNR-g-AAm were slightly higher than those of PPNR. The highest Young's modulus among PPNR and PPENR films was approximately 8 times higher than that of the skin. Adhesion between PPNR or PPENR or PPNR-g-AAm and a commercial acrylate based adhesive, determined by peel test, were 1.4 N/cm for PPNR and greater than 2 N/cm for PPENR and PPNR-g-AAm.

Keywords: Backing film, Natural rubber, Epoxidized natural rubber, Transdermal patch

\* Corresponding author. Address: Department of Chemistry, Faculty of Science, Mahidol University, Bangkok10400, Thailand;

Tel.: +66-2441-9817-20ext 1141; Fax: +66-2441-0511. Email address: scswr@mahidol.ac.th

#### 1. Introduction

Transdermal drug delivery (TDD) is a promising alternative method to deliver drug into human body. By applying a transdermal patch to the skin, drug is transported across the skin to the systemic circulation. In adhesive transdermal patch, drug is typically loaded in pressure sensitive adhesive (PSA) which is sandwiched or entrapped between backing layer and release liner. With the role of protecting the drug matrix and other components of the patch from environment, backing material influences on drug delivery profile, adhesion of the patch to skin, wear ability and severity of skin irritation[1,2]. In order to allow skin movement in a natural way or to provide comfort to user and to cause less skin irritation, Young's modulus of the patch should be comparable to that of the skin(0.1-0.3 MPa) [1,3]. However, most commercial backing films and TDD patches were found to have the Young's modulus at least 100 times higher than that of the skin [1]. Other important required properties for backing materials include optimum water vapor transmission rate (WVTR) and good oxygen transmission rate (OTR). In order for skin to maintain its function, backing materials should have WVTR close to that of transepidermal water loss (5-10 g/m<sup>2</sup>/h) [4,5]. Moreover, it was reported that transportation of moisture vapor affected adhesion of medical device to the human skin [2]. Air-filled channels, which were used as water vapor transport channels, were created on acrylic plastic disks. After that PSA was applied on the disks, which were then adhered to the human body. The disks with air-filled channels remained on the skin three times longer than the disks without the channels because of better water vapor transport. Another important factor is the adhesion between backing film and PSA, which affects the drug delivery as well as durability of the patch. For transdermal patches, adhesion between backing material and PSA is crucial because poor adhesion can lead to un-effective drug delivery as well as poor durability of the patches. The adhesive strength between the backing and the adhesive should be at lease comparable or greater than that between the patch and skin, i.e., 0.4-2.0 N/cm to be sure that the patch will stay intact during use and to be removed cleanly after use [6]. In order to increase adhesion of NR backing films and PSA like acrylate based PSA, either epoxidation reaction or plasma surface modification is required to increase polarity of NR.

Commercial backing layer can be made of single or multiple layers of synthetic plastics, such as polyethylene, polyurethane, ethylene vinyl acetate, poly(vinyl chloride) and polyester, which are known to have much higher Young's modulus than that of the skin. Published papers related to the development of backing films, especially based on natural rubber (NR) are very limited. The uses of elastomeric materials, including NR and NR

blended with polyolefins, as backing materials for transdermal patches were reported in the patent of Venkatraman *et al.*[7]. Their WVTR in a range of 2.4-480 g/m²/day and the Young's modulus in a range of 0.001-100 MPa were reported. It should be noticed that those values were in a wide range with no specific value for each of elastomers. Among polymers that are possibly useful for transdermal patches reviewed by Sukibayashi and Morimoto [8], NR was included as a base with adhesive without providing information related to backing–required properties.

Prevulcanized NR latex is well known as a raw material that can easily be processed into thin film with good mechanical properties. An excellent in flexibility of prevulcanized NR can be benefit when applying the patch onto flexible parts of the body such as elbow. NR latex can be prevulcanized by various systems including sulfur, peroxide and  $\gamma$ -radiation [9]. Drawbacks for sulfur prevulcanized system for food and medical applications may cause by the use of carcinogenic nitrosamine accelerators and the smell of sulfur. Crosslinking via carbon-carbon linkage of peroxide prevulcanization (PP) and  $\gamma$ -radiation systems provides better compression set and heat stability of rubber products than the sulfur system [10, 11]. However, high energy of  $\gamma$ -radiation causes main chain scission, which resulted in deterioration of rubber properties [12].

Properties of NR and epoxidized NR (ENR) were investigated by several research groups [13-15]. Young's modulus of NR, ENR with 25 and with 50 mole % epoxide prevulcanized by sulfur were 2.15, 2.30 and 2.70 MPa, respectively whereas theirs O<sub>2</sub> permeabilities were 24 x10<sup>10</sup>, 5 x10<sup>10</sup> and 2 x10<sup>10</sup> Barrer [13,14]. However, no details related to sample preparation and to backing-required properties of PPNR based films were given. Studies of PPNR and PPENR were focused on particle morphology and secant modulus [16,17]. Therefore, the main purpose of this work was to investigate backing-required properties of PPNR, PPENR and surface modified PPNR (O<sub>2</sub> plasma treatment of PPNR followed by grafting with AAm (PPNR-g-AAm)). Special attention was paid on OTR and WVTR since these two properties have been rarely determined. Young's moduli, obtained from tensile test, of the films were also reported and compared those of skin and of commercial backings. Moreover, adhesion between the backing film and a commercial acrylate based adhesive (DURO-TAK 87-4098) was determined by peel test.

# 2. Experimental

#### 2.1Materials

High ammonia (HA) – NR latex with 60% dry rubber content (DRC) was obtained from Bangkok Rubber Co., Ltd., (Rayong, Thailand). *Tert*-Butyl hydroperoxide (t-BuHP; Purum), D-(-)-Fructose (Bacteriology) and sodium dodecyl sulfate (SDS; GC) were purchased from Fluka (Bangkok, Thailand) whereas acrylamide monomer (AAm) was purchased from Sigma-Aldrich (Bangkok, Thailand). A commercial acrylate based adhesive (DURO-TAK 87-4098), kindly supplied by Henkel Corporation (New Jersey, USA), was an acrylate-co-vinylacetate non-curing PSA without reactive functional groups.

#### 2.2Preparation of PPNR and PPENR Latexes

PPNR latex was prepared as described elsewhere [17]. The formulation used for the preparation of PPNR is shown in Table 1.

**Table 1** Formulation used for preparation of PPNR [17].

Ingredients	Part by wet weight
	(g)
HA-NR latex	166.7
tert- Butyl hydroperoxide(t-BuHP) (30%)	1.25
D-(-)-Fructose	8.5
Sodium dodecyl sulfate (SDS)	1.25
deionized (DI)water	22.4

In the first step, the peroxide emulsion was prepared by mixing *t*-BuHP solution with DI water and SDS solution. The emulsion and D-(-) - fructose solution were then added into HA-NR latex. Finally, the prevulcanization reaction was carried out at 60°C for various reaction times. During prevulcanization, the latex (about 5 g) was taken out at various time intervals and rapidly cooled down to room temperature to prevent further vulcanization and dried on a petri dish. The crosslink density of PPNR film was determined by measuring % swelling ratio of a piece of dried rubber, which was immersed into toluene for 24 h. After blotting its surface with filter paper, the swelling ratio of crosslinked rubber was calculated as follows:

%Swelling ratio = 
$$\frac{W_{wet} - W_d}{W_d} \times 100$$

Where  $W_d$  is an initial weight of dried rubber (g), and  $W_{wet}$  is the weight of swollen rubber at equilibrium swelling (g).

NR latex was also used for preparation of ENR latex by using formic acid and hydrogen peroxide at 50°C as previously described [18]. The epoxide content of ENR was calculated from the spectrum of proton-nuclear magnetic resonance (<sup>1</sup>H-NMR, DPX400, Bruker) spectroscopy as follows [19].

mole % epoxide = 
$$\frac{I_{2.7}}{(I_{2.7} + I_{5.1})} x 100$$

Where  $I_{2.7}$  and  $I_{5.1}$  are integrated area of peaks at 2.7 and 5.1 ppm, respectively.

Similar to PPNR latex, the PPENR latex was also prepared [17].

#### 2.3 Preparation and Characterizations of Backing Film

Rubber film (400  $\mu$ m in thickness) was prepared by casting PPNR or PPENR latex on a glass plate and then dried at room temperature. In order to PPNR film with AAm, PPNR film was subjected to  $O_2$  plasma treatment (Basic plasma kit BP-1, Samco) 100 W, 13.56 MHz under 0.5 Torr, for 15 s before being dipped into an aqueous solution of AAm monomer (5 wt%).

OTR, WVTR, glass transition temperature  $(T_g)$  and Young's moduli of all films were determined by an  $O_2$  permeation tester, a WVTR tester, dynamic mechanical thermal analysis (DMTA) and a tensile tester, respectively.

#### 2.3.1 Determination of OTR and WVTR

The OTR of dried rubber film was measured at  $23^{\circ}$ C using the  $O_2$  permeation tester (Illinois 8000) according to ASTM D3985-02. After keeping in a dry test environment (0% relative humidity; RH) until equilibrium, the specimen was mounted between two chambers. One chamber was slowly purged by a stream of  $N_2$  and the other contained  $O_2$ . As  $O_2$  permeated through the film into  $N_2$  carrier gas,  $O_2$  was transported to the detector.

The WVTR was determined by Mocon Permatran-w 3/33 according to ASTM F1249-90 (reapproved 1995) at  $38^{\circ}$ C and 90% RH. Test cells were divided into two chambers, which separated by the tested film. The inner chamber was filled with  $N_2$  gas while water vapor was in the outer. Molecules of water diffused through the film to the inside

chamber and were transported to the modulated infrared sensor by  $N_2$  gas. This sensor measured the fraction of infrared energy absorbed by the water vapor and produced an electrical signal. The amplitude of the electrical signal was proportional to water vapor concentration and was then used to calculate the WVTR according to the formula described in the ASTM F1249-90 (reapproved 1995);

$$WVTR = C x (ES - EO)$$

where C is a calibration factor expressing rate as a function of voltage. The value of C is derived from tests of a reference film. EO is a permeation system zero level voltage, and ES is an equilibrium voltage obtained with the test specimen.

# 2.3.2 Determination of Tg and Young's modulus

 $T_g$  was measured using a DMTA (Explexor TM 25 N, Gabo) with a heating rate of 5°C/min from -100 to 10°C.

An Instron (model 5569) was used to determine Young's modulus of the samples at room temperature according to the procedure described in ASTM D 412-98a at a crosshead speed of 500 mm/min and the load cell of 1000N.

#### 3. Results and Discussion

#### 3.1 OTR and WVTR

#### 3.1.1 PPNR Films

The swelling ratios, inversely proportional to crosslink density, of PPNR films versus prevulcanization time were determined and the data are shown in Figure 1. It was observed that the swelling ratios rapidly decreased with increasing prevulcanization time in the initial period. After prevulcanization time of 60 min, the swelling ratios reached a constant value of 1300-1400 %, which indicated the maximum crosslinking of PPNR [20].

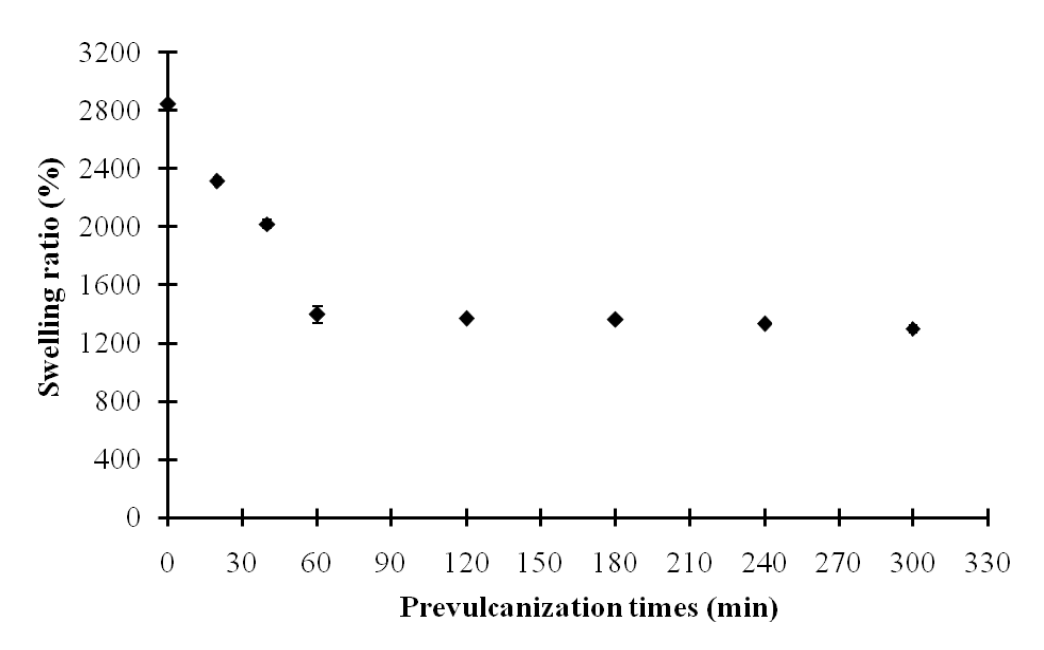


Figure 1 Swelling ratios of PPNR films as a function of prevulcanization times.

Further investigation of the extent of the crosslinking as a function of prevulcanization time was performed by measuring  $T_g$  of the PPNR films using DMTA and the data are presented in Figure 2. Since the formation of network resulted in the reduction of mobility and free volume of rubber chain molecules, it was not surprising that  $T_g$  increased from -64 to -53°C with increasing the prevulcanization time from 0 to 60 min. After 60 min, prevulcanization time had little effect on  $T_g$ , which suggested that the maximum network was obtained [20]. This result corresponded well with the swelling ratios as previously described.

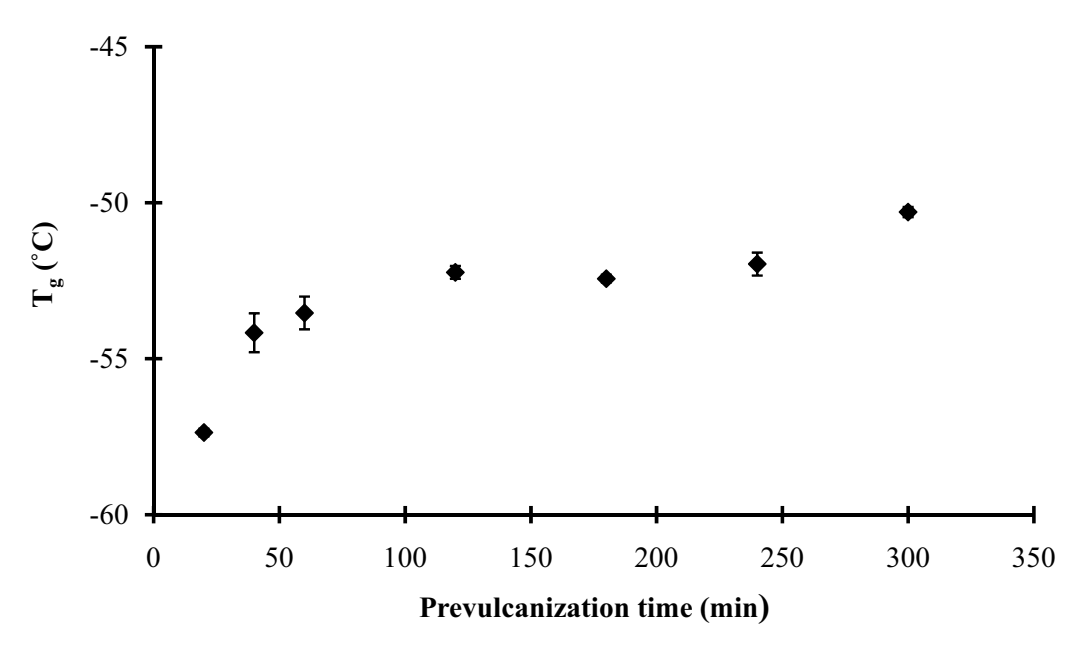


Figure 2 T<sub>g</sub>, determined by DMTA, of PPNR films as a function of prevulcanization times.

The OTR and WVTR of PPNR films as a function of  $T_g$  are displayed in Figure 3. Results showed that both OTR and WVTR values decreased with increasing  $T_g$  of PPNR films. When  $T_g$ s of PPNR films were -57 and -50°C, the OTR were 4333 and 3968 cm<sup>3</sup>/m<sup>2</sup>/day whereas the WVTR were 34 and 22 g/m<sup>2</sup>/day, respectively. It might be due to the formation of crosslinking, which reduced the mobility of rubber chains when increasing  $T_g$  and, hence, the diffusion rate of  $O_2$  or water vapor through PPNR film decreased [13]. These WVTR values of all films were much lower than the transepidermal water loss (TEWL) of human skin), i.e., 120-240 g/m<sup>2</sup>/day.

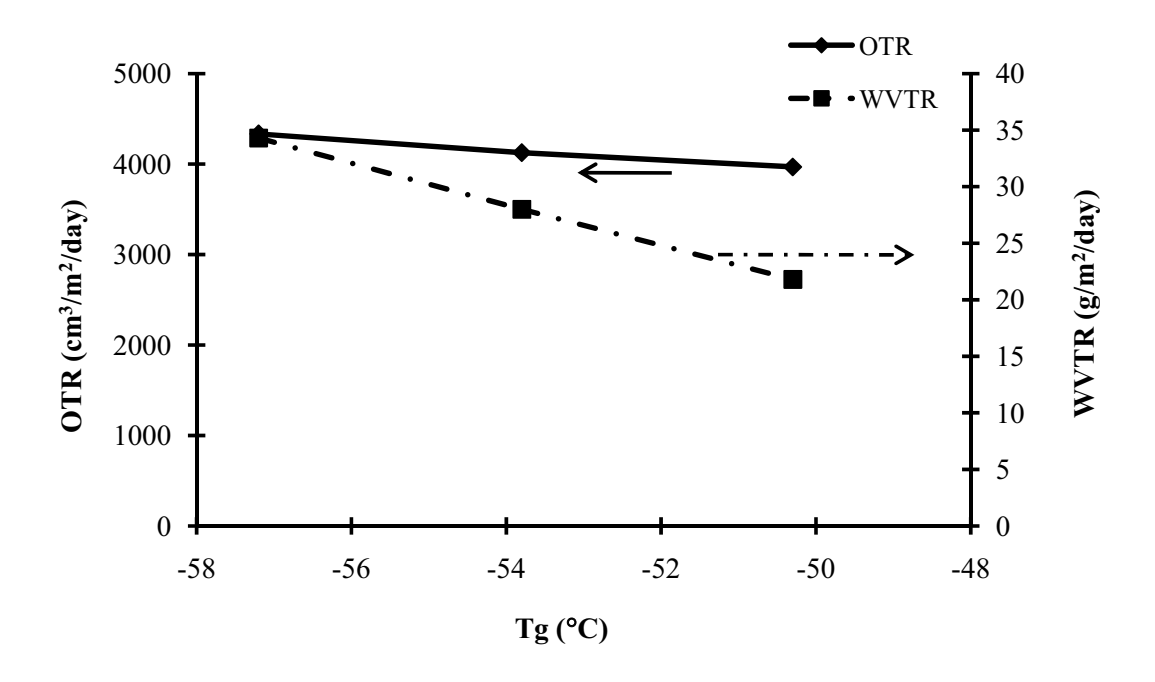


Figure 3 OTR and WVTR of PPNR films as a function of  $T_{\rm g}s$ .

# 3.1.2 PPENR Films

By varying the reaction times from 4 to 24 h, it was found by  $^{1}$ H-NMR that mole % epoxide was in a range of 10-39 % as shown in Figure 4.  $T_{g}$ s of PPENR latex films containing various mole % epoxide, determined by DMTA, are presented in Figure 5. It was noticed that the  $T_{g}$ s increased with increasing reaction times, i.e., with an increase in epoxide groups in rubber molecules because the epoxide or oxirane group reduced mobility and rotational freedom of the rubber molecules [14,18,21].

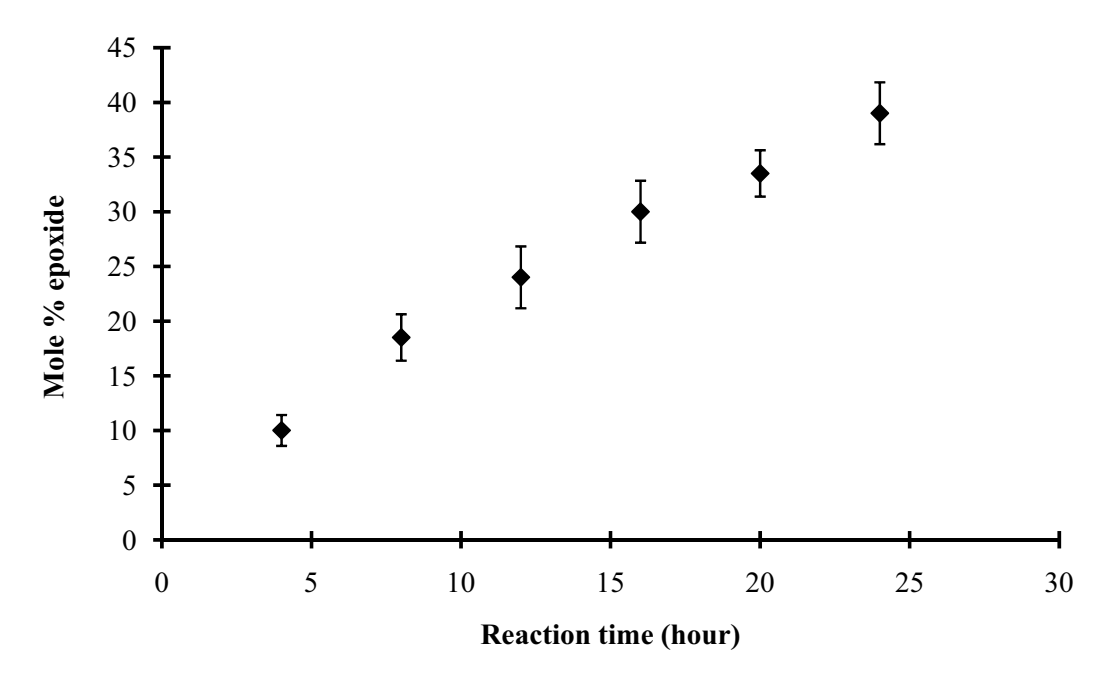


Figure 4 Mole % epoxide as a function of reaction time.

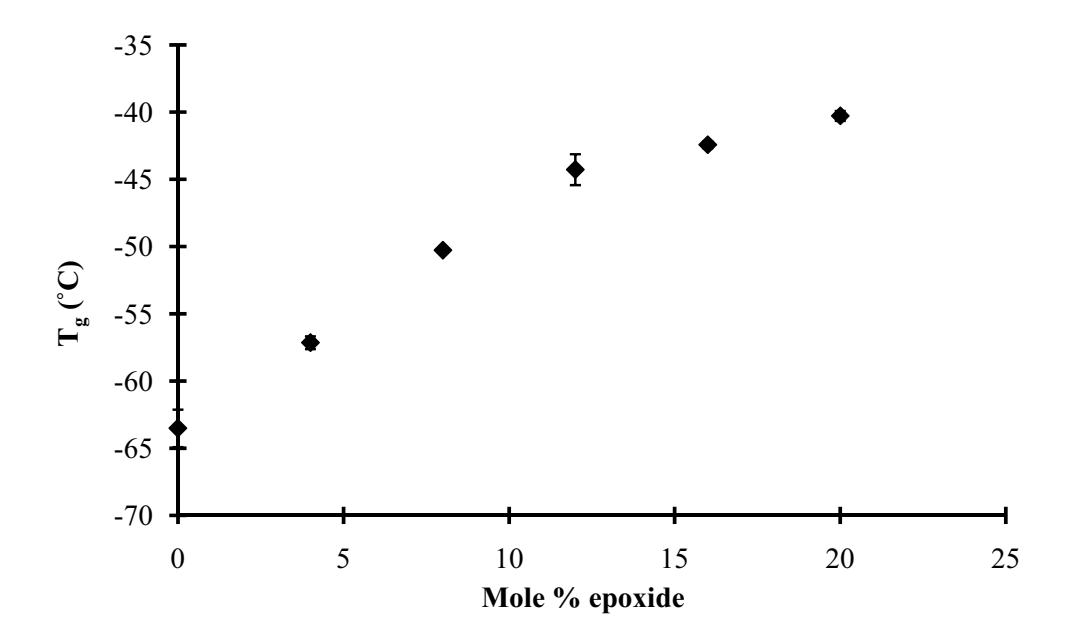
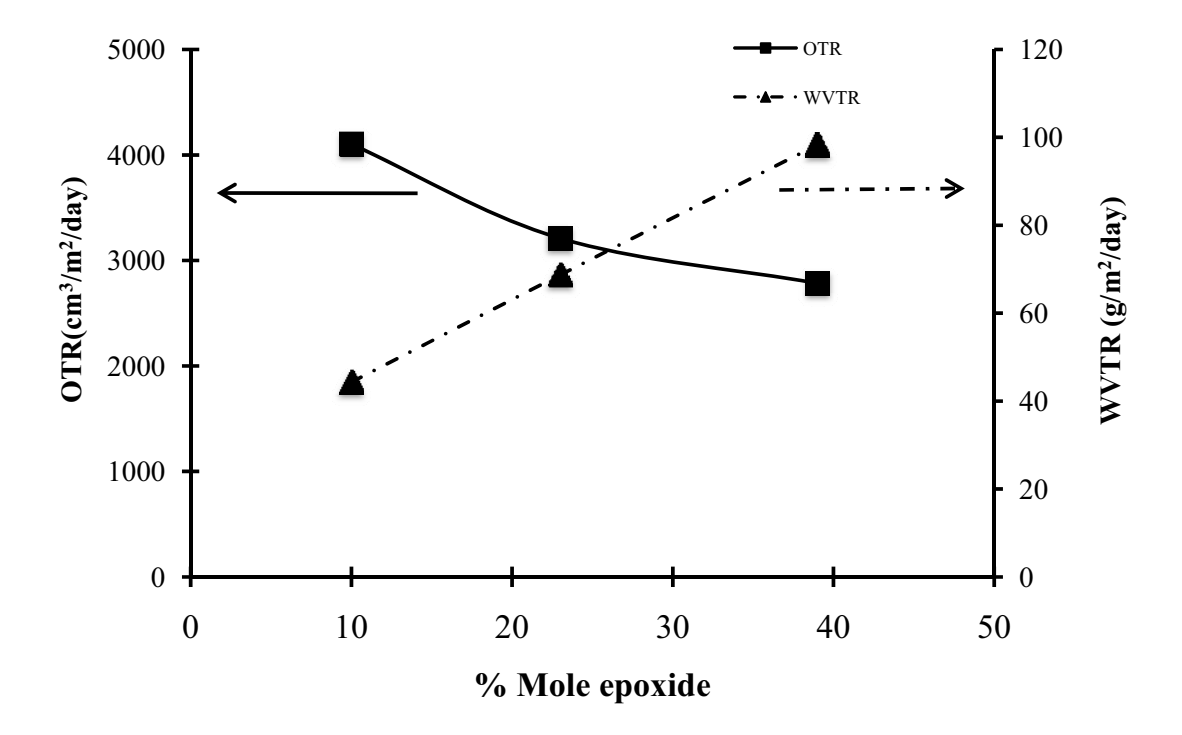


Figure 5  $\,$   $T_{gS}$  of PPENR films with various mole % epoxide.

The OTR and WVTR of PPENR films with prevulcanization time of 60 min as a function of mole % epoxide are shown in Figure 6. The WVTR of PPENR films increased because the epoxide group increased molecular polarity with a consequence of an increase in solubility of water vapor. The WVTR of PPENR with 39 mole % epoxide (prevulcanization time of 20 min) was 112 g/m²/day, which was closed to TEWL of human skin. This suggested that PPENR film had a good potential to be used as a backing film that would be able to maintain the skin functions and cause less skin irritation. However, theirs OTR decreased with increasing mole % epoxide. It was explained that the insertion of oxygen atoms into the rubber molecules resulted in more polar groups in the chains, which reduced theirs mobility and free volume [14,18,21]. As previously observed, the Tg increased with increasing mole % epoxide [13,14].



**Figure 6** OTR and WVTR of PPENR films having various mole % epoxide (prevulcanization time= 60 min)

# 3.1.3 PPNR-g-AAm Films

The presence of acrylamide (AAm) on the surface of PPNR-g-AAm film was confirmed by the decrease of water contact angles of PPNR 91 to 40° after grafting. The OTR and WVTR of PPNR-g-AAm films compared with those of PPNR and PPENR (39 mole %

epoxide) as a function of prevulcanization times are presented in Figures 7 and 8, respectively. Results showed that theirs OTR were slightly higher than those of PPNR films, although the small AAm molecules were presented on the surface of PPNR-g-AAm films. The modification of PPNR might be restricted to the outermost layer [22]. Since oxygen containing functional groups could not be detected by attenuated total reflectance infrared spectroscopy, it was assumed that the modification depth by plasma was less than a micrometer. Therefore, the diffusion of O<sub>2</sub> and water vapor through the bulk of the films remained unaffected. However, the high rigidity of PPENR molecules caused the much lower OTR of PPENR films with 39 mole % epoxide than those of PPNR and PPNR-g-AAm [14,18,21]. The slight increase in WVTR of PPNR-g- compared to that of PPNR film was probably due to better solubility of water vapor at the surface of PPNR-g-AAm film whose surface had higher polarity. It was also observed that the WVTR of PPENR films were 3-4 times higher than those of PPNR and PPNR-g-AAm films. As previously mentioned, the increase in molecular polarity was responsible for an increase in solubility of water vapor throughout the PPENR films.

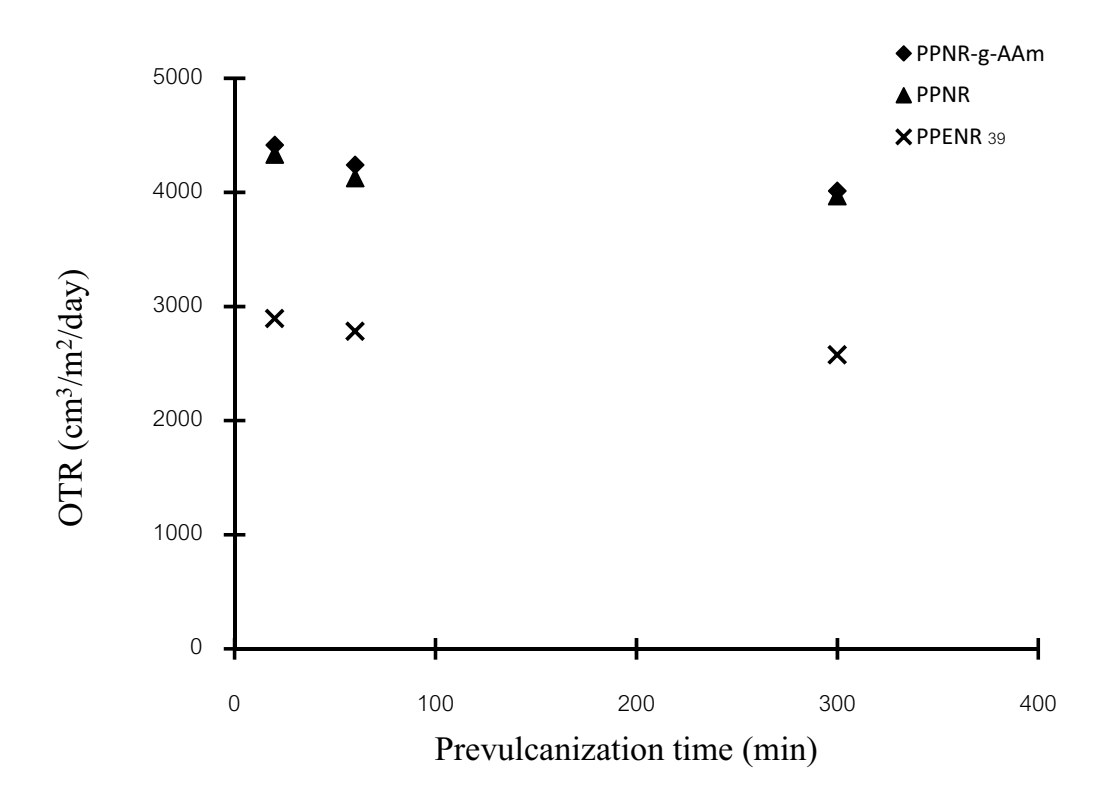


**Figure 7** OTR of PPNR, PPENR(39 mole % epoxide) and PPNR-g-AAm films as a function of prevulcanization times.

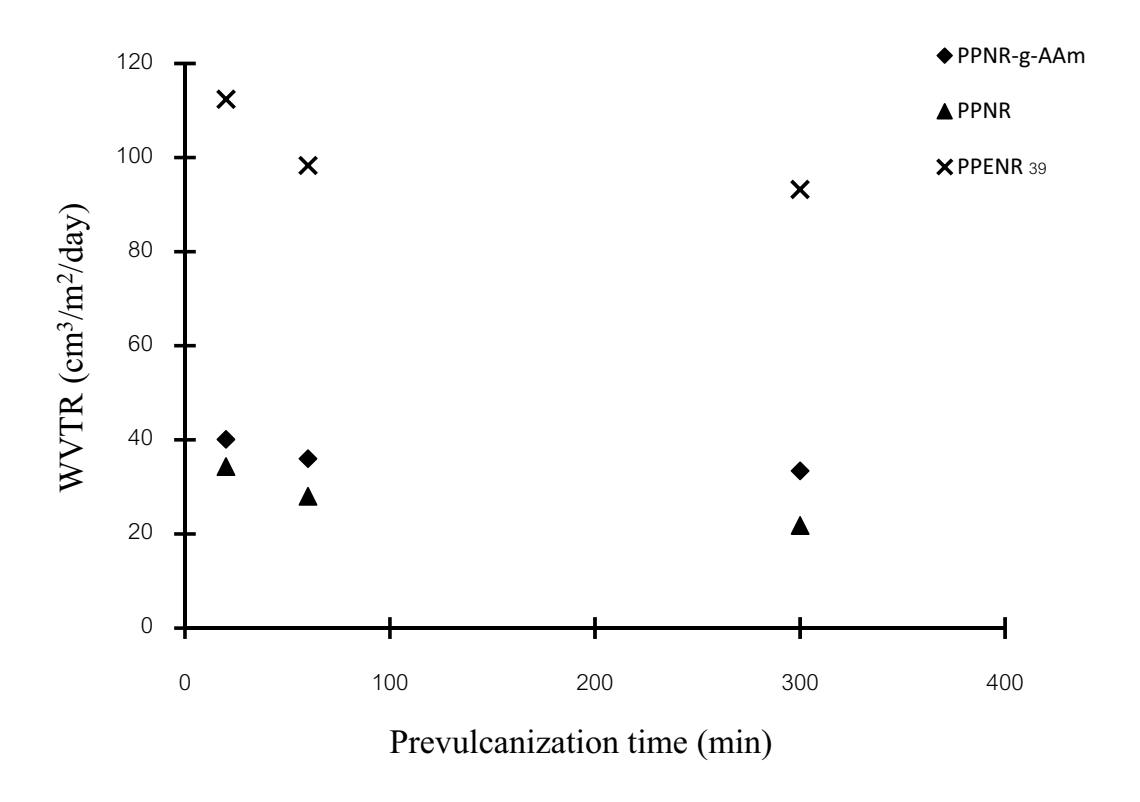


**Figure 8** WVTR of PPNR, PPENR(39 mole % epoxide) and PPNR-g-AAm films as a function of prevulcanization times.

#### 3.2 Young's Modulus and Adhesion to Acrylate Based PSA

# 3.2.1 Young's Modulus

The Young's moduli of PPNR films which increased with increasing prevulcanization times up to 120 min are shown in Figure 9. The highest modulus at prevulcanization time of 120 min was explained by the optimum prevulcanization, which had a suitable fuse of rubber particles [23]. As previously reported, peroxide prevulcanization of NR latex provided heterogeneous network structure inside each rubber particle, i.e., dense crosslink near the surface compared to the central region [23]. At prevulcanization time longer than 120 min, the modulus tended to decrease possibly due to highly crosslink near the surface of rubber particles, which prevented further fuse of rubber particles. It should be mentioned that the highest Young's modulus of PPNR film was approximately 8 times higher than that of the skin (i.e., 0.1–0.3 MPa). These values were much lower than those reported for commercial unlaminated backing films (77, 102 and 2128 MPa) and transdermal patches

(4-501 MPa) [1]. From these data, it could be assumed that PPNR showed promising results to be used as a backing film.

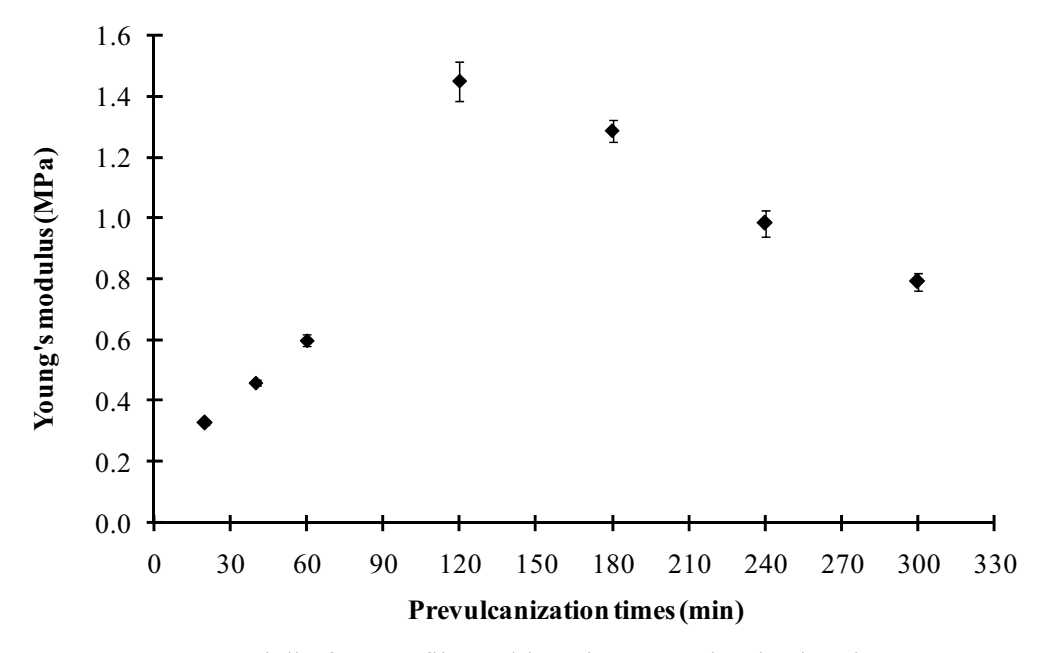
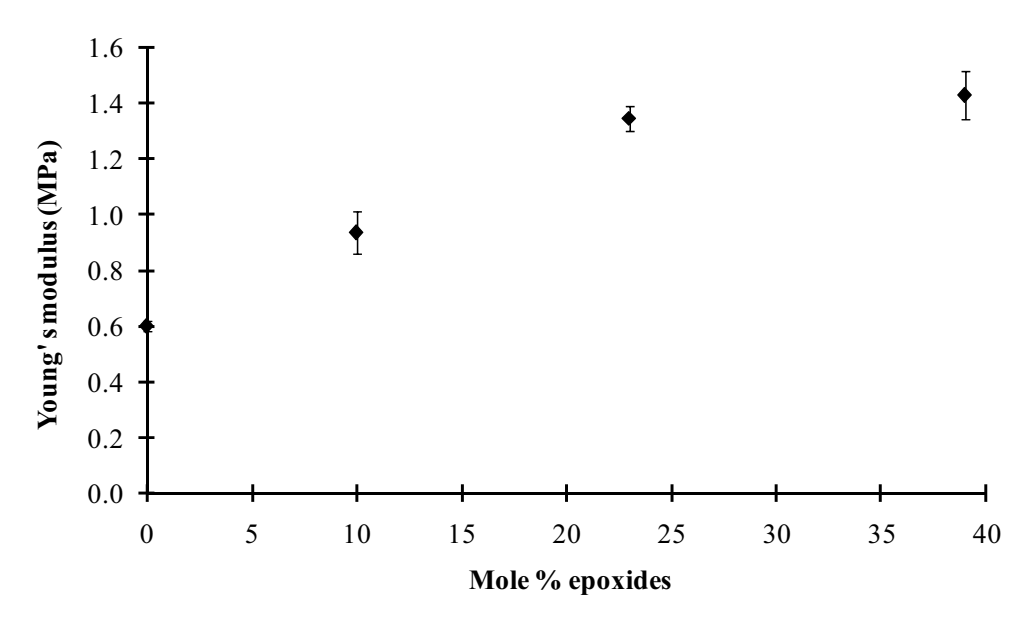


Figure 9 Young's moduli of PPNR films with various prevulcanization times.

As previously mentioned that prevulcanization time longer than 120 min resulted in poor rubber particle fusion, therefore, prevulcanization time of 60 min was selected for further investigation of PPENR films. The Young's moduli of PPENR films having various mole % epoxide are shown in Figure 10. The Young's modulus of the PPENR film was about 1.5-2.0 times higher than that of PPNR film. It might be due to coiled structure of PPNR, i.e. easily to be stretch at low strain level [14,24]. With increasing the epoxy content, the Young's moduli of PPENR increased because of increasing rigidity and reducing mobility of chains as previously explained.



**Figure 10** Young's moduli of PPENR films with various mole % epoxide (prevulcanization time = 60 min).

## 3.2.2 Adhesive Strength

The adhesive strength between PPNR or PPENR or PPNR-g-AAm and acrylate-co-vinylacetate adhesive (DURO-TAK 87-4098) was determined by peel test and the results are shown in Figure 11. With using PPNR and PPNR-g-AAm films, theirs peel strength values were 1.4 and 2.3 N/cm, respectively. The higher peel strength of PPNR-g-AAm compared to that of PPNR was due to the more polarity of PPNR-g-AAm surface as already reported by the water contact angle. The highest peel strength observed for PPENR (39 mole % epoxide) was also explained by the highest polarity of this rubber film.

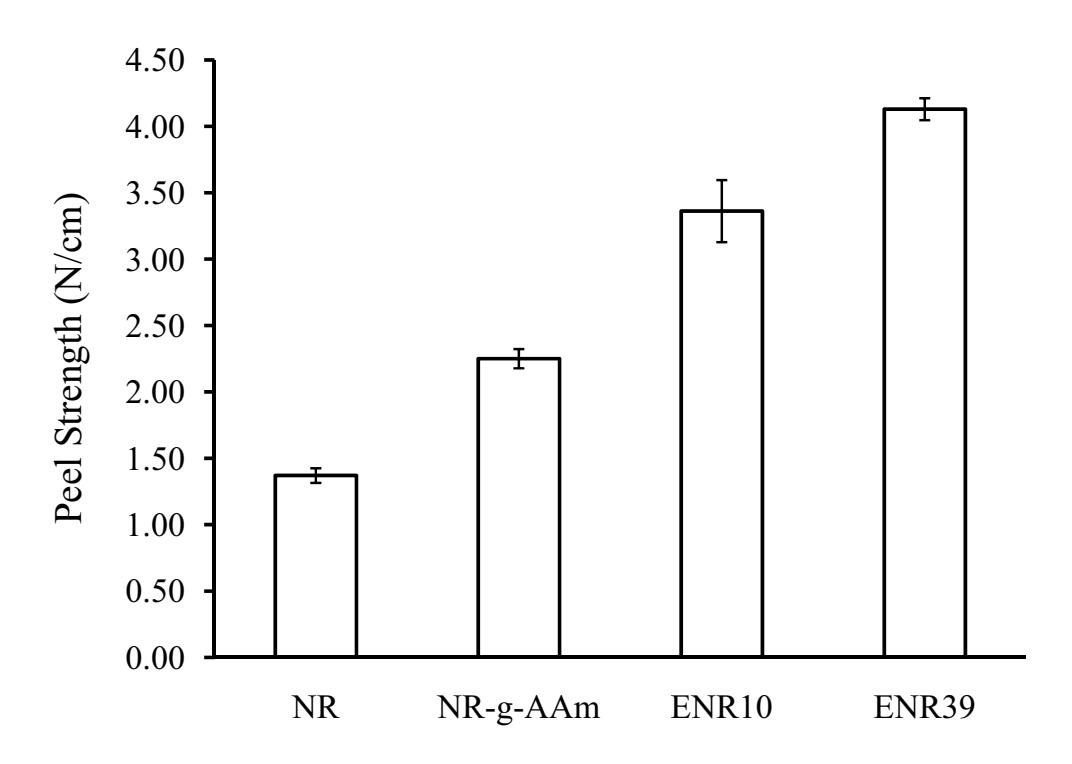


**Figure 11** Peel strength between PPNR or PPENR or PPNR-g-AAm films and DURO-TAK 87-4098.

# 4. Conclusions

PPNR, PPENR and PPNR-g-AAm films had a potential to be used as backing films for trnasdermal patches. For both PPNR and PPENR films, as Tg increased OTR decreased due to the reduction of chain mobility and free volume. However, the lowest OTR obtained from PPENR with 39 mole % epoxide was still greater than 2500 cm³/m²/day. For WVTR of PPENR, as mole % epoxide increased WVTR increased due to more polarity. PPENR films having 39 mole % epoxide had WVTR closed to100 g/m²/day, which is closed to TEWL. Both OTR and WVTR of PPNR-g-AAm were slightly higher than those of PPNR because its surface was covered with small molecules of AAm. Young's moduli of all samples were found to be at most 8 times higher than that of the skin. Adhesive strength, determined by peel test, between PPNR films and DURO-TAK 87-4098 was found to be about 1.4 N/cm whereas those for PPENR and PPNR-g-AAm were greater than 2 N/cm, which is sufficient for making the patch.

#### Acknowledgement

Financial support from The Thailand Research Fund /the Commission on Higher Education (MRG5380023) and the Faculty of Science, Mahidol University, Bangkok, Thailand to S.W. were gratefully acknowledged. P.T. is TRF Senior Researcher.

#### References

- [1] C. Fauth, S. Wiedersberg, R. H. H. Neubert, and M. Dittgen, "Adhesive backing foil interactions affecting the elasticity, adhesion strength of laminates, and how to interpret these properties of braded transdermal patches", Drug Dev. Ind. Pharm., 28 (10), 1251-1259 (2002).
- [2] D. D. Cunningham and M. G. Lowery, "Moisture vapor transport channels for the improved attachment of a medical device to the human body", Biomed.Microdev.,6 (2), 149-154 (2004).
- [3] S. Diridollou, D. Black, J. M. Lagarde, Y. Gall, M. Berson, V. Varbe, F. Patat and L. Vaillant, "Sex- and site-dependent variations in the thickness and mechanical properties of human skin *in vivo*", Int. J. Cosmet.Sci., 22, 421-435 (2000).
- [4] Y. N. Kalia, F. Pirot and R. H. Guy, "Homogeneous transport in a heterogeneous membrane: water diffusion across human stratum corneum in vivo", Biophys. J., 71, 2692-2700 (1996).
- [5] Y. N. Kalia, I. Alberti, N. Sekkat, C. Curdy, A. Naik, and R. H. Guy, "Normalization of stratum corneum barrier function and transepidermal water loss *in vivo*", Pharm. Res., 17 (9), 1148-1150 (2000).
- [6] T. S. Spencer, S. E. Smith and S. Conjeevaram, "Adhesive interaction between polymers and skin in transdermal delivery systems", Polym. Mater.Sci. Eng., 63, 337-339 (1990).
- [7] S. S. Venkatraman, S. E. Smith. "Occlusive, elastomeric backing materials in transdermal drug delivery systems, and associated methods of manufacture and use", US Patent 5,246,705 September 21, 1993.
- [8] K. Sugibayashi and Y. Morimoto, "Polymers for transdermal drug delivery systems" J. Control Release, 29, 177-185 (1994).
- [9] J. T. Varkey, S. S. Rao and S. Thomas, "Effect of prevulcanization on the rheological behavior of natural rubber/styrene butadiene rubber latex blends", J. Appl. Polym. Sci., 62, 2169-2180 (1996).
- [10] A. Ciesielski, An Introduction to Rubber Technology, Rapra Technology Limited Shawbury, Shrewsbury, Shropshire, SY4 4NR, UK, 1999, pp. 35-36.

- [11] A. A. Basfar, M. M. Abdel-Aziz, and S. Motif, "Influence of different curing systems on the physico-mechanical properties and stability of SBR and NR rubbers", Radiat. Phys. Chem., 63, 81-87(2002).
- [12] K. Makuuchi and M. Hagiwara, "Radiation vulcanization of natural rubber latex with polyfunctional monomers, J. Appl. Polym.Sci.,29, 965-976 (1984).
- [13] T. Johnson and S. Thomas, "Nitrogen/oxygen permeability of natural rubber, epoxidised natural rubber and natural rubber/epoxidised natural rubber blends", Polymer, 40, 3223-3228 (1999).
- [14] T. Johnson and S. Thomas, "Effect of epoxidation on the transport behaviour and mechanical properties of natural rubber", Polymer 41, 7511–7522 (2000).
- [15] M. Chen, N. –J Ao, B. –L. Zhang, C. –M. Den, H. –L. Qian and H. –L Zhou, Comparison and evaluation of the thermooxidative stability of medical natural rubber latex products prepared with a sulfur vulcanization system and aperoxide vulcanization system, J. Appl. Polym. Sci., 98, 591-597 (2005).
- [16] P. Tangboriboonrat, D. Polpanich, T. Suteewong, K. Sanguansap, U. Paiphansiri, and C. Lerthititrakul, "Morphology of peroxide prevulcanised natural rubber latex: effect of reaction time and deprotenisation", Colloid Polym. Sci., 282, 177-181 (2003).
- [17] T. Suteewong and P. Tangboriboonrat, Particle morphology of epoxidised natural rubber latex prevulcanized by peroxide system, e-Polymers, 121, 1–9 (2007).
- [18] P. Saendee and P. Tangboriboonrat, "Latex interpenetrating polymer networks of epoxidized natural rubber/poly (methyl methacrylate): an insight into mechanism of epoxidation", Colloid Polym.Sci., 284, 634-643 (2006).
- [19] P. Tangboriboonrat and C. Rakdee, "Effect of epoxidised natural rubber latex on carbon black-natural rubber interaction in bead masterbatch", Plast. Rubber Compos.,29, 258-262 (2000).
- [20] P. Tangboriboonrat and C. Tiyapaiboonchaiya, Novel method for toughening of polystyrene based on natural rubber latex, J. Appl. Polym. Sci., 71, 1333–1345 (1999).
- [21] K. Sanguansap, T. Suteewong, P. Saendee, U. Buranabunya, and P. Tangboriboonrat, "Composite natural rubber based latex particles: a novel approach", Polymer, 46, 1373-1378 (2002).
- [22] C. M. Chan, T. M. Ko, H. Hiraoka, "Polymer surface modification by plasmas and photons", Surf. Sci. Rep., 24, 1–54 (1996).
- [23] P. Tangboriboonrat and C. Lerthititrakul, "Morphology of sulphur and peroxide prevulcanised natural rubber latex", Colloid Polym. Sci., 280, 1097-1103 (2002).

[24] I. R. Gelling, "Modification of natural rubber latex with peracetic acid", Rubber Chem. Technol., 58, 86–96 (1985).

# Synthesis and Characterizations of PLLA/PEG Block Copolymers

Thai Hien Nguyen<sup>1,a</sup>, Atitsa Petchsuk<sup>2,b</sup>, Pramuan Tangboriboonrat<sup>3,c</sup>, Mantana Opaprakasit<sup>4,d</sup>, Alice Sharp<sup>1,e</sup>, and Pakorn Opaprakasit<sup>1,f\*</sup>

<sup>1</sup>School of Bio-Chemical Engineering and Technology, Sirindhorn International Institute of Technology (SIIT), Thammasat University, Pathumthani 12121 Thailand

<sup>2</sup>National Metal and Materials Technology Center (MTEC), Pathumthani 12120 Thailand <sup>3</sup>Department of Chemistry, Mahidol University, Bangkok 10400 Thailand

<sup>4</sup>Department of Materials Science, Chulalongkorn University, Bangkok 10330 Thailand anguyen.th.hien@gmail.com, batitsp@mtec.or.th, cscptb@mahidol.ac.th, dmantana.o@chula.th, ealice@siit.tu.ac.th, pakorn@siit.tu.ac.th

Keywords: PLLA, PEG, copolymer, chain extending, degradable polymer

**Abstract.** Poly(lactic acid-co-ethylene glycol) (PLLA/PEG) copolymers were synthesized and their properties were characterized. The PLLA/PEG/PLLA triblock copolymers were synthesized by ring-opening polymerization from 1-lactide (LLA) and PEG macroinitiator. Stannous octoate, Sn(Oct)<sub>2</sub> was used as a catalyst. Effects of molecular weight of PEG (600, 2000 and 4000), LLA/OH molar ratios (95:5, 98:2) and a sequence of addition of the reactants on properties of the copolymers were investigated. The triblock copolymers were subsequently used in a production of multiblock copolymers by reacting with a chain-extending agent, hexamethylene diisocyanate (HMDI). Chemical structure and molecular weight of the copolymers were characterized by <sup>1</sup>H-NMR, FTIR and GPC. The results showed that molecular weight of triblock copolymers varied from 4,500 to 10,200. After chain extension, multiblock copolymer with molecular weight of 16,490 was produced. Thermal properties of the copolymers were also examined by DSC.

## Introduction

Poly(lactic acid) (PLA) is biodegradable and biocompatible polymer that is particularly attractive in scientific community to use in various applications, especially in medical applications. This aliphatic polyester is polymerized by polycondensation or ring-opening polymerization, where the latter reaction yields higher molecular weight copolymers. However, PLA is hydrophobic, which limits its use in certain applications. On the other hand, poly(ethylene glycol) (PEG) is known as hydrophilic polymer with outstanding properties, such as non-toxicity, non-ionic and biocompatible characteristics. Therefore, copolymerization of PLA and PEG offers an opportunity to combine the advantages of these polymers.

In this study, PLA/PEG copolymers are synthesized and their properties are characterized. The PLLA/PEG/PLLA triblock copolymers are synthesized by ring-opening polymerization using Sn(Oct)<sub>2</sub> as a catalyst. Effects of molecular weight of PEG, LLA:OH(PEG) molar ratios and a sequence of addition of the reactants on structure and properties of copolymer are investigated. Multiblock copolymers are then synthesized by employing a chain extending agent, HMDI. These copolymers are intended for use as biomedical materials, e.g. drug encapsulation, scaffold and controlled release applications.

## **Experimental**

The synthesis procedure of triblock PLLA/PEG/PLLA copolymers was adopted the methodology reported by Yuqing Wan et. al.[1]. L-lactide (LLA) was synthesized in the laboratory by polycondensation of l-lactic acid (88 wt% in water, Carlo Erba), using  $Sn(Oct)_2$  as catalyst. The purified LLA was stored in vacuum flask until use. PEG with  $M_n = 600$ , 2000, 4000 were supplied



by Fluka. Sn(Oct)<sub>2</sub> (Wako) was used as a catalyst. HMDI were purchased from Aldrich. The properties of copolymers were then characterized by <sup>1</sup>H-NMR (Bruker DRX400) and FTIR (ThermoNicolet 6700) spectroscopy and GPC (Waters 150 CV). Thermal properties of copolymer were characterized by Mettler Todedo DSC822<sup>e</sup>

Effects of molecular weight of PEG and LLA/OH molar ratios. PLLA/PEG/PLLA triblock copolymers were synthesized by using PEG with different molecular weight (600, 2000, and 4000) and employing different LLA/OH molar ratios (95:5, 98:2) to yield different EG and LLA block lengths in copolymer chains. Essentially, the monomer mixture and initiator were dried by a vacuum/inert gas technique for 1 hour under dry nitrogen. The mixture was then melted at 130°C and the polymerization was taken place for 24 hours. Finally, chloroform and ethanol were used to purify the copolymer products.

Effects of sequence of adding the reactants. PEG 4000 and a LLA/OH molar ratio of 98:2 were employed in the synthesis using the same temperature and reaction time as described above. Three experiment conditions were employed. In the first experiment, LLA, PEG and Sn(Oct)<sub>2</sub> were added in the flask at the same time (a). In the second experiment, LLA and PEG were melted at 130°C and Sn(Oct)<sub>2</sub> was then added to the mixture (b). In the final experiment, PEG 4000 was melt at 80°C. Then 1%w/w Sn(Oct)<sub>2</sub> was added to PEG solution. After 1 hour, LLA was finally added to the mixture (c).

**Synthesis of multiblock PLLA/PEG copolymer.** The synthesis process was similar to the methodology reported by Cohn et. al.[2], except that Sn(Oct)<sub>2</sub> was used as a catalyst. PLLA/PEG multiblock copolymer was synthesized by chain extension reaction of PLLA<sub>46</sub>/PEG<sub>46</sub>/PLLA<sub>46</sub> triblock copolymer using HMDI as a coupling agent. A molar ratio of triblock copolymer:HMDI of 1.0:1.1 was employed. Triblock copolymer was first dissolved in dioxane. HMDI and Sn(Oct)<sub>2</sub> were then added to the solution, and the reaction was carried out at 80°C for 3 hours (d).

## **Results and Discussion**

Triblock PLLA/PEG/PLLA copolymers were synthesized by ring-opening polymerization of LLA in the presence of PEG and Sn(Oct)<sub>2</sub>, as presented in Figure 1. As a result, OH-capped triblock copolymers were produced.

$$HO - CH_2 - CH_2 - O - H \\ hO - CH_2 - CH_2 - O - H \\ hO - CH_3 \\ hO - CH_3 \\ hO - CH_2 - CH_2 - O - H \\ hO - CH_2 - CH_2 - CH_2 - O - H \\ hO - CH_2 - CH_2$$

Figure 1. Copolymerisation reaction of PEG and LLA by ring-opening polymerization

The chemical structure and composition of the triblock copolymers were characterized by <sup>1</sup>H-NMR. The <sup>1</sup>H-NMR spectrum of the copolymer and signal assignments are shown in Figure 2.

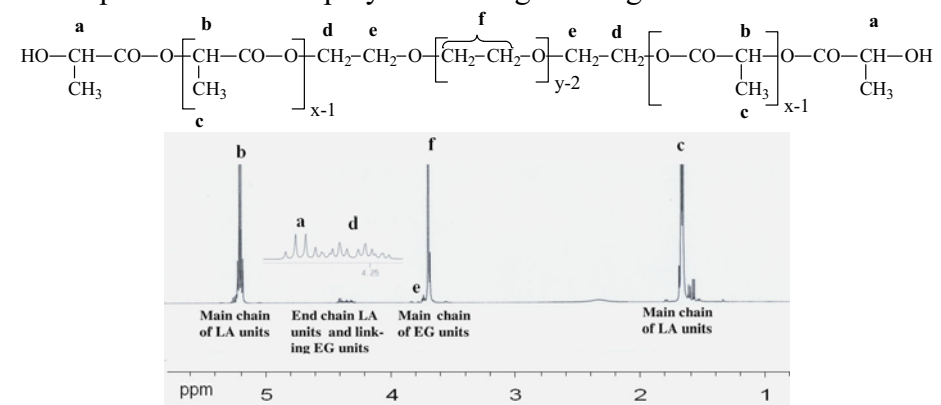


Figure 2. <sup>1</sup>H-NMR spectrum of PLLA<sub>46</sub>/PEG<sub>46</sub>/PLLA<sub>46</sub> triblock copolymer



FTIR spectra of PLLA ( $M_n = 40,000$ ), PEG ( $M_n = 2,000$ ), and PLLA<sub>46</sub>/PEG<sub>46</sub>/PLLA<sub>46</sub> triblock copolymer are compared in Figure 3. The presence of band characteristics of PLLA and PEG were observed in the spectrum of the copolymer. Characteristic of LLA segments were observed at 1713 cm<sup>-1</sup> (C=O stretching). The bands located at 3447 cm<sup>-1</sup> (O-H stretching), 2872 cm<sup>-1</sup> (C-H stretching) are assigned to characteristic of EG segments.

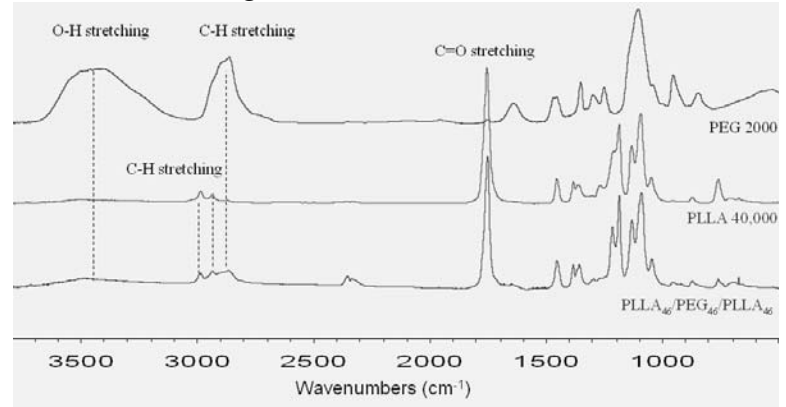


Figure 3. FTIR spectra of PEG 2,000, PLLA 40,000 and PLLA<sub>46</sub>/PEG<sub>46</sub>/PLLA<sub>46</sub> triblock copolymer

Effects of molecular weight of PEG and LLA/OH molar ratios. Triblock copolymers with wide range of molecular weight were obtained by varying molecular weight of PEG and LLA/OH molar ratios, as summarized in Table 1. The results showed that LLA/EG ratios in the products varied from 0.42:1 to 2.78:1, which are dependent on the ratios in feed.

Table 1. Effect of molecular weight of PEG and LLA/OH molar ratios

Copolymers	LLA/OH (mol/mol)	LLA/EG (in feed) (mol/mol)	LLA/EG <sup>a</sup> (in product) (mol/mol)	$\overline{DP}_{PEG}^{b}$	$\overline{DP}_{PLLA}^{^{^{^{}}}$	$M_n^{d}$	M <sub>n</sub> (GPC)
PLLA <sub>27</sub> /PEG <sub>14</sub> /PLLA <sub>27</sub>	95:5	2.78:1	3.90:1	14	27	4,500	5,800
PLLA <sub>28</sub> /PEG <sub>46</sub> /PLLA <sub>28</sub>	95:5	0.84:1	1.26:1	46	28	6,060	6,950
PLLA <sub>46</sub> /PEG <sub>46</sub> /PLLA <sub>46</sub>	98:2	2.16:1	2.04:1	46	46	8,650	10,400
PLLA <sub>14</sub> /PEG <sub>91</sub> /PLLA <sub>14</sub>	95:5	0.42:1	0.31:1	91	14	6,020	10,900
PLLA <sub>43</sub> /PEG <sub>91</sub> /PLLA <sub>43</sub>	98:2	1.08:1	0.95:1	91	43	10,200	12,650

<sup>&</sup>lt;sup>a</sup> Calculated from the ratios of integral intensities of methyne of lactic acid at 5.0-5.3 ppm to methylene of ethylene glycol at 3.5-3.8 ppm,  ${}^{b}\overline{DP}_{PEG} = M_{nPEG} / 44$ ,  ${}^{C}\overline{DP}_{PLLA} = \overline{DP}_{PEG} \times (LLA/EG)/2$ ,  ${}^{d}M_{n} = \overline{DP}_{PEG} \times 44 + \overline{DP}_{PLLA} \times 2 \times 72$ 

Effects of sequence of adding of the reactants. Effects of order of adding of reactants on properties of the resulting copolymers were studied to further optimize suitable synthesis conditions. The results, as shown in Table 2, indicates that comparable LLA block length were obtained from sample (a) and (b). Results from sample (c) showed copolymer with higher molecular weight than those of the former two copolymers.

Table 2. Effects of sequence of adding the reactants on properties of triblock copolymers

Copolymers	Samples	LLA/EG (in feed) (mol/mol)	LLA/EG <sup>a</sup> (in product) (mol/mol)	$\overline{DP}_{PEG}^{\ \ b}$	$\overline{DP}_{PLLA}^{C}$	$M_n^{d}$
PLLA <sub>43</sub> /PEG <sub>91</sub> /PLLA <sub>43</sub>	(a)	1.08:1	0.95:1	91	43	10,250
PLLA <sub>41</sub> /PEG <sub>91</sub> /PLLA <sub>41</sub>	(b)	1.08:1	0.90:1	91	41	9,920
PLLA <sub>48</sub> /PEG <sub>91</sub> /PLLA <sub>48</sub>	(c)	1.08:1	1.05:1	91	48	10,860

**Synthesis of PLLA/PEG multiblock copolymer.** The molecular weights of the multiblock copolymer are summarized in Table 3. As expected, the molecular weight of the resulting copolymer increased from 10,400 to 16,490, as a result from chain-linking reaction.



Table 3. Molecular weight of PLLA/PEG multiblock copolymer after chain coupling reaction

Copolymers	LA/EG <sup>a</sup> (in product) (mol/mol)	$M_n$ (GPC)
PLLA <sub>46</sub> /PEG <sub>46</sub> /PLLA <sub>46</sub>	2.04:1	10,400
(d)	2.40:1	16,490

**Thermal properties.** Thermal characteristics of PLLA/PEG/PLLA triblock copolymers were examined by DSC. The results are summarized in Table 4. In copolymer with PEG length of 14 units, single  $T_m$  was observed. An increase in  $T_m$  was detected, as molecular weight of the copolymers increased. As expected, two  $T_m$  of the copolymer with  $\overline{DP_{PEG}} = 46$  and  $\overline{DP_{PEG}} = 91$ , because each segregated block are large enough to exhibit two separate crystalline domains. On the other hand, DSC curves showed a decrease in  $T_g$  when the degree of polymerization  $\overline{DP_{PEG}}$  increases from 14 to 46.  $T_g$  of copolymer with  $\overline{DP_{PEG}} = 91$  was not detected because it was masked by  $T_m$  of EG block. It was difficult to determine  $T_g$  of LLA block because  $T_g$  of PLLA and  $T_m$  of PEG are very close. DSC exhibit the mutual effects of LLA and EG blocks on  $T_m$  and  $T_g$ , such as  $T_g$  of copolymers is ranging from -7 to -3°C while  $T_g$  of commercial PEG is -40°C [3]. An addition of EG block results in a decrease in  $T_m$  of PLLA blocks (118-156°C), when compared with the  $T_m$  of commercial PLLA (145-186°C) [3]

Table 4. Thermal properties of PLLA/PEG/PLLA triblock copolymers

Copolymers	$T_{g}$		T <sub>m</sub>
Coporymers	[°C]	[°	'C]
PLLA <sub>27</sub> /PEG <sub>14</sub> /PLLA <sub>27</sub>	-3	1	29
PLLA <sub>28</sub> /PEG <sub>46</sub> /PLLA <sub>28</sub>	-7	23	129
PLLA <sub>46</sub> /PEG <sub>46</sub> /PLLA <sub>46</sub>	-6	85	156
PLLA <sub>14</sub> /PEG <sub>91</sub> /PLLA <sub>14</sub>	/	45	118
PLLA <sub>43</sub> /PEG <sub>91</sub> /PLLA <sub>43</sub>	/	42	150

## **Conclusions**

PLLA/PEG/PLLA triblock copolymers are synthesized at  $130^{\circ}$ C by ring-openning polymerization of lactide, PEG as a macroinitiator and Sn(Oct)<sub>2</sub> as a catalyst. Block lengths and chemical structures of the copolymers are characterized by  $^{1}$ H-NMR and FTIR. It was found that the degree of polymerization of LLA block decreased (27, 28 and 14) when the degree of polymerization of EG block increased (14, 46 and 91). The results also indicated that a 98:2 of LLA/OH molar ratio is a suitable ratio for synthesizing high molecular weight copolymers. HMDI was used as a chain-extender to produce higher molecular weights multiblock copolymers. DSC thermograms showed the dependence of  $T_m$  and  $T_g$  on the block lengths of the copolymers.

## Acknowledgements

Financial support of this work is provided by The Thailand Research Fund (TRF), The Commission on Higher Education (CHE), RTA5180003 and Thailand Toray Science Foundation. Thai Hien Nguyen is supported by a scholarship program from SCG Foundation and SIIT, Thammasat University.

#### References

- [1] Yuqing Wan, Wenna Chen, Jian Yang, Jianzhong Bei, Shenguo Wang: Biomaterials, Vol. 24, Issue 13 (2003), p. 2196
- [2] D. Cohn, A. Hotovely-Salomon: Polymer, Vol. 46, Issue 7 (2005), p. 2069
- [3] James E. Mark: *Polymer Data Handbook* (1999), p.632, 545, 628



# **Functionalized and Sensing Materials**

doi:10.4028/www.scientific.net/AMR.93-94

# Synthesis and Characterizations of PLLA/PEG Block Copolymers

doi:10.4028/www.scientific.net/AMR.93-94.198

## References

[1] Yuqing Wan, Wenna Chen, Jian Yang, Jianzhong Bei, Shenguo Wang: Biomaterials, Vol. 24, Issue 13 (2003), p. 2196

[2] D. Cohn, A. Hotovely-Salomon: Polymer, Vol. 46, Issue 7 (2005), p. 2069

[3] James E. Mark: Polymer Data Handbook (1999), p.632, 545, 628



# Preparation and Characterizations of Electrospun Lactide-based Polymeric Nanofibers

C. Thammawong<sup>1,a</sup> A. Petchsuk<sup>2,b</sup> M. Opaprakasit<sup>3,c</sup>

N. Chanunpanich<sup>4,d</sup> P. Tangboriboonrat<sup>5,e</sup> and P. Opaprakasit<sup>1,f\*</sup>

<sup>1</sup>School of Bio-Chemical Engineering and Technology, Sirindhorn International Institute of Technology (SIIT), Thammasat University, Pathumthani 12121 Thailand

<sup>2</sup>National Metal and Materials Technology Center (MTEC), Pathumthani 12120 Thailand

<sup>3</sup>Department of Materials Science, Chulalongkorn University, Bangkok 10330 Thailand

<sup>4</sup>Industrial Chemistry Department, King Mongkut's University of Technology North Bangkok, 10800 Thailand

<sup>5</sup>Department of Chemistry, Mahidol University, Bangkok 10400 Thailand <sup>a</sup>chakrit\_th@windowslive.com, <sup>b</sup>atisasp@mtec.or.th, <sup>c</sup>mantana@sc.chula.ac.th, <sup>d</sup>ncn@kmutnb.ac.th, <sup>e</sup>scptb@mahidol.ac.th, <sup>f</sup>pakorn@siit.tu.ac.th

**Keywords:** Polylactic acid; Electrospinning; Porosity; Nanofiber; Copolymer.

**Abstract.** Poly(L)lactide (PLLA), aliphatic polyester, and poly(LLA-co-DLLA) copolymers consisting of 2.5, 7.5, 50% of DLLA content were also synthesized. PLLA was successfully electrospun by using 15wt% solution in (1DMF:3CHCl<sub>3</sub>) mixed solvent. 2.5, 7.5, 50% P(LLA-co-DLLA) copolymers were then spun at 8, 10, and 15wt% concentration in a single chloroform solvent, respective. The lactide-based polymeric nanofibers were characterized by Scanning Electron Microscope (SEM). Smooth surface morphology was observed in nanofibers produced from PLLA and 50% P(LLA-co-DLLA) copolymer. However, surface porosity was observed in the corresponding fibers from 2.5 and 7.5% P(LLA-co-DLLA) copolymers. These nanofibers have high potential for wide range of applications such as filter media, nano-sensor, drug delivery and tissue scaffold, especially, those derived from 2.5 and 7.5% P(LLA-co-DLLA) copolymers which contain high degree of porosity.

## Introduction

Electrospun nanofibers have recently attracted vast attention in research community, especially in biomedical applications. Diameters of polymer nanofibers are smaller than micron (e.g.  $10\times10^{-3}$  -  $100\times10^{-3}$  µm). The materials show many interesting characteristics, i.e., very large surface area to volume ratio, flexibility, and superior mechanical performance (e.g. stiffness and tensile strength), compared to traditional materials. Polymeric nanofibers are commonly produced by an electrospinning technique from polymer solutions. There are three basic components for electrospinning process. First, a high voltage power supply is used to produce high voltage electric field to induce the charged solution jet out of the capillary tip to the metal collector. Second, a capillary is connected with a syringe. Finally, a metal collecting screen is used to collect the solution jet which has travelled along an ambient air [1]. For the experimental setup, a positive charge is placed to the capillary tube and another connected to the collector. In most case, the collector is simply grounded.

Many parameters have influences on the transformation of polymer solution into nanofibers through electrospinning [2], including (i) system parameters such as molecular weight, molecular weight distribution and architecture (branched, linear and etc.) of the polymer, and polymer solution properties (viscosity, conductivity, dielectric constant, surface tension, and charge carried by the spinning jet) and (ii) process parameters such as electric potential, flow rate and concentration, distance between capillary and collection screen, ambient parameters (temperature, humidity and air



velocity in the chamber) and finally motion of the target screen.

Polylactide (PLA) is aliphatic polyester, which has been widely used in medical, industrial, and agricultural applications. The advantages of this polymer are its degradability and renewable monomer resources. As PLA's repeat unit consists of chiral center, the polymer presents in two enantiomeric form, i.e. poly(L-lactide), PLLA, and poly(D-lactide), PDLA. A mixture of PLLA and PDLA results in a formation of stronger crystalline structure, a stereocomplex, compared to the homopolymer counter parts. This also leads to differences in mechanical properties of the materials. In addition, optimization of the polymer system can be achieve by copolymerization of DLA and LLA to yield poly(DL-lactide) by varying the copolymer composition with 0, 2.5, 7.5 and 50% DLLA content were synthesized. In this study, poly(LLA-co-DLLA) copolymers has a good mechanical properties as tensile strength, modulus, and elongation at break, i.e., 2.5, 7.5, and 50% [3]. The (co)polymers are then fabricated into nanofibers by an electrospinning technique. Properties and morphology of fibers are then characterized.

## **Experimental**

## Materials

All copolymers samples were synthesized by ring-opening polymerization of lactide using stannous(II) octoate as catalyst [3].

## **Equipments**

High voltage supplier (GAMMA, High voltage research) and a syringe pump (kd Scientific, Model 781100) were employed in the electrospinning process.

## Characterizations

The morphology of the electrospun nanofibers was examined by an SEM (HITASHI S3400N) after platinum coating. The average diameter and diameter distribution were examined by using image analyzer (PC SEM).

#### **Results and Discussion**

Lactide-based (co)polymers were successfully electrospun by using difference conditions, i.e., solvent system, spinning distance, applied voltage, and solution flow rate. The electrospinning conditions and properties of the resulting nanofibers are summerized in Table 1.

**Table 1.** Electrospinning conditions and properties of the resulting nanofibers.

		Concentration	Conditions			Fiber	Surface	Average
Polymers	Solvents	(wt%)	V (kV)	Q (ml/hr)	D (cm)	appearance	morphology	diameter (µm)
PLLA	DMF:Chloroform (1:3)	15	5	1	10	Some beads	Smooth	0.5
2.5%P(DLLA- co-LLA)	Chloroform	8	6	1	15	Perfect fiber	Porous	7.5
7.5% P(DLLA- co-LLA)	Chloroform	10	7	1	15	Perfect fiber	Porous	7.0
50% P(DLLA- co-LLA)	Chloroform	15	5	1	12	Perfect fiber	Smooth	6.3

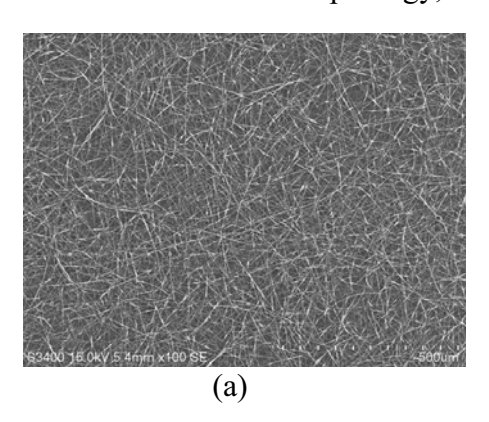
V = Applied voltage (kV)

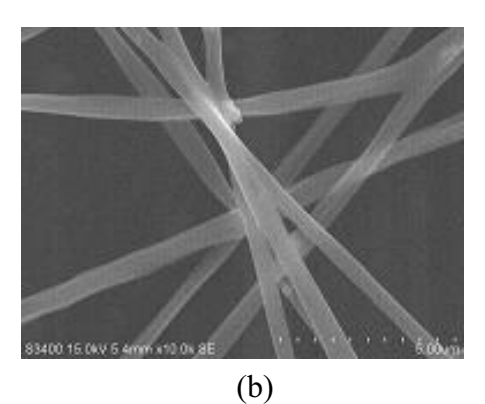
Q = Flow rate (ml/hr)

D = Spinning distance (cm)



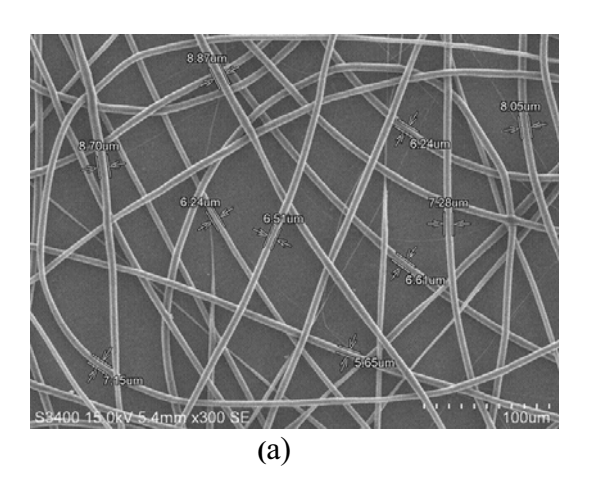
PLLA (Mn 40,000) was electrospun by using a 1DMF:3CHCl<sub>3</sub> mixed solvent at 15wt% concentration. The resulting fibers contain some beads in the fiber filaments, as can be seen in Figure 1(a). Fibers with average diameter of 0.5μm were obtained, which is the smallest compared to other samples in this lactide-based system. High magnification SEM image of the nanofibers show smooth surface morphology, as can be seen in Figure 1(b).





**Fig 1.** SEM images of PLLA (Mn 40,000) at; (a) 100x, (b) 10,000x

Three samples of P(LLA-co-PDLLA) copolymers were successfully electrospun by dissolving in a chloroform single solvent. Initially, 2.5% P(LLA-co-DLLA) copolymer was dissolved in a chloroform solvent at concentration of 6 wt%. Results on fibers showed some defects from beads and the fiber filaments were not uniform. Consequently, the concentration was increased to 8wt% in order to improve the chain entanglement. The resulting fibers showed no beads, as shown in SEM images in Figure 2. Average fiber diameter of 7.5  $\mu$ m was obtained from this copolymer.



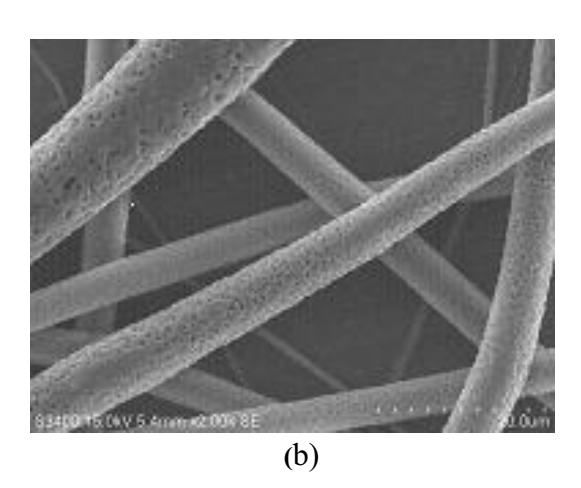
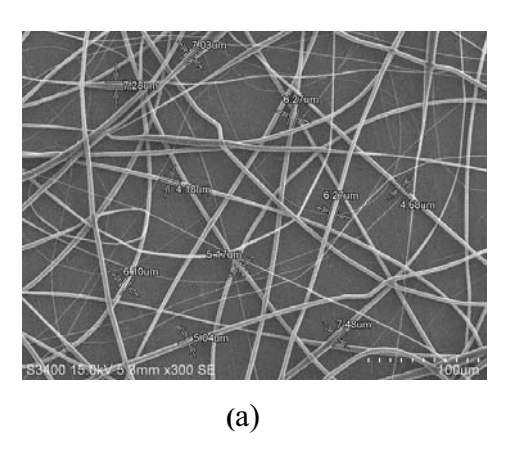


Fig 2. SEM images of 2.5% P(DLLA-co-LLA) at; (a) 300x, (b) 2000x

The corresponding fibers of a 7.5% P(LLA-co-DLLA) copolymer was spun using a chloroform solvent at concentration of 10 wt%. Perfect fibers were also produced, as shown in Figure 3.





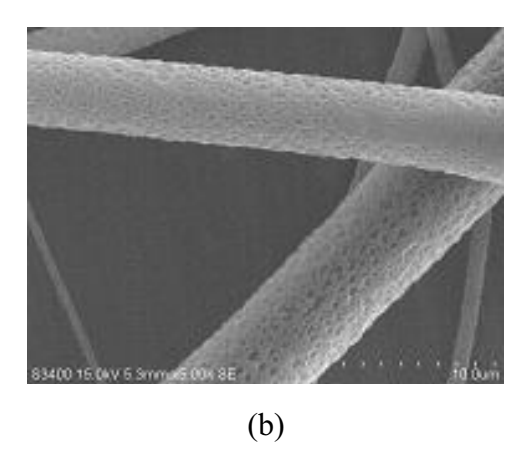
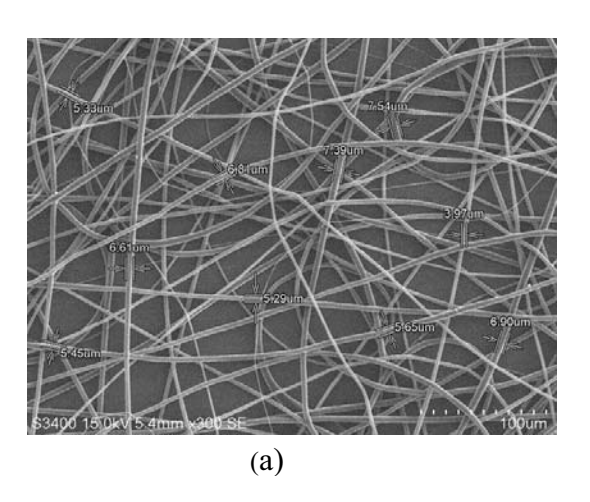


Fig 3. SEM images of 7.5% P(DLLA-co-LLA) at; (a) 300x, (b) 5000x

Interrestingly, nanofibers produced from copolymers containing 2.5 and 7.5% DLLA content showed high degree of porosity on the surface, as shown in Figure 2(b) and Figure 3(b).

The corresponding nanofibers obtained from 50% P(LLA-co-DLLA) copolymer at a concentration of 15 wt% in chloroform contains no beads beads, as shown in Figure 4(a). However, surface porosity was not observed in this sample.



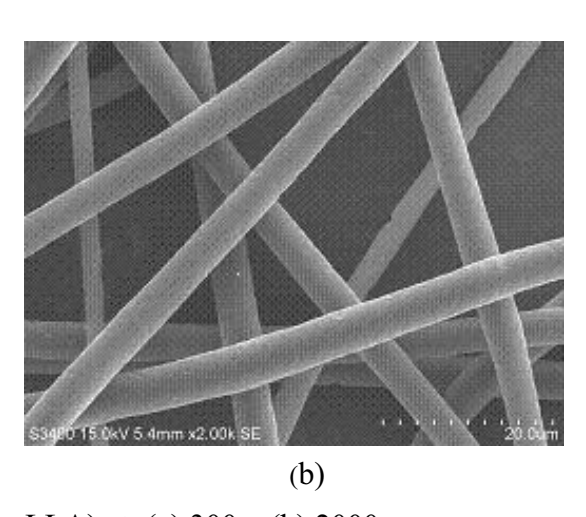


Fig 4. SEM images of 50%P(DLLA-co-LLA) at; (a) 300x, (b) 2000x

## **Summary**

Nanofibers of biodegradable/biocopatible lactide-based (co)polymers fabricated by an electrospinning technique were prepare for use in applications. PLLA and P(LLA-co-DLLA) copolymers containing 2.5, 7.5, and 50 % DLLA content were successfully spun by using 15 wt% in 1DMF:3CHCl<sub>3</sub>, and 8, 10, and 15 wt% concentration in CHCl<sub>3</sub>, respectively. Nanofibers with different surface morphology and fiber diameter were obtained. This is due to the differences in chemical structures of (co)polymers and interactions of the (co)polymers and solvents, resulting in formation of fibers with different properties.

## Acknowledgements

Financial support of this work is provided by Thailand Research Fund (TRF), The commission of Higher Education (CHE), RTA5180003, and Thailand Toray Science Foundation. Chakrit Thammawong is supported by a scholarship program from SIIT, Thammasat University.

#### References

- [1] A. Frenot, I.S. Chronakis, Polymer nanofibers assembled by electrospinning, Curr. Opin. Colloid Interf. Sci. 8 (2003) 64–75.
- [2] Ioannis S. Chronakis: Journal of Materials Processing Technology 167 (2005) 283–293
- [3] S. Buchatip, A Petchsuk, and K Kongsuwan: Journal of Metals, Materials and Minerals. Vol.18 No.175-180, 2008.



# **Functionalized and Sensing Materials**

doi:10.4028/www.scientific.net/AMR.93-94

# **Preparation and Characterizations of Electrospun Lactide-Based Polymeric Nanofibers**

doi:10.4028/www.scientific.net/AMR.93-94.377

## References

[1] A. Frenot, I.S. Chronakis, Polymer nanofibers assembled by electrospinning, Curr. Opin. Colloid Interf. Sci. 8 (2003) 64–75. doi:10.1016/S1359-0294(03)00004-9

[2] Ioannis S. Chronakis: Journal of Materials Processing Technology 167 (2005) 283–293 doi:10.1016/j.jmatprotec.2005.06.053

[3] S. Buchatip, A Petchsuk, and K Kongsuwan: Journal of Metals, Materials and Minerals. Vol.18 No.175-180, 2008.



# Improving Malaria Diagnosis via Latex Immunoagglutination Assay in Microfluidic Device

Raweewan Thiramanas<sup>1,a</sup>, Rujira Wanotayan<sup>2,b</sup>, Sakon Rahong<sup>1,c</sup>, Kulachart Jangpatarapongsa<sup>3,d</sup>, Pramuan Tangboriboonrat<sup>4,e</sup> and Duangporn Polpanich<sup>1,f</sup>

<sup>1</sup>National Nanotechnology Center, Thailand Science Park, Pathumthani, 12120 Thailand <sup>2</sup>Department of Nanoengineering, Faculty of Engineering, Chulalongkorn University, Bangkok, 10330 Thailand

<sup>3</sup>Department of Clinical Microbiology, Faculty of Medical Technology, Mahidol University, Bangkok, 10700 Thailand

> <sup>4</sup>Department of Chemistry, Faculty of Science, Mahidol University, Bangkok, 10400 Thailand

<sup>a</sup>raweewan@nanotec.or.th, <sup>b</sup>smiley\_rujira@hotmail.com, <sup>c</sup>sakon@nanotec.or.th, <sup>d</sup>mtkip@mahidol.ac.th, <sup>e</sup>scptb@mahidol.ac.th, <sup>f</sup>duangporn@nanotec.or.th

**Keywords:** latex immunoagglutination assay, microfluidic device, malaria diagnosis.

Abstract. Attempt to improve latex immunoagglutination assay, a rapid method in medical diagnostics, reporting as quantitative results was interested in this study by using microfluidic device. Sensitized latex was produced by physical adsorption of human polyclonal IgG antibody to *Plasmodium falciparum* malaria parasite onto carboxylated polystyrene particle. Conventional latex agglutination assay was firstly performed to verify specific interaction of antibody on the bead surface versus antigen in malaria plasma. The agglutinate size around 30 µm was observed under optical microscope. The proportion of the plasma and the particle was optimized, and an appropriate ratio was applied in microfluidic device. Three patterns of the device were used with the agglutinate size comparison after 10 min as followed: rapid mixing > U-shaped loop > straight capillary Y-junction patterns. However, compared with patient plasma, small agglutinates were also observed when using normal serum.

## Introduction

Malaria is a life-threatening disease caused by parasite of the genus *Plasmodium* which causes nearly one million deaths yearly [1]. If this disease is not treated promptly with effective medicines, especially *P. falciparum* malaria can cause severe illness to death. Polpanich D and co-workers reported the success in rapid detection of malaria disease using latex agglutination assay with 90% sensitivity and 80% specificity [2]. The interaction occurred between the antibody and the antigen forming network structure resulted in the particle clumping which can be seen *via* naked eyes [2,3]. However, the assay has limitation which based the result on qualitative analysis. The combination of the assay and other devices which provide the quantitative data is the great challenge. Recently, a few researches have attempted to establish procedure using the latex agglutination assay in a Y-junction microfluidic device [4-6]. It was expected that the agglutination in the microfluidic device would be even easier than its large-sized, commercialized counter part [5]. Moreover, using the particle as mobile solid support dramatically increased surface area and allowed the device to be reused many times [4]. However, a limited success due to the difficulty in mixing in the microchannel was reported. The ideal mixing has not properly been demonstrated so far. In this preliminary study, latex agglutination assay was applied in the microfluidic device having different channel patterns to



find the suitable mixing system for further develop a quantitative assay for malaria detection. The highly carboxylated polystyrene (PS) particle conjugated with human polyclonal IgG antibody to *P. falciparum* malaria was prepared. The agglutination reaction on the glass slide and microfluidic device was investigated under optical microscope (OM).

# **Experimental**

**Preparation of antibody:** Blood samples were collected from acutely *P. falciparum* infected patients examined by Giemsa stained thick blood film at Malaria Clinic, Mae-Sod, Tak province, Thailand. Malaria naive volunteers from non-malaria endemic area were recruited as negative control. This study was approved by the Committee on Human Rights Related to Human Experimentation, Mahidol University. Informed consent was obtained from each individual.

Ammonium sulfate precipitation (33% saturation) of the malaria infected plasma was performed in an ice bath with gently stir for 2 h. The precipitate was dissolved and then dialyzed with 1x PBS (pH 7.4) at 4°C overnight by using dialysis membrane (SpectraPor<sup>®</sup>, MWCO 100kDa). After that, the human polyclonal IgG antibody was purified using Protein G column (Nunc, USA) according to manufacture's instruction. The purified antibody was checked in sodium dodecyl sulfate-polyacrylamide gel electrophoresis for purity and kept at 4°C until use.

*Preparation of antibody-latex conjugate*: The sensitized latex was produced by physical adsorption of the purified human polyclonal IgG antibody to *P. falciparum* onto the highly carboxylated PS particle (hydrodynamic diameter of 422 nm). Adsorption was prepared by mixing the purified antibody (30 μg/ml) and the latex (2% (w/v), 5 μl) in adsorption buffer (0.01 M) with different pHs (6.4 to 8.0) in total volume of 500 μl. The mixture was incubated at 25°C for 2 h with shaking (Thermomixer Comfort, Eppendorf, Germany). After that, the reaction was centrifuged (17,800g, 20°C for 20 min), supernatant was then collected to measure the amount of unbound BSA by Bradford assay. The adsorbed amount ( $\Gamma_{ads}$ ) was calculated according to the previous study [7].

Latex agglutination assay: The antibody-latex conjugate (1% (w/v), 5 μl) was dropped onto a glass slide and the various amount of malaria plasma was subsequently added. The slide was swirled and the mixture was mixed thoroughly for 2 min, and then the agglutinates were investigated under an inverted OM (Body: IX71, CCD: DP71, Olympus, Japan). The PBS was used as negative control. The appropriate ratio of the particle and the malaria plasma was then applied in microfluidic device.

Microfluidic-latex agglutination assay: Microfluidic channels (200 μm (width) x 100 μm (depth)) were fabricated using standard soft lithography with the polydimethylsiloxane (PDMS) molding technique [8]. Three patterns were used namely: straight capillary Y-junction (Fig. 1(a)), rapid mixing (Fig. 1(b)) and U-shaped loop (Fig. 1(c)) patterns. The channel's inlet and outlet were attached with silicone tube (diameter 0.5 mm, Cole-Parmer, USA). Syringe pump (PHD 2000, Harvard apparatus, USA) was used to control the flow rate of the system. After the antibody-latex conjugate and the malaria plasma were injected into the microchannel and met at the Y-junction, the flow rate was reduced to 5 nl/min. The specific interaction of antigen and antibody was observed and was photographed by the OM (Body: BX51, CCD: DP71, Olympus, Japan). The experiment was repeated twice.



Figure 1. Schematic drawings of three microfluidic patterns namely: straight capillary Y-junction (a), rapid mixing (b) and U-shaped loop (c).



#### **Results and Discussion**

**Preparation of antibody-latex conjugate:** The pH of medium was optimized to find the appropriate condition for preparing the *P. falciparum* antibody-carboxylated latex conjugate. From our results, the high  $\Gamma_{ads}$  value of  $8.96\pm0.08$  mg/m² was obtained at pH 6.4, whereas the value was decreased to  $6.54\pm0.09$  and  $6.63\pm0.08$  mg/m² at pH 7.0 and 8.0, respectively. Although, at pH 6.4, the highest  $\Gamma_{ads}$  value can be obtained, the prepared sensitized particle seemed to lose the stability during adsorption so called "spontaneous agglutination" which can be inhibited by increasing pH [9]. The conjugated particle adsorbed at pH 8.0 was more stable and was chosen for preparing antibodylatex conjugate.

Agglutination assay on glass slide: Several cases of the malaria infected plasma and PBS were tested with the sensitized particle. Results showed that the 50% of the total infected cases can produce the large size of the immune complexes, whereas the rest exhibited too small size of the agglutinates. It can be pointed out that the amount of antigen and antibody play an important role in the agglutinate size [2]. The proportion of the malaria infected plasma and the prepared antibodylatex conjugate were optimized. As shown in Fig. 2(a)-(e), the size of agglutinate grew up with increasing the amount of the infected plasma, i.e., increasing the amount of antigen. The optimum ratio of the sensitized particle to the undiluted infected plasma equal to 5:1 with average agglutination size of 30 µm was chosen for further experiment.

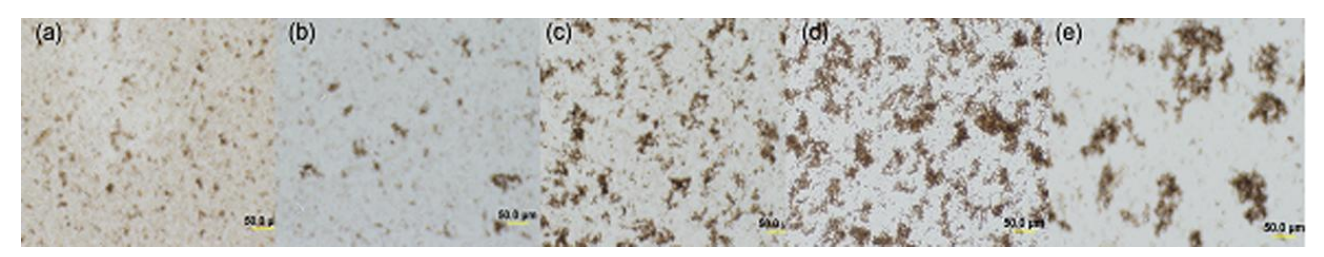


Figure 2. Immunoagglutination of the prepared antibody-latex conjugate (5  $\mu$ l) in the presence of PBS (a) and the malaria infected plasma: diluted 10 times (5  $\mu$ l) (b), diluted 5 times (5  $\mu$ l) (c) undiluted (0.5 $\mu$ l) (d), undiluted (1 $\mu$ l) (e).

Microfluidic-latex immunoagglutination assay: It was reported that the highly carboxylated particle enhanced particle mobility in the microfluidic channel and simultaneously reduce the nonspecific reaction leading to the low false-positive result [5]. In our work, the agglutination of the sensitized highly carboxylated PS latex in the presence of the infected plasma in various patterns of the microchannel was investigated under OM. The boundary between the two streams of the P. falciparum antibody conjugated particle and the plasma was clearly observed at the beginning. After decreasing the flow rate to 5 nl/min, the agglutination reaction was then significantly occurred. Most distinguishable interaction time was about 10 min after both solutions first met. The pictures of the immune complexes with using the malaria plasma compared with the normal control were captured for each pattern and shown in Fig. 3(a)-(f). It can be seen that the small agglutinates was observed in the case of normal plasma, however, larger agglutinate size was detected in the case of the patient plasma. The comparison between three microchannel patterns were ranked from biggest agglutinate size as followed: rapid mixing, U-shaped loop and straight capillary Y-junction. Due to the low flow rate and the small dimension of the microchannel, the flow in microfluidic devices is normally laminar with slow diffusive mixing which takes place at low Reynolds number (Re), i.e., 0.01-100. Re is defined as  $lU\rho/\mu$ , where l is the capillary diameter (m), U is the flow velocity (m/s),  $\rho$  is the fluid density (kg/m·s) and  $\mu$  is the fluid velocity (kg/m·s) [10]. To improve the diffusive mixing between two fluids, the rapid mixing (Fig. 1(b)) and U-shaped loop microchannel patterns (Fig. 1(c)) were employed. As expected the agglutinates occurred when using these patterns were larger than the straight capillary Y-junction pattern (Fig. 1(a)). However, the high curvature channel in the rapid mixing pattern might be rendered the larger size of the occurred immune complexes.



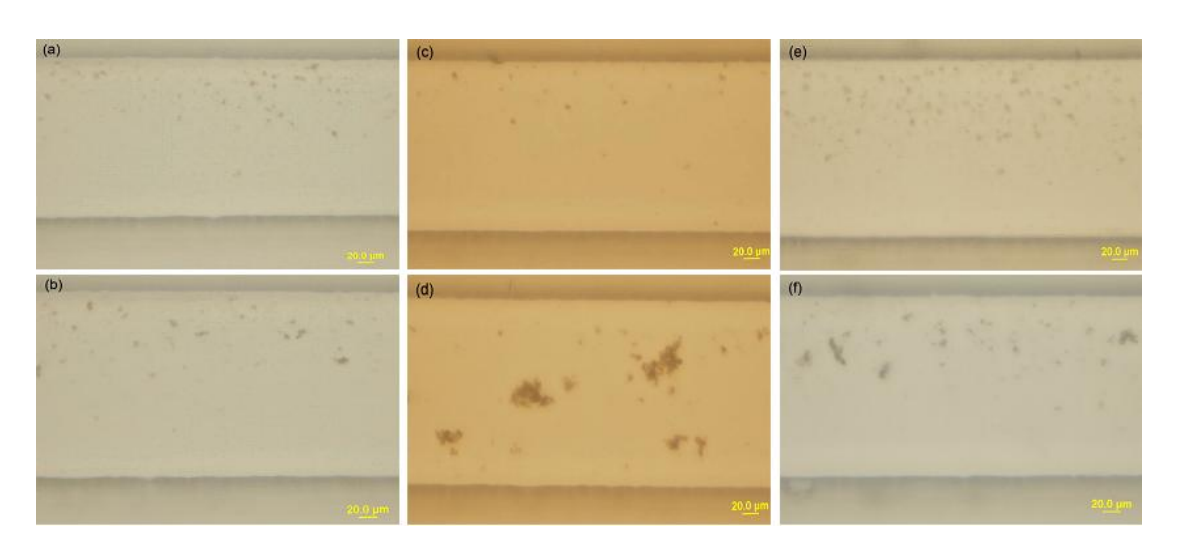


Figure 3. Microfluidic-latex immunoagglutination results for various patterns of the microchannel: straight capillary Y-junction (a,b), rapid mixing (c,d) and U-shaped loop (e,f) by using the normal plasma (a,c,e) and the malaria infected plasma (b,d,f).

## **Summary**

The human polyclonal IgG antibody adsorbed onto the highly carboxylated PS particle was achieved by using Tris-HCl pH 8.0 (0.01M),  $25^{\circ}$ C for 2 h. The agglutination between the sensitized latex and the malaria infected plasma was clearly observed under OM with average size of 30  $\mu$ m. After applying in three patterns of microfluidic device, agglutination results were compared ranking from biggest agglutinate size: rapid mixing, U-shaped loop and straight capillary Y-junction. In malaria plasma, the agglutinate size was bigger than that observed in normal plasma for all patterns. Quantitative results would be further obtained by interfacing spectrophotometer to the microfluidic device with the rapid mixing pattern to measure the optical density of agglutinate.

## Acknowledgement

Research grant given by The Thailand Research Fund and Commission on Higher Education is gratefully acknowledged.

## References

- [1] on http://www.who.int/topics/malaria/en/ (August, 2009)
- [2] D. Polpanich, P. Tangboriboonrat, A. Elaissari and R. Udomsangpetch: Anal. Chem. Vol. 79 (2007), p. 4690.
- [3] L.B. Bangs: Pure Appl. Chem. Vol. 68 (1996), p. 1873.
- [4] L.J. Lucas, J.-H. Han, J. Chesler and J.-Y. Yoon: Biosens. Bioelectron. Vol. 22 (2007), p. 2216.
- [5] J.-H. Han, K.-S. Kim and J.-Y. Yoon: Anal. Chim. Acta Vol. 584 (2007), p. 252.
- [6] J.-H. Han, B.C. Heinze and J.-Y. Yoon: Biosens. Bioelectron. Vol. 23 (2008), p. 1303.
- [7] J. Revilla, A. Elaissari, P. Carriere and C. Pichot: J. Colloid Interf. Sci. Vol. 180 (1996), p. 405.
- [8] Y. Xia, G.M. Whitesides: Annu. Rev. Mater. Sci. Vol. 28 (1998), p. 153.
- [9] I.A. Gritskova, P.V. Nuss, I.G. Krasheninnikova, I. Grzywa-Niksińska, Ye.A. Dorokhova, S.A. Gusev and E. Grzywa: Polimery Vol. 40 (1995), p. 229.
- [10] H. Song, J.D. Tice and R.F. Ismagilov: Angew. Chem. Int. Ed. Vol. 42 (2003), p.768.





# Preparation of Novel Composite from Natural Rubber, Bagasse and Plaster

Sa-Ad Riyajan<sup>1</sup>, Isara Intharit<sup>1</sup>, Suthikiat Thaiprasansup<sup>1</sup> and Pramuan Tangboriboonrat<sup>2</sup>

- 1. Department of Materials Science and Technology, Bioplastics Research Unit, Faculty of Science, Prince of Songkla University, Hat Yai, Songkhla 90112, Thailand
- 2. Department of Faculty of Science, Mahidol University, Bangkok 10400, Thailand

Received: February 23, 2010 / Accepted: March 8, 2010 / Published: August 30, 2010.

**Abstract:** The sugar cane bagasse was treated with chemical treatment including sodium hydroxide and silane. The characterization of the modified bagasse was achieved with Fourier transform infrared spectroscopy (FTIR), and scaning electron microscopy (SEM). Results showed that the presence Si-CH<sub>3</sub> group occurred on bagasse surface after chemical modification. In addition, the roughness of the modified bagasse was higher than that of unmodified bagasse due to chemical modification from sodium hydroxide. Two polymer composite types, namely (1) natural rubber NR/sugar cane bagasse and (2) NR/plaster via two-roll mill method, were prepared. The optimum cure (t<sub>90</sub>) and torque of the NR/plaster increased with increasing plaster loading in composite. In case of NR/bagasse, the t<sub>90</sub> of this sample decreased as a function of sugar cane bagasse while torque of this sample increased with increasing sugar cane bagasse. The modulus of the resulting composite increased with increasing both plaster and sugar cane bagasse, but the tensile strength and elongation at break of the composite decreased as a function of both plaster and sugar cane bagasse in composite.

Key words: Natural rubber, composite, bagasse, plaster, chemical modification.

## 1. Introduction

Nowadays, many works have reported the natural fibre as reinforcement of polymer matrix including both natural polymer and synthetic polymer due to environment problem [1]. The advantages of natural fiber are available in Asian country, cheap, biodegradable polymer and easily degradation in soils with many microorganisms leading to a good environment in the further. Bagasse is a solid lignocellulosic residue left after extraction of juice from the sugar cane stalk [2]. In addition, the applications of bagasse are used in burnt for energy supply in sugar cane factory, pulps, board materials and composites [3-6]. In the previous work, it was found that bagasse is a raw material blended with other polymer including poly (vinyl alcohol), PVA [2],

**Corresponding author:** Sa-Ad Riyajan, asst. Prof., research field: polymer science and technology. E-mail sa-ad.r@psu.ac.th, saadriyajan@hotmail.com.

polypropylene [4], phenol formaldehyde (PF) resin [3] waste gelatin [7] and polystyrene [8]. PVA composites sheet [2] was prepared from PVA, and lignocellulosic fillers, corn starch, presence of water and glycerol by compression molding. Results showed that the resulting polymer composite based on PVA and starch with apple wastes and sugarcane bagasse fillers were much harder than samples prepared with orange wastes. E. Chiellini, and co-worke [9, 10] reported the preparation and mechanical properties of composite films from biorelated agro-industrial waste including sugar cane and apple and orange fruit juice extraction and PVA cast from PVA aqueous solutions. They found that composite obtained from orange fruit gave to be suitable for blending in higher amounts by weight than other samples. This is the first study of its kind wherein the preparation and physical testing of polymer composite obtained from natural rubber, sugar cane bagasse and plaster. The obtained polymer

composite from NR, sugar cane bagasse and plaster was prepared by two-roll mill method. In addition, the modified sugar cane bagasse with sodium hydroxide and silane treatment was analyzed by Attenuated Total Reflection Fourier Transform Infrared (ATR-FTIR), scanning electron microscope (SEM) and atomic force microscopy (AFM). The characterization of novel polymer composite was studied through curing properties and tensile strength.

#### 2. Materials and Methods

#### 2.1 Materials

Natural rubber grade STR 5L was supplied by Chalong Latex Industry Co., Ltd. Sugar cane bagasse was obtained from local in Thailand. Then, sugar cane bagasse fibers were obtained by milling using a laboratory blender. Plaster was purchased from Siam Nakarin Co., Ltd.. All other ingredients used were a commercial grade. The commercial Bis-(3-triethoxy-silyl propyl)-tetrasulfide, which is a coupling reagent, was provided by Sigma-Aldrich Company. The vulcanizing agent including zine oxide, steric acid, sulfur and tetramethyl thiuram disulfide (TMTD) were reagent grade and were obtained commercially.

## 2.2 Modified Sugar Cane Bagasse

The resulting sugar cane bassage was immersed in 10% sodium hydroxide solution for 24 h. After sugar cane bagasse was treated with sodium hydroxide, it was washed with water for many times and reached to neutral pH. Thus, the resulting sugar cane bagasse was coated with silane by stiring an immersion of 10 g of sugar cane bagasse in silane for 5 h.

# 2.3 Preparation of Polymer Composite

Formulation of mixes used for polymer composite from NR/sugar cane bagasse and NR/plaster in this the present work is shown in Table 1 and Table 2, respectively. NR was masticated on the mill for 5 min followed by addition of tphe ingredients as shown in Table 1 and Table 2. The resulting polymer composite

materials were prepared in a two-roll mill. The condition of operation including the nip gap, speed ratio, mill roll and the number of passes for two-mill was controlled at the same in all the mixes at 50  $^{\circ}$ C. The resulting samples were milled for sufficient time to disperse the sugar cane bagasse or plaster with different loading in the NR matrix at a mill opening of 1.55 mm. The silane as a coupling agent was added in NR compound during mixing to improve the interaction between sugar cane bagasse/plaster and NR matrix. Then, the resulting NR composite was kept at  $28 \pm 2$  °C for overnight in a closed container before cure analysis using an Alpha Moving Die rheometer (MDR 2000). The t<sub>90</sub>, cure time and max torque were measured from the MDR 2000. Then, each specimen was placed in a mold (140  $\times$  140  $\times$  1.5 mm) and the NR compounds were vulcanized at 150 °C and the pressure of 6.89  $MN/m^2$  for 20-30 min for a optimum cure (t = 90) or

Table 1 Formulation of polymer composite obtained from NR and sugar cane bagasse.

Chemical		Formulation					
(phr)	1	2	3	4			
STR 5 CV60	100	100	100	100			
Wigstay L	2	2	2	2			
Sulfur	2	2	2	2			
Steraric acid	2	2	2	2			
ZnO	3	3	3	3			
TMTD	1.3	1.3	1.3	1.3			
DPG	0.7	0.7	0.7	0.7			
Sugar can Bagasse	e 2	5	10	20			
Silane	0.5	0.5	0.5	0.5			

Table 2 Formulation of polymer composite obtained from NR and plaster.

Chemical		Formulation					
(phr)	1	2	3	4	5		
STR 5 CV60	100	100	100	100	100		
Wigstay L	2	2	2	2	2		
Sulfur	2	2	2	2	2		
Steraric acid	2	2	2	2	2		
ZnO	3	3	3	3	3		
TMTD	1.3	1.3	1.3	1.3	1.3		
DPG	0.7	0.7	0.7	0.7	0.7		
Plaster	5	30	50	70	100		
Silane	0	0.18	0.3	0.42	0.60		

tc<sub>90</sub>). The polymer composite was compressed by compression molding machine to give the polymer composite sheet.

# 2.4 Characterization of Modified Sugar Cane Bagasse and Testing of Polymer Composite

The chemical structure of the modified sugar cane was observed by FTIR-ATR. ATR-FTIR spectra were studied with Fourier transformed infrared; FTIR (Bruker, EQUINOX 55) spectral data, taking 100 scans for each sample with resolution 3 cm<sup>-1</sup>, and raging from 400-4000 cm<sup>-1</sup> and the ATR-FTIR of samples were obtained to detect any chemical interactions between silane and sugar cane bagasse. The aim of the SEM study was to obtain a topographical characterization of the modified and unmodified sugar cane bagasse. In addition, the morphology of fractured polymer composite sheet was analyzed by SEM. The sample was deposited on a brass hold and sputtered with platinum. SEM photographs were taken with a JSM 6400 Scanning Microscope (Japan) at the required magnification at ambient temperature. SEM was performed at an accelerating voltage of 20 kV. The height and deflection images were recorded with the resolution of 512 lines. Then, the resulting polymer composite was kept at 28 ± 2 °C for overnight in a closed container before cure analysis using an Alpha Moving Die rheometer (MDR 2000). The t<sub>90</sub>, cure time and max torque were measured from the MDR 2000.

The testing crosshead speed of 500 mm/min was applied with load cell of 1 kg-N. The physical testing of dried latex film was analyzed by universal testing machine Gotech brand model TCS 2000 based on ASTM D 412. Five dumbbell test pieces were cut from each film and the average thickness was calculated and then attached between the grips of a tensile testing machine and pulled at a rate of 500 mm. The thermogravimetric (TG) analysis was performed on a TGA7, PERKIN ELMER: TGA. The mass of each sample was roughly 5.00-6.00 mg. The carrier gas was air with a flow rate of 50 mL/min. The temperature rose from 50 to 800 °C at heating rates of 10 °C/min.

#### 3. Results and Discussion

## 3.1 Characterization of Modified Sugar Baggage

The characterization of modified sugar cane bagasse was investigated by SEM and FTIR. The chemical structure of modified sugar cane bagasse was analyzed by FTIR as shown in Fig. 1. The ester-linkage or OC=O stretching of modified sugar cane was observed at 1085 and 1238 cm<sup>-1</sup>. In addition, the wavelength at 1321 cm<sup>-1</sup> of modified sugar cane bagasse indicated the stretching C-O. The new peak of modified sugar cane was observed at 1180 and 1225 cm<sup>-1</sup> referred to Si-O-Si and Si-O-cellulose, respectively. This result responds with this in Ref. [1]. These results revealed the successfully modified surface of sugar cane bagasse. The morphology of modified sugar cane and unmodified

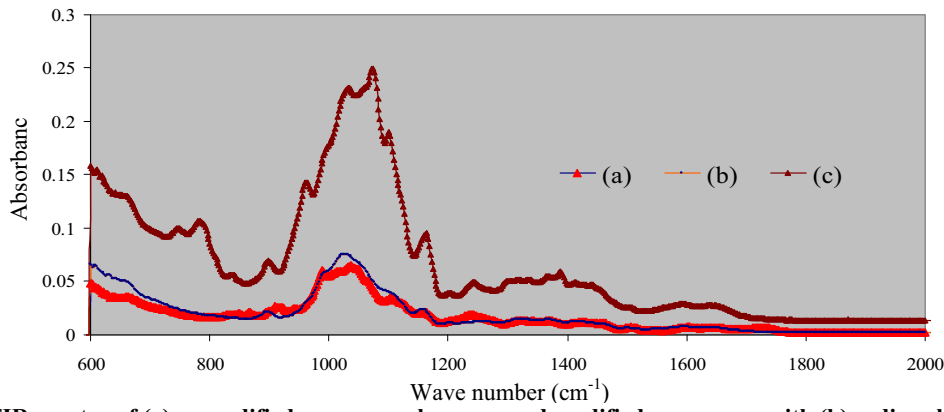


Fig. 1 ATR-FTIR spectra of (a) unmodified sugar cane bagasse, and modified sugar cane with (b) sodium hydroxide and (c) silane treatment.

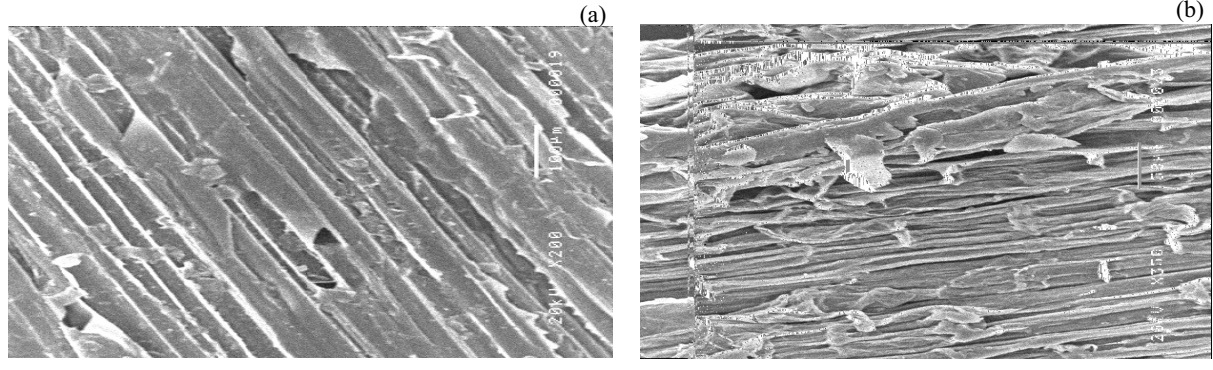


Fig. 2 SEM image of surface of (a) unmodified sugar cane and (b) modified sugar cane with sodium hydroxide.

sugar cane bagasse is shown in Fig. 2. It was found that the surface of unmofidified sugar cane bagasse showed lower roughness comparing to sample with modified with chemical treatment as shown in Fig. 2. This result indicated that the fat acid on surface of bagasse was removed by sodium hydroxide. The diameter of sugar cane was roughly 0.1 mm.

#### 3.2 Curing Properties of Polymer Composite

When the addition of plaster in NR matrix was subjected to tc<sub>90</sub> of polymer composite presence of 30, 50, 70 and 100 phr of plasters was 2.33, 2.51, 2.42 and 2.41 min, respectively as shown in Fig. 3 (a). Torque of polymer composite containing 0 phr of plaster was about 2 dNm while the torque of this polymer composite in the presence of 30, 50 and 70 phr plaster was 3, 6 and 11 dNm, respectively as shown in Fig. 3(b). Moreover, when plaster was added in polymer composite, the properties of the resulting polymer composite exhibited a hardness behavior due to elastic modulus of plaster observing from torque. In the case of bagasse, it was found that the curing time of polymer composite decreases as a function of bagasse content as shown in Fig. 4 (a). The curing time of polymer composite containing 2, 5 and 10 phr of bagasse was 1.75, 1.6 and 1.4 min, respectively. The torque of polymer composite in the presence of 2, 5 and 10 phr of bagasse was 2.6, 3 and 4.4 dNm, respectively as shown in Fig. 4 (b).

## 3.3 SEM of Polymer Composite

The morphology of polymer composite is a relationship with the physical properties of polymer composite. The morphology of polymer composite was obtained from NR and sugar cane bagasse contents and plaster contents as shown in Fig. 5. It is clear that the plasters and sugar cane bagasse are hard to disperse in NR matrix due to difference in surface component between NR and plaster. The morphology of polymer composite showed the more roughness as a function of amount of plaster content in polymer composite. In the case of polymer composite containing 70 phr of plaster, a large number of voids were clearly visible on the fracture surface leading to poor adhesion between NR matrix and plaster. In addition, the sugar cane bagasse is difficult to disperse in NR matrix due to difference in polar groups between sugar cane bagasse and NR matrix.

## 3.4 Mechanical Properties

The modulus of NR filled with plaster and bagasse increased with increasing percentage of plaster and bagasse loading as shown in Fig. 6 (a). It is noted that the maximum of modulus was observed in sample in the presence of 20 phr of sugar cane bagasse and 70 phr of plaster. Fig. 6 (b) shows the influence of both sugar cane bagasse and plaster on the tensile strength of polymer composite. The tensile strength of the polymer composite containing 70 phr of plaster was about 2 MPa. The elongation at break of polymer composite dramatically decrease after addition of more amount of sugar cane bagasse and plaster as shown in Fig. 6 (c).

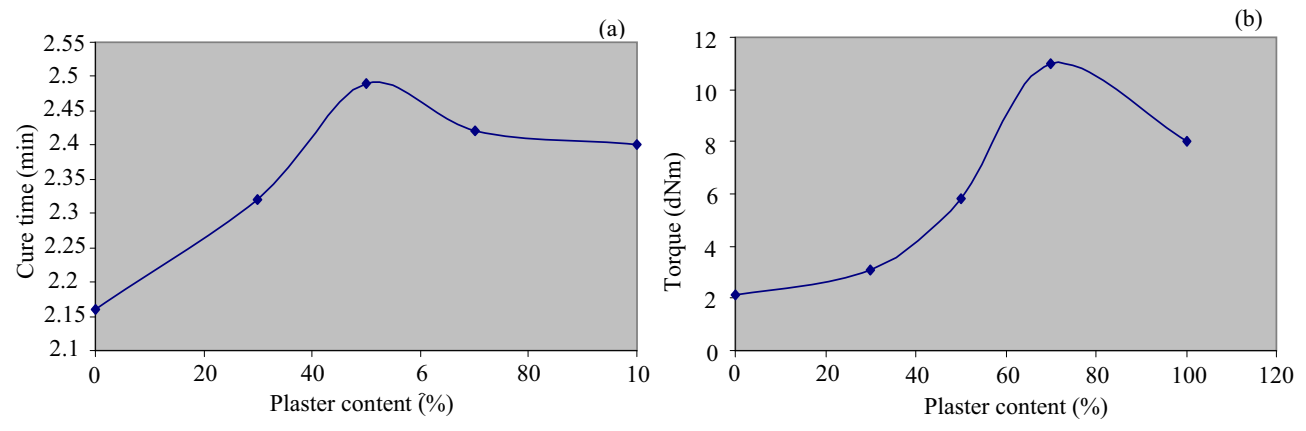


Fig. 3 Effect of plaster on (a) the cure property and (b) torque of polymer composite.

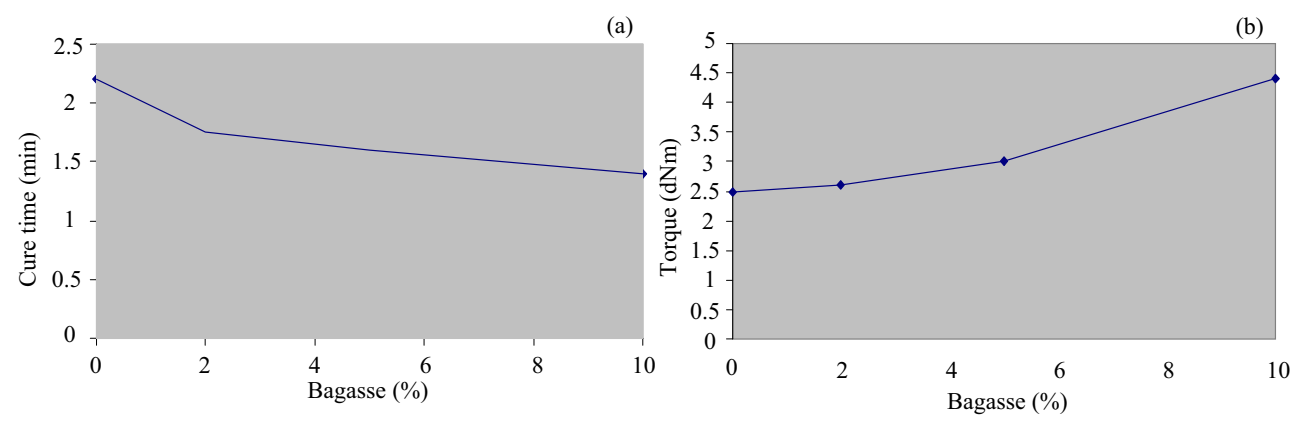


Fig. 4 Effect of bagasse on (a) the cure property and (b) torque of polymer composite.

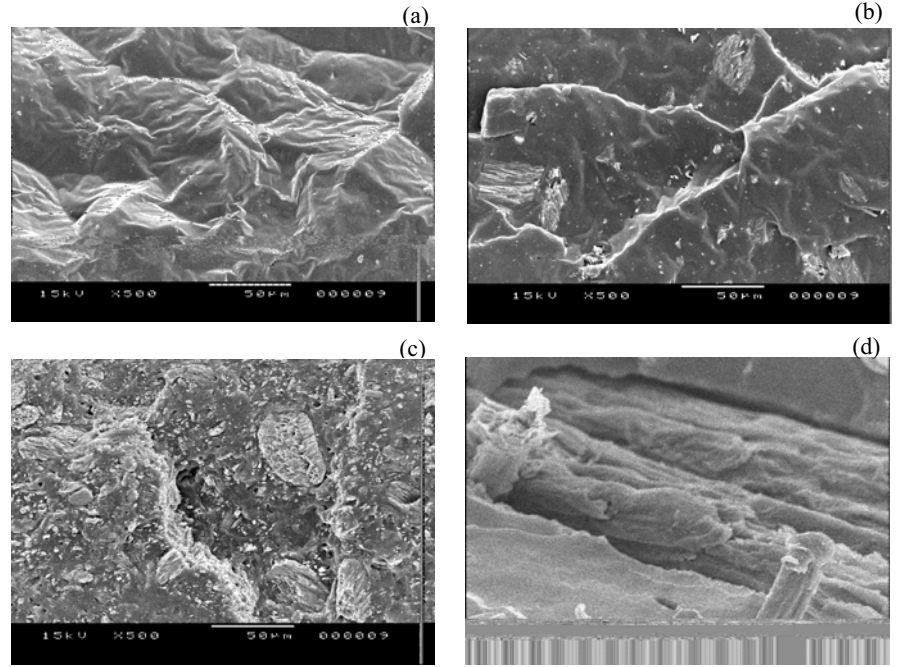


Fig. 5 Morphology of natural rubber alone (a), polymer composite in the presence of (b) 30, (c) 0 phr of plaster and (d) 20 phr of sugar cane bagasse observed from SEM.

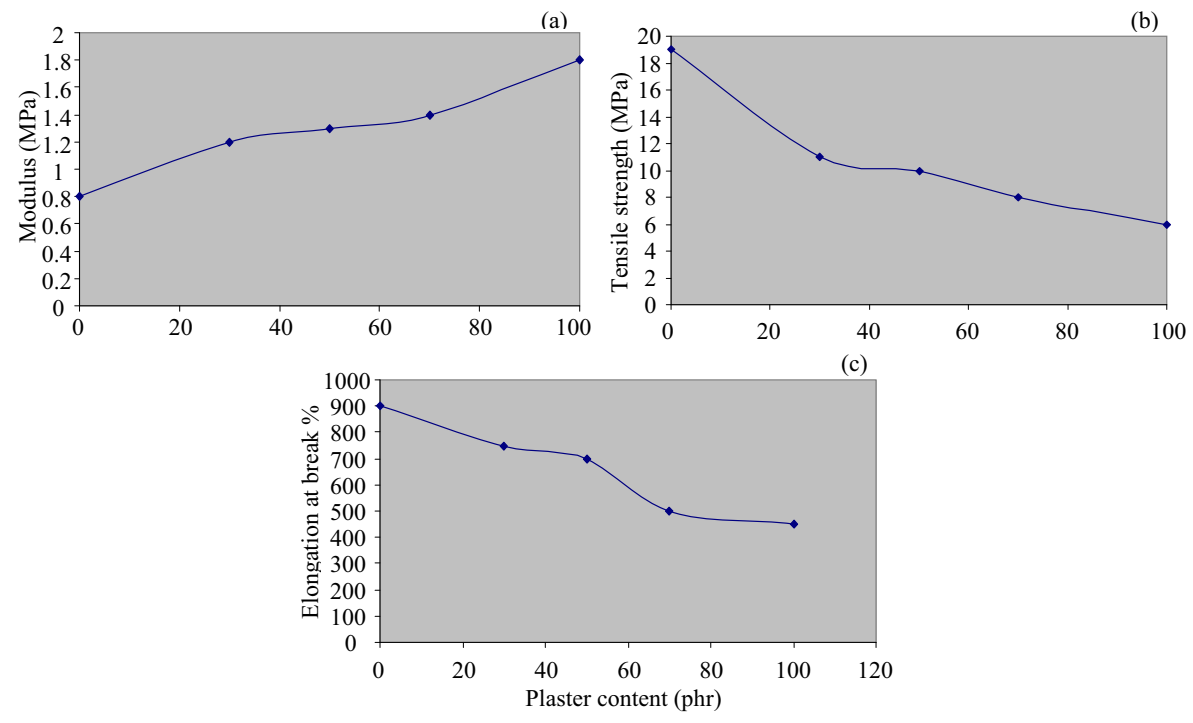


Fig. 6 Effect of plaster on (a) modulus, (b) tensile strength and (c) elongation of polymer composite.

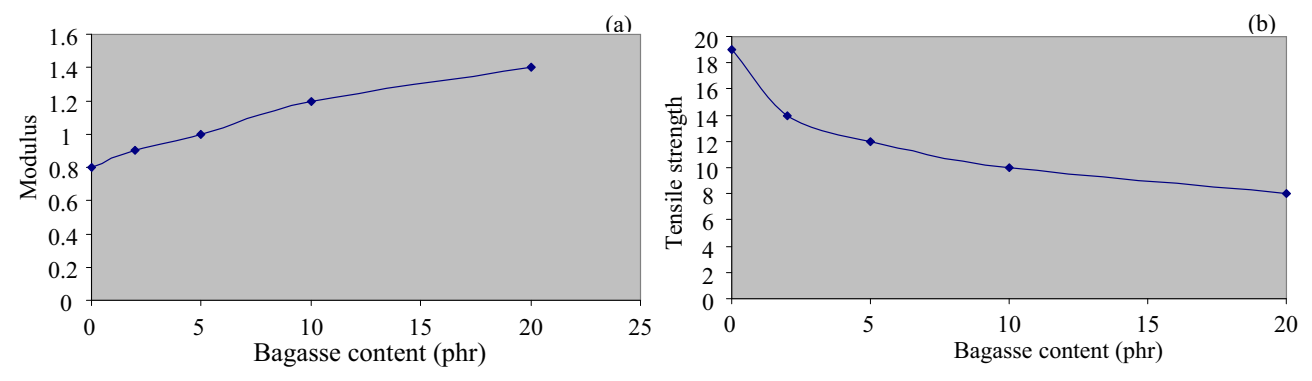


Fig. 7 Effect of sugar cane bagasse on (a) modulus, and (b) tensile strength of polymer composite.

This result is explained that the reduction of the tensile strength can be attribution to the more dewetting of NR matrix at the interface between NR and filler and more amount of agglomeration of plaster leading to generation of weak to structure due to creating stress concentration [8].

Fig. 7 (a) and Fig. 7 (b) exhibit the effect of bagasse on modulus and tensile strength of polymer composite. Results showed that the modulus of polymer composite increased as a function of bagasse. But the tensile strength of this sample decreased after addition of more amount bagasse.

## 4. Conclusions

The achievement in the preparation of polymer composite was obtained from natural rubber, bagasse and plaster. The chemical stretching of the modified bagasse showed the occurrence of Si-CH<sub>3</sub> group after chemical modification. The roughness of bagasse modified with sodium hydroxide was higher than that of unmodified bagasse, leading to removing fatty acid from sugar cane. The torque of the polymer composite increased with increasing both plaster content and bagasse content. The modulus of the polymer composite increased as a function of the both bagasse

and plaster contents in polymer composite. The possible applications of the resulting polymer composite are applied in board and container.

## Acknowledgements

The authors thank Department of Materials Science and Technology, Faculty of Science, Prince of Songkla University for using laboratory space. This study was supported by Faculty of Science Research Fund, Prince of Songkla University and Thailand Research Fund (RTA518003).

## References

- [1] S.M. Luz, J.D. Tio, G.J.M. Rocha, A.R. Gonçalves, J.A.P. Del'Arco, Cellulose and cellulignin from sugarcane bagasse reinforced polypropylene composites: effect of acetylation on mechanical and thermal properties, Comp. Part A: Appl. Sci. Manuf. 39 (2008) 1362-1369.
- [2] P. Cinelli, E. Chiellini, S.H. Imam, Hybrid composite based on poly(vinyl alcohol) and fillers from renewable resources, J. Appl. Polym. Sci. 109 (2008)1684-1691.
- [3] C.N. Zarate, M.I. Aranguren, M.M. Reboredo, Thermal degradation of a phenolic resin, vegetable fibers, and derived composites, J. Appl. Polym. Sci. 107 (2008) 2977-2985.

- [4] S.M. Luz, A.R. Gonçalves, J.A.P. Del'Arco, Mechanical behavior and microstructural analysis of sugarcane bagasse fibers reinforced polypropylene, Comp. Part A: Appl. Sci. Manuf. 38 (2007) 1455-1461.
- [5] N. Kiattipanich, N. Kreua-ongarjnukool, T. Pongpayoon, C. Phalakornkule, Properties of polypropylene composites reinforced with stearic acid treated sugarcane fiber, J. Polym. Eng. 27 (2007) 411-428.
- [6] F.J.F. Talavera, J.A.S. Guzmán, H.G. Richter, R.S. Dueñas, J.R. Quirarte, Effect of production variables on bending properties, water absorption and thickness swelling of bagasse/plastic composite boards, Indus. Crop. Prod. 26 (2007) 1-7.
- [7] E. Chiellini, P. Cinelli, E.G. Fernandes, E.R.S. Kenawy, A. Lazzeri, Gelatin-based blends and composites. Morphological and thermal mechanical characterization, Biomacromolecules 2 (2001) 806-811.
- [8] L.T. Furlan, M.A. Rodrigues, M.A. De Paoli, Sugar cane bagasse lignin as stabilizer for rubbers: Part III-Styrene/butadiene rubber and natural rubber, Polym. Degrad. Stab. 13 (1985) 337-350.
- [9] E. Chiellini, P. Cinelli, S.H. Imam, L. Mao, Composite films based on biorelated agro-industrial waste and poly(vinyl alcohol), preparation and mechanical properties characterization, Biomacromolecules 2 (2001) 1029-1037.
- [10] E. Chiellini, P. Cinelli, R. Solaro, M. Laus, Thermomechanical behavior of poly (vinyl alcohol) and sugar cane bagasse composites, J. Appl. Polym. Sci. 92 (2004) 426-432.

# Improvement of biocompatibility of natural rubber by PLA-PEG-PLA triblock copolymer

Rattaporn Thonggoom<sup>1,2,\*</sup>, Narudom Srisawang<sup>2,3</sup>, Supa Wirasate<sup>1,2</sup>, Atitsa Petchsuk<sup>4</sup>, Pramuan Tangboriboonrat<sup>1</sup>

<sup>1</sup>Department of Chemistry, Mahidol University, Rama 6 Rd., Phyathai, Bangkok 10400 Thailand <sup>2</sup>Center for Surface Science and Engineering, Faculty of Science, Mahidol University, <sup>3</sup>Salaya, Nakornpathom 73170 Thailand

<sup>3</sup>Materials Science and Engineering Graduate Programme, Faculty of Science, Mahidol University, Rama 6 Rd., Phyathai, Bangkok 10400 Thailand

<sup>4</sup>National Metal and Materials Technology Center, National Science and Technology Development Agency, Pathumthani 12120 Thailand

E-mail: scrtg@mahidol.ac.th

## Abstract

The PELA with various molecular weights having PEG:PLA molar ratio of 1:1 was synthesized by ring-opening polymerization, and then coated onto NR surface to enhance its biocompatibility. The chemical structure and composition were determined by Proton nuclear magnetic resonance. The presence of PELA on the NR surface was examined by Attenuated total reflection-Fourier transform infrared spectroscopy. The AFM morphologies supported ATR-FTIR result in that PELA was introduced onto NR surface and there is no phase separation between PLA and PEG segment. The results from water contact angle measurement indicated the improved hydrophilicity of NR/PELA film. The effect of various PELA molecular weights on the elastic modulus was investigated using Nanoindentation. The reduced modulus of NR/PELA films increases with increasing PELA molecular weights. The NR/PELA-20k exhibited a comparable reduced modulus to that of unmodified NR. Finally, the cytotoxicity results showed that the surface modification of NR film by PELA could effectively improve biocompatibility of NR.

**Keywords:** Copolymer, natural rubber, biocompatibility, hydrophilicity, nanoindentation

## Introduction

Natural rubber (NR) is a biomaterial that has received a great deal of attention in the field of medical applications due to its excellent elasticity, high strength and high stretching ability. It is recognized that NR latex has been used to produce medical related products, ranging from surgical gloves, contraceptive devices, tubings, catheters to balloons etc. However, a recent emergence of latex allergy has prevented any direct biomedical applications of this material in comparison to those of silicones and polyurethanes. Therefore, the surface treatment applied to improve biocompatibility, while still simultaneously maintain the characteristics of the bulk properties, are necessary. Very few efforts have been conducted to solve this problem. For instance, by using UV-induced graft copolymerization method, NR grafted poly(ethylene glycol) methacrylate (PEGMA) was found to reduce protein adsorption [1]. Hoven et al. [2] also reported that NR grafted PEGMA containing grafting yield more than 1% could improve blood compatibility without compromising the mechanical properties of NR film.

Biocompatible and biodegradable polymers based on copolymers of polylactic acid(PLA) and polyethylene glycol(PEG) have been of great experimental interest for drug delivery [3-6], gene therapy [7-9] and tissue engineering [10-12]. In this study, copolymer structures featuring PEG soft segment with PLA hard segment; namely, triblock copolymer of PLA-PEG-PLA (PELA) were chosen to modify NR surface to enhance its biocompatibility. For utility purpose, the evaluation of biocompatibility of biomaterials was required using a standard method of in vitro cytotoxicity. And, nanoindentation technique is used to determine the mechanical properties, in particular elastic modulus, of these PELA modified surfaces of NR. Nanoindentation technique is the most advanced method to study a small-scale mechanical behavior of "soft" matters such as polymer, biomaterial, and cell membrane [13-19].

In this present study, a series of triblock copolymers of PLA-PEG-PLA (PELA) having PEG:PLA molar ratio of 1:1 were synthesized by ring-opening polymerization in the presence of varying PEG molecular weight (MWs 2,000, 8,000, 14,000, 20,000), and then coated onto NR surface to study the effect of PELA molecular weight on hydrophilicity, morphology, nanomechanical behaviors, and in vitro cytotoxicity. If improvement in biocompatibility of NR could be achieved, the biomedical applications of NR could be greatly extended.

## **Experimental**

## Materials

All molecular weights (MWs 2,000, 8,000, 12,000 and 20,000) of Poly(ethylene glycol) hydroxyl terminated (PEG), lactide monomer and stannous 2-ethylhexanoate (Sn(Oct)<sub>2</sub>) were purchased from Aldrich. High ammonia NR latex was obtained from Rayong Bankok Rubber Co.,Ltd., Thailand. And all solvents such as dichloromethane and ethanol were used of AR grade and supplied by Lab Scan.

# **Synthesis of PELA**

The PLA-PEG-PLA triblock copolymer was synthesized by ring-opening polymerization of lactide in bulk process using stannous 2-ethylhexanoate (Sn(Oct)<sub>2</sub>) as a catalyst. The PEG and Sn(Oct)<sub>2</sub> were introduced into a three-necked round bottomed flask equipped with magnetic stirring. The flask was connected to a vacuum system and immersed in an oil bath. The flask was heated to 50 °C for 1 h. A predetermined content of lactide monomer (PEG:PLA molar ratio is fixed at 1:1) was added. The temperature of the reaction mixture was raised to 170 °C and maintained constant for 24 h. Then, the synthesized copolymer was dissolved in dichloromethane and precipitated in methanol and dried under vacuum. Proton nuclear magnetic resonance (<sup>1</sup>H-NMR) spectra, which were taken with a Bruker DPX-300 operating at 300 MHz using CDCl<sub>3</sub> as a solvent was used to determine chemical structure and composition. Chemical shift (δ) was measured in ppm using tetramethylsilane (TMS) as an internal reference. And, the molecular weight of PELA was calculated by the following equation:

$$M_{nPLA} = LA/EO \times 72/44 \times M_{nPEG}$$
  
 $M_{nPELA} = M_{nPLA} + M_{nPEG}$ 

where LA/EO is the molar ratio of the lactide to ethylene oxide in the copolymer determined by  ${}^{1}$ H-NMR and M<sub>n</sub> is the number-average molecular weight

## Preparation of PELA modified NR film

Natural rubber (NR) latex films with a thickness about 2.0 mm were prepared from commercial NR latex concentrate (Rayong Bangkok Rubber Co., Ltd., Thailand). A dried NR film was prepared from casting the NR latex on a glass plate at room temperature. The NR strip (2x5 cm<sup>2</sup>) was held onto a glass slide without any use of adhesive. The sample surface was cleaned by

sonicating sequentially with ethanol and water for 15 minutes in each step before drying under vacuum at room temperature. A solution of 5% w/v PELA in dichloromethane was prepared. The cleaned NR strip was then immersed into the PELA solution for 24 h at room temperature. Then, the modified surface was rinsed with dichloromethane before drying under vacuum at room temperature.

## Attenuated Total Reflectance Fourier Transform Infrared Spectroscopy (ATR-FTIR)

Attenuated total reflection (ATR) mode was characterized for all samples. The chemical characteristic of NR and modified NR surfaces were obtained. ATR-FTIR spectra were taken using diamond crystal for a single reflection mode and Nicolet 6700 FT-IR. The measurements were performed with sixty-four scans at resolution of 4 cm<sup>-1</sup> over the range of 4,000 to 600 cm<sup>-1</sup>

## **Atomic Force Microscopy (AFM)**

The morphology of the NR and PELA modified NR sheet was determined by using a Scanning Probe Microscope (SPM) with Nanoscope IV controller (Digital Instrument) in tapping mode with the scan size of  $10x10 \ \mu m^2$ . The surface root mean squared roughness ( $R_{rms}$ ) was directly calculated from Nanoscope software using the following equation:

$$R_{rms} = \sqrt{\frac{1}{n} \sum_{i=1}^{n} Z_i^2}$$

where

 $Z_i$  = current difference between the height and the mean plane

n = number of points in the image

## Water Contact Angle measurement

A deionized water droplet (approximately 5  $\mu$ L) was dropped on the NR and modified NR surface. And, sessile drop contact angle measurement was performed with a contact angle goniometer (G-1, Kruss). For each angle reported, at least five sample readings were averaged.

## Nanoindentation testing

Nanoindentaion experiments were performed using Nano Test system (Micro Material Ltd. Wrexham, UK) with a  $100~\mu m$  radius diamond spherical indenter tip manufactured by Micro Materials.

The experimental conditions for all indentation tests were as follows:

Initial load: 0.01 mN

The maximum load: 0.25 mN

Loading and unloading rate: 0.10 mN/s

Dwell time or holding time at maximum load: 60 s.

The stiffness was obtained by fitting a power law function, proposed by Oliver and Pharr [20], on the unloading curve. And, the reduced elastic modulus  $(E_r)$  was determined from average forty-eight data points using the following equation, deduced from Hertz analysis:

$$E_r = \sqrt{\frac{8^3}{6RP}}$$

where S is the stiffness. R and P values are the nominal radius of curvature of the spherical indenter and the applied load, respectively.

## In vitro cytotoxicity test

## Cells

A mouse connective tissue fibroblast cell line, L929 was cultured in Dulbecco's minimum eagle medium (DMEM) supplemented with 10% fetal calf serum and 4 mM glutamine. The cultures were cultivated in an incubator at 37°C 90% r.h. and 5% CO<sub>2</sub>, until cell monolayers attained confluence, which occurred after 24 h Then, the cultures were harvested using trypsin solution. Stock cultures were seeded in 60 mm diameter cell culture petri dishes at a density of 0.1 x 10<sup>6</sup> cells/cm<sup>3</sup> and subcultured once a week. Assays were always performed in the exponential growth phase of the cells. The cell line was periodically assayed for mycoplasma.

## Extraction method

Extracts of the polymers were prepared using 0.2 g polymer per ml serum-supplemented culture medium (DMEM) containing 4 mM glutamine. The extracts were maintained in an incubator for 24 h at 37°C. If necessary, the extracts were neutralized to exclude the effect of pH and filtered through a 0.2  $\mu$ m membrane filter. The cells were seeded into 96-well microtiter plates at a density of 1 x 10<sup>4</sup> cells/well. Then, after 24 h the culture medium (100  $\mu$ l) was replaced with

serial dilutions of the extracts. After an incubation period of 24 h, the viability of the cells was evaluated by the MTT assay.

## MTT assay

MTT (3-(4,5-dimethylthiazol-2-yl)-2,5-diphenyl tetrazolium bromide) was dissolved in PBS (phosphate-buffered solution) at 5 mg/ml and filtered for sterilization. A total of 50  $\mu$ l of this stock solution was added to each well, reaching a final concentration of 0.5 mg MTT per ml and the plates were incubated for 2 h. Unreacted dye was removed by aspiration and the purple formazan product was dissolved in 100  $\mu$ l/well isopropanal and quantified by spectrophotometer at wavelengths of 570 and 650 nm. The % cell viability related to control wells containing cell culture medium without extracts was calculated by the following equation (A = absorbance):

% cell viability = 
$$\underline{[A]_{test}}$$
 x 100  $[A]_{control}$ 

## Results and discussion

# Synthesis and characterization of PELA

## NMR spectra

Typical <sup>1</sup>H-NMR spectra of PELA is shown in Fig. 1. A series of PELA having a fixed PEG:PLA molar ratio of 1:1 were successfully synthesized by varying the PEG molecular weight (chain length) in the middle block. The obtained PELA are denoted as PELA-Xk, where X is for the number of molecular weight of PEG. By predetermination of the content of lactide monomer attached to the PEG middle block, the molar ratio of PLA:PEG could be controlled to be closely 1.0:1.0. The characteristics of PELA are presented in Table 1. The obtained PEG:PLA molar ratios were within a confined range between 1.1:1.0 and 1.2:1.0.

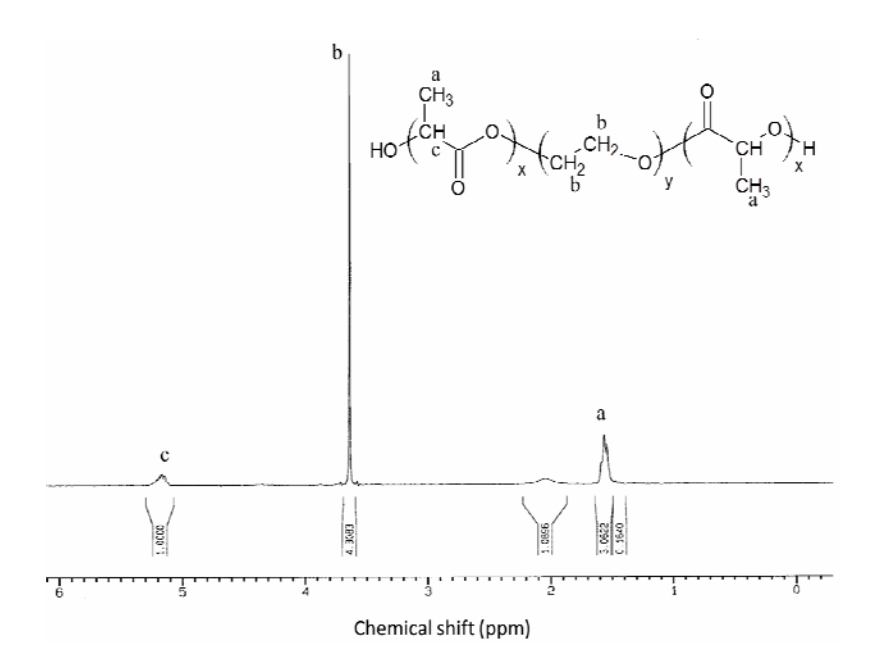


Fig.1 <sup>1</sup>H-NMR spectra of PELA-8k

Table 1 Structural characteristic and molecular weight of PLA-PEG-PLA triblock copolymer

Polymer	M <sub>n</sub> of PEG g/mol	EG:LA (theory)	EG:LA (Exp.)	M <sub>n</sub> (NMR)of PELA g/mol
PELA-2k	2,000	1.0:1.0	1.2:1.0	4,700
PELA-8k	8,000	1.0:1.0	1.1:1.0	22,100
PELA-12k	12,000	1.0:1.0	1.2:1.0	28,900
PELA-20k	20,000	1.0:1.0	1.1:1.0	41,000

Note:  $M_n$  is a number average molecular weight

## Characterization of modified NR surface

## **FTIR**

The presence of PELA on the surface of modified NR film was characterized by ATR-FTIR, a technique well suited for investigating surface chemical species, and the spectra are presented in Fig.2. It was apparent that the ATR-FTIR spectra of the modified NR films were different from that of the unmodified NR. The characteristic absorbance peak at 1740 cm<sup>-1</sup>, corresponding to C=O stretching, was clearly observed in all NR surfaced modified with PELA indicating that PELA was introduced into the NR surface. Together with a decrease in the intensity of absorbance peak at 1380 cm<sup>-1</sup> of NR, it could be inferred that the surfaces of all modified NR film were completely covered by PELA of all molecular weights. Moreover, it could be suggested that the formation of PELA onto NR surface involves only physical bonding.

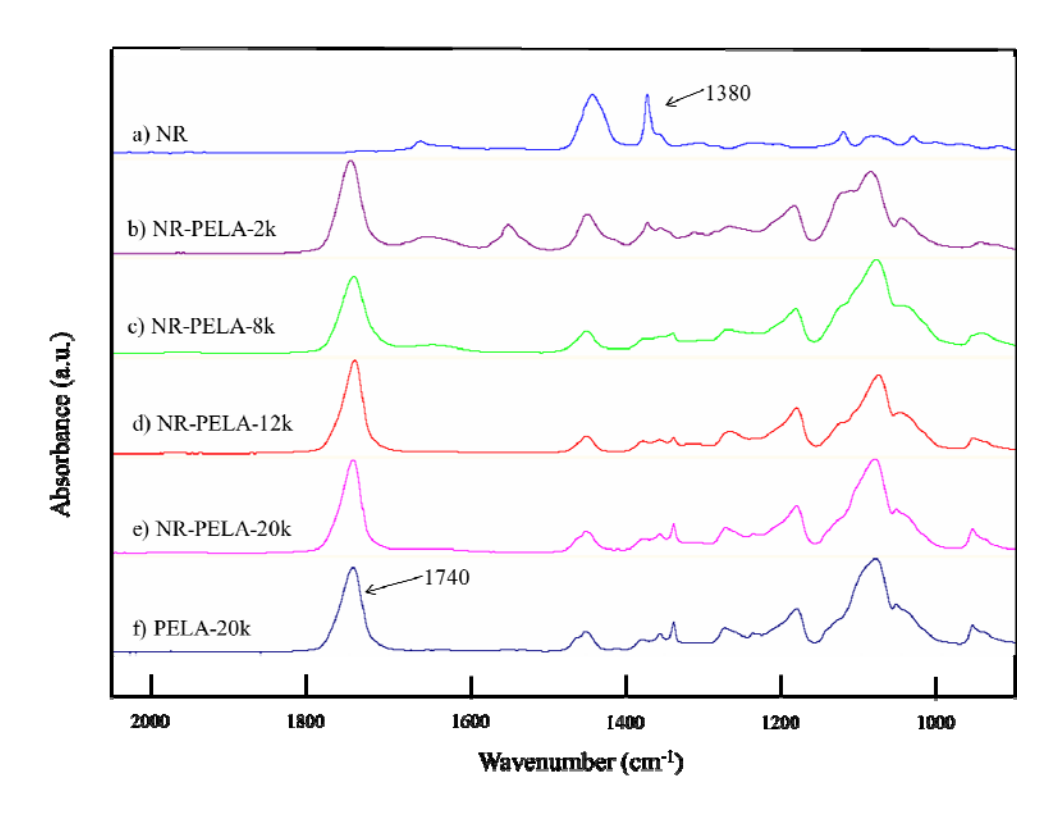


Fig.2 The ATR-FTIR spectra of of unmodified NR and modified NR with various molecular weight PELA

# Morphology of modified NR surface

The surface morphologies of unmodified NR and NR modified by PELA investigated by AFM were shown in Fig. 3, with the topographic or height images on the left, and the phase images on the right. The AFM micrographs of unmodified NR are apparently different from those of PELA modified NR surfaces. The topographic image showed the relative flat and smooth surface of the unmodified NR, as seen in Fig. 3a. Whereas, globular particle like morphologies were observed on the PELA modified NR of all molecular weights, as shown in Fig 3(b-e). According to the surface root mean squared roughness ( $R_{rms}$ ), the surfaces of all PELA modified NR, which are in the range of 43 to 196 nm., are slightly rougher than that of unmodified NR ( $R_{rms}$  = 29 nm). Also, the phase images of all NR modified by various PELA molecular weights, as seen in Fig.3(g-j), show no character; i.e. particularly no phase separation. This can be explained by the fact that dichloromethane is considered a good solvent for both pure PLA and PEG. Therefore, both components of PELA; namely PLA and PEG, can dissolve to form particle like morphology instead of phase-separated structure. In addition, These AFM results suggested that the orientation between PLA and PEG segment of PELA are randomly oriented, and the chain length of PELA in the scope of this study is not sufficient to induce phase separation.

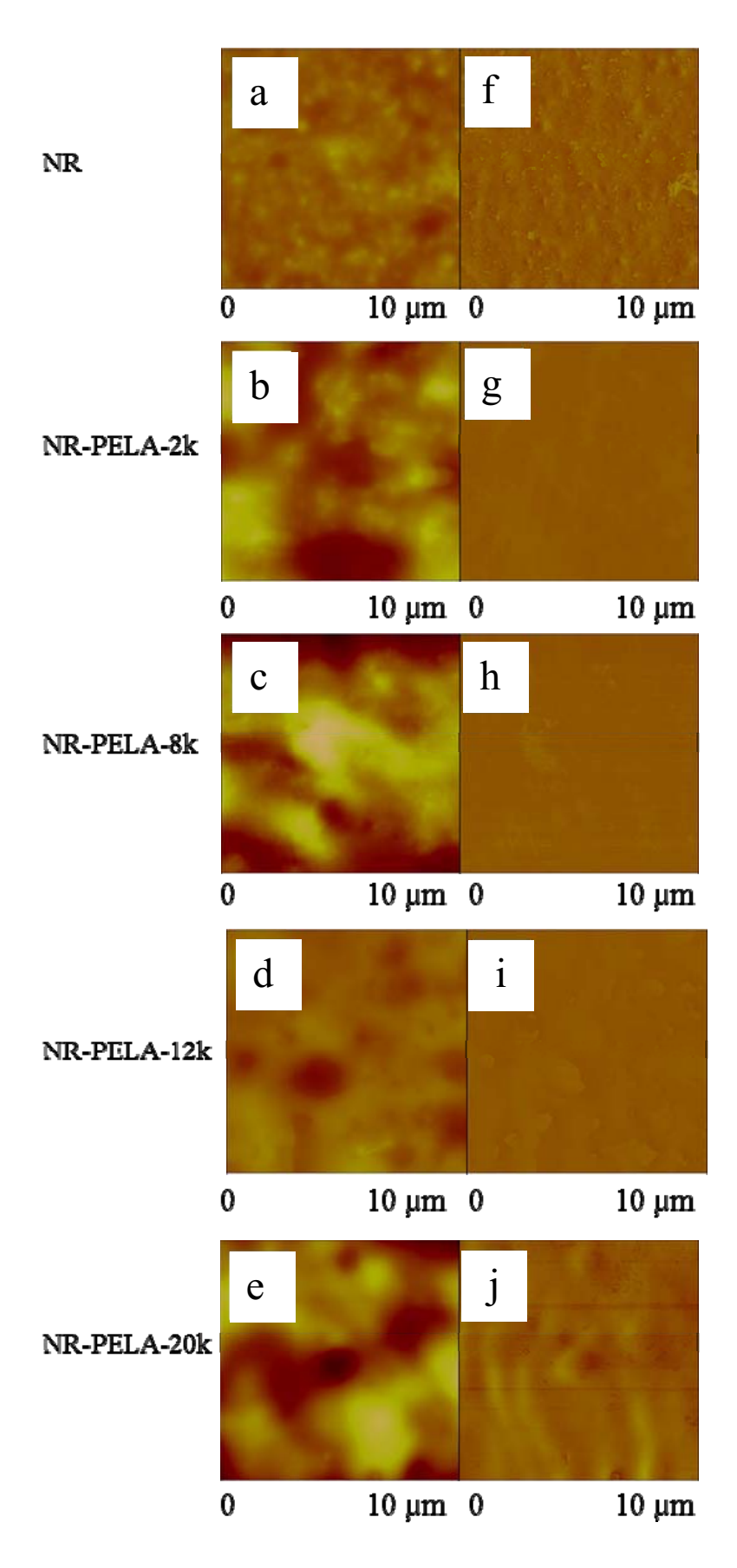


Fig.3 AFM topoghapic micrographs of (a) unmodified NR film and (b-e) modified NR with PELA-2k, PELA-8k, PELA-12k and PELA-20k, and AFM phase images of (f) unmodified NR film and (g-j) modified NR with PELA-2k, PELA-8k, PELA-12k and PELA-20k, respectively

## **Water Contact Angle**

Table 2 Water contact angle of unmodified NR and modified NR with various molecular weight PELA

Sample	Water Contact Angle (°)
NR	$87.3 \pm 1.3$
NR-PELA-2k	$37.3 \pm 2.2$
NR-PELA-8k	$44.8 \pm 2.4$
NR-PELA-12k	$46.0 \pm 1.7$
NR-PELA-20k	$46.6 \pm 2.0$

To determine the relative hydrophilicity of various molecular weight PELA, WCA measurements were conducted, and the results are depicted in Table 2. A decrease in WCAs on the PELA modified surfaces of NR of all molecular weight in comparison to that of unmodified NR surface indicates that the modification of NR surface by PELA can enhance hydrophilicity of NR surface.

#### Nanoindentation behavior

To reduce the viscoelastic or time-dependent effect, the methodology of inserting the holding period of 60 s between loading and unloading was used to determine elastic modulus in this study. Load-displacement curves of unmodified NR and PELA modified NR with various molecular weights were shown in Fig. 4. The average values of reduces modulus data extracted from the loading/unloading curves were presented in Table 3 and presented in Fig. 5. The PELA-2k exhibited the lowest reduced modulus. With an increase in the PELA molecular weight, the reduced modulus of all PELA modified NR surfaces were found to increase monotonously. It is worth noting that the PELA-20k exhibited a comparable reduced modulus to that of unmodified NR. It could be suggested that the PELA with molecular weight of PEG-20k is the best candidate for modifying the NR surface in order to enhance biocompatibility, while the mechanical property still remained intact.

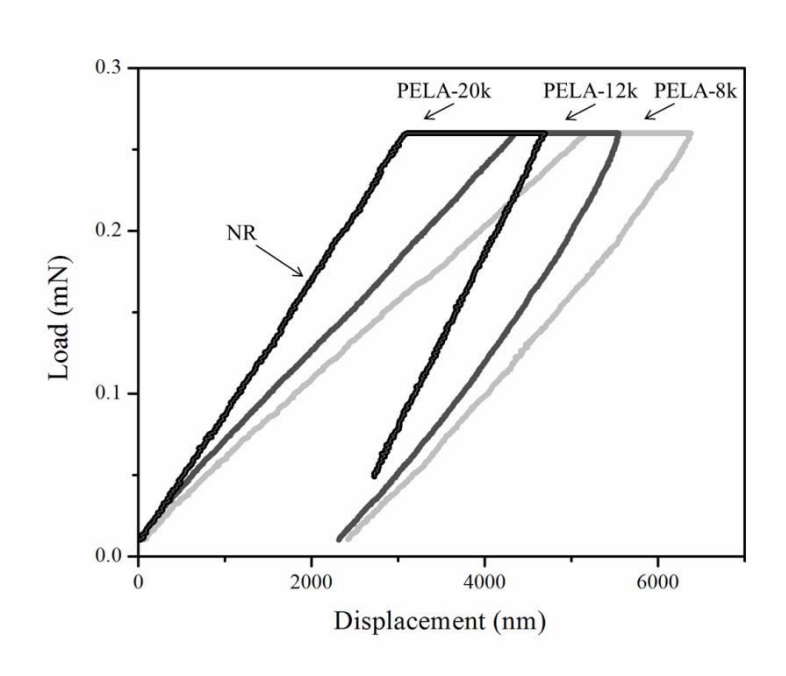


Fig. 4 Load-displacement curves of unmodified NR and modified NR with various molecular weight PELA

Table 3 Reduced modulus of unmodified NR and modified NR with various molecular weight PELA

Sample	Reduced modulus (MPa)
NR	$2.45 \pm 0.08$
NR-PELA-2k	$0.97 \pm 0.04$
NR-PELA-8k	$1.20 \pm 0.10$
NR-PELA-12k	$1.63 \pm 0.09$
NR-PELA-20k	$2.35 \pm 0.20$

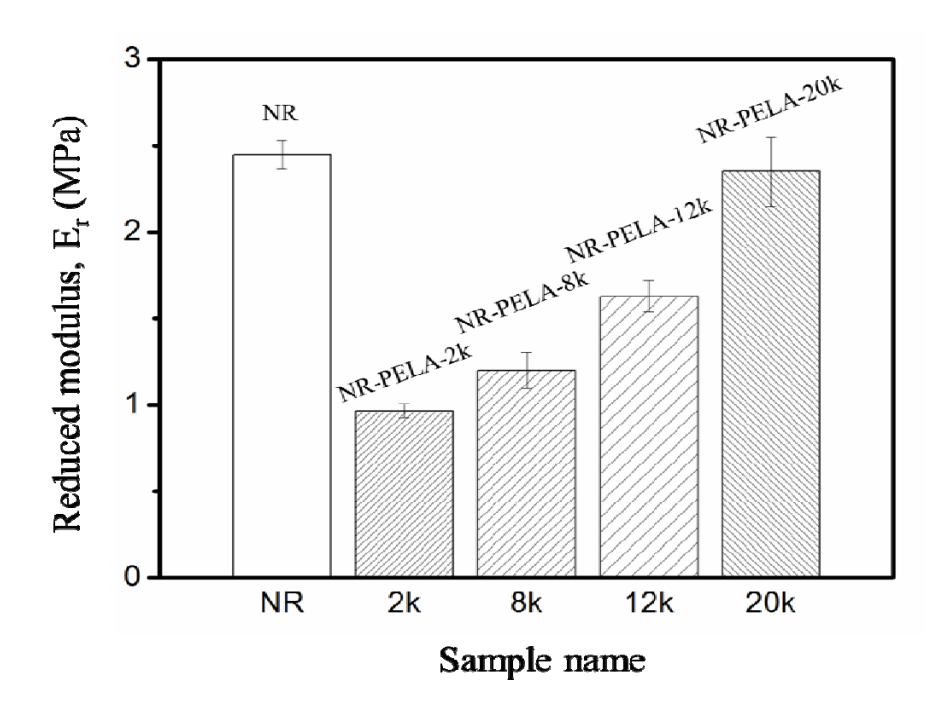


Fig. 5 The reduced modulus of unmodified NR and modified NR with various molecular weight PELA

## Cytotoxicity of NR modified by PELA

The MTT assay was conducted to evaluate the cytotoxicity of all tested NR modified by PELA. This standard method was based on the colorimetric analyses of cell viability. The specimens of NR modified by PELA were tested using dimethyl sulfoxide (DMSO) as a positive control, micro covered glass as negative control, and Dulbecco's minimum eagle medium (DMEM) as a control. The results showed that % cell viability of NR was 20%, while all of those of NR modified by PELA were greater than 70%. According to the standard procedure, if cell viability was found to be greater than 70% of that of control, this tested sample was considered biocompatible material. Therefore, it was apparent that the surface modification of NR by PELA could effectively improve the biocompatibility of NR.

## **Conclusions**

To enhance the biocompatibility of NR film, the surface modification of NR film by PELA of various molecular weights was successfully prepared, and characterized. Their nano-mechanical properties were investigated using Nanoindentation technique by taking viscoelastic effect into an account. The ATR-FTIR result suggests that the formation of PELA onto NR surface involves only physical bonding. The AFM morphologies supported ATR-FTIR result in that PELA was introduced onto NR surface and there is no phase separation between PLA and PEG segment. The

NR surfaces modified by PELA of all molecular weight exhibit enhanced hydrophilicity in comparison to that of unmodified NR, and their reduced modulus was found to increase with an increasing PELA molecular weight. In addition, the NR-PELA-20k showed a comparable reduced modulus to the unmodified NR. Finally, it was apparent that the improvement of biocompatibility of NR could be successfully achieved by the surface modification of NR by PELA.

## Acknowledgement

Research grants from The Thailand Research Fund (TRF) to P.Tangboriboonrat and R.Thonggoom are gratefully acknowledged. The authors thank K.Phomphrai for valuable suggestions. Special thank to N.Promawan and N.Pancharoentavon for performing Nanoindentation.

## References

- [1] Chei Sara HY, Tan Peng Wang KL, Ho CC, Kang ET. Surface modification of natural rubber latex films via grafting of poly(ethylene glycol) for reduction in protein adsorption and platelet adhesion. J Mat Sci Mater Med 2001; 12: 377-384.
- [2] Hoven VP, Chombanpaew K, Iwasaki Y, Tasakorn P. Improveing Blood Compatibility of Natural Rubber by UV-induced Graft Polymerization of Hydrophilic Monomers. J Appl Polym Sci 2009; 112: 208-17.
- [3] Steele Terry WJ, Huang Charlotte L, Effendi Widjaja, Boey Freddy YC, Loo Joachim SC and Venkatraman Subbu S. The effect of polyethylene glycol structure on paclitaxel drug release and mechanical properties of PLGA thin films. Acta Biomater 2011; 7: 1973-83.
- [4] Danquah M, Fujiwara T, Mahato RI. Self-assembling methoxypoly(ethylene glycol)-b-poly(carbonate-co-L-lactide) block copolymers for drug delivery. Biomaterials 31 (2010) 2358-70.
- [5] Kumari A, Yadav SK, Yadav SC. Biodegradable polymeric nanoparticles based drug delivery systems. Colloid Surface B 2010; 75: 1-18.
- [6] Nampoothiri KM, Nair NR, John RP. An overview of the recent developments in polylactide (PLA) research. Bioresource Technol 2010; 101: 8493-501.
- [7] Wang H, Zhao P, Su W, Wang S, Liao Z, Niu R, Chang J. PLGA/polymeric liposome for targeted drug and gene co-delivery. Biomaterials 2010; 31: 8741-48.
- [8] Rungsardthong U, Deshpande M, Bailey L, Vamvakaki M, Armes SP, Garnett MC, Stolnik S. Copolymers of amine methacrylate with poly(ethylene glycol) as vectors for gene therapy. J Control Release 2001; 73: 359-80.

- [9] Barton KN, Stricker H, Kolozsvary A, Kohl R, Heisey G, Nagaraja TN, Zhu G, Lu M, Kim JH, Freytag SO, Brown SL. Polyethylene Glycol (Molecular Weight 400 DA) Vehicle Improves Gene Expression of AdenovirusMediated Gene Therapy. J Urology 2006; 175: 1921-25.
- [10] Zhu J. Bioactive modification of poly(ethylene glycol) hydrogels for tissue engineering. Biomaterials 2010; 31: 4639-56.
- [11] Bettahalli NMS, Steg H, Wessling M and Stamatialis D. Development of poly(L-lactic acid) hollow fiber membranes for artificial vasculature in tissue engineering scaffolds. J Membrane Sci 2011; 371: 117-26.
- [12] Armentano L, Dottori M, Fortunati E, Mattioli S and Kenny JM. Biodegradable polymer matrix nanocomposites for tissue engineering: A review. Polym Degrad Stabil 2010; 95: 2126-46.
- [13] Lu YC, Fulcher JT, Tandon GP, Foster DC, Baur JW. Microscale thermomechnical characterization of environmentally conditioned shape memory polymer. Polym Test 2011; 30: 563-70.
- [14] Liao Q, Huang J, Zhu T, Xiong C and Fang J. A hybrid model to determine mechanical properties of soft polymers by nanoindentation. Mech Mater 2010; 42: 1043-47.
- [15] Gupta S, Carrillo F, Li C, Pruitt L and Puttlitz C. Adhesive forces significantly affect elastic modulus determination of soft polymeric materials innanoindentation. Mater Lett 2007; 61: 448-51.
- [16] Ebenstein Donna M and Pruitt Lisa A. Nanoindentation of biological materials. Nano Today 2006; 1: 26-33.
- [17] McDaniel Dennis P, Shaw Gordon A, Elliott John T, Kiran Bhadriraju, Curt Meuse, Koo-Hyun Chung and Plant Anne L. The Stiffness of Collagen Fibrils Influences Vascular Smooth Muscle Cell Phenotype. Biophys J 2007; 92: 1759-69.
- [18] Zhu J, Sabharwal T, Kalyanasundaram A, Guo L, Wang G. Topographic mapping and compression elasticity analysis of skinned cardiac muscle fibers in vitro with atomic force microscopy and nanoindentation. J Biomech 2009; 42: 2143-50.
- [19] Leong PL and Morgan EF. Measurement of fracture callus material properties via nanoindentation. Acta Biomater 2008; 4: 1569-75.
- [20] Oliver WC, and Pharr GM. An Improved Technique for Determining Hardness and Elastic Modulus Using Load and Displacement Sensing Indentation Experiments. J Mater Res 1992; 7: 1564-83.
- [21] Rho JY, Pharr GM. Effects of Drying on the Mechanical Properties of Bovine Femur Measured by Nanoindentation. J Mat Sci Mater Med 1999; 10: 1-4.

## Synthesis and Characterizations of Poly(lactic acid-co-ethylene glycol) (PLLA/PEG) Block-copolymers

Thai Hien Nguyen<sup>a</sup>, Atitsa Petchsuk<sup>b</sup>, Pramuan Tangboriboonrat<sup>c</sup>,
Mantana Opaprakasit<sup>d</sup>, , and Pakorn Opaprakasit<sup>a</sup>,\*

<sup>a</sup>School of Bio-Chemical Engineering and Technology, Sirindhorn International Institute of Technology (SIIT), Thammasat University, Pathumthani, 12121, Thailand
 <sup>b</sup>National Metal and Materials Technology Center, Thailand Science Park,
 Pathumthani, 12120 Thailand

<sup>c</sup>Department of Chemistry, Mahidol University, Bangkok 10400 Thailand <sup>d</sup>Department of Materials Science, Chulalongkorn University, Bangkok 10330 Thailand

Abstract. Poly(lactic acid-co-ethylene glycol) (PLLA/PEG) copolymers were synthesized and their properties were characterized. The PLLA/PEG/PLLA triblock copolymers were synthesized by ring-opening polymerization from 1-lactide (LLA) and PEG. Stannous octoate, Sn(Oct)<sub>2</sub> was used as a catalyst. Effects of molecular weight of PEG (600, 2000 and 4000), LLA/OH molar ratios (95:5, 98:2) and sequence of addition of the reactants on properties of the copolymers were investigated. The triblock copolymers were subsequently used in a production of multiblock copolymers by reacting with chain-extending agents, hexamethylene diisocyanate (HMDI) and maleic anhydride (MA). Effects of chain-extending agent and reaction temperature on chainlinking reaction were studied. Chemical structure and molecular weight of the copolymers were characterized by <sup>1</sup>H-NMR, FTIR and GPC. The results showed that molecular weight of triblock copolymers varied from 4,500 to 10,200. After chain extension, multiblock copolymer with molecular weight of 16,490 was produced. Thermal properties of the copolymers were also examined by DSC. The morphology of copolymer was determine by XRD and were examined by comparing with the results from DSC.

## 1 Introduction

Nowadays, fossil fuel plays an important part in human living. The petroleum-based commodity plastics present everywhere from household utilities to industrial products. Most of these are non-degradable plastics which are considered as the source of environmental pollution. One of the disposing methods of these plastic wastes is landfills. However, this method presents an ugly and unhygienic seen. This littering effect on the rate of rain water percolating, results in lower of the undercurrent water level. The soil fertility deteriorates as the plastic bags form part of manure remains in the soil for years. Futhermore, the rapid increase in the demand of plastic products and the decrease of landfill site causes a formidable amount of plastic wastes. In fact, the recycling method was recommended to overcome environmental issue. This method, however, requires more manual labor, energy and time. This method, in turn, emits some toxic gases in the process. Therefore, biodegradable plastics have been considered as a new method to reduce the impact of plastic waste on the environment.

One of the biodegradable plastics is poly(lactic acid) (PLA). PLA is produced from lactic acid (2-hydroxyl propanoic acid). Lactic acid has an asymmetric carbon atom and two optically active configurations, l- and d- enantiomers. Lactic acid can be produced either by chemical synthesis or by fermentation. The chemical synthesis can procedure a racemic mixture while fermented lactic acids can be optically pure isomer [1]. PLA is considered as a renewable material because its monomer, lactic acid, is produced by fermentation from sucrose or fructose, which can be derived from agricultural product. PLA is biodegradable and biocompatible polymer that is particularly an attractive material for various applications, especially in medical applications. This aliphatic polyester is polymerized by polycondensation or ring-opening polymerization, where the later can yield high molecular weight copolymers [2]. It is a high strength and high modulus thermoplastic. PLA degrade by simple hydrolysis of the ester bond and does not require the presence of enzymes to catalyze hydrolysis. The degradation products of PLA are nontoxic to living organisms since lactic acid itself occurs in the metabolism. PLA and its copolymers have been used for applications like drug delivery system, protein encapsulation and delivery, etc [2]. PLA also finds applications in household products such as degradable rubbish bags, thermoformed trays for fruits and vegetables, disposable plates and cup, toys, cutlery, fiber and composites, etc. In addition, this polymer is used in agricultural applications such as mulch films, temporary replanting pots, delivery system for fertilizers and pesticides, etc [2]. However, PLA is hydrophobic, which limits its use in certain applications.

On one hand, poly(ethylene glycol) (PEG) is known as hydrophilic polymer with outstanding properties, such as non-toxicity, non-ionic and biocompatible characteristics. Poly(ethylene oxide) (PEO), otherwise known as poly(oxide ethylene) or poly(ethylene glycol) ( PEG), is synthesized form ethylene oxide or ethylene glycol. The term PEG refers to polymer chain with molecular weight below 20,000, while PEO refers to the higher molecular weight [3]. PEG is soluble in water, methanol, benzene, dichloromethane and insoluble in diethyl ether and hexane. It can be filtered through kidney when the molar mass is below 30,000[4, 5]. Especially, it lacks in antigenicity and immunogenicity, so it is suitable for drug formulations [5]. PEG is used in various biomedical applications to increase the stability of blood contacting materials [6]. It has been applied in protein pharmaceuticals as stabilizer and emulsifier to prevent aggregation and inactivation of proteins [7]. The high molecular weight PEG-grafted pericardium is used to enhance the biostability and calcium resistance of biomaterials [8]. The highly crosslinked PEG-rich networks can be produced by containing PEG bridges and PEG grafts. So the three-dimensional structure can control delivery of proteins from hydrogels containing PEG [8] and modified with galactose moieties to enhance interactions with liver cells [9]. Moreover, two hydroxyl groups at the end chain of PEG play as functional groups which can be reactive with other functional groups, especially carboxyl group. Therefore, copolymerization of PLA and PEG offers an opportunity to combine the advantages of these polymers.

Many reports in the literature focused on the synthesis and characterizations of PLLA/PEG block copolymers [4-6, 10-14]. However, to our knowledge, these reports lacked of information on the effect of reaction conditions on the structure and properties of copolymer.

In this study, PLA/PEG copolymers are synthesized and their properties are characterized. The triblock PLLA/PEG/PLLA copolymers are synthesized by ring-opening polymerization using tin(II)hexyl ethanoate, Sn(Oct)<sub>2</sub>, as a catalyst. Effects of

molecular weight of PEG, LLA/OH(PEG) molar ratios and a sequence of addition of the reactants on structure and properties of copolymer are investigated. Multiblock copolymers are then synthesized by employing chain extending agents, HMDI and MA. These copolymers were used as a crosslink agent in chemical modification of natural rubber.

## 2 Experimental

#### 2.1 Materials

L-lactic acid (88wt% in water) was purchased from Carlo Erba. L-lactide (LLA) was synthesized according the method of Zhang et.al [15] and of Sutawan et.al [16]. First, l-lactic acid was distilled to dehydrate at 120°C. Polycondensation was then employed to convert l-lactic acid to its short chain oligomers (8-15 units) at 140°C. These oligomers were then depolymerized to form a cyclic l-lactide (LLA) by heating at 170°C in a presence of Sn(Oct)<sub>2</sub> (Wako) as a catalyst. The resulting LLA was recrystallized three times in cool ethyl acetate and was then vacuum dried at 40°C for 24 hours. The purified LLA was stored in a vacuum flask for further use. PEG with molecular weight of 600, 2000, 4000 g/mol were supplied by Fluka. Chain-linking agents, i.e. HMDI and MA, were purchased from Aldrich.

2.2 Synthesis of

PLLA/PEG/PLLA

triblock copolymers

The synthesized procedure of PLLA/PEG/PLLA triblock copolymers was adopted from the methodology reported by Y.Wan et. al. [11]. Effects of molecular weight of PEG, LLA/OH molar ratios, and a sequence of addition of the reactants on the properties of the resulting copolymers were investigated. PEG with different molecular weights (600, 2000, and 4000) and LLA/OH(PEG) molar ratios of 95:5, 98:2 were employed to vary PEG and PLLA block lengths in copolymer chains. Essentially, a mixture of monomer and 1%w/w catalyst were dried by a vacuum/inert gas technique for 1 hour. The mixture was then melted at 130°C and the polymerization was taken place for 24 hours.

Chloroform and ethanol were used to purify the copolymer products at least two times. Finally, the samples were dried under vacuum at 40°C for 24 hours.

In the study on effects of a sequence of addition of the reactants, PEG 4000 and an LLA:OH molar ratio of 98:2 were employed in the synthesis using similar reaction temperature and time, as described above. Three experiments conditions were employed. First, LLA, PEG and Sn(Oct)<sub>2</sub> were added in the flask at the same time (A). In the second experiment, LLA and PEG were melted at 130°C, and Sn(Oct)<sub>2</sub> was then added to the mixture (B). In the final experiment, PEG was melted at 80°C, followed by an addition of 1%w/w Sn(Oct)<sub>2</sub>. After 1 hour, LLA was finally added to the mixture (C).

2.3 Synthesis of
multiblock PLLA/PEG
copolymers

Multiblock PLLA/PEG copolymers were synthesized by a chain extension reaction of triblock copolymer obtained from a reaction of PEG2000 with an LLA/OH ratio of 98:2. HMDI and MA were used as coupling agents. A 1.0:1.1 molar ratio of triblock copolymer/HMDI (or MA) was employed. Effect of synthesis conditions on properties of the copolymers was investigated by conducting reactions in bulk and by using a solvent. Reaction in bulk was conducted by drying the triblock copolymer using vacuum/inert gas technique for 1 hour. The reactant was melted at 160°C under vacuum pressure and a coupling agent, i.e., MA (D) or HMDI (E), was added. The reaction was carried out for 1.5 hours. The mixture was then precipitated in ethanol and dried under vacuum at 40°C for 24 hours.

The synthesis procedures of reaction in solvent were similar to the methodology reported by Cohn et. al [12], except that Sn(Oct)<sub>2</sub> was used as a catalyst. The triblock copolymer was first dried by vacuum/inert gas technique for 1 hour and dissolved in dried dioxane. HMDI was then added to the mixture. The reaction temperature was kept at 80°C for 3 hours. The product was precipitated in ethanol (F). Additionally, a similar reaction was conducted with an employment of Sn(Oct)<sub>2</sub> as a catalyst (G). The sample was finally dried under vacuum at 40°C for 24 hours.

# 2.4 Characterizations of copolymers

Chemical structure and composition of the triblock copolymers were characterized by <sup>1</sup>H-NMR on a Bruker DRX400 using chloroform-d as a solvent. FTIR spectra were recorded on a ThermoNicolet 6700 model spectrometer in a transmission mode. A copolymer film was prepared by casting a 5% solution in chloroform on a KBr pellet. Molecular weights of the copolymers were examined by employing a Waters 150 CV Gel Permeation Chromatography (GPC). THF was used as a solvent, with a flow rate of 1 ml/min. Polystyrene standards were employed to construct a standard curve.

Thermal properties of copolymer were characterized on a Mettler Todedo DSC822° machine. The samples were scanned from -60°C to 200°C with heating and cooling rates of 20°C/min. Glass transition temperature ( $T_g$ ), melting temperature ( $T_m$ ) and heat of melting ( $\Delta H_m$ ) were derived from the second heating thermograms. The decomposition temperatures ( $T_d$ ) of copolymers were determined on a Mettler Toledo TGA/SDTA 851 instrument, under oxygen atmosphere. The temperature was increased from 50°C to 1000°C with a heating rate of 20°C/min. Differential TGA plots (DTGA) were used in the determination of degradation temperature ( $T_d$ ) and degradation composition. X-ray diffraction (XRD) traces were obtained on a JEOL JDX-3530 machine, using CuK $_{\alpha 1}$  radiation. The sample films were scanned from a 20 of 5°-50° in a 0.02 step size, 1 second step size.

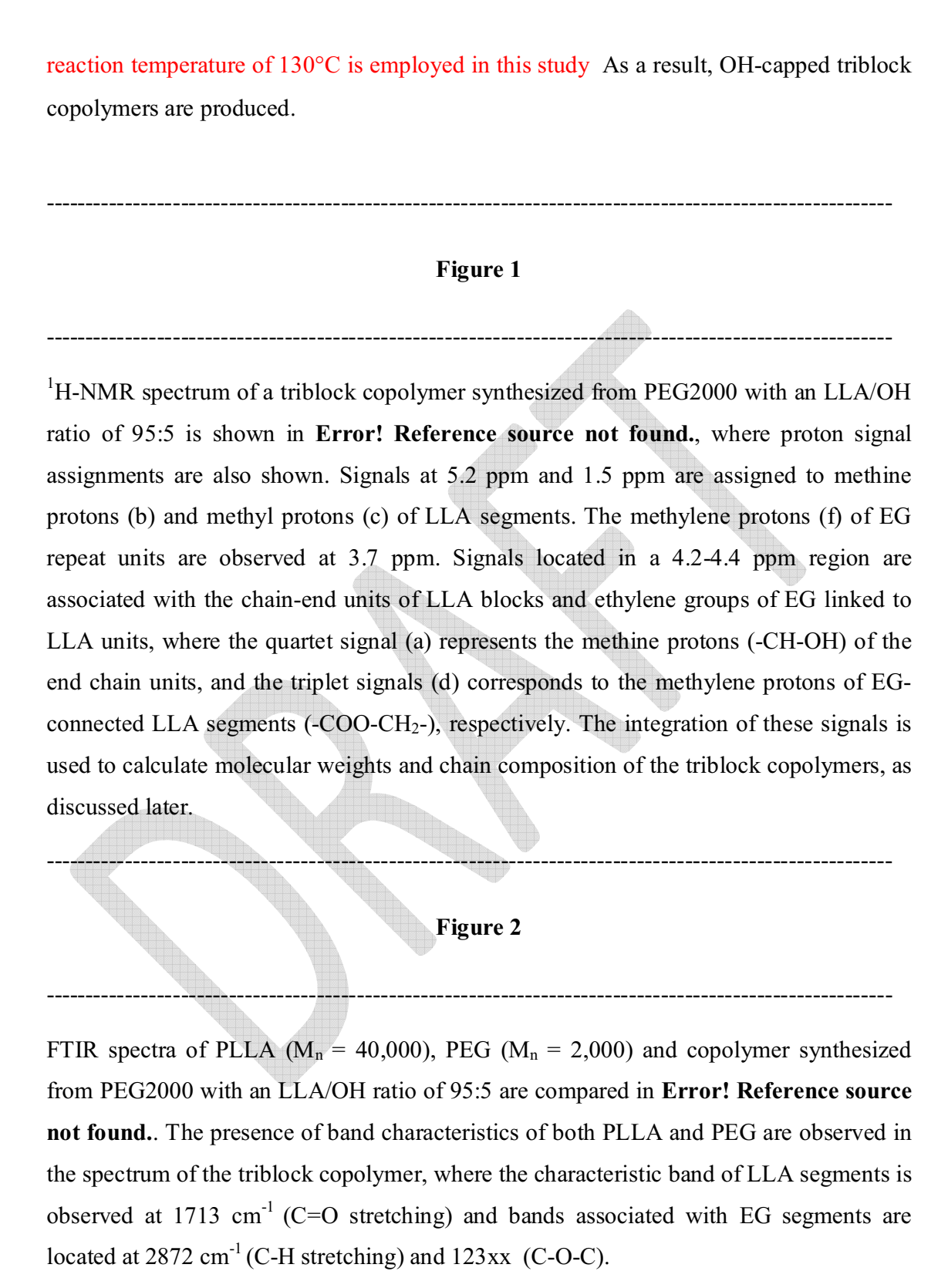
## 3 Results and Discussion

3.1 Synthesis of

PLLA/PEG/PLLA

triblock copolymers

Triblock PLLA/PEG/PLLA copolymers are synthesized by a ring-opening polymerization of LLA in the presence of PEG and Sn(Oct)<sub>2</sub>, as presented in **Error! Reference source not found.**. As the catalyst is more effective at high temperature to initiate the OH groups of PEG that take part in the ring opening polymerization [17], a



\_\_\_\_\_

Effects of molecular weights of PEG and LLA/OH molar ratios. Triblock copolymers with wide range of molecular weights and chain composition are obtained by varying PEG size and LLA/OH molar ratios, as summarized in Error! Reference source not found. The results show that LLA/EG ratios in the copolymer chain structure range from 0.31:1 to 3.90:1, which are dependent on the ratios in feed. The effect of PEG size on chain structure and molecular weight of the copolymer is revealed in samples prepared from the 95:5 LLA/OH feeding ratio. With the use of low molecular weight PEG (samples 1 and 2), the molar ratios of LLA/EG in product are significantly higher than those in feed. However, opposite trend is observed when higher molecular weight PEG is employed (samples 4 and 5). This is probably because the bigger sized PEG leads to a reduction in reactivity of OH groups at the end chains, which act as reactive sites in the polymerization of LLA blocks. LLA/EG/LLA block lengths of the copolymer products are summarized in Table 1, and will be used to refer to the copolymers from now on.

------

## Table 1

Effects of sequence of addition of the reactants. Effect of order of adding of reactants on properties of the resulting copolymers is studied to further optimize suitable synthesis conditions. The results, as shown in Error! Reference source not found., indicates that comparable LLA block length are obtained from sample (A) and (B). Sample (C) composts copolymer chains with significantly higher molecular weight than those of the former two counterparts. This is probably because  $Sn(Oct)_2$  acts as co-initiator by initiating hydroxyl groups of PEG, which readily reacts with LLA in the latter stage. On the other hand, when  $Sn(Oct)_2$  is added into the mixture at the same time with LLA and

Table 2									
3.1.1 Synthesis of PLLA/PEG multiblock copolymers.									
Results on the effects of types of chain linking agent and the reactions conditions con									
nolecular weight of PLLA/PEG multiblock copolymer are summarized in Error!									
Reference source not found. Molecular weight distributions plot of multiblock									
opolymers obtained form GPC experiments are also shown in Error! Reference source									
not found. The results show a decrease in molecular weight of samples obtained from									
he reactions in bulk (samples 6 and 7), compared to the original 46/46/46 triblock									
copolymer. The changes in molecular weight distribution are also clearly observed in									
amples 6 and 7. The unimodal distribution of sample 6 shifts to the right (shorter chain),									
ndicating chain-breaking of the copolymer structures as a result from high reaction									
emperature. A broader trimodal distribution observed in GPC curve of sample 7									
probably indicates that both chain breaking and linking processes take place.									
Table 3									
Figure 4									

It is likely to conclude that HMDI is more effective than MA in chain-linking process of these copolymers. In sample 7, bond breaking due to high reaction temperature (160°C), occurs in the early stage, followed by chain-linking of the resulting fragment by HMDI. However, the less effective MA may not be able to reform longer chains in sample 6. This results in a reduction in overall chain lengths. Unsurprisingly, the results indicate that reaction in solvent with the use of HMDI as a coupling agent is an effective process to increase the copolymer chain lengths, as mild reaction conditions are employed. A slight increase in molecular weight of sample 7 is observed, probably due to chain linking of some low molecular weight fractions, as seen in GPC curve. Interestingly, when Sn(Oct)<sub>2</sub> is used as a catalyst in sample 8, a large increase in molecular weight of the resulting copolymer from 10,400 to 16,490 g/mol is observed. An apparent shift in peak maximum of GPC and a disappearance of smaller sized fractions indicate an effectiveness of chain linking reaction on all copolymer chains, reflecting in an increase in average molecular weight of almost twofold.

## Thermal properties of PLLA/PEG/PLLA triblock copolymers

Thermal characteristics of PLLA/PEG/PLLA triblock copolymers are examined by DSC and TGA experiments. The results are summarized in Error! Reference source not found. In copolymer with PEG length of 14 units, single  $T_m$  is observed as a result from LLA segment. As expected, two  $T_m$ s are observed in copolymers with  $\overline{DP}_{PEG} = 46$  and  $\overline{DP}_{PEG} = 91$ , because each segregated block are large enough to exhibit two separate crystalline domains.  $T_m$  of each component is strongly dependent on its corresponding block length. On the other hand, DSC thermograms of copolymers synthesized from PEG show  $T_g$  in the range of -3°C to -7°C, which are higher than that of pure PEG 2000 with  $T_g = -95$ °C [18, 19].  $T_g$  of copolymer with  $\overline{DP}_{PEG} = 91$  can not be detected because it is masked by  $T_m$  of EG block in the temperature range of 42°-50°C [18]. In addition, it is difficult to determine  $T_g$  of LLA block, because  $T_g$  of PLLA and  $T_m$  of PEG were very close. DSC exhibit the mutual effects of LLA and EG blocks on  $T_m$  and  $T_g$ , such as  $T_g$  of copolymers is ranging from -7 to -3°C while  $T_g$  of PEG 2000 is -95°C [18]. An addition

of EG block results in a decrease in  $T_m$  of PLLA blocks (118-156°C), compared with the  $T_m$  of commercial PLLA (145-186°C) [20]. This indicates strong interaction of PEG segments with PLA segments.

TGA was used to determine decomposition temperature  $T_d$  related to change in weight of PLLA/PEG/PLLA triblock copolymers. There were two main decompositions, in there; LA chain was degraded first with  $T_d$  of PLLA blocks were observed between 270°C and 310°C, whereas  $T_d$  of PEG blocks were between 390°C and 415°C.  $T_d$  of PEG blocks increased gradually with  $\overline{DP}_{PEG}$ : 390°C for PEG<sub>14</sub>, 410°C for PEG<sub>46</sub> and 415°C for PEG<sub>91</sub>. In contrast,  $T_d$  of PLLA blocks decreased when their degree of polymerization increased, as showed in **Error! Reference source not found.** In the effect of PEG blocks,  $T_d$  of PLLA blocks (288-310°C) are quite higher than  $T_d$  of commercial PLLA (235-255°C) [20]

Thermal characteristics of PEG/PLLA multiblock copolymers.  $T_g$  and  $T_m$  of sample (G) was examined and compared with the original material, PLLA<sub>46</sub>/PEG<sub>46</sub>/PLLA<sub>46</sub> triblock copolymer. The result in **Error! Reference source not found.** showed that  $T_m$  and  $T_g$  did not change after chain linking reaction. However,  $\Delta H_m$  of multibock copolymer slightly changed. For example,  $\Delta H_m$  PLLA block increased to 41.12 J/g in the case of multiblock copolymer, in contrast to 40.32 J/g in the case of triblock copolymer. The increase of  $\Delta H_m$  of PLLA block leaded to the higher of  $T_m$  of PLLA block, this implied that the chain of multiblock copolymer was longer due to the reaction between the original copolymers. HMDI was success in linking two PLLA blocks together to make a multiblock copolymer with longer PLLA block

Morphological Characterization by X-ray diffraction. The morphology of PEG2000 (PEG<sub>46</sub>), PLLA40000 (PLLA<sub>555</sub>) and triblock copolymers were determined by X-ray diffraction, as shown in Error! Reference source not found. PEG<sub>46</sub> exhibited two main diffraction peaks located at 9.6 and 11.6° whereas two main peaks of PLLA<sub>555</sub> were observed at 8.3 and 9.4°. PEG blocks were not always able to crystalline in copolymers. The presence of PLLA blocks in copolymer decreased the crystallizability of PEG block.

This was shown through the absence of two main diffraction peaks of PEG in diffractogram (PLLA<sub>27</sub>/PEG<sub>14</sub>/PLLA<sub>27</sub>,). Even though  $\overline{DP}_{PEG}$  was equal  $\overline{DP}_{PLLA}$ , the crystallizability of PLLA block still remained on advantages than that of PEG block (PLLA<sub>28</sub>/PEG<sub>46</sub>/PLLA<sub>28</sub>, PLLA<sub>43</sub>/PEG<sub>91</sub>/PLLA<sub>43</sub>). Only when  $\overline{DP}_{PEG}$  was significant higher than  $\overline{DP}_{PLLA}$ , the diffraction peaks of PEG block could be observed (PLLA<sub>14</sub>/PEG<sub>91</sub>/PLLA<sub>14</sub>).

The volume fraction crystallinity  $\phi$  of each block was summarized in **Error! Reference** source not found., based on the interpolation of XRD data. Assumed that the volumer fration crystallinity equaled with the mass fraction crystallinity  $\psi$ , The XRD data is in good agreement with DCS data, as shown in **Error! Reference source not found.**. In the case of PEG<sub>91</sub>, the longer LLA blocks were, the lower the crystallinity of EG blocks were. Similar to the effect of EG blocks onto the crystallinity of LLA blocks, the longer EG blocks were, the lower the crystallinity of LLA blocks were. This can be observed in the case of PLLA<sub>27</sub> vs. PLLA<sub>28</sub> and PLLA<sub>43</sub> vs. PLLA<sub>46</sub>. That is understandable because the attachment of one block reduce the chain mobility of another block. That makes the crystallinity of each block decrease when compare with that of pure PLLA or PEG.

#### 4 Conclusions

PLLA/PEG/PLLA triblock copolymers are synthesized at 130°C by ring-opening polymerization of lactide, PEG as a macroinitiator and Sn(Oct)<sub>2</sub> as a catalyst. Block lengths and chemical structures of the copolymers are characterized by <sup>1</sup>H-NMR and FTIR. It was found that the degree of polymerization of LLA block decreased (27, 28 and 14) when the degree of polymerization of EG block increased (14, 46 and 91). The results also indicated that a 98:2 of LLA/OH molar ratio is suitable ratio for synthesizing high molecular weight copolymers. HMDI was used as a chain-extender to produce higher molecular weights multiblock copolymers.

### 5 Acknowledgements

Financial support of this work is provided by The Thailand Research Fund (TRF), The Commission on Higher Education (CHE), RTA5180003 and Thailand Toray Science

Foundation. Thai Hien Nguyen is supported by a scholarship program from SCG Foundation and SIIT, Thammasat University.

- [1] N. Narayanan, P.K. Roychoudhury, A. Srivastava, L (+)lactic acid fermentation and its product polymerization, Electron. J. Biotechnol. 7(2) (2004) 167-U162.
- [2] A.P. Gupta, V. Kumar, New emerging trends in synthetic biodegradable polymers Polylactide: A critique, Eur. Polym. J. 43(10) (2007) 4053-4074.
- [3] N.A. Peppas, K.B. Keys, M. Torres-Lugo, A.M. Lowman, Poly(ethylene glycol)-containing hydrogels in drug delivery, Journal of Controlled Release 62(1-2) (1999) 81-87.
- [4] L. Yang, Z. Zhao, J. Wei, A. El Ghzaoui, S. Li, Micelles formed by self-assembling of polylactide/poly(ethylene glycol) block copolymers in aqueous solutions, J. Colloid Interface Sci. 314(2) (2007) 470-477.
- [5] I. Rashkov, N. Manolova, S.M. Li, J.L. Espartero, M. Vert, Synthesis, Characterization, and Hydrolytic Degradation of PLA/PEO/PLA Triblock Copolymers with Short Poly(l-lactic acid) Chains, Macromolecules 29(1) (1996) 50-56.
- [6] S.K. Agrawal, N. Sanabria-DeLong, J.M. Coburn, G.N. Tew, S.R. Bhatia, Novel drug release profiles from micellar solutions of PLA-PEO-PLA triblock copolymers, Journal of Controlled Release 112(1) (2006) 64-71.
- [7] I.J. Castellanos, R. Crespo, K. Griebenow, Poly(ethylene glycol) as stabilizer and emulsifying agent: a novel stabilization approach preventing aggregation and inactivation of proteins upon encapsulation in bioerodible polyester microspheres, Journal of Controlled Release 88(1) (2003) 135-145.
- [8] S.C. Vasudev, T. Chandy, Polyethylene glycol-grafted bovine pericardium: a novel hybrid tissue resistant to calcification, Journal of Materials Science: Materials in Medicine 10(2) (1999) 121-128.
- [9] S.T. Lopina, G. Wu, E.W. Merrill, L. Griffith-Cima, Hepatocyte culture on carbohydrate-modified star polyethylene oxide hydrogels, Biomaterials 17(6) (1996) 559-569.
- [10] S. Popelka, L.k. Machová, F. Rypácek, Adsorption of poly(ethylene oxide)-block-polylactide copolymers on polylactide as studied by ATR-FTIR spectroscopy, J. Colloid Interface Sci. 308(2) (2007) 291-299.
- [11] Y. Wan, W. Chen, J. Yang, J. Bei, S. Wang, Biodegradable poly(-lactide)-poly(ethylene glycol) multiblock copolymer: synthesis and evaluation of cell affinity, Biomaterials 24(13) (2003) 2195-2203.

- [12] D. Cohn, A. Hotovely-Salomon, Biodegradable multiblock PEO/PLA thermoplastic elastomers: molecular design and properties, Polymer 46(7) (2005) 2068-2075.
- [13] M. Yuan, D. Liu, C. Xiong, X. Deng, Polymerization of lactides and lactones 6. Synthesis of poly-lactide and polyethylene glycol-co-poly-lactide copolymer with allylmagnesium chloride, Eur. Polym. J. 35(12) (1999) 2139-2145.
- [14] S.M. Li, I. Rashkov, J.L. Espartero, N. Manolova, M. Vert, Synthesis, Characterization, and Hydrolytic Degradation of PLA/PEO/PLA Triblock Copolymers with Long Poly(l-lactic acid) Blocks, Macromolecules 29(1) (1996) 57-62.
- [15] H.-p. Zhang, J.-m. Ruan, Z.-c. Zhou, Y.-j. Li, Preparation of monomer of degradable biomaterial poly(L-lactide), Journal of Central South University of Technology 12(3) (2005) 246-250.
- [16] Sutawan Buchatip, Atitsa Petchsuk, K. Kongsuwan, Synthesis and Mechanical Properties of Poly (LLA-co-DLLA) Copolymers, Journal of Metals, Materials and Minerals 18 (2009) 175-180.
- [17] H.R. Kricheldorf, I. Kreiser-Saunders, A. Stricker, Polylactones 48. SnOct2-Initiated Polymerizations of Lactide: A Mechanistic Study, Macromolecules 33(3) (2000) 702-709.
- [18] H.R. Kricheldorf, S. Rost, C. Wutz, A. Domb, Stereocomplexes of Aâ^Bâ^A Triblock Copolymers Based on Poly(l-Lactide) and Poly(d-Lactide) A Blocks, Macromolecules 38(16) (2005) 7018-7025.
- [19] R. Mladenova, T. Petrova, N. Manolova, M. Ignatova, I. Rashkov, P. Kubisa, Preparation, Characterization, and Biological Activity of Amides and Esters from 8-Hydroxyquinoline-2-Carboxylic Acid and Jeffamines ED(R) Or Poly(Ethylene Glycol)S, Journal of Bioactive and Compatible Polymers 16(4) (2001) 259-276.
- [20] J.E. Mark, Polymer Data Handbook, Oxford University Press, 1999.

## Enhancement of Mechanical Properties of Poly(L-lactide-co-D,L-lactide) Copolymers by Physical Crosslinks Derived from Configuration Interlocks

Pakorn Opaprakasit<sup>d</sup>,\* Atitsa Petchsuk<sup>a</sup>,\*, Sutawan Buchatip<sup>a</sup>, Mantana Opaprakasit<sup>b</sup>,

Pramuan Tangboriboonrat<sup>c</sup>

<sup>a</sup>National Metal and Materials Technology Center, Pathum Thani, 12120 Thailand
 <sup>d</sup>Department of Materials Science, Chulalongkorn University, Bangkok 10330 Thailand
 <sup>c</sup>Department of Chemistry, Mahidol University, Bangkok 10400 Thailand
 <sup>d</sup>School of Bio-Chemical Engineering and Technology, Sirindhorn International Institute of Technology (SIIT), Thammasat University, Pathum Thani, 12121, Thailand

**ABSTRACT**— Copolymerization of enantiomeric lactides has been extensively investigated as a useful route to modify the chemical structure of PLA in order to achieve desirable properties. Various compositions of high molecular weight poly(L-lactide-co-D,L-lactide), P(LLA-co-DLLA), copolymers successfully synthesized by ring-opening were polymerization (ROP) of L-lactide (LLA) and D,L-lactide (rac-lactide, DLLA) using stannous (II) ethylhexanoate [Sn(Oct<sub>2</sub>)] as a catalyst. Properties of the copolymers were investigated through thermal analysis and tensile testing. The copolymers exhibited lower glass transition temperature (Tg), melting temperature (Tm) and % crystallinity than those of PLLA homopolymer. T<sub>g</sub> and T<sub>m</sub> of the copolymers decreased as DLLA content increased. An enhancement in mechanical properties of the copolymers was observed, with the degree of improvement dependent on the DLLA contents. Results on Young's modulus and tensile strength showed that optimum properties were obtained when 7.5% DLLA was employed, and tended to decrease as rac-lactide composition increased. Interestingly, copolymer synthesized from 50% DLLA showed remarkable improvement in modulus, strength and elongation at break. The origin of this properties enhancement was studied by polarized FTIR spectroscopy. The result showed vibrational mode originated from a formation of point interaction between DL and LL diads of copolymer chains, which acts as a "physical crosslink" in the amorphous phase of the copolymers.

#### **Keyword:**

\*Corresponding author

#### Introduction

Polylactide or polylactic acid (PLA) has been extensively researched and widely used in various applications, due mainly to its degradability and biocompatibility. This polymer is producible from renewable resources, very low or nontoxic in natural environments. In addition, PLA has good mechanical properties comparable to those of commodity thermoplastics. However, its rigidity and brittleness has limited its use in certain applications [1-3]. As a result, various PLA-based copolymers and blend systems have been developed to improve the materials mechanical properties [1, 4-9].

PLA is commonly synthesized by the ring-opening polymerization of lactide, its cyclic dimer derived from 2 units of lactic acid [10, 11]. Since lactic acid contains a chiral carbon, lactide occurs in three enantiomeric forms: D-lactide (DLA), L-lactide (LLA), and meso-lactide. Consequently, PLA may be synthesized in the forms of poly(L-lactide) (PLLA) or poly(D-lactide) (PDLA), which mainly consists of S or R lactate repeat units, respectively. In addition, syndiotactic polylactide may be produced when meso-lactide is employed.

It is well known that an enantiomeric mixture of PLLA and PDLA forms a stereocomplex, i.e. a stronger crystal structure that exhibits higher  $T_m$  compared to those of its single component counterparts, as a result from a formation of C-H··O=C hydrogen bonding[12-15]. Mechanical properties of the stereocomplex are also superior to those of the PLLA or PDLA single component counterparts [1, 5, 6]. This stereocomplexation is therefore used to further improve the versatile characteristics of polylactide, and to widen the materials applications[1]. In recent years, however, the applications of PLA stereocomplex have been limited because of an unavailability of PDLA in an industrial scale.

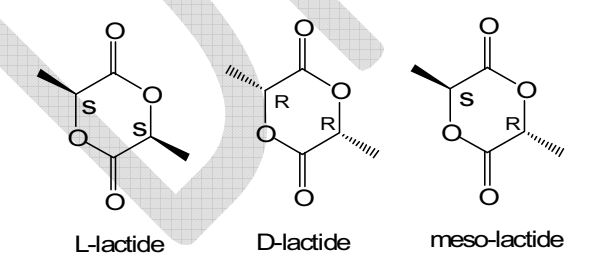


Figure 1. Structures of different stereoforms of lactide.

Copolymerization is an alternative method to modify properties of polymers for specific applications [8, 16, 17]. Polymerization of lactides with different stereoisomerism results in a formation of materials with different properties. For example, a racemic mixture of 1:1 LLA/DLA (DLLA) is used to synthesize PDLLA copolymers, which are amorphous materials. In addition, the composition of DL-lactate groups in the PDLLA copolymers can

be varied by using a mixture of racemic DL-lactide/L-Lactide at various compositions in order to optimize the copolymers crystalline content and hence thermal and mechanical properties [8, 16-18].

In this work, copolymers of DLLA and LLA with various DL-lactate contents are systematically synthesized by the ring-opening polymerization [19-21]. This copolymers is referred to as P(DLLA-co-LLA)<sub>x</sub> copolymers, where x indicates molar composition of DL-lactate groups. Intriguingly, characterization results on the synthesized copolymers reveal a drastic enhancement in mechanical properties of the copolymers consisting of certain DL-lactide compositions, especially those containing DLLA content lower than 7.5%, and the copolymer consisting of DLLA content of 50%. Insight into the origin of the mechanical properties enhancement in terms of structural conformations and interactions are investigated.

Urayama and Kimura analyzed microstructure of PDLLA copolymers in amorphous phase and found that an increase in length of L-lactate sequence resulted in an increase in helical nature, causing an increase in Tg value but a decrease in density. FTIR results indicated that band intensity of C=O stretching mode is independent on conformational change of the copolymers. Information on conformation of the chain structure can be monitored by employing the 1265 and 1210 cm<sup>-1</sup> modes, corresponding to  $(\delta_{CH}+\nu_{COO})$  and  $(\nu_{as\ COC}+r_{as\ CH3})$ .[8]

## **Experimental**

#### Materials

A racemic mixture of DL-lactide and Tin octoate [Sn(Oct<sub>2</sub>)] was purchased from Wako Co., Ltd. L-lactide was synthesized in this laboratory by depolymerization of low molecular weight poly(lactic acid) using antimony (III) oxide catalyst (Sb<sub>2</sub>O<sub>3</sub>).

## Synthesis of P(DLLA-co-LLA)<sub>x</sub> copolymers

P(DLLA-co-LLA)<sub>x</sub> copolymers were synthesized via a ring-opening polymerization of DLLA and LLA using 0.075 % wt. Sn(Oct<sub>2</sub>) as a catalyst. The reactions were conducted at 120°C for 5 hours. Molar composition of DLLA in feed was varied from 0, 2.5, 5, 7.5, 10, 20, 30, 50 and 100%. The resulting copolymers were purified by dissolving in chloroform and precipitating in methanol.

## Molecular Weight and Structural Characterizations

The average molecular weight and molecular weight distributions ( $\overline{M}_n$ ,  $\overline{M}_w$  and polydispersity) of the copolymers were measured using a Waters 150-CV gel permeation chromatography (GPC), comparative to mono-disperse polystyrene standard. Thermal properties of the copolymers were recorded on a DSC822° Mettler Toledo DSC. The sample was scanned twice from -20 to 200°C with heating and cooling rates of 10.0 °C/min. Results on  $T_m$  and  $T_g$  were determined from the second scan thermograms. Structural information of copolymers was examined on an AVENCE 300 MHz Digital NMR spectrometer (Bruker Biospin; DPX-300). <sup>13</sup>C NMR spectra were recorded at a frequency of 75 MHz. Tensile tests were carried out on an Instron tensile testing machine with a crosshead speed of 50 mm/min, using rectangular specimens with 50 mm gauge length and 15 mm width, according to ASTM D882. Copolymer films were prepared by casting from polymer solutions in chloroform. The resulting polymer film's thickness is roughly 10-60  $\mu$ m. The specimens were pulled in tension until rupture. The values of modulus, tensile strength, and elongation at break were recorded, and the average value from 3-4 specimens was reported.

Density of the copolymers was measured by employing gas displacement technique on an Ultrapycnometer 1000, Quantachrome. Helium gas was employed in the measurements conducted at  $23.3 \pm 0.1$ °C. All samples were dried at 80°C overnight in a vacuum oven before measurements. The reported density values were averaged from 5 measurements.

XRD traces of the film samples were recorded on a JEOL JDX-3530 Diffractometer, using  $CuK_{\alpha 1}$  radiation. The sample films were scanned from 20 of 5°- 40° at a 0.02 step size. FTIR spectra of the copolymer samples were recorded in transmission mode on a Fourier Transform Infrared Spectrophotometer (a NICOLET 6700 FT-IR) at a resolution of 2 cm<sup>-1</sup> by coadding of 64 scans. Typical and polarized FTIR spectra were recorded.

#### **Results and Discussion**

## Microstructure and Physical Properties

Microstructure of the synthesized P(DLLA-co-LLA)<sub>x</sub> copolymers is investigated by <sup>13</sup>C NMR spectroscopy employing resonances due to carbonyl carbons, where three signals are observed in the 169 ppm region. These signals correspond to various triad sequences in the copolymer chain, where the resonance at 169.6 ppm was assigned to the isotactic sequence of carbonyls of homo-sequence (mm triad). The signals at 169.3 and 169.1 ppm was tentatively assigned to heterotactic sequence (mr triad), and syndiotactic sequence (rr

triad), respectively.[8, 22-24] The percentage of these triads calculated from signals integration is summarized in Table 1. The calculated percentage of isotactic and syndiotactic sequences are comparable to those obtained from theoretical calculation employing the Bernoullian addition mechanisms[8], reflecting a success in the systematic synthesis of these random copolymers. Nevertheless, slight deviations of the values from the theory may perhaps due to racemization or intermolecular transesterification during the synthesis [8, 24]. In addition, results on molecular weight and molecular weight distribution of the P(DLLA-co-LLA)<sub>x</sub> copolymers are also summarized in Table 1. It is clearly seen that all copolymers have comparable molecular weight in the range of  $5.8 \times 10^4$  to  $11.8 \times 10^4$  g/mol, with polydispersity (PD) values ranging from 1.7-3.5. This enables a systematic comparison of copolymers properties by neglecting the effect of the copolymer molecular weight [25].

Table 1. Results on properties characterizations of  $P(DLLA-co-LLA)_x$  copolymers.

Samples	DLLA in feed	Chain Microstructure <sup>1</sup>			$\overline{M}_n$	PD	T <sub>g</sub> (°C)	T <sub>m</sub> (°C)	Average Density	Crystallinity <sup>2</sup> (%)
	(mol %)	% mm, δ <sub>169.6</sub>	% mr, $\delta_{169.3}$	% rr, δ <sub>169.1</sub>					(g/cm <sup>3</sup> )	
PLLA	0	99.6	0.0	0.4	91,370	1.79	68.3	169.9	1.542±0.007	48.1
P(DLLA-co-LLA) <sub>2.5</sub>	2.5	92.4	6.2	1.4	83,340	3.58	59.2	159.7	1.454±0.007	30.4
P(DLLA-co-LLA) <sub>5</sub>	5	88.6	9.2	2.2	67,870	1.99	57.4	154.2	1.304±0.005	29.7
P(DLLA-co-LLA) <sub>7.5</sub>	7.5	85.9	10.6	3.5	118,250	2.68	55.9	147.6	1.537±0.007	0.7
P(DLLA-co-LLA) <sub>10</sub>	10	85.8	11.1	3.1	81,140	1.98	54.0	143.7	1.530±0.007	1.7
P(DLLA-co-LLA) <sub>20</sub>	20	69.1	22.9	8.0	82,660	1.85	55.5	ı	1.337±0.009	-
P(DLLA-co-LLA) <sub>30</sub>	30	61.6	29.2	9.2	60,660	1.99	53.4	ı	1.267±0.007	-
P(DLLA-co-LLA) <sub>50</sub>	50	46.1	40.6	13.3	80,880	2.23	51.1	ı	1.204±0.008	-
P(DLLA-co-LLA) <sub>100</sub>	100	27.9	54.2	17.9	58,920	1.79	45.3	-	1.263±0.008	-

<sup>&</sup>lt;sup>1</sup> calculated from <sup>13</sup>C NMR spectra,

<sup>2</sup>crystallinity (%) = 
$$\frac{\Delta H_m - \Delta H_c}{\Delta H_f^{\circ}} \times 100$$
, where  $\Delta H_f^{\circ} = 96$  J/g [26]

Density results of the copolymers, as also summarized in table 1, show a decrease in the density values when the DLLA content of the copolymer increases from 0-5 %. However, when the DLLA content reaches 7.5%, a sudden increase in the value to 1.537±0.007 g/cm³ is observed. Upon further increasing the DLLA content in the copolymer

chain, a decreasing trend of the density values is re-observed. The former decreasing trend is probably originated from a decrease in the crystalline content of the copolymers, calculated from DSC thermograms as also summarized in Table 1. However, a sudden increase in the value and the latter decreasing trend observed in the complete amorphous copolymers series with DLLA content of higher than 7.5% is intriguing. This is probably associated with formation of different chain arrangement, which will be explained later.

Thermal properties of the copolymers derived from the second-heating cycle DSC thermograms are also summarized in Table 1. The results show that PLLA exhibits a glass transition temperature ( $T_g$ ) at 68°C. As DLLA is incorporated into the copolymer chains, the  $T_g$  of the copolymers decreases with an increase in DLLA content, i.e., an increase in  $T_g$  from 59.2 to 45.3°C is observed for copolymers derived from DLLA contents of 2.5 to 100 mol%. Melting characteristic peak is only observed in thermograms of PLLA homopolymer and copolymers containing DLLA contents of less than 10 mol%, reflecting the maximum DLLA content to produce semi-crystalline copolymers. The melting temperature ( $T_m$ ) of the copolymers also decreases as DLLA content increases in the copolymer chains, due to shorter sequences of LLA in the copolymer chains.

Similar trend is also observed on crystallinity of the corresponding copolymers consisting of low DLLA contents, where crystallinity decreases from 48.1% to 1.7% for PLLA and P(DLLA-co-LLA)<sub>10</sub>, respectively. On the other hand, copolymers consisting of DLLA content higher than 10 mol% exhibit amorphous characteristic. This indicates that the incorporated DLLA units act as defects in LLA segments, resulting in an interruption of crystal formation that leads to reduction of  $T_g$  and  $T_m$  values, as well as crystallinity of the copolymers.

#### Mechanical properties

Tensile properties of P(DLLA-co-LLA)<sub>x</sub> copolymers as a function of DLLA contents are summarized in Figure 1. The results on modulus, tensile strength and elongation at break of PLLA and P(DLLA-co-LLA)<sub>100</sub> observed in this study are comparable to those reported earlier [1, 5, 17]. Figure 1 clearly shows that the characteristic trends of tensile strength and modulus of the copolymers as a function of DLLA content are almost identical. An enhancement of these two properties is achieved by introducing DLLA comonomer into PLLA chains at DLLA contents of up to 7.5%. This mechanical property enhancement is intriguing, given that the introduction of DLLA units causes a reduction in crystallinity, T<sub>g</sub>,

and T<sub>m</sub> of the copolymers, as previously discussed. This is coincided with the sudden increase in density of the P(DLLA-co-LLA)<sub>7.5</sub> copolymer, which may also associated with the same origin. However, further increase in the DLLA content results in a drastic drop in the copolymers strength and modulus. This is in concert with the amorphous nature of the copolymers, as discussed earlier. The drop in the properties is mainly due to a destruction of crystalline domains in the copolymer matrix. Interestingly, an unusual increase in tensile strength and modulus was re-observed in copolymer containing DLLA content of 50%, i.e. P(DLLA-co-LLA)<sub>50</sub>, which are much higher than those of PLLA and P(DLLA-co-LLA)<sub>100</sub> counterparts.

\_\_\_\_\_\_

**Figure 1.** Young's modulus, Tensile strength and Elongation at break of PLLA and P(LLA-co-DLLA)<sub>x</sub> copolymers as a function of DLLA composition. The dotted line indicates those of PLLA/PDLA stereocomplex [5].

In addition, Figure 1 also shows data on elongation at break of the copolymers as a function of DLLA content. The results indicate that the elongation is independent on the DLLA composition, when the content is kept lower than 20%. A drastic increase in the value is observed upon increasing the DLLA content from 30% to 50%, where the maximum elongation of 150% is achieved. The corresponding value of P(DLLA-co-LLA)<sub>100</sub>, however, decreases to 40%. Given the mechanical properties of PDLA/PLLA stereocomplex reported by Tsuji et al.[5] (See Figure 1), it is clearly seen that the stereocomplex showed higher strength and modulus, compared to PLLA and PDLA homopolymers, and P(DLLA-co-LLA)<sub>100</sub>. However, these are still inferior to those of the P(DLLA-co-LLA)<sub>7.5</sub>. In addition, it is obvious that mechanical properties of these copolymers are strongly dependent on the monomer compositions. As a result, these materials are suitable candidates for producing degradable polyesters with tunable mechanical properties.

#### Effects of structure and interactions on mechanical properties

To obtain an insight into the origin of the enhancement in mechanical properties of  $P(DLLA-co-LLA)_x$ , XRD and FTIR spectroscopy are employed to study the nature of chain structures and interactions. XRD spectra of PLLA, PDLA/PLLA stereocomplex and the copolymers are compared in Figure 2. The spectrum of PLLA shows crystal characteristics signal at  $2\theta = 14.6^{\circ}$ ,  $16.6^{\circ}$ ,  $18.9^{\circ}$ , which is corresponding to 110,  $110\alpha/220\alpha$ ,  $203\alpha$  planes in

its  $10_3$  helical conformation[27]. The corresponding spectrum of PDLA/PLLA stereocomplex shows signals located at  $2\theta = 11.9^{\circ}$ ,  $20.8^{\circ}$  and  $24^{\circ}$ , which reflects 110, 300, and 220 planes in the  $3_1$  helical conformation of stereocomplex crystalline domains[27].

**Figure 2.** XRD traces of PLLA (a), PDLA/PLLA stereocomplex (b), P(LLA-*co*-DLLA)<sub>2.5</sub> (c), P(LLA-*co*-DLLA)<sub>7.5</sub> (d), P(LLA-*co*-DLLA)<sub>50</sub> (e), and P(LLA-*co*-DLLA)<sub>100</sub> (f).

.....

The corresponding spectra of P(LLA-co-DLLA)<sub>x</sub> copolymers show a broad pattern covering 20 angle of 10° to 25°, reflecting the amorphous characteristics of the samples. Weak crystalline patterns are observed only in P(LLA-co-DLLA)<sub>2.5</sub>, which is similar to those found in neat PLLA. This finding slightly differs from those obtained from DSC experiments, where crystalline melting peaks are observed in copolymers consisting of DLLA content of up to 10%. This is probably because the crystalline domains present in P(LLA-co-DLLA)<sub>7.5</sub>and P(LLA-co-DLLA)<sub>10</sub> consists of shorter LLA sequence than the detectable limit of XRD experiments. Nevertheless, DSC thermograms of the particular copolymers show weak T<sub>m</sub> peaks located at much lower temperature and lower  $\Delta H_{m}$ , compared to those of neat PLLA. Interestingly, weak but sharp signals located at  $2\theta = 9.4^{\circ}$ , 28.7°, and 44.4°, corresponding to d-spacing of 9.4, 3.1 and 2.0 Å, respectively, are observed in all copolymer samples. The signals are not observed in the spectra of homopolymers and the stereocomplex blend. This indicates a presence of order structures with respective dspacings in the copolymers, which is probably an origin of the mechanical property enhancement in certain P(LLA-co-DLLA)<sub>x</sub> copolymers.

FTIR spectroscopy is employed to study chain structures and interactions of the copolymers. Given that polylactides and PLLA/PDLA blend can form various types of crystal structures, i.e.,  $\alpha$ ,  $\alpha$ ',  $\gamma$  and  $\beta$ , this can be characterized by FTIR spectroscopy by employing vibrational modes of carbonyl, C-C backbone,  $C_{\alpha}$ -H, and  $-CH_3$  groups, as these are sensitive to chain structures and conformations [12, 13, 28, 29]. In neat PLLA or PDLA, the chains are in a  $10_3$  helical conformation, and dipole-dipole interaction is formed. The band characteristic of this crystal structure is observed at 921 cm<sup>-1</sup> (coupling of C-C stretching with the -CH<sub>3</sub> rocking mode). On the other hand, a stronger C=O··H-C hydrogen bonds formed in the crystal structure of the stereocomplex blend, where the polymer chains are in a  $3_1$  helical conformation. This is reflected by a characteristic band located at 909 cm<sup>-1</sup> [12, 13, 28-30].

FTIR spectra in the 1000-900 cm<sup>-1</sup> region of P(LLA-*co*-DLLA)<sub>x</sub> copolymers as a function of DLLA content are shown in Figure 3, where those of PLLA and stereocomplex are also compared. The spectra of PLLA homopolymer and P(LLA-*co*-DLLA)<sub>x</sub> copolymers with DLLA contents of up to 10% exhibit a characteristic band of single crystallite at 924 cm<sup>-1</sup>. A unique band characteristic of stereocomplex located at 909 cm<sup>-1</sup> is not observed in all copolymers, reflecting that a formation of such structure is unlikely in these copolymers at all compositions. Intriguingly, a higher frequency band is observed at 935 cm<sup>-1</sup> in copolymer samples containing DLLA contents of up to 7.5%, and at 50%. The appearance of this band in the spectra of these particular samples, which show relatively higher modulus, strength, and elongation, indicates that this vibrational mode is probably derived from structural conformations that are responsible for the improved properties, especially in P(LLA-*co*-DLLA)<sub>50</sub>, which is an amorphous sample. Given the correlation of band position and helical structure of 10<sub>3</sub> and 3<sub>1</sub> of the homocrystalite and stereocomplex, located at 920 and 909 cm<sup>-1</sup>, respectively, the new band observed here (at higher frequency) probably indicates lower strain in the helical structure.

\_\_\_\_\_

**Figure 3.** FTIR spectra in the 1000-900 cm<sup>-1</sup> region of PDLA/PLLA stereocomplex (a), PLLA (b), and P(LLA-co-DLLA)<sub>x</sub> copolymers with DLLA content of: 2.5% (c), 7.5% (d), 10% (e), 30% (f), 50% (g), and 100% (h).

\_\_\_\_\_

Directional behavior of the vibrational modes in the 1000-900 cm<sup>-1</sup> region is studied by examining parallel and perpendicular spectra of the copolymers, as shown in Figure 4 (lower and top spectrum, respectively). The spectra of semi-crystalline PLLA and P(LLA-co-DLLA)<sub>7.5</sub> show that the intensity of the 924 cm<sup>-1</sup> band (due to the 10<sub>3</sub> helical conformations) is dependent on the measurement directions, as this is originated from anisotropic arrangement of the single crystalline domains. The 935 cm<sup>-1</sup> band observed in the copolymers, however, is directional independent, as evidenced from the spectrum of P(LLA-co-DLLA)<sub>50</sub>. This indicates that conformational structures that are origins of this vibrational mode are randomly aligned in the amorphous matrix.

**Figure 4.** Polarized FTIR spectra in the 1000-900 cm<sup>-1</sup> region of PLLA (a), P(LLA-co-DLLA)<sub>7.5</sub> (b), P(LLA-co-DLLA)<sub>50</sub> (c), and P(LLA-co-DLLA)<sub>100</sub> (d). (Top: perpendicular, lower: parallel spectrum)

.....

Information on interactions in polylactides structure can also be derived from band position of the C-H stretching modes located in the 3000 cm<sup>-1</sup> region, where three groups of band are assigned orderly from high to low frequency as  $\nu(C_{\alpha}H)$ ,  $\nu_s(CH_3)$ ,  $\nu_{as}(CH_3)$ , respectively. It was reported that a red shift of the three bands to lower frequency indicated formation of strong C=O·H-C hydrogen bonding in stereocomplex [30]. FTIR spectra of the P(LLA-co-DLLA)<sub>x</sub> copolymers in the C-H stretching region are shown in Figure 5. It is clearly seen that the 3 vibrational modes of the copolymers are located in the middle of that of the two extreme of PLLA and stereocomplex and dependent on copolymer compositon, which probably indicate of formation of interation

-CH<sub>3</sub> vibrational mode of PLLA and stereocomplex is located at 2994 and 2998 cm<sup>-1</sup>, respectively. The corresponding band of the copolymers is located in between the two extremes at 2996 cm<sup>-1</sup>. The relatively higher frequency of the band, compared to those of the coupled C-C backbone vibrational mode in the structures of homocrystalite and stereocomplex, indicates weaker interactions associated with the corresponding -CH<sub>3</sub> and C=O functional groups.

\_\_\_\_\_

**Figure 5**. FTIR spectra in the –CH<sub>3</sub> stretching mode region of PDLA/PLLA stereocomplex (a), PLLA (b), and P(LLA-co-DLLA)<sub>x</sub> copolymers with DLLA content of: 2.5% (c), 7.5% (d), 10% (e), 30% (f), 50% (g), and 100 % (h).

\_\_\_\_\_\_

Interestingly, a new band centered ~3030 cm<sup>-1</sup> is clearly observed in FTIR spectra of all P(LLA-*co*-DLLA)<sub>x</sub> copolymers. This unusual band is not found in those of PLLA and PDLA/PLLA stereocomplex. A close examination on the vibrational mode indicates an increase in band intensity as a function of DLLA content for copolymers with low DLLA compositions, where the most intense band is observed in P(LLA-*co*-DLLA)<sub>30</sub>. When the DLLA content is further increased, however, the band inversely shifts to lower frequency. The presence of this band is similar to that observed in crystallization of PHBV reported by Hu et. al.[31], which were assigned to a formation of C-H OC hydrogen bonding[32]. As the

repeat unit of PHBV contain longer repeat unit, compared to that of PLA, and its CH3 groups is located at beta postion, it is likely that this is derived from the higher flexibility of the -CH<sub>3</sub> groups in the repeat units, which enables more freedom for placement of the groups in structural arrangement. In the case of copolymer it is lock conofitmation. The formation of this band at 3030 indicate even strong interaction between the CH3 and C=O groups.

Important structural information can also be obtained from the C-O-C band located in the 1330-1290 cm<sup>-1</sup> region, as shown in Figure 6 [xxx]. The spectra show that the vibrational mode is sensitive to structural conformation, where those of PLLA single crystallite show split bands located at 1304 and 1295 cm<sup>-1</sup>, which is probably due to crystalline splitting. The corresponding spectrum of stereocomplex also show bands spitting, but located at higher frequency at 1307 and 1300 cm<sup>-1</sup>, indicating higher strain in the helical structure. The spectrum of ...similar to those observed in methylene bridge of phenolic resin where linear and helix structure are dependent on the band location.

As relatively thick films were used in this study, quantitative information cannot be obtained from the carbonyl stretching band. However, the overtone bands of these vibrational modes can be employed. [11] Similar results to those obtained from the C-C backbone characteristics were observed. Spectrum of PLLA homopolymer shows overtone band due to single crystallite at 3508 cm<sup>-1</sup>, while that of stereocomplex exibhits a band at lower frequeny at 3485 cm<sup>-1</sup>, indicating stronger interaction involving C=O functional groups. The corresponding sprecta of copolymers show a broad band located at 3508cm<sup>-1</sup> and a showlder at 3560 cm<sup>-1</sup>. This is a mode that corresponding to probably free C=O, due to its lower interaction in the structure, probably associated with those present in the amorphous region. The spectrum of PDLLA7.5 show very sharp band at 3500 cm<sup>-1</sup> and the shoulder, perhaps due to an enhancement in the arragment.

This is probably derived from a formation of segmental interactions between the -CH<sub>3</sub> and C=O groups of DL and LL diads in the chain structure of copolymer in the amorphous domain. The similarity of the band intensity and pattern observed in the polarized spectra reflects that these point interactions are isotropic in nature. The randomly-distributed point interactions, perhaps, act as "physical crosslink" in the amorphous domain, which collectively results in an improvement of the copolymers bulk properties. The results also indicate that the formation of such structures is strongly dependent on the DLLA content of the copolymer, where optimum value was observed at 50%. In addition, the isotropic placement of the "physical crosslinks" also improves elastic behavior of amorphous copolymers, which is reflected in superior elongation at break of the P(LLA-co-DLLA) 50, as

proposed in Figure 8. A formation of such network-like structure was also observed by He et.al. in their study on effect of initial melt states of PDLA/PLLA stereocomplex on its crystallization behaviors. It was found that when PDLA/PLLA stereocomplex was melt at high temperature or longer melting time, the subsequent stereocomplex crystallization of the sample was depressed. This was because the strong CH<sub>3</sub> ·· O=C interaction between PDLA and PLLA chains was completely destroyed during the melting process, and the enantiomeric chains homogenously inter-penetrated one another in the blend matrix. This resulted in a random formation of the CH<sub>3</sub> ·· O=C strong interactions between segments of PDLA and PLLA in the melt, which subsequently prevented a crystallization of larger domain-sized stereocomplex.[24] Given its entropic driving force and its superior collective strength, the formation of such random segmental interactions is able to prevent melt crystallization of stereocomplex. It is therefore likely that similar structure is present in the structure of PDLLA copolymers, where a random formation of segmental interaction is also responsible for the enhancement in the materials properties, especially their high elongation at break.

#### **Conclusions**

P(LLA-co-DLLA) copolymers have been synthesized by ring-opening polymerization of L-lactide and D,L-lactide using Sn(II)-ethylhexanoate [Sn(Oct<sub>2</sub>)] as a catalyst. The resulting high molecular weight copolymers have Mn in the range of  $5.8 \times 10^4$  to  $11.8 \times 10^4$ . The incorporation of DLLA units results in a modification of thermal and mechanical properties of the copolymers.  $T_g$  and  $T_m$  of the copolymers decreased with an increase in DLLA comonomer in copolymer chains. The Young's modulus and tensile strength were obviously improved upon addition of DLLA comonomer units, where an optimum value was achieved in copolymer with 7.5 mol% monomer in feed. In addition, elongation at break of the copolymers is also affected by the DLLA content, where the largest improvement was observed in copolymer with 50 mol% of DLLA. The origin of this properties enhancement was investigated by polarized FTIR spectroscopy. The result indicated a formation of point interaction between DL and LL diads of the copolymer chain, which acts as a "physical crosslink" in the amorphous phase of the copolymers.

## Acknowledgement

Financial support of this work is provided by The Thailand Research Fund (TRF)/ The Commission on Higher Education (CHE), RTA5180003, and Thailand Toray Science Foundation.



#### References

- [1] Albertsson AC, Stridsberg KM, Ryner M. Controlled Ring-Opening Polymerization: Polymers with designed Macromolecular Architecture. Advances in Polymer Science 2002; 157: 41-65.
- [2] Jacobsen S, Degee PH, Fritz, HG, Dubois PH, Jerome R. Polylactide(PLA)-A new way of production. Polymer Engineering and Science 1999; 39:1311-1319.
- [3] Ouchi T, Ichimura S, Ohya Y. Synthesis of branched poly(lactide) using polyglycidol and thermal, mechanical properties of its solution-cast film. Polymer 2006; 47: 429-434.
- [4] Tsuji H, Ikada Y. Stereocomplex formation between enantiomeric poly(lactic acid)s. XI. Mechanical properties and morphology of solution-cast films. Polymer 1999; 40: 6699-6708.
- [5] Kimura Y, Fukushima K. Stereocomplexed polylactide (Neo-PLA) as high-performance bio-based polymers: their formation, properties, and application. Polymer International 2006; 55: 626-642.
- [6] Chen GX, Kim HS, Kim ES, Yoon JS. Synthesis of high-molecular-weight poly(L-lactic acid) through the direct condensation polymerization of L-lactic acid in bulk state. Europian Polymer Journal 2006; 42: 468-472.
- [7] Lima LT, Aurasb R, Rubinob M. Processing technologies for poly(lactic acid). Progress in Polymer Science 2008 (article in press).
- [8] Zhang J, Sato H, Tsuji H, Noda I, Ozaki Y. Infrared spectroscopic study of CH<sub>3</sub>·· O=C interaction during poly(L-lactide)/poly(D-lactide) stereocomplex formation, Macromolecules 2005; 38: 1822-1828.
- [9] Zhang J,Tashiro K, Tsuji H, Domb AJ. Investigation of phase transitional behavior of poly(L-lactide)/poly(D-lactide) blend used to prepare the highly-oriented stereocomplex. Macromolecules 2007; 40: 1049-1054.
- [10] Meaurio E, Zuza E, Lopez-Rodriguez N, Sarasua JR. Conformational behavior of poly(L-lactide) studied by infrared spectroscopy. Journal of Physical Chemistry B 2006; 110: 5790-5800.
- [11] Opaprakasit P, Opaprakasit M, Tangboriboonrat P. Crystallization of polylactide and its stereocomplex investigated by two-dimensional Fourier Transform Infrared correlation spectroscopy employing carbonyl overtones. Applied Spectroscopy 2007; 61: 1352-1358.

- 1. Fukushima, K. and Y. Kimura, *Stereocomplexed polylactides (Neo-PLA) as high-performance bio-based polymers: Their formation, properties, and application.* Polymer International, 2006. **55**(6): p. 626-642.
- 2. Lindblad, M.S., et al., *Polymers from renewable resources*, in *Advances in Polymer Science*. 2002. p. 139-161.
- 3. Lim, L.T., R. Auras, and M. Rubino, *Processing technologies for poly(lactic acid)*. Progress in Polymer Science (Oxford), 2008. **33**(8): p. 820-852.
- 4. Tsuji, H., *Poly(lactide) stereocomplexes: Formation, structure, properties, degradation, and applications.* Macromolecular Bioscience, 2005. **5**(7): p. 569-597.
- 5. Tsuji, H. and Y. Ikada, *Stereocomplex formation between enantiomeric poly(lactic acid)s. XI. Mechanical properties and morphology of solution-cast films.* Polymer, 1999. **40**(24): p. 6699-6708.
- 6. Brizzolara, D., et al., *Mechanism of the stereocomplex formation between enantiomeric poly(lactide)s.* Macromolecules, 1996. **29**(1): p. 191-197.
- 7. Urayama, H., T. Kanamori, and Y. Kimura, *Properties and biodegradability of polymer blends of poly(L-lactide)s with different optical purity of the lactate units.* Macromolecular Materials and Engineering, 2002. **287**(2): p. 116-121.
- 8. Urayama, H., S.I. Moon, and Y. Kimura, *Microstructure and thermal properties of polylactides with different L- and D-unit sequences: Importance of the helical nature of the L-sequenced segments.* Macromolecular Materials and Engineering, 2003. **288**(2): p. 137-143.
- 9. Ouchi, T., S. Ichimura, and Y. Ohya, Synthesis of branched poly(lactide) using polyglycidol and thermal, mechanical properties of its solution-cast film. Polymer, 2006. 47(1): p. 429-434.
- 10. Stridsberg, K.M., M. Ryner, and A.C. Albertsson, *Controlled ring-opening polymerization: Polymers with designed macromolecular architecture*, in *Advances in Polymer Science*. 2002. p. 41-65.
- 11. Jacobsen, S., et al., *Polylactide (PLA) a new way of production*. Polymer Engineering and Science, 1999. **39**(7): p. 1311-1319.
- 12. Opaprakasit, P., M. Opaprakasit, and P. Tangboriboonrat, *Crystallization of polylactide and its stereocomplex investigated by two-dimensional Fourier transform infrared correlation spectroscopy employing carbonyl overtones.* Applied Spectroscopy, 2007. **61**(12): p. 1352-1358.
- 13. Zhang, J.M., et al., *Infrared spectroscopic study of CH3 center dot center dot center dot O=C interaction during poly(L-lactide)/poly(D-lactide) stereocomplex formation*. Macromolecules, 2005. **38**(5): p. 1822-1828.
- 14. Zhang, J.M., et al., Structural changes and crystallization dynamics of poly(L-lactide) during the cold-crystallization process investigated by infrared and two-dimensional infrared correlation spectroscopy. Macromolecules, 2004. **37**(17): p. 6433-6439.
- 15. Zhang, J.M., et al., Weak intermolecular interactions during the melt crystallization of Poly(L-lactide) investigated by two-dimensional infrared correlation spectroscopy. Journal of Physical Chemistry B, 2004. **108**(31): p. 11514-11520.
- 16. Fukuzaki, H., et al., Synthesis of copoly(d,l-lactic acid) with relatively low molecular weight and in vitro degradation. European Polymer Journal, 1989. **25**(10): p. 1019-1026.
- 17. Ferguson, S., D. Wahl, and S. Gogolewski, *Enhancement of the mechanical properties of polylactides by solid-state extrusion. II. Poly(L-lactide), poly(L/D-lactide), and poly(L/DL-lactide).* Journal of Biomedical Materials Research, 1996. **30**(4): p. 543-551.

- 18. Bigg, D.M., *Polylactide copolymers: Effect of copolymer ratio and end capping on their properties.* Advances in Polymer Technology, 2005. **24**(2): p. 69-82.
- 19. Albertsson, A.C. and I.K. Varma, *Aliphatic polyesters: Synthesis, properties and applications*, in *Degradable Aliphatic Polyesters*. 2002. p. 1-40.
- 20. Stridsberg, K.M., M. Ryner, and A.C. Albertsson, *Controlled ring-opening polymerization: Polymers with designed macromolecular architecture*, in *Degradable Aliphatic Polyesters*. 2002. p. 41-65.
- 21. von Schenck, H., et al., *Ring-opening polymerization of lactones and lactides with Sn(IV) and Al(III) initiators.* Macromolecules, 2002. **35**(5): p. 1556-1562.
- 22. Chabot, F., et al., Configurational structures of lactic acid stereocopolymers as determined by 13C{1H} n.m.r. Polymer, 1983. **24**(1): p. 53-59.
- 23. Chen, G.X., et al., Synthesis of high-molecular-weight poly(l-lactic acid) through the direct condensation polymerization of l-lactic acid in bulk state. European Polymer Journal, 2006. **42**(2): p. 468-472.
- 24. He, Y., et al., *Unique crystallization behavior of poly(l-lactide)/poly(d-lactide)* stereocomplex depending on initial melt states. Polymer, 2008. **49**(26): p. 5670-5675.
- 25. Pan, P., et al., *Polymorphous crystallization and multiple melting behavior of poly(L-lactide): Molecular weight dependence.* Macromolecules, 2007. **40**(19): p. 6898-6905.
- 26. Lin, Y., et al., Study of Hydrogen-Bonded Blend of Polylactide with Biodegradable Hyperbranched Poly(ester amide). Macromolecules, 2007. **40**(17): p. 6257-6267.
- 27. Fujita, M., et al., Stereocomplex Formation through Reorganization of Poly(l-lactic acid) and Poly(d-lactic acid) Crystals. Macromolecules, 2008. 41(8): p. 2852-2858.
- 28. Meaurio, E., et al., *Conformational behavior of poly(L-lactide) studied by infrared spectroscopy.* Journal of Physical Chemistry B, 2006. **110**(11): p. 5790-5800.
- 29. Zhang, J., et al., *Investigation of phase transitional behavior of poly(L-lactide)/* poly(D-lactide) blend used to prepare the highly-oriented stereocomplex. Macromolecules, 2007. **40**(4): p. 1049-1054.
- 30. Sarasua, J.R., et al., *Stereoselective crystallization and specific interactions in polylactides*. Macromolecules, 2005. **38**(20): p. 8362-8371.
- 31. Hu, Y., et al., *C-H*\(\text{\gamma}\)*O=C hydrogen bonding and isothermal crystallization kinetics of poly(3-hydroxybutyrate) investigated by near-infrared spectroscopy.*Macromolecules, 2006. **39**(11): p. 3841-3847.
- 32. Zhang, J., et al., Conformation rearrangement and molecular dynamics of poly(3-hydroxybutyrate) during the melt-crystallization process investigated by infrared and two-dimensional infrared correlation spectroscopy. Macromolecules, 2005. **38**(10): p. 4274-4281.

## Property Modification of Epoxidized Natural Rubber: Crosslinking by Reactive Blend Technique of Poly(L-Lactic Acid-co-Ethylene Glycol) Block Copolymers

Thai-Hien Nguyen<sup>1</sup>, Pramuan Tangboriboonrat<sup>2</sup>, Nittaya Rattanasom<sup>3</sup>, Atitsa Petchsuk<sup>4</sup>, Mantana Opaprakasit<sup>5</sup>, Pakorn Opaprakasit<sup>1</sup>\*

<sup>1</sup> School of Bio-Chemical Engineering and Technology, Sirindhorn International Institute of Technology (SIIT), Thammasat University, Pathum Thani 12121, Thailand

<sup>2</sup> Department of Chemistry, Mahidol University, Bangkok 10400 Thailand

<sup>3</sup>Institute of Molecular Biosciences, Mahidol University, Salaya, Nakhon Pathom 73170, Thailand

Tel: +66 (0) 2986 9009 Ext. 1806

Fax: +66 (0) 2986 9009 Ext. 1801

E-mail: pakorn@siit.tu.ac.th

<sup>&</sup>lt;sup>4</sup> National Metal and Material Technology Center (MTEC), Pathum Thani 12120, Thailand

<sup>&</sup>lt;sup>5</sup> Department of Materials Science, Chulalongkorn University, Bangkok 10330, Thailand

<sup>\*</sup> Corresponding author

#### **Abstract**

Property modification of epoxidized natural rubber (ENR) was studied by croslinking with Poly(L-Lactic Acid-co-Ethylene Glycol) Block Copolymers (PLLA<sub>46</sub>/PEG<sub>46</sub>/PLLA<sub>46</sub>) using a Moving Rheometer (MDR, TechPro MD+). Chemical structure and properties of the products were characterized by <sup>1</sup>H-NMR. Curing characteristic, swelling behavior and thermal properties of the blends cured using ENR and PLLA<sub>46</sub>/PEG<sub>46</sub>/PLLA<sub>46</sub> triblock copolymer were investigated. Results indicate that the maximum elastic and viscous torque increased as a function of increasing copolymer content. However, a reverse trend was observed for tanð. The swelling ratio increased with decreasing ENR composition in the blend. Thermal stability property was determined by TGA.

Keywords: Epoxidized natural rubber, PLLA/PEG copolymer, blend, curing characteritics



#### 1. Introduction

Epoxidized natural rubber (ENR) is chemical modified natural rubber (NR) product obtained from the introduction of epoxide groups into NR backbone to enhance its properties such as higher hysteresis, oil resistance and lower air permeability [1-3]. ENR contains both epoxide and unsaturated sites, in which epoxide groups are reactive toward nucleophilic reagents, while the double bond is conventionally use as typical crosslink points by using various curing agents [4-14]. Reaction through epoxide groups were carried out by reactive blending of ENR with other polar components such as carboxylated nitrile rubber [4,5], chlorosulfonated polyethylene rubber,[5,6] polychloroprene rubber [4,7], polypropylene [8], ethylene vinyl acetate [9,10], *p*-phenylenediamine [11-13], butylphosphate [14].

LLA/EG/LLA triblock copolymers are materials that combine good characteristics of PEG and PLLA polymers, biocompatibility and biodegradability [15-22]. Moreover, OH-capped in chain-end of triblock copolymer play as nucleophilic reagents to react with epoxide groups of ENR. There are several papers in the literature regarding to addition of hydroxyl groups onto ENR has been initiated for recent years and some accomplishments have been achieved so far [23-25]. Elastomeric rubber-plastic materials have become a great interest in rubber industry nowadays because they have properties of rubber and thermoplastic material [26]. Thus, this study focuses on the use of PLLA/PEG block copolymer with the OH-capped at the chain-end as a macromolecular crosslink agent for ENR to obtain elastomeric materials, which exhibits biocompatible and biodegradable properties for use in biomedical applications. Thus, crosslinking of ENR-PLLA/PEG block copolymer by a reactive blend process was conducted to obtain elastormeric material. In this process mixtures of ENR and the copolymer and catalyst were prepared and then subjected to elastic torque measurement to study its *in situ* crosslinking characteristics. In this study, the mixing torque value, swelling ratio as well as thermal properties of ENR-PLLA/PEG blend were investigated.

## 2. Experimental

#### 2.1 Materials

LLA<sub>46</sub>/EG<sub>46</sub>/LLA<sub>46</sub> triblock copolymer was synthesized by the methodology reported in the previous study [27]. ENR with 20% epoxidation was synthesized from commercial high ammonia (HA)-preserved NR latex concentrate (Rayong Bangkok Rubber, Thailand). Epoxidation procedure was similar to that reported by Saendee et al. [28]. Dried tetrahydrofuran (THF) was used as a solvent in a mixing process. Sn(Oct)<sub>2</sub> (Wako) was used as a catalyst in the curing of the materials.

## 2.2 Crosslinking of ENR by LLA/EG copolymer

Crosslinking of ENR by OH-capped LLA/EG copolymer was conducted by a reactive blend process. This is achieved by reactions of OH groups of copolymer with epoxide groups of ENR through ring opening reaction with Sn(Oct)<sub>2</sub> as a catalyst [29]. A mixture of ENR/copolymer and the catalyst was first prepared. Essentially, ENR and copolymer were separately dissolved in dried THF at 50°C. ENR solution was then cooled to 30°C. Sn(Oct)<sub>2</sub> catalyst was added in the copolymer solution and stirred for 1 hour. The solution of copolymer and catalyst was slowly added into the ENR solution. Finally, homogeneous mixtures of ENR, copolymer and catalyst were obtained by evaporation of the solvent under vacuum pressure. Compositions of ENR and copolymers of various mixtures, 4/1, 2/1, 1/1 by weight, are referred to as T41, T21, and T11, respectively.

The cure characteristics of ENR-LLA/EG sample in the reactive blend process were assessed *in situ* by using a moving die rheometer (MDR, TechPro MD+) at 80 °C in accordance with ISO 6502. Elastic and viscous torques were measured as function of curing time.

Soxhlet extraction experiments were carried out to determine the content of soluble and insoluble fractions by using THF at 110°C for 24 hours. The insoluble (denoted by "I") and soluble fractions (denoted by "S") of each sample were recovered by evaporation of the solvent and dried in a vacuum oven at room temperature until a constant weight was reached.

Chemical structure and chain composition of the triblock copolymers were characterized by <sup>1</sup>H-NMR on a Bruker DRX400 using CDCl<sub>3</sub> as a solvent. Decomposition temperatures (T<sub>d</sub>) of the cured samples were determined on a Mettler Toledo TGA/SDTA 851, using nitrogen atmosphere. The samples were scanned from 50°C to 1000°C with a heating rate of 20°C/min.

The crosslink density was measured by using the swelling method. A piece of crosslinked sample (approximately 0.2 g) was accurately weighed and immersed in toluene (40ml) at room temperature in a dark cabinet. At equilibrium swelling time (about 7 days), the test piece was removed from toluene, wiped with filter paper, and its weight was recorded. The swelling ratios were calculated as follows:

%Swelling = 
$$\frac{W_{eq} - W_o}{W_o} \times 100$$

where  $W_0$  = original weight of dried sample (g)

 $W_{eq}$  = weight of swollen sample at equilibrium swelling time(g)

Solvent taken up by the swollen samples after equilibrium swelling was then completely removed by air dry at room temperature for at least 1 month until a constant weight was reached. The remaining weight was recorded, and the weight loss of the sample, which reflect weight fractions of sample dissolved into toluene solvent during the swelling experiment were calculated, as follows:

% weight loss = 
$$\frac{W_o - W_d}{W_o} \times 100$$

where  $W_0$  = weight of original dried sample before swelling experiment (g)

 $W_d$  = remaining weight of dried sample after swelling experiment (g)

# 3. Results and Discussion

In previous study, OH-capped LLA/EG triblock copolymer is used as crosslinking agent for ENR by using Sn(Oct)<sub>2</sub> as a catalyst with chemical reaction technique. <sup>1</sup>H-NMR spectra indicate formation of chemical bond between copolymer and ENR by ring opening reaction of epoxide groups by OH end chain of copolymer [29]. With the application of Sn(Oct)<sub>2</sub> catalyst, formation of crosslinked ENR with the copolymer takes places, resulting in further increase in the tensile properties [29].

# 3.1 Curing characteristics of samples during reactive blending process

The steady-state elastic torques of ENR/copolymer mixture as a function of compositions are shown in Figure 1. The maximum torque increases with an increase in the copolymer content, reflecting an increase in modulus of the mixtures. This is probably because the presence of the copolymer in the rubber matrix results in a mobility restriction of ENR molecules and consequently increases the elastic torque of the mixture. In addition, epoxide of ENR is able to react with the hydroxyl end groups of copolymer to form crosslinked network. This significantly contributes to the decrease in chain flexibility and the increase in the elasticity of the structure with increasing copolymer content.

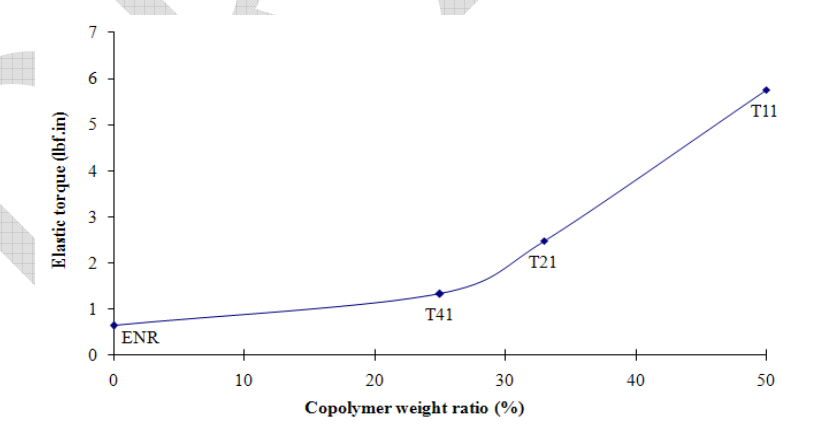


Figure 1 Maximum elastic torques as a function of ENR/copolymer compositions

Figure 2 shows that the maximum viscous torques also increase with an increase in the copolymer composition. This is surprising, as it was expected that the formation of crosslinked ENR by using LLA/EG block copolymer should lead to a decrease in viscous

torques. This is probably due to a combination of crosslinking and simple blending characteristic of ENR and copolymer in the mixtures. Although increasing of copolymer composition in the mixture provides higher amount of OH groups for enhancements of improves crosslinking reaction, this may lead to an excess amount of copolymers which are not crosslinked. It is likely that some copolymer chains may react with ENR only one end (grafting) or may not react (simple blend), as the copolymer is macromolecule crosslinker. This results in an increase in the flow characteristics of the mixture and, in turn, increases the viscous torques or damping behavior of the material.

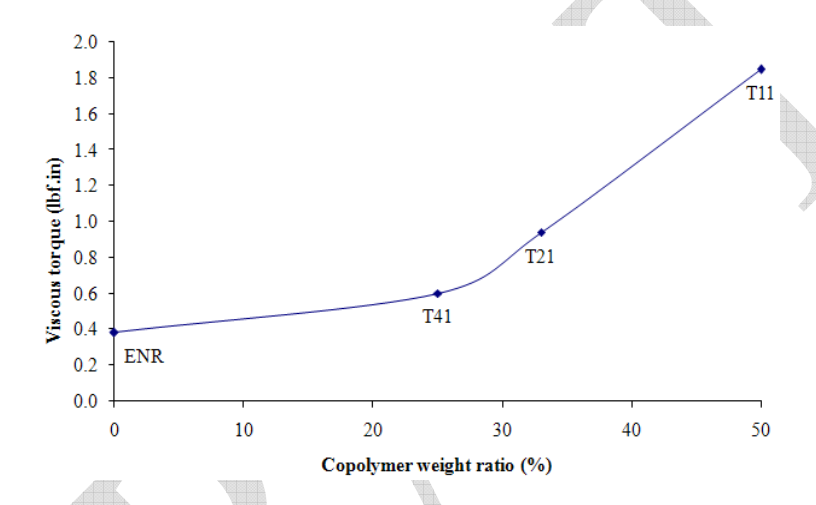


Figure 2 Maximum viscous torques as a function of ENR/copolymer compositions

Loss tangent (tan  $\delta$ ) at maximum elastic torque of samples at various ENR/copolymer compositions is shown in Figure 3. Tan  $\delta$  is the ratio of viscous to elastic torque, indicating relative viscous/elastic behaviors. A decrease in tan  $\delta$  with an increase in copolymer content indicates that the relative elastic behavior of the crosslinked samples improves with an increase in copolymer composition. This indicate a higher effectiveness of crosslinking process as a function of copolymer content, as this results in an improvement in elasticity of the material, compared to damping behavior derive from simple blend.

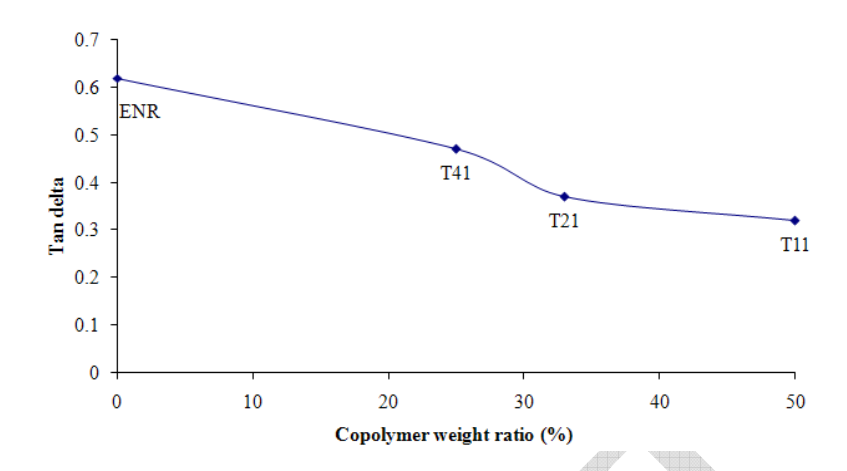


Figure 3 Maximum tan δ as a function of ENR/copolymer compositions

# $3.2^{-1}$ H-NMR characterization

Results on copolymer composition of samples after reactive blend process are summarized in Table 1. The results indicate that the presence of copolymer in insoluble samples TI, decreases with increasing ENR content. The disappearance of copolymer in TI11 can be explained base on its hard crosslink network because of high concentration of copolymer. This hard crosslink network cannot dissolve in CDCl<sub>3</sub> which is the solvent for <sup>1</sup>H-NMR. Therefore, the <sup>1</sup>H-NMR cannot detect integrated peak area value of one methine proton (5.10 ppm) of monomer of copolymer in rubber network.

Table 1 Weight compositions of copolymers in extracted products of samples after reactive blending

process					
	C(%)	wt (%)			
TII1	N/A	25			
TS11	100	72			
TI21	21	35			
TS21	86	62			
TI41	19	47			
TS41	42	42			

# 3.3 Degree of crosslinking

Degree of crosslinking of T and TI samples were carried out in toluene based on the completely soluble characteristic of ENR and LLA/EG/LLA triblock copolymer and the insoluble behavior of cured sample after crosslinking at room temperature. Figure 4 shows

that the swelling ratios of crosslinked samples decrease with increasing copolymer composition. T and TI represent the original samples before THF Soxhlet extraction and the THF insoluble fraction of sample after extraction, respectively. The swelling ratio of both T and TI fraction are more than 400 %. Aprem et al. reported that the swelling ration of sulfur vucalnization of natural rubber is less than 550 % [30]. It is probably because the copolymer acts as long chain-linking junction that creates more vacance in the rubber network. In the sample with higher copolymer content, the crosslink reaction is dominant and a high crosslinked network is formed, leading to a decrease in the swelling ratio. This confirms the result on <sup>1</sup>H-NMR spectra, where no signal due to copolymer is observed, as previously discussed in Table 1. TI11 sample has a hard crosslinked network because of high concentration of copolymer, so it cannot be dissolved in CDCl<sub>3</sub> which is the solvent for <sup>1</sup>H-NMR experiment. Therefore, the <sup>1</sup>H-NMR cannot detect integrated peak area value of one methyne proton (5.10 ppm) of monomer of copolymer in rubber network.

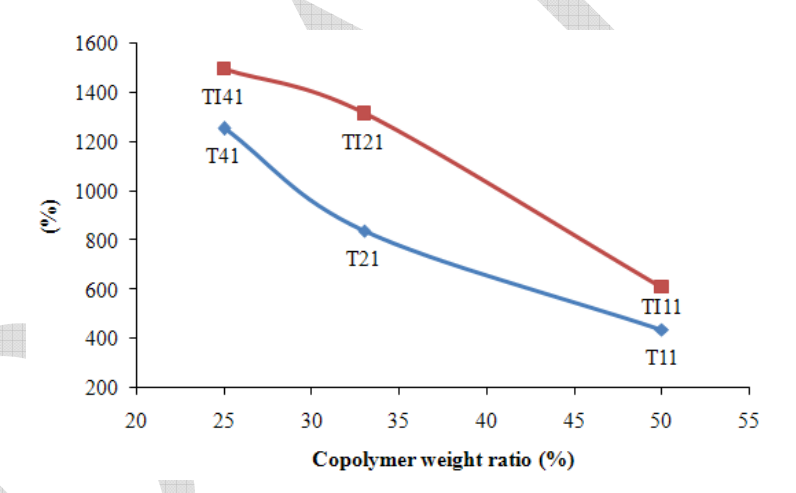


Figure 4 Swelling behavior of samples from reactive blend process as a function of ENR/copolymer composition

The weight losses of samples after swelling experiments are shown in Figure 5. The weight losses decrease as a function of increasing copolymer content. This confirms the results on swelling ratio, where the composition of 1/1 gives the highest crosslink density, lowest swelling ratio, or weight loss whereas the composition of 4/1 gives the lowest crosslink density, highest swelling ratio, or highest weight loss. This also confirms the presence of copolymer either as grafted or crosslinked copolymer on the ENR backbone. In samples with

lower copolymer content, 2/1 and 4/1, the grafting reaction is dominant, leading to a higher weight loss values because simple grafting or lightly crosslink can dissolve in toluene.

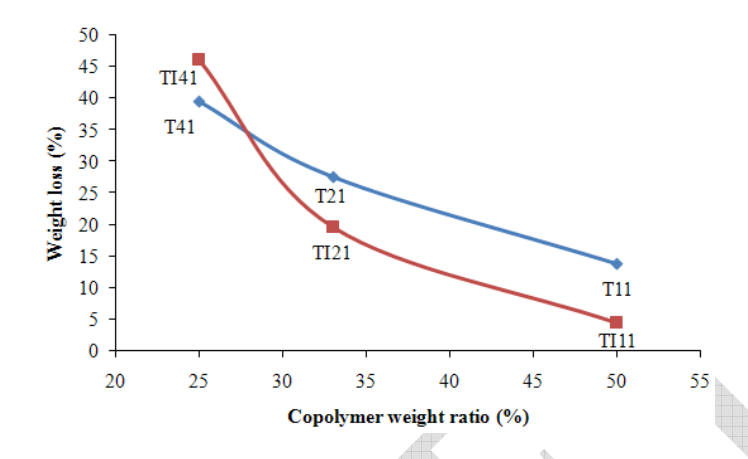


Figure 5 Weight losses after swelling ratio experiments

# 3.4 TGA thermogram

Thermal stability of samples as a function of ENR/copolymer composition is examined. Figure 6 (a) and Figure 7 (a) show TGA curves of THF insoluble (TI) and soluble fractions (TS) after Soxhlet extraction. It is clearly seen that the degradation temperatures of TI and TS start at 287°C and complete at 490°C. Thermal degradation temperatures of copolymer and ENR, T<sub>dC</sub> and T<sub>dE</sub>, are conveniently determined from DTGA curves, as shown in Figure 6 (b) and Figure 7 (b). The degradable characteristics of sample are summarized in Figure 8, where four steps of degradation are observed from the second derivative TGA curve. LLA block in copolymer chain that react with ENR only with ENR only with one chain end (grafted LLA) and unreacted LLA blocks degrade first in the early stage at the temperature T<sub>d LLAg,f</sub> approximately 300°C. It was observed that T<sub>d</sub> of LLA in pure LLA/EG copolymer showed T<sub>d</sub> at 298°C [31]. The second degradation step is associated with junction LLA block. This presence of this degradation temperature (T<sub>d LLAc</sub>) at approximately 350°C indicates formation of ENR crosslinked network, leading to a higher thermal stable LLA blocks. ENR then degrades in the third step with T<sub>d ENR</sub> closer to 400°C. The results show that crosslinked LLA junction degrades at the temperature close to that of ENR matrix. This is clearly visible in the subtracted thermogram. The close temperature indicates the link of the two

components by strong covalent bonds. Final step is the degradation of EG block ( $T_{d\ EG}$ ) at higher temperature around 470°C.

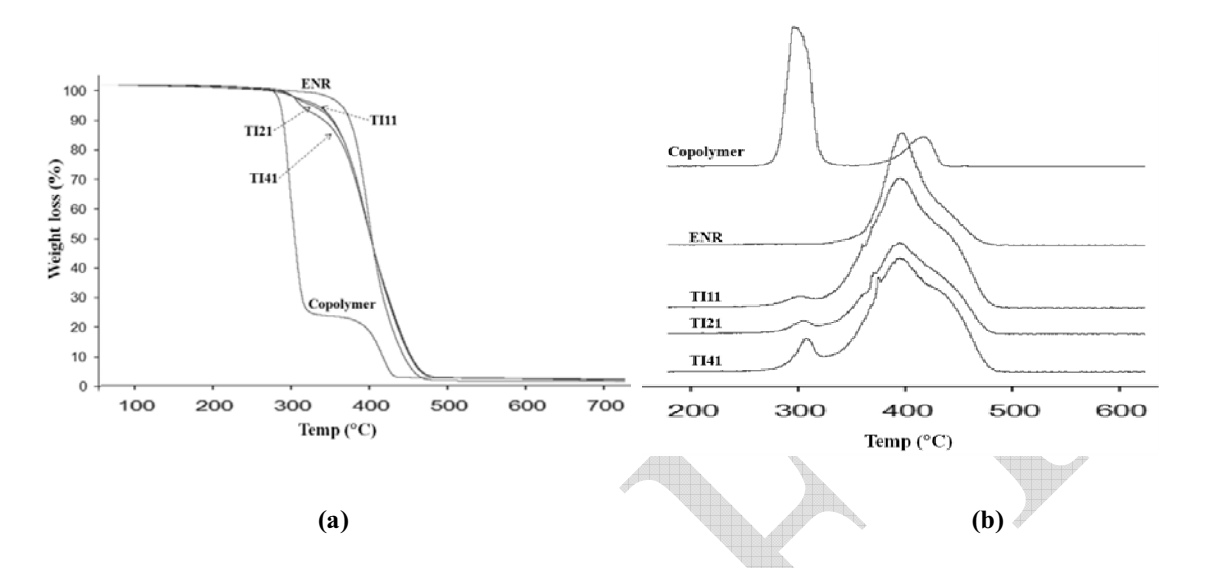


Figure 6 (a) TGA thermograms of ENR, copolymer, and THF insoluble products after Soxhlet extraction of cured sample and (b) the corresponding DTGA plots

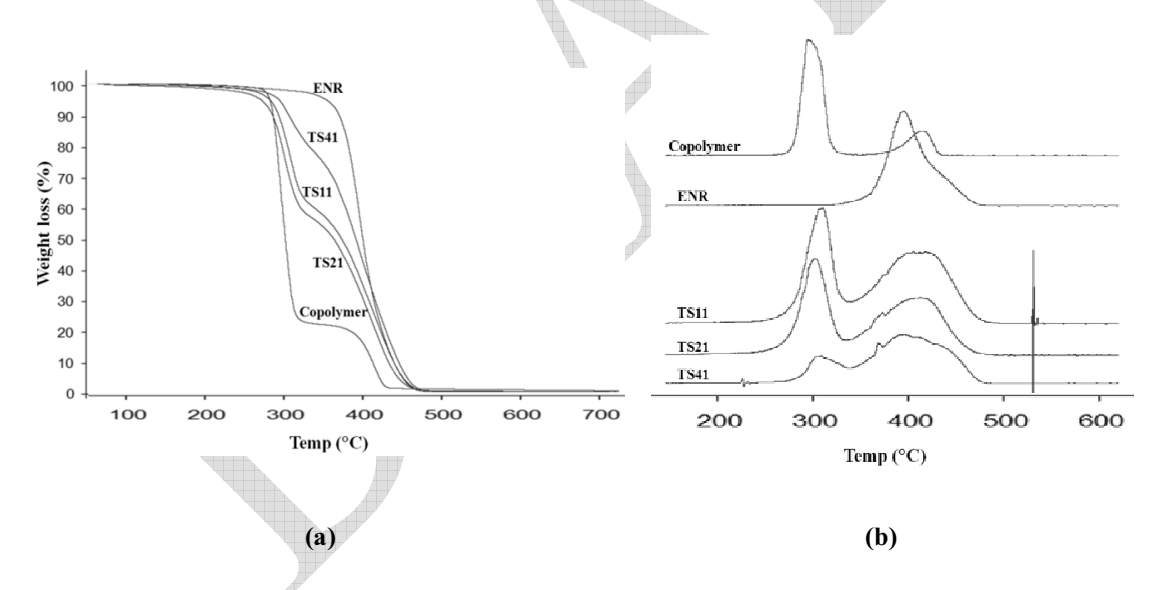


Figure 7 (a) TGA thermograms of ENR, copolymer, and THF soluble products after Soxhlet extraction of cured sample and (b) the corresponding DTGA plots

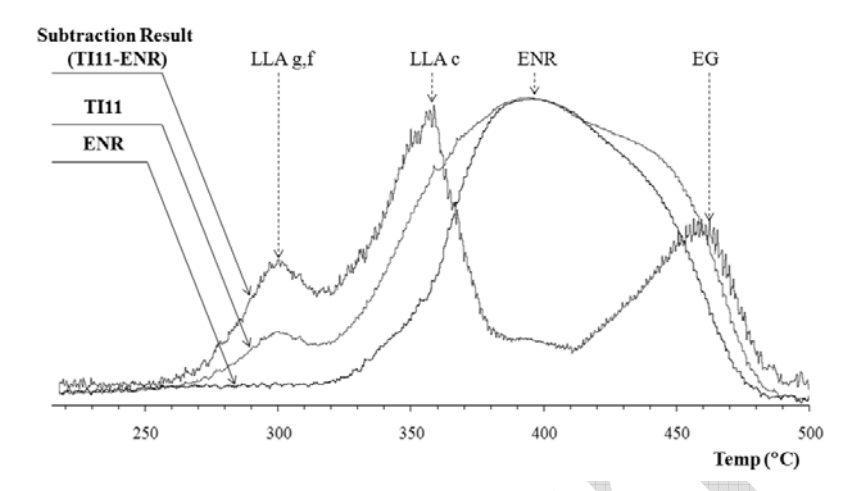


Figure 8 Illustration of degradable temperature (T<sub>d</sub>) from DTGA thermograms

Weight percentage of each component in the cured samples in calculated form curve resolved DTGA thermogram, as illustrated in Figure 9. Peak integrations of each component are as follows.  $A_{LLA\ g,f}$ : unreacted and grafted LLA blocks,  $A_{EG}$ : EG block,  $A_{ENR+LLA\ c}$ : ENR and crosslinked LLA block which are overlapped and hardly determined separately.

Percentage of LLA block of copolymer is therefore calculated as follows:

$$A_{LLA} = \frac{2.04}{1} \times \frac{A_{EG}}{44} \times 72$$

where  $\frac{2.04}{1}$  is the  $\frac{LLA}{EG}$  molar ratio of LLA<sub>46</sub>/EG<sub>46</sub>/LLA<sub>46</sub>, 44 is the molecular weight of EG unit, 72 is the molecular weight of LLA unit.

Percentage of copolymer in the sample, C(%), is calculated as follows:

$$C(\%) = A_{EG} + A_{LLA}$$

Percentage of crosslinked copolymer in the sample, C<sub>crosslink</sub>(%), is calculated as follows:

$$C_{crosslink}(\%) = (A_{LLA} - A_{LLAg,f}) + \frac{1}{2.04} \times \frac{(A_{LLA} - A_{LLAg,f})}{72} \times 44$$

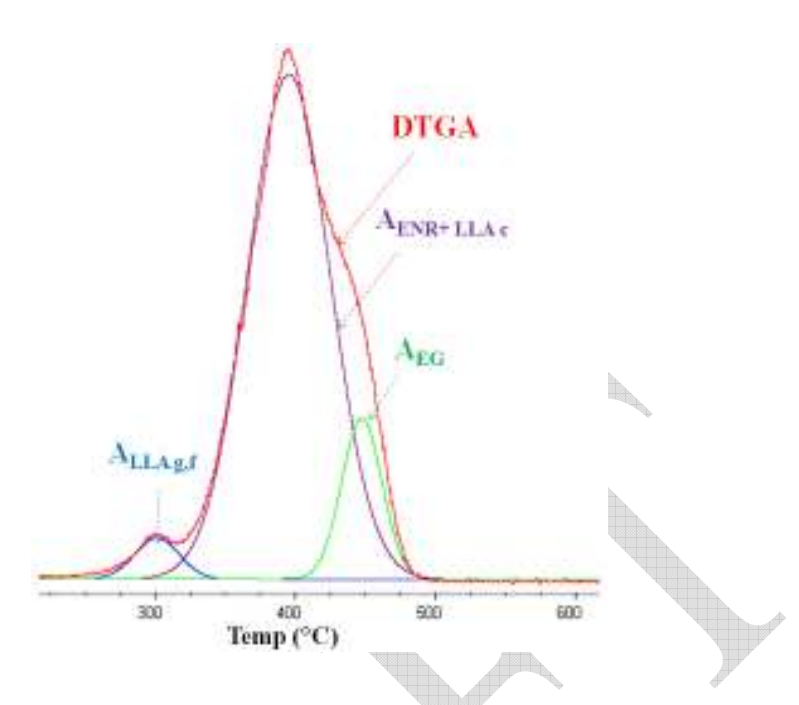


Figure 9 Curve fitting and band assignment of DTGA thermogram of TI11

The thermal degradable properties obtained from TGA are summarized in Table 2. The results show that the percentages of crosslinked copolymer in samples prepared from the reactive blend process improve with an increase in copolymer content, especially in THF insoluble fraction (TI). These results are in good agreement with those from swelling experiments and <sup>1</sup>H-NMR characterizations, as shown in Figure 4 and Table 1, respectively. The drastic reductions in percentage of copolymer and crosslinked copolymer indicate that the copolymers do not completely react with ENR as crosslinked blocks, but partially present as grafted copolymer on ENR backbone or stay unreacted, especially for samples of THF soluble part.

Table 2 Degradable temperatures of THF insoluble parts (TI) and THF soluble parts (TS) of blends

Samples	T <sub>dC</sub> (°C)			$T_{dE}(^{\circ}C)$	C (%)	C <sub>crosslink</sub> (%)
ENR	-			394	0	0
4	LA block		EG block	-	100	0
Copolymer	293		410			
	$T_{dLLAg,f}$	$T_{dLLAc}$	410			
TI11	298	356	459	394	56	42
TI21	303	356	457	394	30	23
TI41	304	356	457	394	26	18
TS11	308	359	430	398	56	8
TS21	301	-	425	397	47	0
TS41	305	356	459	392	26	2

# 4. Conclusions

In situ crosslink network of ENR and PLLA/PEG triblock copolymer were prepared by using reactive blending technique. Higher value of elastic torque and lower value of tangent  $\delta$  were observed in an increase in copolymer composition.

Results from <sup>1</sup>H-NMR indicate formation of chemical bond between copolymer and ENR. After the incorporation of ENR and copolymer, crosslink density of rubber matrix increase with increasing copolymer composition. Moreover, these crosslinked samples exhibit better thermal stability, compared to the original copolymer constituents.

# 5. Acknowledgements

Financial support of this work is provided by The Thailand Research Fund (TRF), The Commission on Higher Education (CHE), RTA5180003 and Thailand Toray Science Foundation. Thai Hien Nguyen is supported by a scholarship program from Siam Cement Foundation and SIIT, Thammasat University.

#### **References and Notes**

- 1. Gelling IR. MODIFICATION OF NATURAL RUBBER LATEX WITH PERACETIC ACID. *Rubber Chemistry and Technology*, 58(1), 86-96 (1985).
- 2. Gelling IR. Epoxidised Natural Rubber. *Journal of Natural Rubber Research*, 6(3), 184-205 (1991).
- 3. Akiba M, Hashim AS. Vulcanization and crosslinking in elastomers. *Progress in Polymer Science*, 22(3), 475-521 (1997).
- 4. Alex R, De PP, De SK. Self-vulcanizable ternary rubber blend based on epoxidized natural rubber, carboxylated nitrile rubber and polychloroprene rubber: 1. Effect of blend ratio, moulding time and fillers on miscibility. *Polymer*, 32(13), 2345-2350 (1991).
- 5. Roychoudhury A, De PP, Bhowmick AK, De SK. Self-crosslinkable ternary blend of chlorosulphonated polyethylene, epoxidized natural rubber and carboxylated nitrile rubber. *Polymer*, 33(22), 4737-4740 (1992).
- 6. Park CY, Kim BK. Self-Vulcanization of ENR/CSM Blends. *Polymer (Korea)*, 17(5), 537-542 (1993).
- 7. Bandyopadhyay S, De PP, Tripathy DK, De SK. Dynamic mechanical spectroscopic studies on the miscibility of polychloroprene--epoxidized natural rubber blend in presence of carbon black filler. *Polymer*, 36(10), 1979-1984 (1995).
- 8. Nakason C, Wannavilai P, Kaesaman A. Effect of vulcanization system on properties of thermoplastic vulcanizates based on epoxidized natural rubber/polypropylene blends. *Polymer Testing*, 25(1), 34-41 (2006).
- 9. Yong MK, Ismail H, Ariff ZM. Comparison Properties of Natural Rubber (SMR L)/Ethylene Vinyl Acetate (EVA) Copolymer Blends and Epoxidized Natural Rubber (ENR-50)/Ethylene Vinyl Acetate (EVA) Copolymer Blends *Polymer-Plastics Technology and Engineering*, 46(4), 361 366 (2007).
- 10. Yong MK, Ismail H, Ariff ZM. The Effect of Epoxidized Natural Rubber (ENR-50) or Polyethylene Acrylic Acid (PEA) as Compatibilizer on Properties of Ethylene Vinyl Acetate (EVA)/Natural Rubber (SMR L) Blends. *Polymer-Plastics Technology and Engineering*, 46(10), 1001 1009 (2007).
- 11. Hashim AS, Kohjiya S. Curing of epoxidized natural rubber with *p*-phenylenediamine. *Journal of Polymer Science Part A: Polymer Chemistry*, 32(6), 1149-1157 (1994).
- 12. Jayawardena S, Reyx D, Durand D, Pinazzi CP. Synthesis of macromolecular antioxidants by reaction of aromatic amines with epoxidized polyisoprene, 3.

- Reaction of 4-anilinoaniline with epoxidized 1,4-polyisoprene. *Die Makromolekulare Chemie*, 185(10), 2089-2097 (1984).
- 13. Perera MCS. Reaction of aromatic amines with epoxidized natural rubber latex. *Journal of Applied Polymer Science*, 39(3), 749-758 (1990).
- 14. Derouet D, Radhakrishnan N, Brosse J-C, Boccaccio G. Phosphorus modification of epoxidized liquid natural rubber to improve flame resistance of vulcanized rubbers. *Journal of Applied Polymer Science*, 52(9), 1309-1316 (1994).
- 15. Popelka S, Machová Lk, Rypácek F. Adsorption of poly(ethylene oxide)-block-polylactide copolymers on polylactide as studied by ATR-FTIR spectroscopy. *J. Colloid Interface Sci.*, 308(2), 291-299 (2007).
- 16. Yang L, Zhao Z, Wei J, El Ghzaoui A, Li S. Micelles formed by self-assembling of polylactide/poly(ethylene glycol) block copolymers in aqueous solutions. *J. Colloid Interface Sci.*, 314(2), 470-477 (2007).
- 17. Agrawal SK, Sanabria-DeLong N, Coburn JM, Tew GN, Bhatia SR. Novel drug release profiles from micellar solutions of PLA-PEO-PLA triblock copolymers. *Journal of Controlled Release*, 112(1), 64-71 (2006).
- 18. Wan Y, Chen W, Yang J, Bei J, Wang S. Biodegradable poly(-lactide)-poly(ethylene glycol) multiblock copolymer: synthesis and evaluation of cell affinity. *Biomaterials*, 24(13), 2195-2203 (2003).
- 19. Cohn D, Hotovely-Salomon A. Biodegradable multiblock PEO/PLA thermoplastic elastomers: molecular design and properties. *Polymer*, 46(7), 2068-2075 (2005).
- 20. Yuan M, Liu D, Xiong C, Deng X. Polymerization of lactides and lactones 6. Synthesis of poly-lactide and polyethylene glycol-co-poly-lactide copolymer with allylmagnesium chloride. *Eur. Polym. J.*, 35(12), 2139-2145 (1999).
- 21. Li SM, Rashkov I, Espartero JL, Manolova N, Vert M. Synthesis, Characterization, and Hydrolytic Degradation of PLA/PEO/PLA Triblock Copolymers with Long Poly(l-lactic acid) Blocks. *Macromolecules*, 29(1), 57-62 (1996).
- 22. Rashkov I, Manolova N, Li SM, Espartero JL, Vert M. Synthesis, Characterization, and Hydrolytic Degradation of PLA/PEO/PLA Triblock Copolymers with Short Poly(I-lactic acid) Chains. *Macromolecules*, 29(1), 50-56 (1996).
- 23. Derouet D, Brosse J-C, Challioui A. Alcoholysis of epoxidized polyisoprenes by direct opening of oxirane rings with alcohol derivatives 1. Modelization of the reaction. *European Polymer Journal*, 37(7), 1315-1326 (2001).
- 24. Derouet D, Brosse J-C, Challioui A. Alcoholysis of epoxidized polyisoprenes by direct opening of oxirane rings with alcohol derivatives 2. Study on epoxidized 1,4-polyisoprene. *European Polymer Journal*, 37(7), 1327-1337 (2001).

- 25. Nakason C, Kaesaman A, Sainamsai W, Kiatkamjonwong S. Rheological behavior of reactive blending of epoxidized natural rubber with cassava starch and epoxidized natural rubber with natural rubber and cassava starch. *Journal of Applied Polymer Science*, 91(3), 1752-1762 (2004).
- 26. Bhowmick AK, Stephens HL. Handbook of Elastomers. (2001).
- 27. Nguyen T-H, Petchsuk A, Tangboriboonrat P, Opaprakasit M, Sharp A, Opaprakasit P. Synthesis and Characterizations of PLLA/PEG Block Copolymers. *Advanced Materials Research* 93 94, 198-201 (2010).
- 28. Saendee P, Tangboriboonrat P. Latex interpenetrating polymer networks of epoxidised natural rubber/poly(methyl methacrylate): an insight into the mechanism of epoxidation. *Colloid & Polymer Science*, 284(6), 634-643 (2006).
- 29. Nguyen T-H, Tangboriboonrat P, Rattanasom N, Petchsuk A, Opaprakasit M, Opaprakasit P. Property Modification of Epoxidized Natural Rubber by Polymerization of Poly(L-Lactic Acid-co-Ethylene Glycol) Block Copolymers. (Ed.^(Eds) (2010)
- 30. Aprem AS, Joseph K, Mathew T, Altstaedt V, Thomas S. Studies on accelerated sulphur vulcanization of natural rubber using 1-phenyl-2, 4-dithiobiuret/tertiary butyl benzothiazole sulphenamide. *European Polymer Journal*, 39(7), 1451-1460 (2003).
- 31. Nguyen TH, Thammawong C, Tangboriboonrat P *et al.* L-Lactide/Ethylene Glycol Block Copolymers and Their Applications: Nanofibrous Materials and Surface Modification of Epoxidized Natural Rubber. *Express Polymer Letters*, (2010).

# Morphology and Interactions of Naproxen-loaded Fe<sub>3</sub>O<sub>4</sub> magnetic nanoparticles coated PLA-co-PEG block copolymer

# 1. Introduction

Owing to the magnetic properties and the ability to function at the cellular and molecular level of biological interactions of magnetic nanoparticles (MNP), they have a number of potentials to be used in medical applications such as contrast agents for magnetic resonance imaging (MRI) [1-4], cell engineering [1-3], and carriers for drug delivery [1, 2]. Especially, in the last decade, nanostructure mediated drug delivery or nanomedicine has been realized with the potential to enhance drug bioavailability, improve the timed release of drug molecules, enable precision drug targeting, reduce drug toxicity, and increase the efficiency in drug distribution [5, 6]. That is, the technology has developed so that it is possible to synthesize, characterize and tailor the functional properties of magnetic nanoparticles for medical applications.

Many methods have been proposed for the synthesis of iron oxide nanoparticles. These includes co-precipitation, reactions in constrained environments, hydrothermal and high-temperature reactions, sol-gel reactions, polyol methods, flow injection syntheses, electrochemical methods, aerosol/vapor methods, and sonolysis [7-9].

For drug delivery application, the use of magnetic nanoparticles, magnetite ( $Fe_3O_4$ ) can give rise to a precise drug delivery to a specific target site by application of external magnetic fields [10]. However, there are some limitations that are needed to be overcome in using nanoparticles in the drug delivery applications—especially the short blood circulation time due to rapid elimination of the nanoparticles from the blood stream, poor cell internalization, poor biocompatibility, and any other processes that might affect their behaviors in vivo [6].

To overcome these limitations, it is necessary that some adjustments for suitable composition, size, morphology, and surface chemistry are carried out before being used in order to avoid those limitations and thereby achieve the utmost effectiveness. For the simplest approach to increasing the blood circulation time, the magnetic nanoparticles are coated with hydrophilic polymers as many recent researches have focused on [7, 11-13] such as poly(ethylene glycol) or PEG to disperse particles, increase blood circulation time, biocompatibility, and improve cell internalization [6]. In addition to a simple hydrophilic polymer coating, it is also possible to coat

MNPs with copolymer such as PEG-co-PLA with the help of hydrophobic compounds such as oleic acid, as shall be the formulation used in this work.

Tapan K. Jain, et al. reported using Pluronic F-127 to coat oleic acid (OA) pre-stabilized MNP and encapsulate an anticancer agent, doxorubicin [7]. As a result of this study, the obtained particles, mean particle size measured by TEM being 9-13 nm, can be loaded easily with high doses of water insoluble anticancer agents. In addition, the sustained release behavior of the encapsulated drug is observed over 2 weeks under in vitro conditions. Similarly, Rutnakornpituk, M., et al. employed OA to stabilized the MNP, before using different block length mPEG-PCL diblock copolymers to coat the drug delivery system [11]. The particles obtained had the diameter of 9 nm measured by TEM. Furthermore, it was found that increase of Mn of hydrophilic mPEG blocks in the enhanced the particle dispersability in water, while increase of Mn of hydrophobic PCL blocks improved their adsorbing ability to the hydrophobic inner layer of the particles. Nonetheless, particle size and magnetic properties did not depend on copolymer coating. For the particle stability, they were stable in water for one month period before aggregation was observed..S. Kayal and R.V. Ramanujan successfully coated the MNP with a conjugate of doxorubicin (DOX) and PVA and the average particle size was 10 nm analyzed by TEM [13]. DOX loading and release profiles showed that up to 45% of adsorbed drug was released in 80 h. Another different polymer is used by Bakandritsos, A., et al. in their research [12]. They apply PLA or PEG-PLA diblock copolymer to the MNP where the magnetic nanoparticles are organized in superclusters inside the hydrophobic core of the polymers. As a result, they found that the hydrodynamic diameter of MNPs-loaded PLA is approximatelt 250 nm, while that of MNPs-loaded PLA-PEG micelles is much lower ( around 100 nm) and thus suitable with applications where prolonged blood circulation is required. Moreover, PLA-PEG magnetic hybrids showed remarkable colloidal stability in human blood plasma. However, no drug encapsulation was mentioned in this report.

PEG-PLA block copolymers are interesting in the use to coat magnetic nanoparticles. This is because the PLA part, with the help of hydrophobic compounds such as oleic acid, would serve as the hydrophobic area excellent for encapsulation of hydrophobic drugs [12] while the PEG part of the polymer chain offers hydrophilic properties to the complex, which is useful in stabilizing MNP in water. According to the work of Bakandritsos, A., et al., they employed diblock PLA-PEG copolymer with PLA and PEG molecular weight 10,000 and 5,000 Da, respectively, to coat the MNP. This drug delivery complex is also similar to the system of water-dispersible oleic acid (OA)-Pluronic-coated iron oxide magnetic nanoparticle illustrated in the work of Tapan K. Jain, et al. except the polymer in their work is Pluronic [7]. The schematic representation is shown in Fig 1.

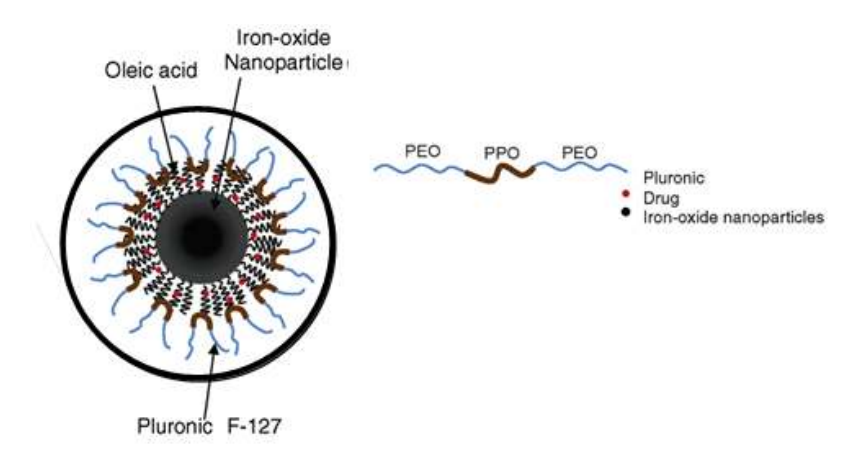


Fig. 1 Schematic representing formulation of iron oxide nanoparticles with oleic acid (OA) and pluronic (PEO-PPO-PEO) [7]

Modified MNP have a potential to act as drug carriers for a variety of therapeutic agents such as etoposide, doxorubicin, methotrexate, etc. The design of structural features, such as coating material, interaction between drug and coating, etc, determines the characteristics such as loading capacities and drug release profiles [14].

Naproxen is a hydrophobic anti-inflammatory agent. Liversidge G. and Conzentino P. has demonstrated that having high concentration of this drug can trigger gastric mucosal damage. They have also proven that lowering the drug particle size by suspension of drug in pluronic F-68 has lower the damaging effects [15]. Another experiment done be Maver U., *et al.*, synthesized a novel magnetic nanoparticle complex incorporated with naproxen which can readily be released [16]. The coating substance is, however, inorganic silica and drug encapsulation is done by incorporation into the porous silica area, not by hydrophobic and hydrophilic interaction.

In this work, oleic acid (OA)-PLA-PEG-PLA-coated magnetic iron oxide nanoparticles is successfully synthesized with and without drug encapsulation. The magnetic nanoparticle core is completed using the conventional co-precipitation method. Different weight ratio of polymer to MNP was used to find a suitable amount for coating. Also, incorporation of the therapeutic agent naproxen into the delivery complex is achieved.

#### 2. Experiment

#### 2.1 Materials

Iron(II) chloride tetrahydrate ( $FeCl_2.4H_2O$ ) and iron(III) chloride anhydrous ( $FeCl_3$ ) were purchased from Acros Organics. Oleic acid, n-hexane and methyl alcohol were from Carlo Erba

Reagents. Ammonia solution 25% (NH<sub>4</sub>OH) was bought from Merck. THF is obtained from Fischer Scientific. Chloroform is from Lab-Scan analytical sciences. Naproxen drug is purchased from Andenex-Chemie GmbH; Germany. PLA-PEG-PLA triblock copolymer (MW=) was obtained from... All solvents are of analytical grades. All reagents and solvents are used without further purification. Reversed Osmosis (RO) water was used throughout the experiment.

#### 2.2 Preparation of oleic acid stabilized Fe<sub>3</sub>O<sub>4</sub> magnetic fluid

Magnetic nanoparticles were synthesized using the co-precipitation method reported by Rutnakornpituk, M., et al. with slight modification. That is 3 g of FeCl<sub>2</sub>.4H<sub>2</sub>O and 4.98 g of FeCl<sub>3</sub> were separately dissolved in 40ml of water. The mixtures were then sonicated using an ultrasonic bath, with interval stirring, for 1 hour. Finally, they were mixed together with stirring followed by rapid addition of ammonium hydroxide solution (25 vol%; 20 mL) to stimulate a basic environment for reaction I.

$$Fe^{2+} + Fe^{3+} + 80H^{-} \rightarrow Fe_3O_4 + 4H_2O$$
 (I)

Oleic acid (9 mL) was subsequently added dropwise to the black liquid with stirring which continued for a further 30 minute. Afterwards, the oleic-coated magnetic nanoparticles were separated by magnetic decantation using a neodymium magnet. They were washed with water 5 times to remove excess oleic acid. Finally, the particles were suspended in THF.

#### 2.3 Surface modification of oleic acid stabilized Fe<sub>3</sub>O<sub>4</sub> with PLA-PEG-PLA copolymer

The surface modification was carried out with a few number of steps. The solution of polymer (PLA-PEG-PLA) in THF was prepared (10%, 25%, 50% and 100%, wt polymer/wt oleic acid coated magnetic nanoparticles). The suspension of magnetic nanoparticles was added into the polymer solution prior to ultrasonic bath sonication for 30 minutes. Then, deionized water was added, followed by further sonication until 2 hours is reached. The mixture was undergone rotary evaporation (vacuum, 50 °C) to change medium—from THF to water. Afterwards, suspended nanoparticles in water were sonicated for 5 minutes using (strong sonicator). Lastly, the surface-modified magnetic nanoparticles suspended in water were centrifuged at 4000 rpm for 5 minutes to precipitate large aggregates. The supernatant was filtered and collected.

#### 2.4 Drug encapsulation

For drug incorporation in nanoparticles, naproxen is primarily the represent of hydrophobic drug. Naproxen 10 mg was dissolved in 5 ml of methyl alcohol. The prepared drug solution is added

dropwise to 15 ml of (OA)-PLA-PEG-PLA-coated magnetic iron oxide nanoparticles suspended in water with stirring and heating at 60°C. The stirring and heating is continued for 20 minutes to evaporate the methyl alcohol. The mixture is sonicated using the (strong sonicator) for 2 minutes. Excess drug is removed by centrifugation at 3000 rpm for 5 minutes followed by filtration.

#### 2.5 Characterization

- 2.5.1 Transmission Electron Microscope (TEM)
- 2.5.2 Scanning Electron Microscope (SEM)
- 2.5.3 Environmental Scanning Electron Microscope (ESEM)
- 2.5.4 RAMAN Spectroscopy: NTEGRA Spectra. Helium neon laser ( $\lambda = 632.8$  nm). Objective lens 100x
- 2.5.5 Confocal RAMAN Spectroscopy:
- 2.5.6 Thermogravimetric Analysis (TGA)
- 2.5.7 Dynamic Light Scattering (DLS)

The morphology of the magnetic nanoparticles was characterized using transmission electron microscope (TEM) model JEOL JEM - 2010, (200kV) and scanning electron microscope (SEM) model JEOL JSM 6301F. For TEM, the nanoparticle suspended in water is drop onto a carbon coated copper grid and left overnight. As for the SEM preparation, the samples are drop onto aluminum foil and heated overnight. Structure of the samples were observed using confocal RAMAN spectroscopy (NTEGRA Spectra, Helium neon laser ( $\lambda$  = 632.8 nm), Objective lens 100x), Fourier Transform infrared spectroscopy (FTIR) NICOLET 6700 FTIR and thermogravimetric analysis (TGA) METTLER TOLEDO TSO801RO. Samples are dried on a glass slide for confocal RAMAN spectroscopy. Dried powder samples are employed for TGA. Particle size distribution and colloidal stability (zeta potential) is done using dynamic light scattering (DLS) Zetasizer Nanoseries ZS Model 3600 (Malvern, UK). Nanoparticles suspended in water are sonicated before measurement.

#### Also have VSM and XRF left

#### 3. Result and Discussion

X-ray Fluorescence (XRF) was used to confirm the existence of iron oxide. Fig.2 illustrates the intensity in the range of 60 to 120 degree of 2 thetas in which the synthesized magnetic nanoparticles show the peak whereas the medium—water—has no peak of iron. Thus, it reassures the presence of iron oxide suspended in water. There are other different compounds including silicon,

phosphate and calcium ion exist in the synthesized nanoparticles; however, these impurities already present in water used in the experiment as shown in Table 1.

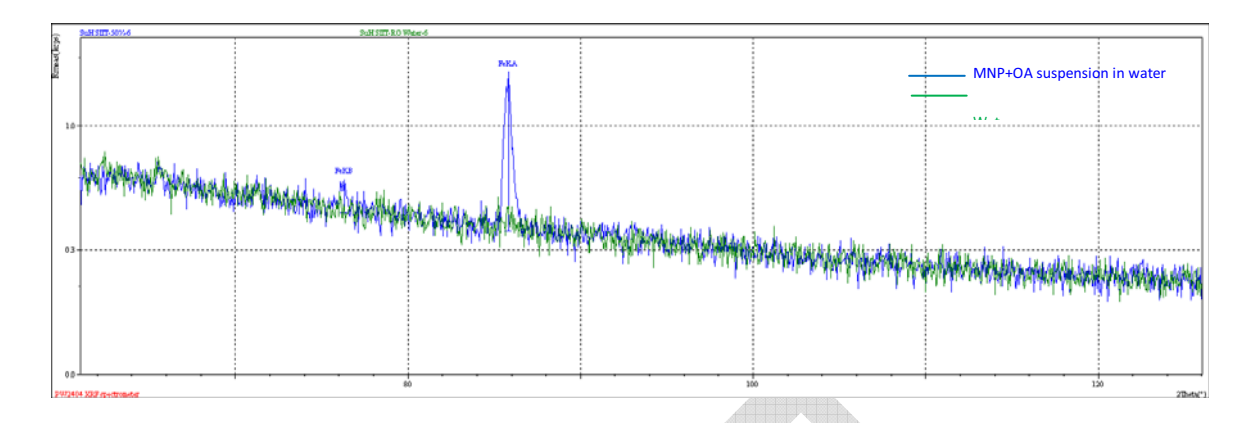
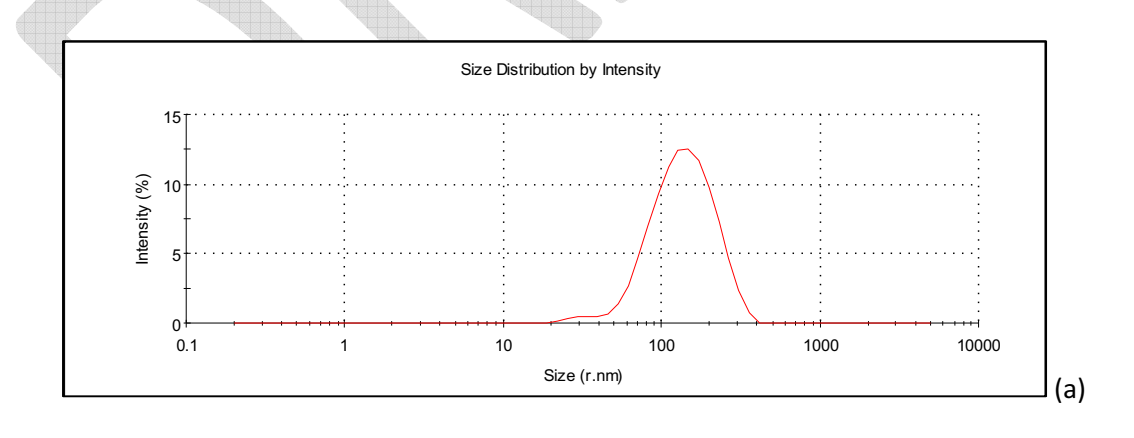
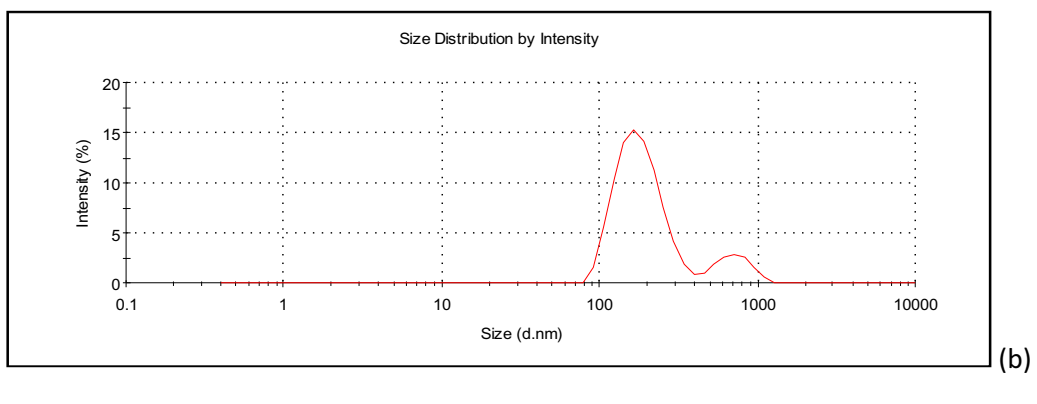


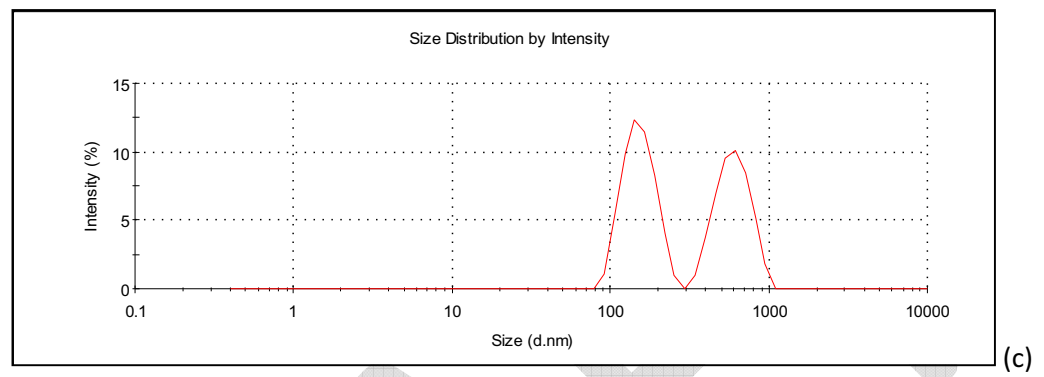
Fig. 2 XRF spectra of MNPs+OA in comparison with the medium (water)

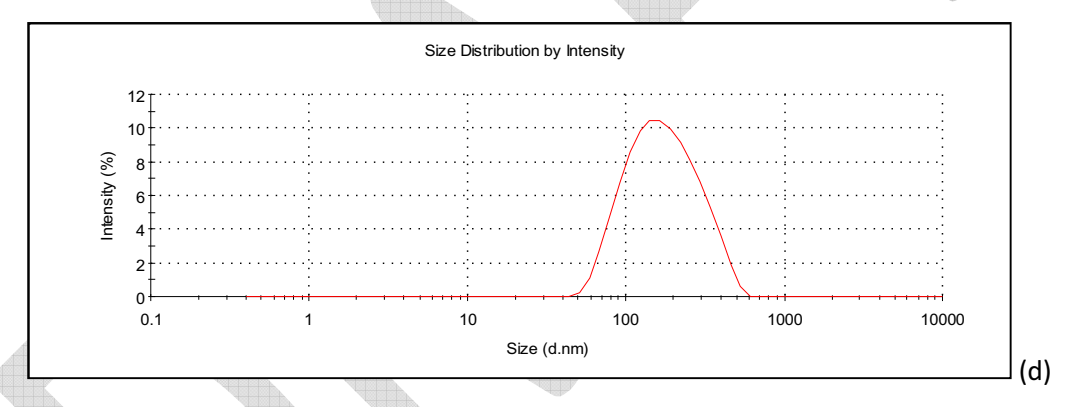
Table 1. XRF Quantification of water and MNPs+OA suspended in water

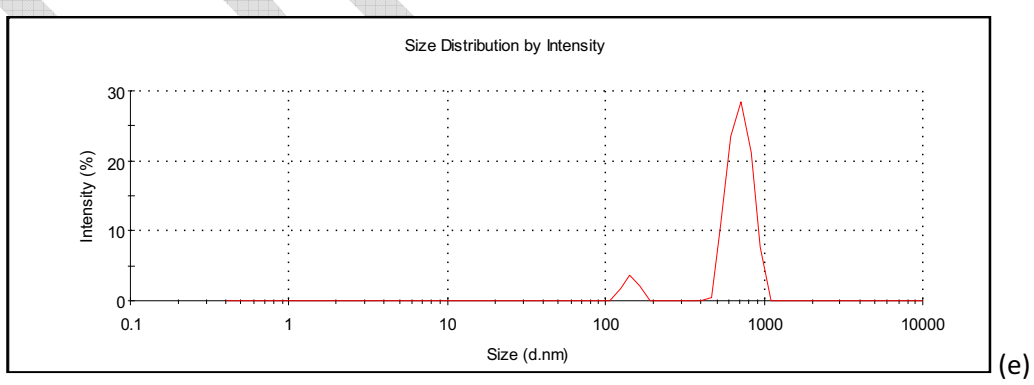
	Conce	entration (%)
Compound	Water	MNPs+OA suspended in water
Si	0.02	0.02
P	0.13	0.17
Ca	0.13	0.12
Fe		0.14











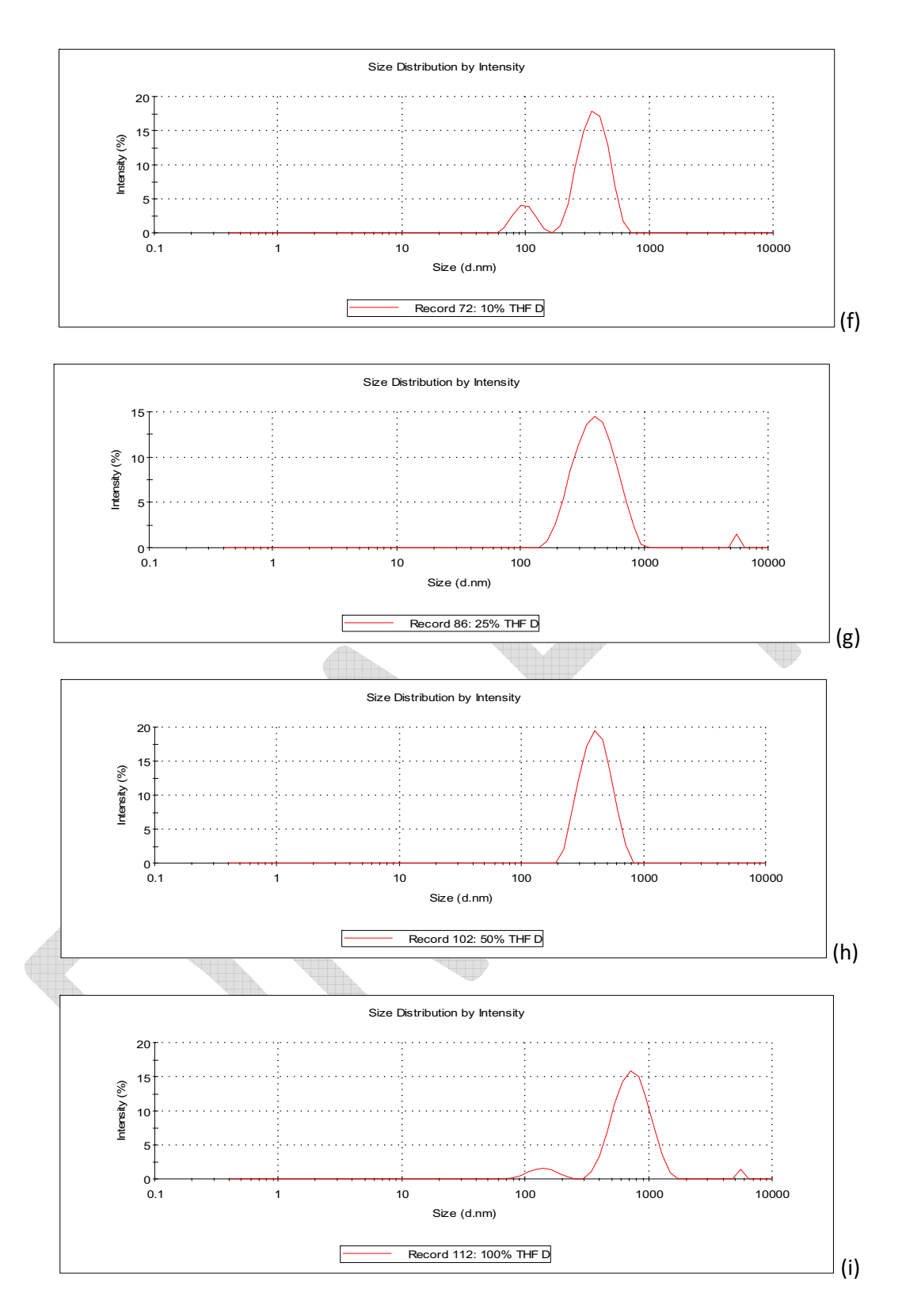
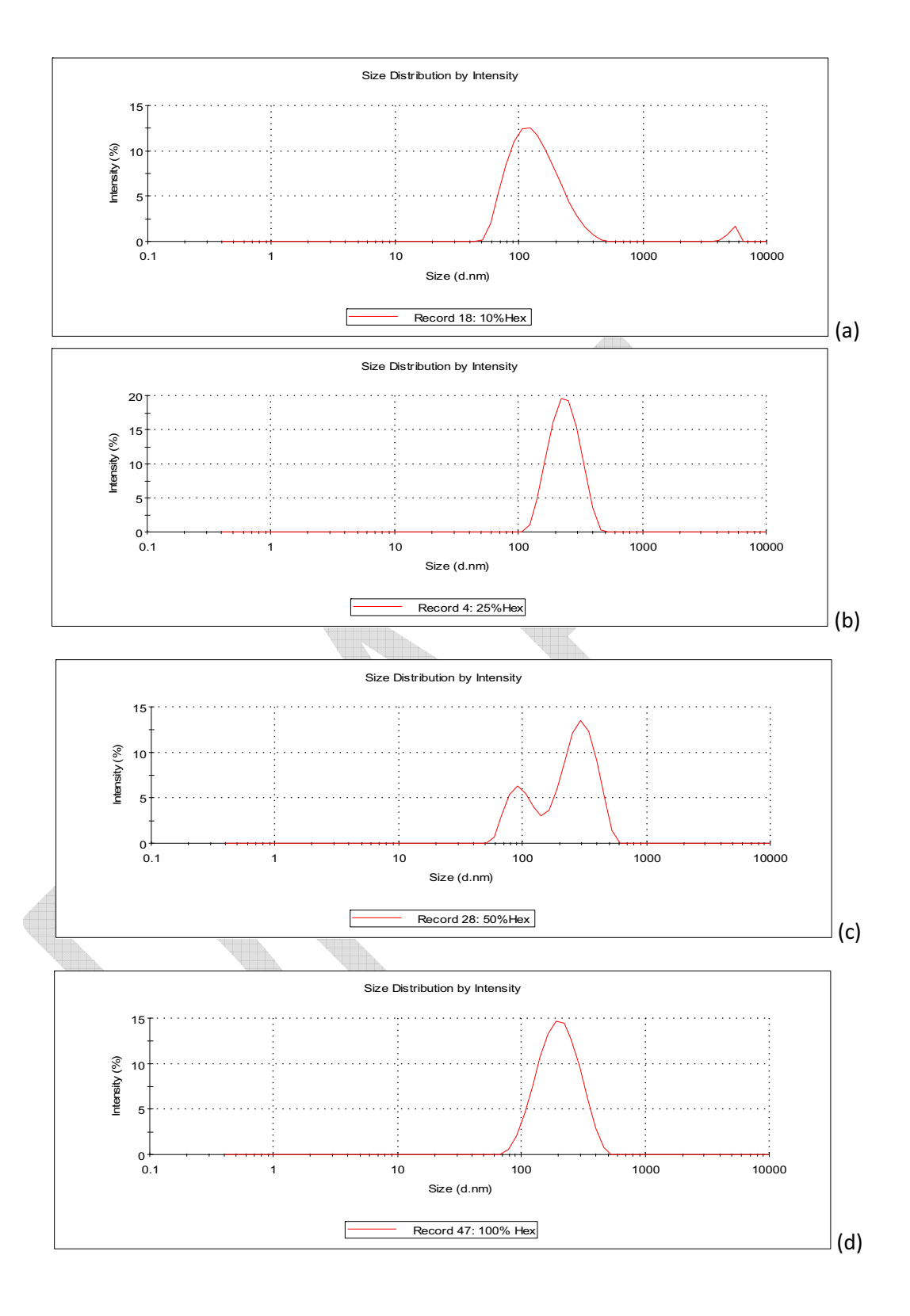


Fig. 3 Size distribution of PLA-PEG-PLA loaded magnetic nanoparticles synthesized in THF suspended in water

(a) no polymer coating (b) 10 wt% polymer (c) 25 wt% polymer (d) 50 wt% polymer (e) 100 wt% polymer (f) 10 wt% polymer with drug (g) 25 wt% polymer with drug

(h) 50 wt% polymer with drug (i) 100 wt% polymer with drug



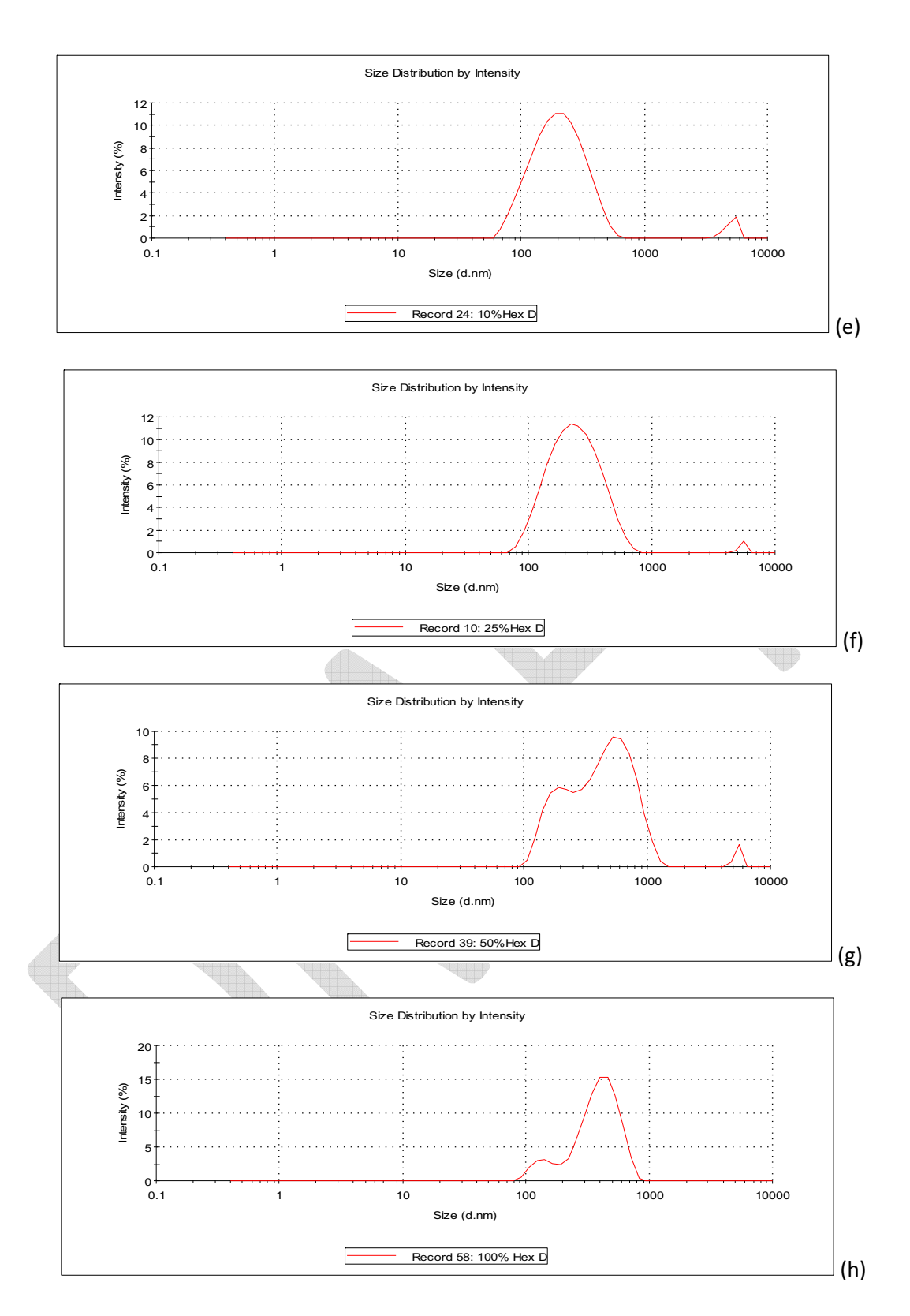


Fig. 3 Size distribution of PLA-PEG-PLA loaded magnetic nanoparticles synthesized in hexane suspended in water

(a) 10 wt% polymer (b) 25 wt% polymer

(c) 50 wt% polymer (d) 100 wt% polymer (e) ) 10 wt% polymer with drug (f) 25 wt% polymer with drug

(g) 50 wt% polymer with drug (h) 100 wt% polymer with drug

Table 2. Summary of hydrodynamic size and zeta potential

Solvent	Concen	tration (wt%)	hydrodynamic size (nm)	zeta potential (mV)
Hexane	No drug	10	145.07	-23.27
		25	332.00	-26.20
		50	227.27	-26.60
		100	228.00	-27.70
	Drug	10	232.30	-17.73
		25	252.53	-17.67
		50	423.00	-12.20
		100	509.00	-13.03
ТНБ	No drug	10	390.00	-52.2
		25	302.00	-29.23
		50	216.00	-16.18
		100	285.00	-22.77
	Drug	10	404.00	-20.37
		25	441.00	-15.77
		50	499.00	-15.53
		100	780.00	-14.23

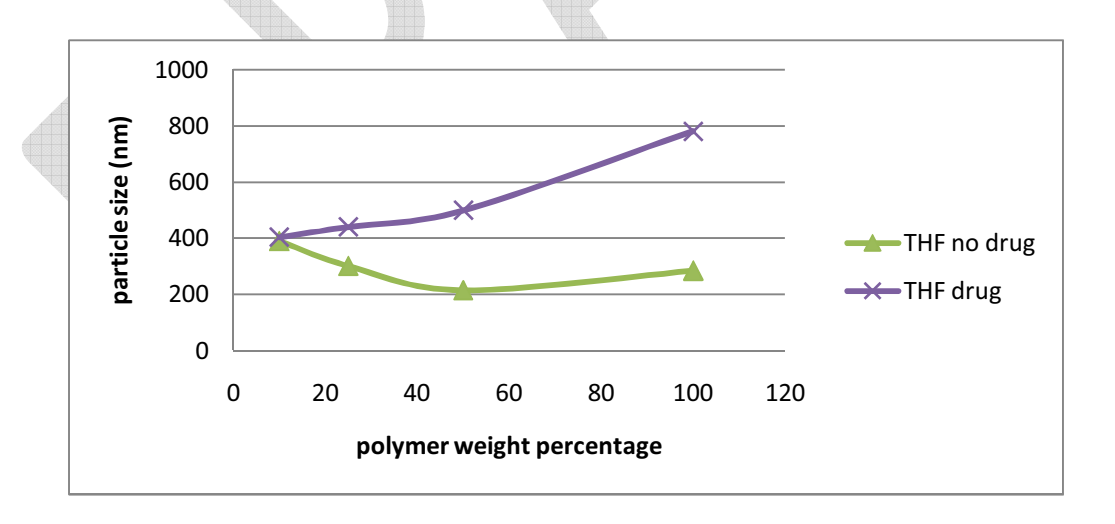


Fig x, summary of DLS synthesized in THF

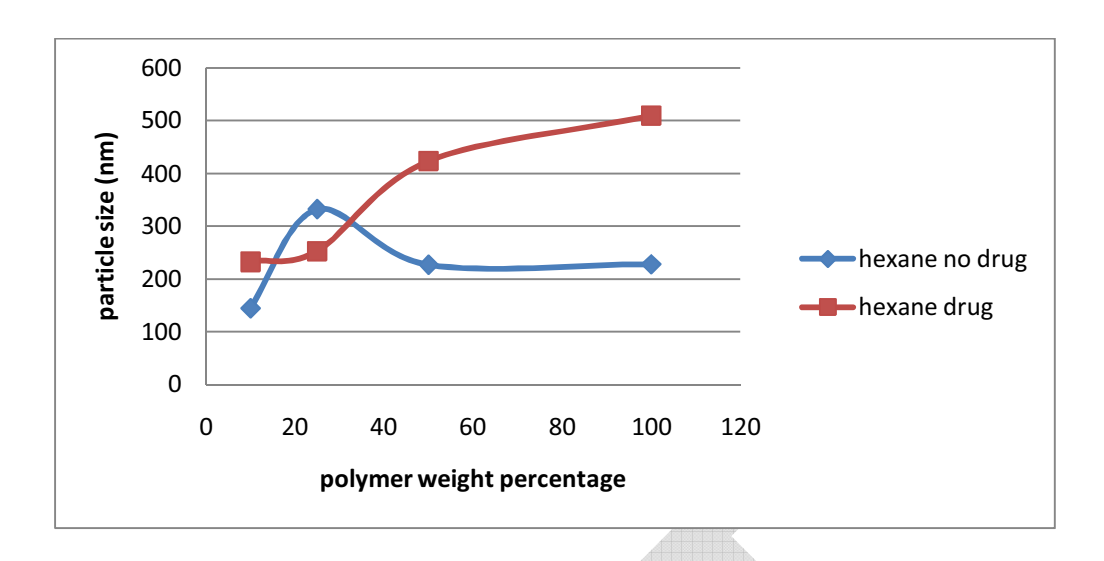
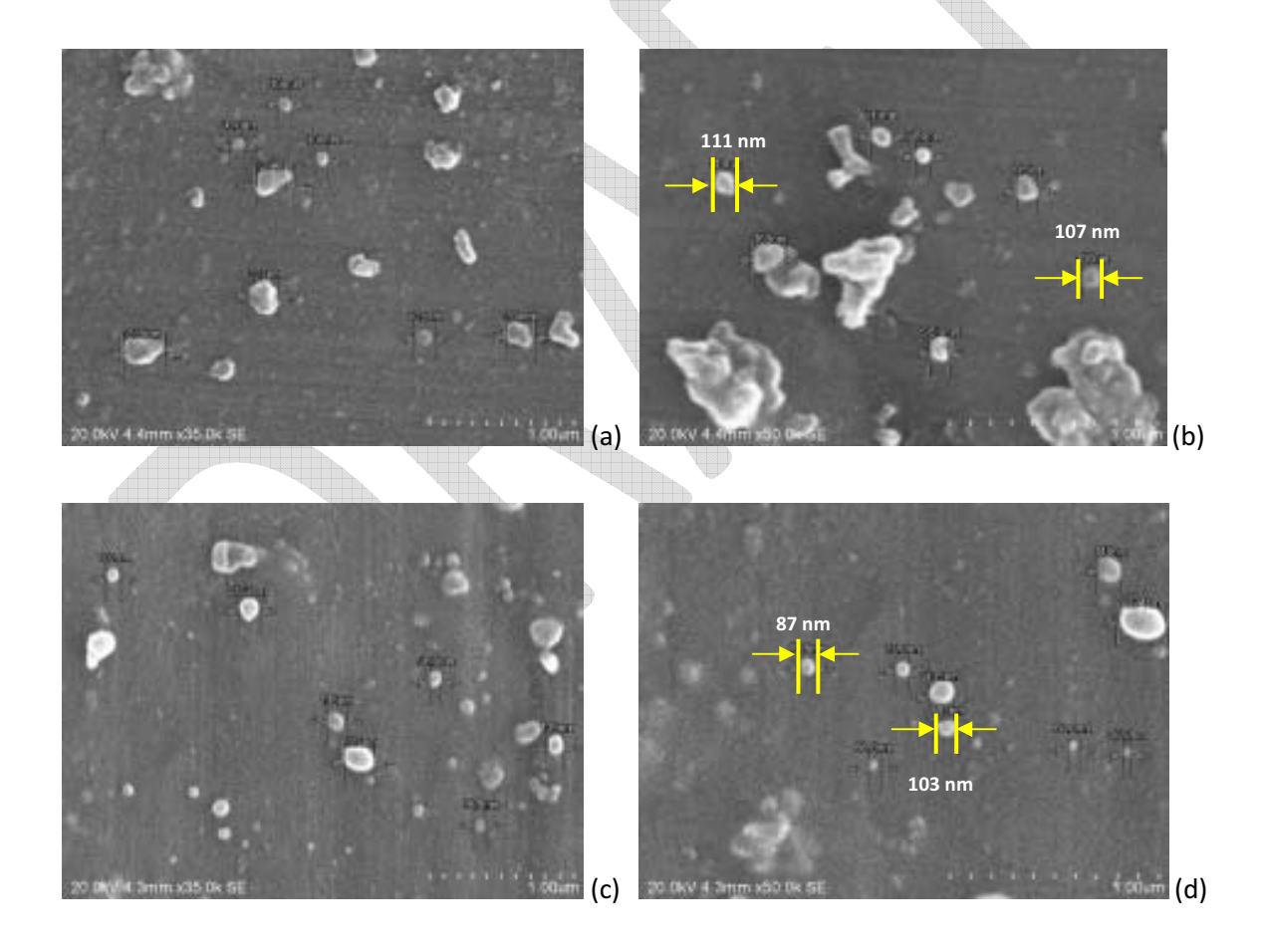
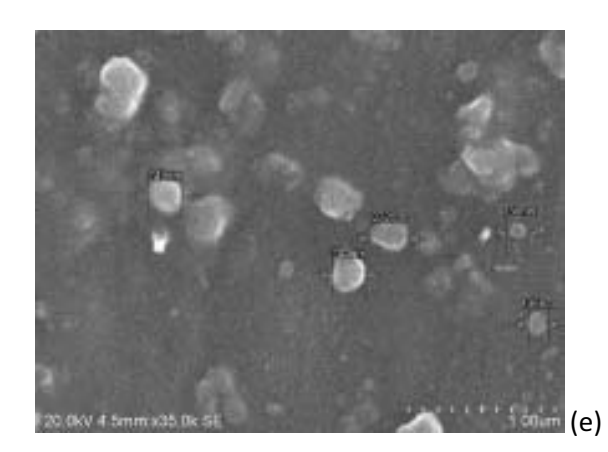


Fig x, summary of DLS synthesized in Hex





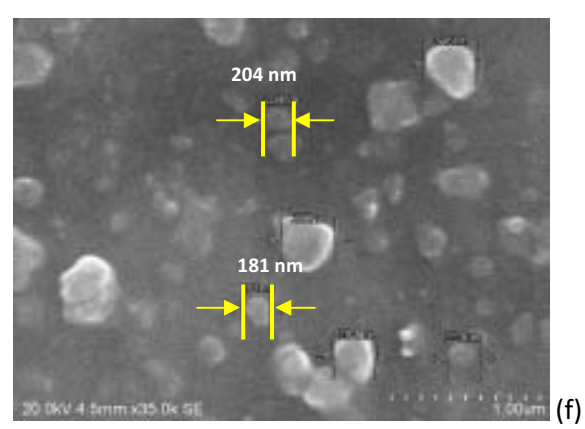


Fig. 4 SEM pictures of PLA-PEG-PLA loaded iron oxide nanoparticles

- (a) 25 wt% polymer without drug encapsulation (35k magnification)
- (b) 25 wt% polymer without drug encapsulation (50k magnification)
- (c) 50 wt% polymer without drug encapsulation (35k magnification)
- (d) 50 wt% polymer without drug encapsulation (50k magnification)
  - (e) 50 wt% polymer with drug encapsulation (35k magnification)
  - (f) 50 wt% polymer with drug encapsulation (50k magnification)

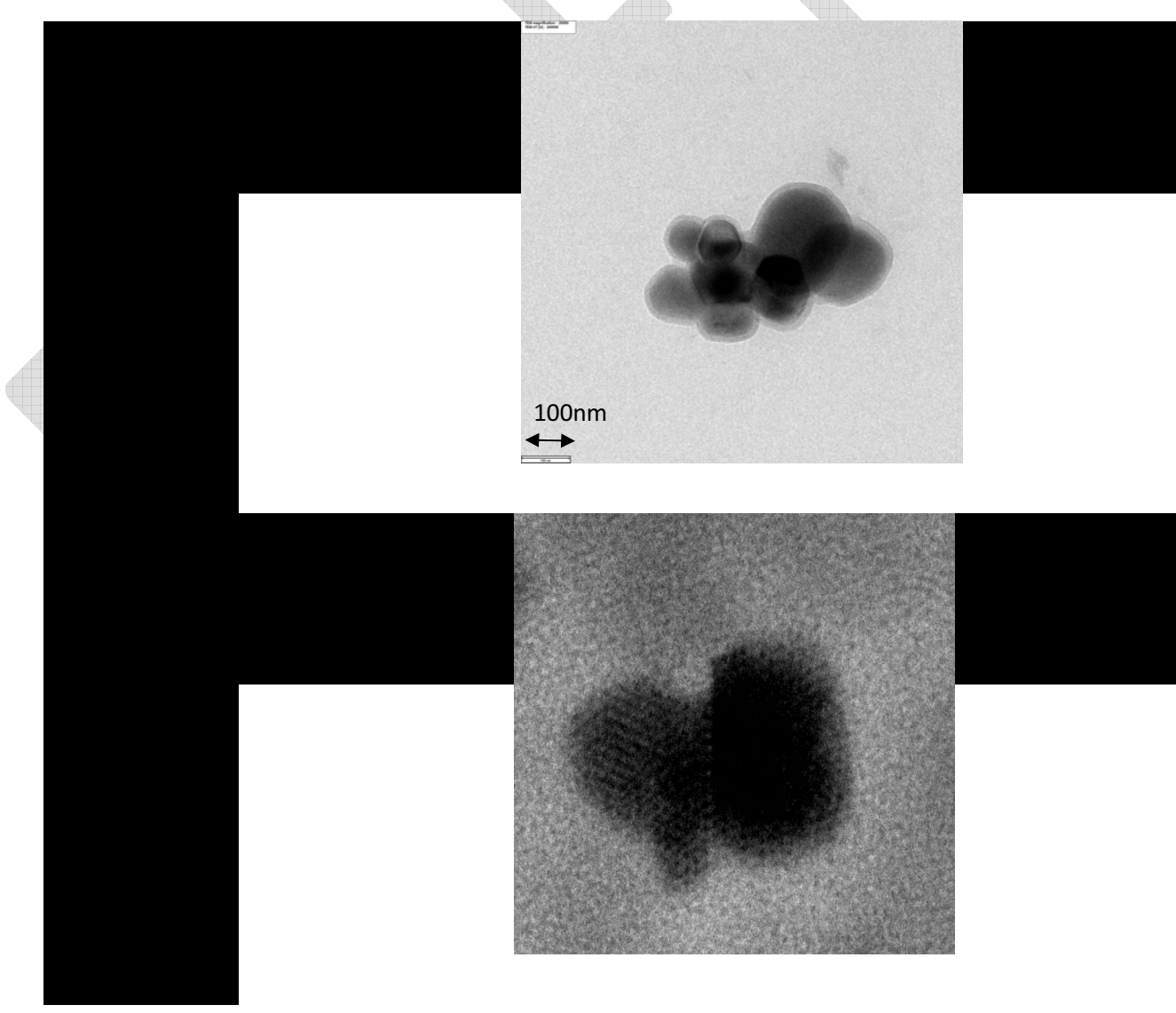


Fig 5. TEM pictures of PLA-PEG-PLA loaded iron oxide nanoparticles

- a) 50 wt% polymer without drug encapsulation
- b) 50 wt% polymer with drug encapsulation
- c) TEM showing iron oxide nanoparticle grain
- d) Zoomed region illustrating the lineup of atomic lattice of iron oxide

The pictures from TEM (Fig.5) illustrate the feature of the particles and size as well as SEM pictures do. Both pictures of particles of 50 wt% polymer with and without drug encapsulation show that there are some agglomerations. The scale bar on the bottom left hand side is 100 nm showing that the size of each particle is around 100-150 nm and 120-200 nm for particles without and with drug encapsulation, respectively. In addition, Fig 5c and d represents the atomic lattice of the iron oxide nanoparticles. The texture of the nanoparticles can be seen to be distinct from other surfaces.

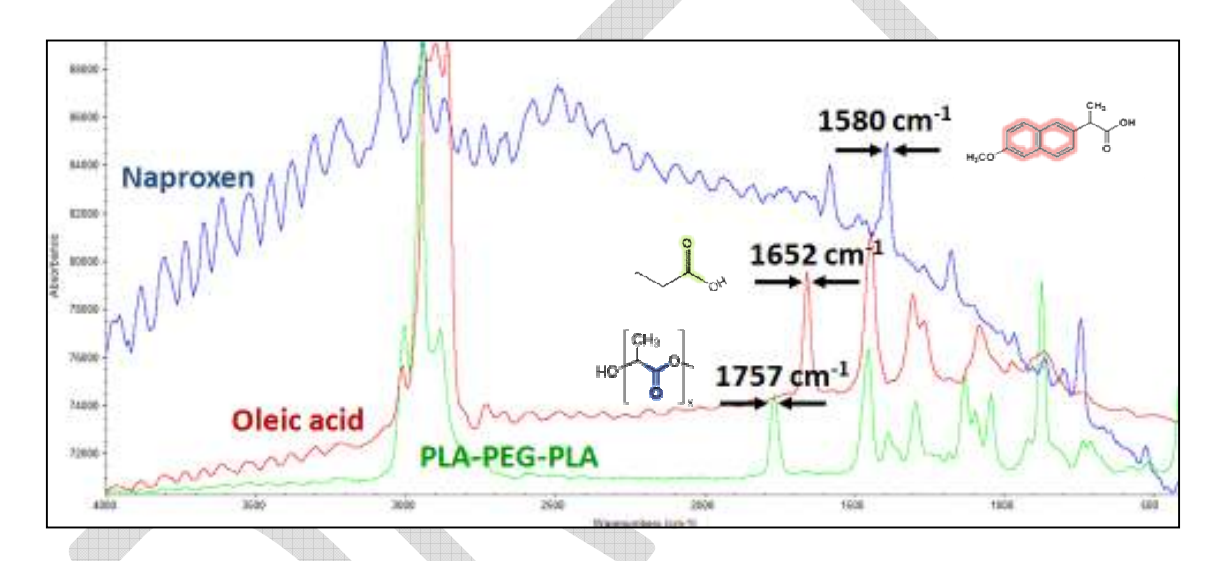


Fig. 6 RAMAN Spectra for pure oleic acid, drug, and polymer

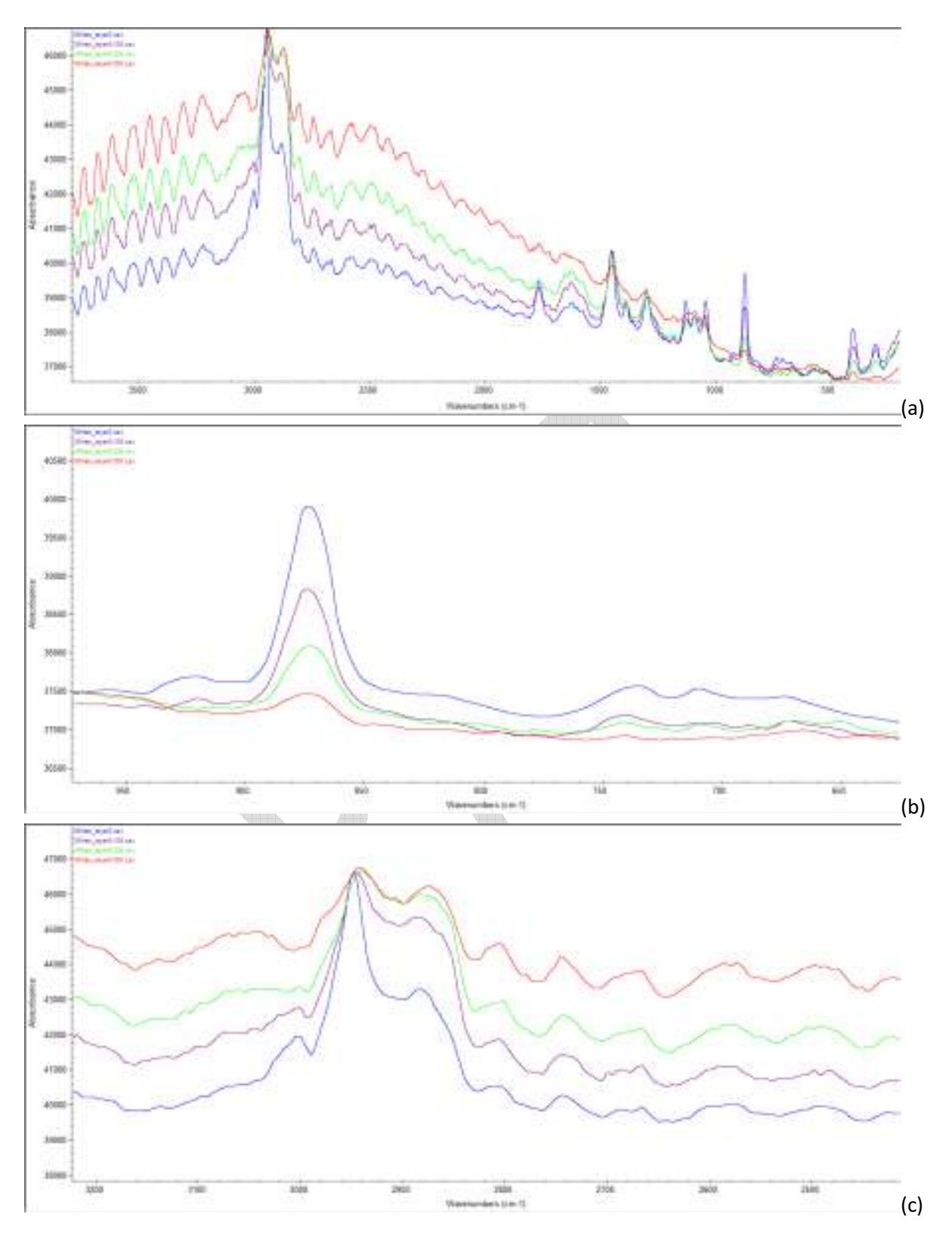


Fig. 7 RAMAN Spectra of PLA-PEG-PLA loaded iron oxide nanoparticles prepared by drug encapsulation together with polymer

- a) Overall spectrum
- b) Peak at wavenumber 875 cm<sup>-1</sup> coresponding to polymer
- c) Peaks at wavenumber 2880cm<sup>-1</sup> and 3040cm<sup>-1</sup> corresponding to oleic acid and naproxen, respectively

Figure 7 illustrate the coating morphology of the magnetic nanoparticle with drug encapsulation simultaneously with polymer coating. The peak present at wavenumber 875, 2880 and 3040cm<sup>-1</sup> corresponds to the polymer, oleic acid and naproxen, respectively. It can be seen from figure 7b that the intensity of the polymer peak decreases with the increase in dept into the MNP. The same can be said for the profile of the naproxen drug. However, an opposite trend is observed with the oleic acid peak (figure 7c). The further into the nanoparticle results in an increase in oleic acid peak intensity. From this information, it can be modeled that this drug delivery complex is composed of different layers in the same way that has been reported by others, with the magnetic nanoparticles surrounded by an oleic acid and polymer layer in succession with the drug partitioning in the oleic acid layer [7, 11]. The schematic representation is shown in figure 8.

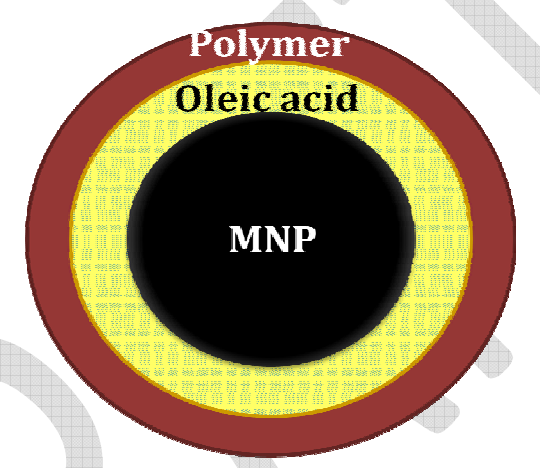


Fig. 8 Schematic representation of PLA-PEG-PLA loaded iron oxide nanoparticles prepared by drug encapsulation together with polymer

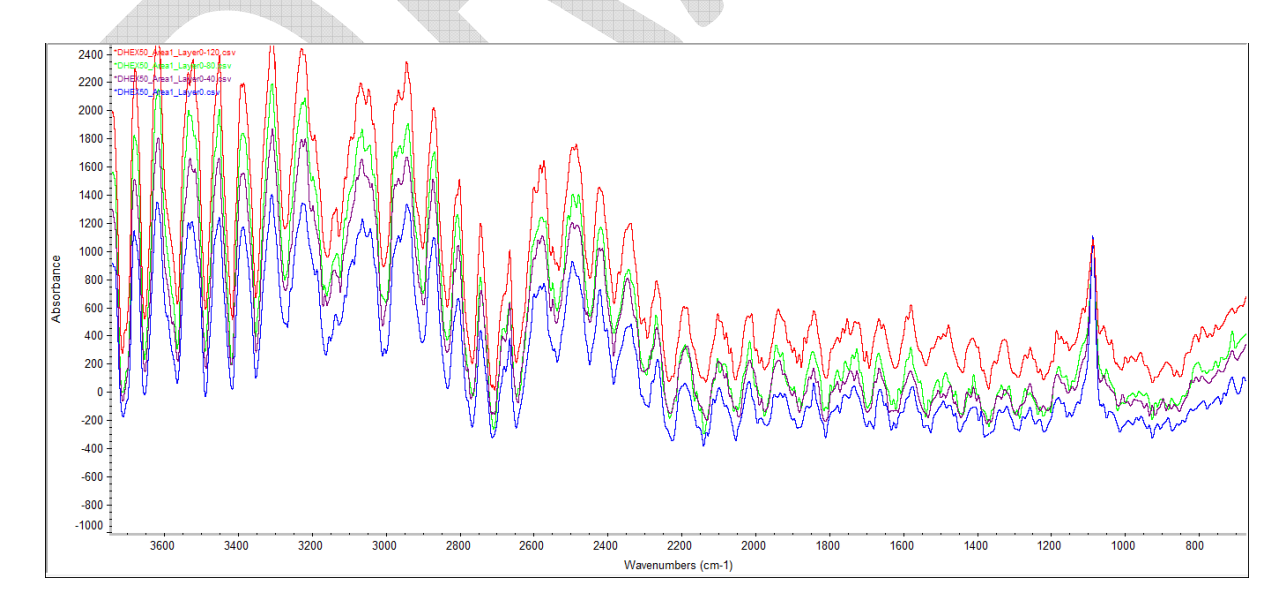


Fig. 9 RAMAN Spectra of PLA-PEG-PLA loaded iron oxide nanoparticles prepared by drug encapsulation after polymer coating

Figure 9 shows the RAMAN spectrum of the complex with drug encapsulation after polymer encapsulation. Unlike the other drug encapsulation method, where drug is mixed and entrapped together with the polymer, this method gives different nanoparticle morphology. It is seen that all peaks change in the same trend with relatively the same quantity. This indicates that instead of a bilayer coating consisting of oleic acid and polymer, the magnetic nanoparticles are coated with a mixed single layer of polymer and oleic acid. The schematic representation of this morphology is shown in Fig 10.

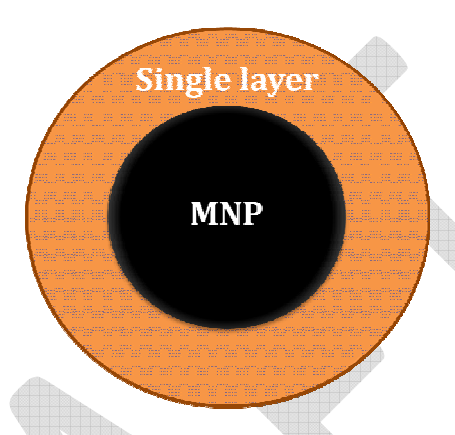


Fig. 10 Schematic representation of PLA-PEG-PLA loaded iron oxide nanoparticles prepared by drug encapsulation after polymer coating

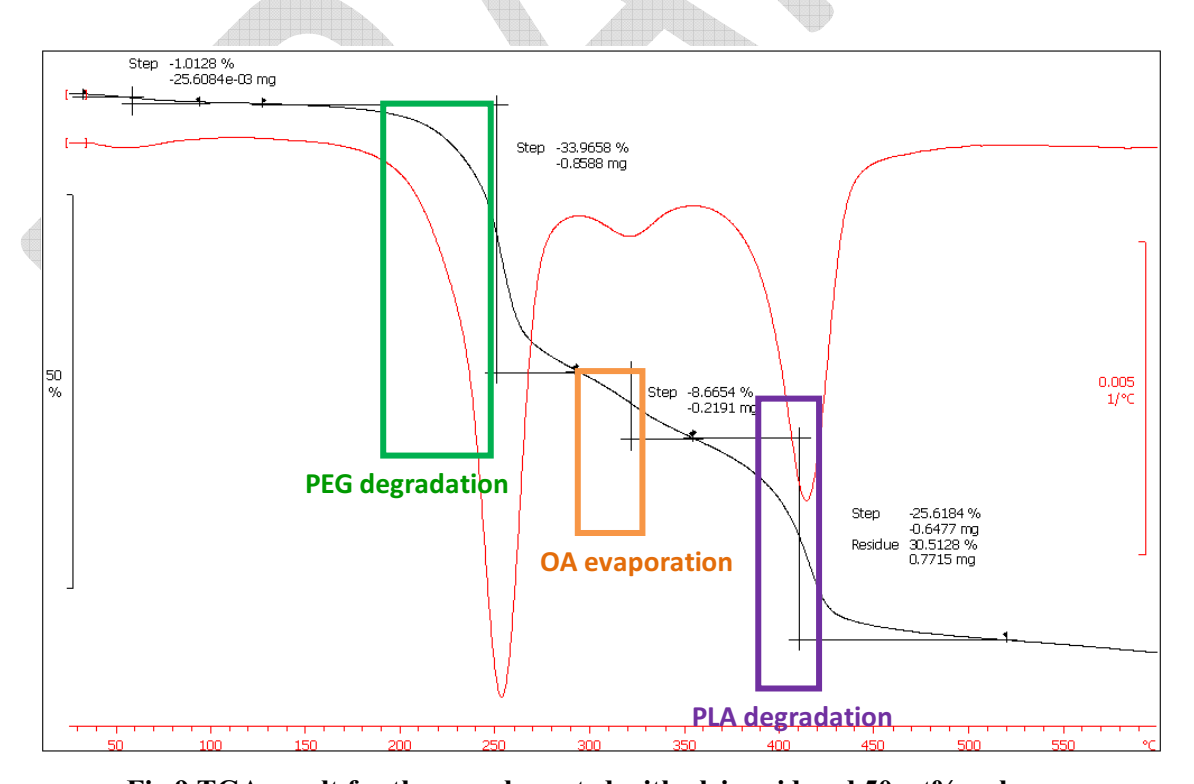


Fig.9 TGA result for the sample coated with oleic acid and 50 wt% polymer

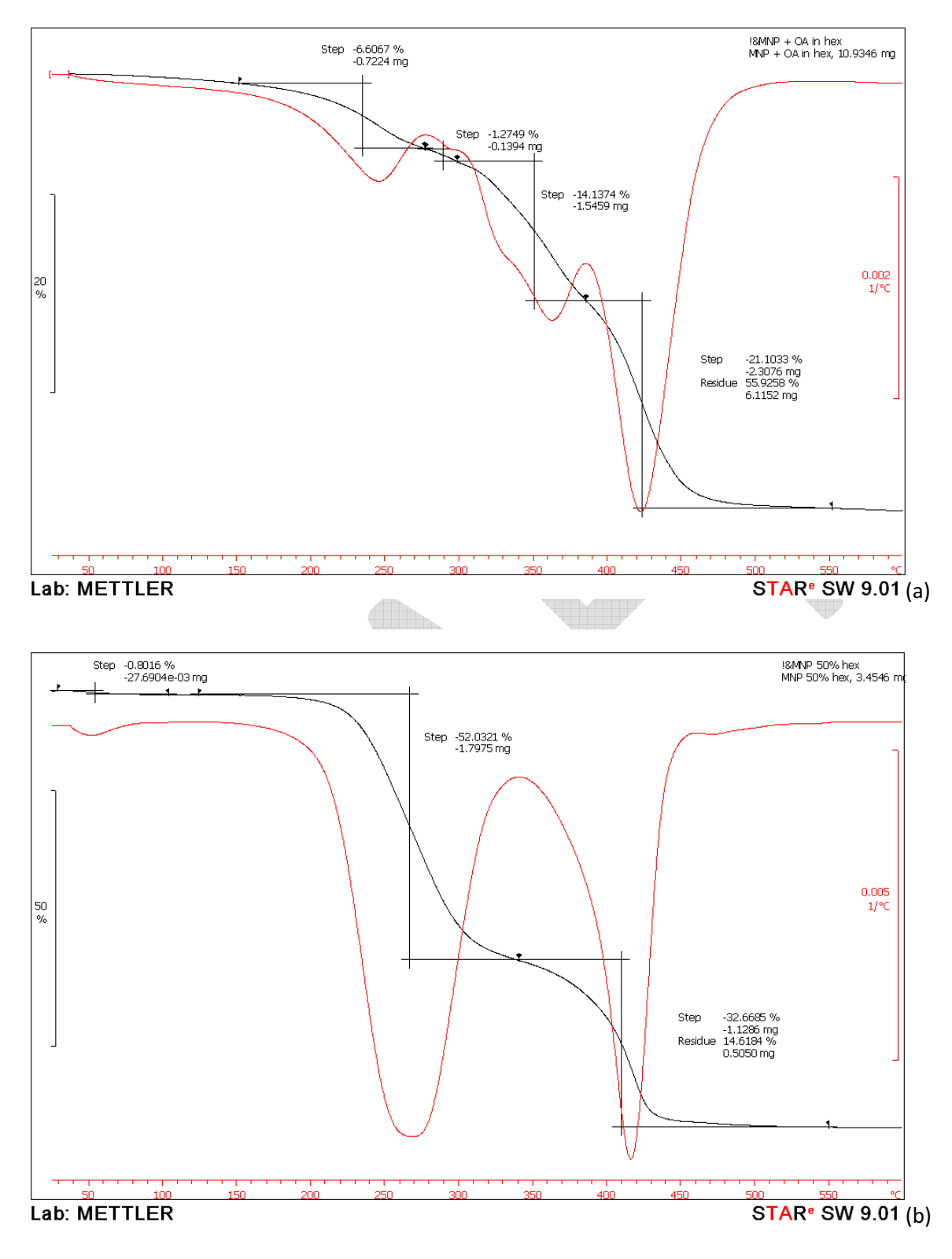


Fig.10 TGA result for (a) MNP+OA in hexane (b) MNP coated with 50% polymer

#### References

- 1. Gupta, A.K. and M. Gupta, *Synthesis and surface engineering of iron oxide nanoparticles for biomedical applications*. Biomaterials, 2005. **26**(18): p. 3995-4021.
- 2. Mahmoudi, M., et al., Superparamagnetic Iron Oxide Nanoparticles with Rigid Cross-linked Polyethylene Glycol Fumarate Coating for Application in Imaging and Drug Delivery. The Journal of Physical Chemistry C, 2009. **113**(19): p. 8124-8131.
- 3. Suh, W.H., et al., *Nanotechnology, nanotoxicology, and neuroscience*. Progress in Neurobiology, 2009. **87**(3): p. 133-170.
- 4. Corot, C., et al., *Recent advances in iron oxide nanocrystal technology for medical imaging.* Advanced Drug Delivery Reviews, 2006. **58**(14): p. 1471-1504.
- 5. Ajay K. Gupta, A.C., Surface Modification of Superparamagnetic Iron Oxide Nanoparticles and Their Intracellular Uptake. European Cells and Materials, 2002. **4**(Suppl.2): p. 101-102.
- 6. Sun, C., J.S.H. Lee, and M. Zhang, *Magnetic nanoparticles in MR imaging and drug delivery*. Advanced Drug Delivery Reviews, 2008. **60**(11): p. 1252-1265.
- 7. Jain, T.K., et al., *Iron Oxide Nanoparticles for Sustained Delivery of Anticancer Agents.* Molecular Pharmaceutics, 2005. **2**(3): p. 194-205.
- 8. Zhang, X., et al., *Synthesis and characterization of the paclitaxel/MPEG-PLA block copolymer conjugate.* Biomaterials, 2005. **26**(14): p. 2121-2128.
- 9. Laurent, S., et al., Magnetic Iron Oxide Nanoparticles: Synthesis, Stabilization, Vectorization, Physicochemical Characterizations, and Biological Applications. Chemical Reviews, 2008. **108**(6): p. 2064-2110.
- 10. Venkatraman, S.S., et al., *Micelle-like nanoparticles of PLA-PEG-PLA triblock copolymer as chemotherapeutic carrier.* International Journal of Pharmaceutics, 2005. **298**(1): p. 219-232.
- 11. Rutnakornpituk, M., et al., *Magnetic core-bilayer shell nanoparticle: A novel vehicle for entrapmentof poorly water-soluble drugs.* Polymer, 2009. **50**(15): p. 3508-3515.
- 12. Bakandritsos A, M.G., Zboril R, Bouropoulos N, Tucek J, Fatouros DG, Avgoustakis K., *Preparation, stability and cytocompatibility of magnetic/PLA-PEG hybrids.* Nanoscale, 2010. **2**(4).
- 13. Kayal, S. and R.V. Ramanujan, *Doxorubicin loaded PVA coated iron oxide nanoparticles for targeted drug delivery*. Materials Science and Engineering: C, 2010. **30**(3): p. 484-490.
- 14. Yasugi, K., et al., *Preparation and characterization of polymer micelles from poly(ethylene glycol)-poly(,-lactide) block copolymers as potential drug carrier.* Journal of Controlled Release, 1999. **62**(1-2): p. 89-100.
- 15. Liversidge, G.G. and P. Conzentino, *Drug particle size reduction for decreasing gastric irritancy and enhancing absorption of naproxen in rats.* International Journal of Pharmaceutics, 1995. **125**(2): p. 309-313.
- 16. Maver, U., et al., *Incorporation and release of drug into/from superparamagnetic iron oxide nanoparticles*. Journal of Magnetism and Magnetic Materials, 2009. **321**(19): p. 3187-3192.

# Preparation and characterizations of $Fe_3O_4$ magnetic nanoparticles coated PLA-grafted Chitosan copolymer as potential drug delivery material for naproxen

#### 1. Introduction

Magnetic nanoparticles possess special physical and chemical properties suitable for use in many industrial and biomedical applications. Fe<sub>3</sub>O<sub>4</sub> iron oxide nanoparticles can be dispersed in various solvents by using surfactants to assist its suspension present as magnetic nanoparticles colloid in selected media. Many research has been focused on the materials potential use, such as magnetic drug targeting, pigment, recording material, magnetic sensing, and separation, etc [1-4]. Various methods of Fe<sub>3</sub>O<sub>4</sub> nanoparticles preparation have been reported in the literatures, such as microemulsions [5], laser ablation [6], high temperature decomposition of organic precursor [7], etc. However, one of the convenient and economical technique is chemical coprecipitation, due to the well-dispersed in water-base solution of Fe<sub>3</sub>O<sub>4</sub> (magnetite) nanoparticles, which offers low temperature processing.

Chitosan,  $\beta$ -(1-4) linked 2-amino-2-deoxy-D-glucose, is linear cationic polysaccharide obtained by deacetylation of chitin, which is derived from crab and shrimp shells. This polymer is known to be non-toxic, good biocompatible, highly flexible, and low cost material [8]. As a result, this biopolymer is widely use in many applications, especially in biomedical and agricultural fields. Polylactide (PLA) is aliphatic polyester derived from agricultural sources, such as corn and starch. PLA has attracted vast attention due to its good mechanical properties, bio-degradability and biocompatibility [9]. However, its hydrophobicity limits its use in certain biomedical applications. Combining of PLA and chitosan by copolymerization produces copolymers with improved mechanical properties, adjustable crystallinity and hydrophilicity. In addition, a variation in PLA/Chitosan composition in the copolymer chain results in the change in amphiphilic property of the copolymer, which behave as polymeric surfactant.

Naproxen is a non-steroidal anti-inflammatory drug (NSAID), which possess a very poor water-solubility (0.025mg/ml at 25°C). Several approaches have been attempted to improve the naproxen dissolution properties. Encapsulation is one of the effective procedures. This technique not only provides an enhancement in water solubility of drug by the encapsulation material, but also reduces the irritation of gastrointestinal and provides long lasting release of selected drug as controlled release drug delivery [10]. Chitosan and its derivative have demonstrated as an efficient material to promote dissolution of naproxen [11].

In this study, magnetic nanoparticles coated PLA/Chitosan copolymers are prepared for use as potential drug delivery material for naproxen. The drug–encapsulated magnetic nanoparticles are prepared by one step coating of  $Fe_3O_4$  magnetic nanoparticles synthesized via chemical coprecipitation using ammonium hydroxide (NH $_3$ .H $_2O$ ) solution. This material is obtained without the use of external surfactant as the PLA/Chitosan copolymer (low molecular weight) functions as encapsulation and coating material and as well as a surfactant. Properties of the drug-encapsulated materials are then characterized.

#### 2. Experimental

#### 2.1. Materials

Ferric chloride anhydrous (FeCl<sub>3</sub>) and ferrous chloride tetrahydrate (FeCl<sub>2</sub>.4H<sub>2</sub>O) were purchased from Acros organics. Chitosan oligomers (97.0% deacetylation) were obtained from Taming Enterprises Co., Ltd., Thailand. Lactic acid (commercial grade, 10% weight water), n-hexane, and ammonium hydroxide (NH<sub>4</sub>OH, 25% of ammonia) were acquired from Carlo Erba reagents. Tin (II) chloride was received from Sigma Aldrich. Naproxen was purchased from Andenex-Chemie Gmblt, Germany. All chemicals were analytical grade reagents, and were used without further purification. Deionized water was used throughout this work.

#### 2.2. Synthesis of PLA/Chitosan copolymer

PLA/Chitosan copolymer was synthesized by grafting of PLA chain from hydroxyl groups of chitosan structure employing condensation reaction of lactic acid. Essentially, 100 mL of lactic acid was heated to 120°C for 1 hour. The temperature was increased to 140°C for 1 hour, and 1.1 g chitosan (1 wt% of pure lactic acid) was then added to the system. The temperature of the mixture was kept at 140°C for 1 hour, then 0.55 g SnCl<sub>2</sub> catalyst (0.2 mol % pure lactic acid) was added. The temperature was kept at 140°C for 3 hours. Vacuum system was applied for 1 hour to remove small molecular weight by products. Consequently brown copolymer in viscous liquid form was obtained.

# 2.3. Preparation of Fe<sub>3</sub>O<sub>4</sub> nanoparticles coated PLA/chitosan copolymer with loaded naproxen

Magnetic nanoparticles were prepared by chemical coprecipitation, where 1 g (0.005 mol) FeCl<sub>2</sub>.4H<sub>2</sub>O and 1.66 g (0.01 mol) FeCl<sub>3</sub> were dissolved in 40 ml of deionization water, then stirred at 350 rpm for 10 min. Ammonium hydroxide (NH<sub>4</sub>OH, 25% of ammonia) was then added dropwise to the iron salt solution. Precipitate was observed and the mixture was vigorously stirred for 30 min at room temperature. The Fe<sub>3</sub>O<sub>4</sub> precipitate was then washed twice with ethyl alcohol and deionization water. In a separate container, naproxen was dissolved in viscous PLA/Chitosan copolymer and the mixture was heated at 60°C to form a homogeneous phase mixture. The mixture was then added dropwise to the Fe<sub>3</sub>O<sub>4</sub> with slowly stirred motion. Subsequently, 20 ml of n-hexane was added to the system as a dispersing medium. Deionized water (100 ml) was added and the mixture was stirred for 30 min to evaporate n-hexane. The resulting magnetic nanoparticles colloid was centrifuged at 2500 rpm for 15 min, and the liquid supernatant was kept as the magnetic nanoparticles dispersed in the water medium.

#### 2.4. Characterizations

# 2.4.1. X-Ray diffraction

The crystal structure of the magnetic nanoparticles was characterized by X-ray diffraction (XRD) recorded by using a Rigaku TTRAX III diffractometer with CuK $\alpha$  radiation (1.5418 Å). The conditions are  $\theta/2\theta$  scan, 50 kV, 300 mA, 0.2°/ step, 2°/min, Ds = Ss =  $(\frac{1}{2})^{\circ}$ , fix monochomator, and focusing beam method were used.

# 2.4.2. TEM and particle size analyzer

The morphology and size of the magnetic nanoparticles were investigated by using transmission electron microscope (JEOL, JEM-2010) at accelerating voltage of 200 keV. The samples were prepared by placing drops of diluted medium dispersed of the nanoparticles on the copper grids. Size distribution was determined by Particles Size Analyzer (ZETA-SIZER, MALVERN Nano-Zs90). The real and imaginary reflective indexes were used at 1.59 and 0.0, respectively. The following parameters were used for the experiment: medium refractive index 1.330, medium viscosity 1.0 mPa.s and a dielectric constant of 80.4. The size analysis of each sample consisted of 30 measurements.

### 2.4.3. Raman spectroscopy

The liquid sample was dropped on the glass slide and placed into the vacuum oven at room temperature for 24 hours. Then, the magnetic nanoparticles were characterized by using Raman spectroscopy (NT-MDT NTEGRA Spectra). Laser light source is 632.8 nm and confocal raman scanning mode were applied.

# 2.4.4. Fourier transform infrared spectroscopy (FTIR)

FTIR spectra of the PLA/Chitosan copolymer and naproxen drug were investigated using Fourier Transform Infrared Spectrophotometer (Nicolet 6700 FT-IR).

# 2.4.5. Vibrating Sample Magnetometer

The magnetic properties were investigated by using room temperature vibrating sample magnetometer (VSM, Lakeshore 7400, Lakeshore) at an applied maximum field of 10,000 G.

#### 3. Results and Discussion

#### 3.1. Particle size distribution and zeta potential

Preliminary study on preparation of Fe<sub>3</sub>O<sub>4</sub> magnetic nanoparticles, coated by PLA/chitosan copolymer as a surfactant was conducted by varying MNP/copolymer compositions. Effect of the mixture compositions on average particles size and surface charge of the nanoparticles are shown in Figures 1 and 2. Figure 1 shows that average size of the copolymer-coated magnetic nanoparticles increases when Fe<sub>3</sub>O<sub>4</sub> contents increases. This reveals that the decrease in copolymer content compared to Fe<sub>3</sub>O<sub>4</sub> leads to less effective coating of the copolymer on the nanoparticles surface, resulting in agglomeration of the magnetic particles to form larger particles. Figure 2 shows results from zeta potential of the resulting nanoparticles as a function of pH and weight ratio of Fe<sub>3</sub>O<sub>4</sub>/copolymer. The result show that copolymer-coated nanoparticles prepared from different weight ratio contains significantly similar values of surface charge at all composition range, accept at acidic pH of 3, where those prepared from a 1:1 ratio show much higher positive value. Moreover, results on zeta potential of the nanoparticles as a function of pH show moderate negative value at pH 7, indicating appreciable stability of the particles however base solution exhibits more stable particles than acidic and neutral solution. This probably, the charge of the basic solution can assist particles to stabilize in the medium.

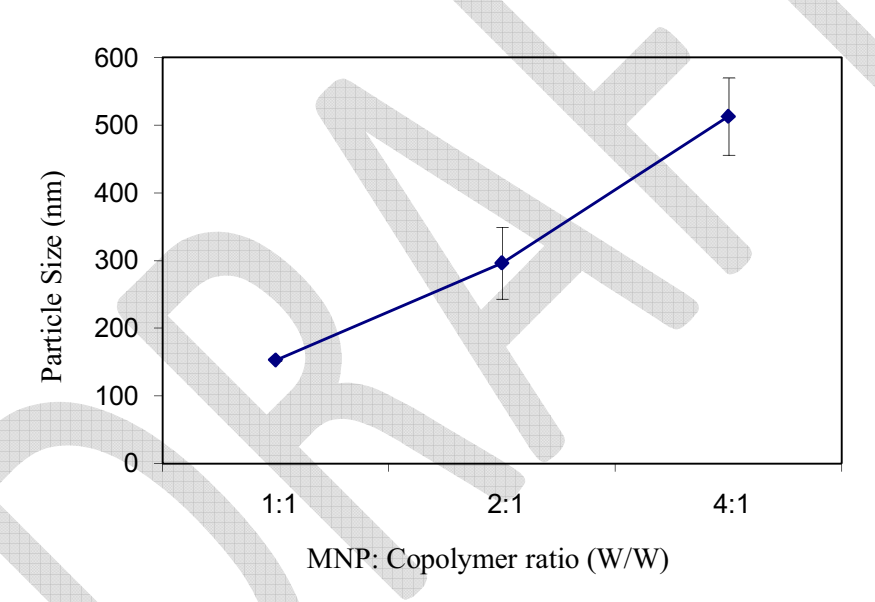


Figure 1. Average size of copolymer-coated magnetic nanoparticles as a function of Fe<sub>3</sub>O<sub>4</sub> to copolymer ratios.

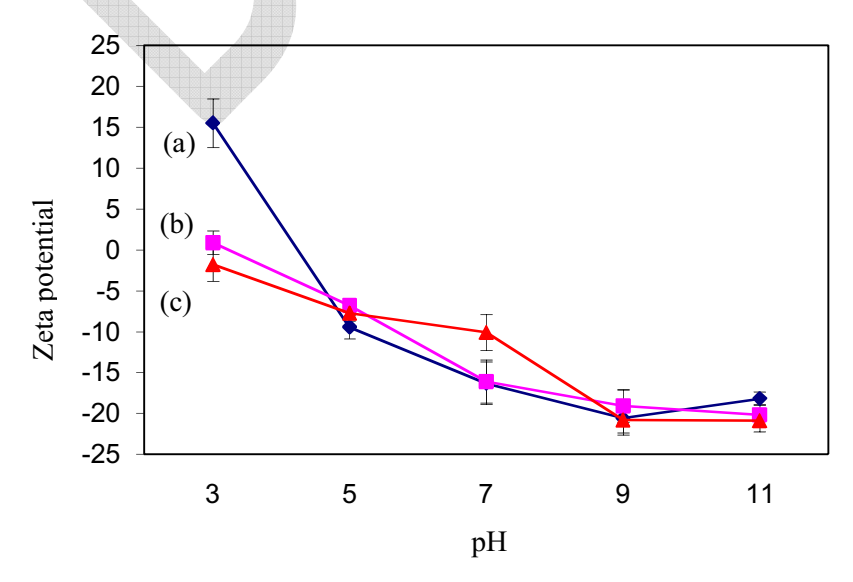


Figure 2. Effect of pH on surface charge of copolymer-coated magnetic nanoparticles prepared from various  $Fe_3O_4$ /copolymer ratio: (a) 1.1, (b) 2:1, and (c) 4:1

PLA/Chitosan copolymer-coated MNP with loaded naproxen is then prepared by the same procedure as previous discussed, except that 3 wt% of naproxen is mixed with the copolymer before the coating process. Results on average diameters, yield, and surface charge of the resulting drugloaded nanoparticles are shown in Figures 3 and 4. The results show that the average size of the nanoparticles decrease from 351 nm to138 nm with an increase in Fe<sub>3</sub>O<sub>4</sub>/copolymer ratios from 1:1 to 4:1. This is intriguing, as this is opposite to those previously observed in the system not containing naproxen. This is probably due to the presence of naproxen along with PLA/Chitosan copolymer, which prevents the magnetic nanoparticles to aggregate. Yield of suspended magnetic nanoparticles is also determined from weight percentage of suspended particle per original magnetic particle. The yield results show an increasing trend with increasing MNP and the surface charge with loaded naproxen, which enable the particles to be more stable in the neutral solution, compared to the MNP without naproxen. This can be explain in term of naproxen perform as the co-surfactant [12], resulting in the smaller sizes and also make the MNP well disperse in the neutral medium. It has been clearly seen that the magnetic nanoparticles is stable at basic solution (pH>7), from this result, 2:1 ratio was prepared the basic medium in order to study the affect of the particles size and the yield product as a function of pH. Consequently, the results show that percent yield of 2:1 ratio of MNP: PLA/Chitosan with naproxen in basic solution was increased from 59 to 79 percent, and particles size was slightly decreased from 225 nm to 185 nm with the standard deviation is 11.

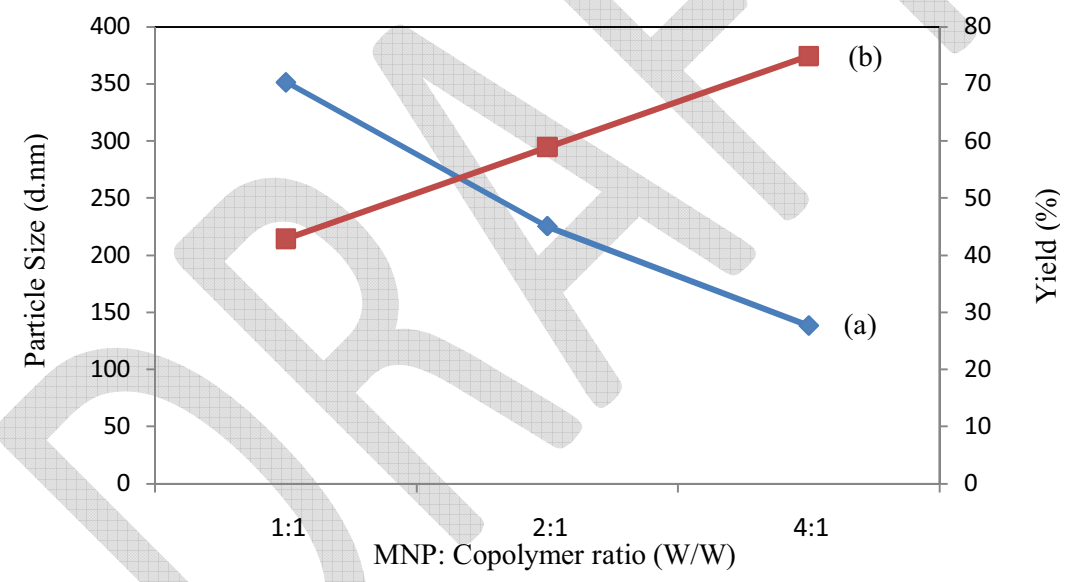


Figure 3. Average size and yield of naproxen-encapsulated magnetic nanoparticles as a function of MNP/copolymer ratios; (a) average particle size and (b) yield.

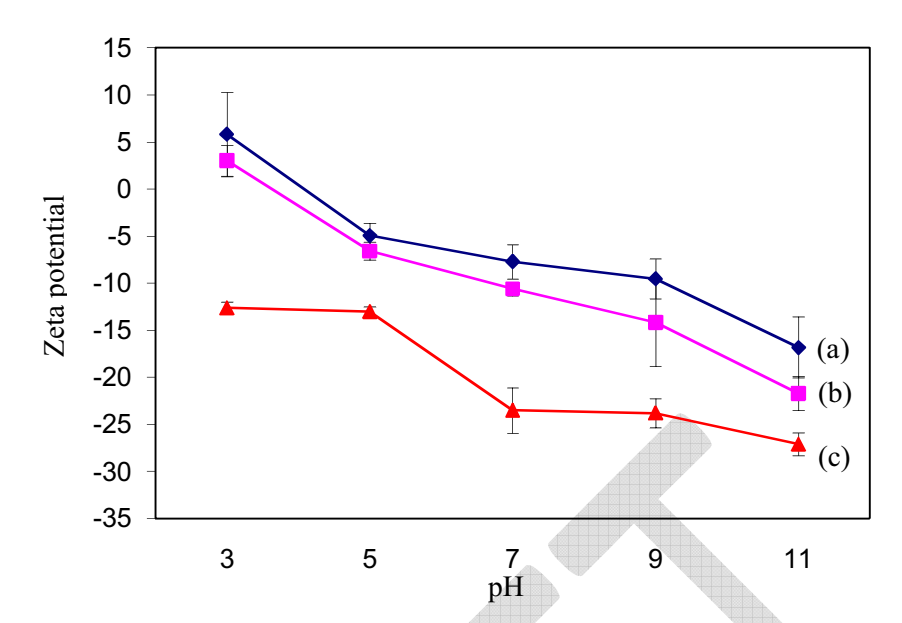


Figure 4. Effect of pH on surface charge of naproxen loaded PLA/Chitosan-MNP; (a) 1.1, (b) 2:1, and (c) 4:1



### 3.2. Morphology of naproxen loaded PLA/Chitosan-MNP.

TEM images of naproxen-loaded PLA/chitosan-MNP prepared at various MNP/copolymer ratio, shown in Figure 5. The images reveals that at 1:1 MNP/copolymer ratio, cluster of magnetic Fe3O4 nanoparticles are represent in the bulk polymer matrix as shown in Figure 5(a). However, when the 2:1 and 4:1 ratios are used, smaller particles are obtained, especially 4:1 shows the diameters smaller than 20 nm (Figure 5(c)). Moreover, the core shell of 2:1 ratio of MNP: PLA/Chitosan with naproxen in basic medium is also observed, as shown in Figure 5(d). It should be noted that all the pictures that show in Figure 5, the sizes are smaller than the results from the size distribution because of the swelling of the organic phase in the solution we obtained.

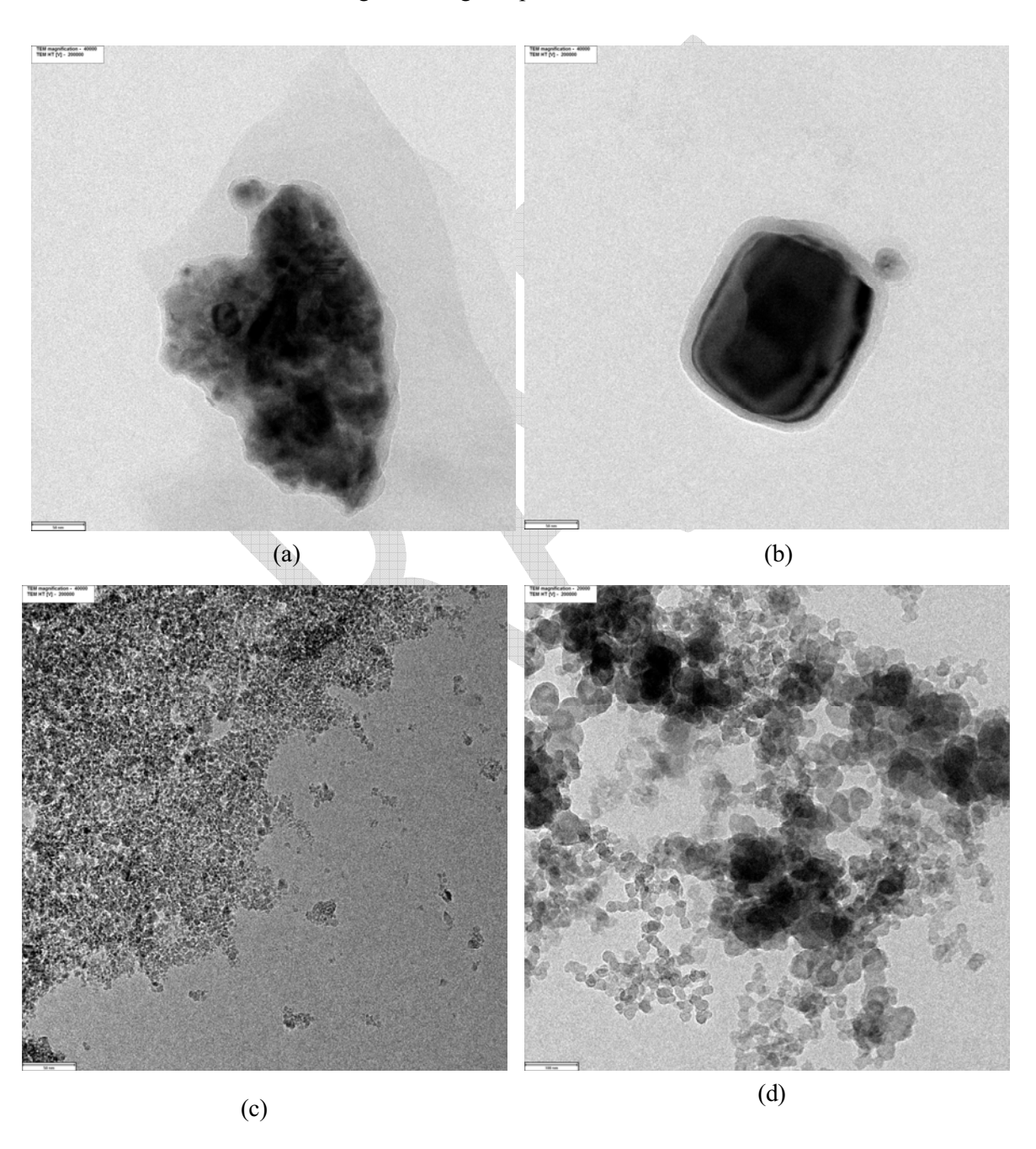


Figure 5. The TEM images of PLA/Chitosan-MNP with naproxen (a) 1:1, (b) 2:1, (c) 4:1 (d) 2:1 in pH 11.

## 3.3. Confocal Raman spectroscopy of PLA/Chitosan-Fe3O4 with loaded naproxen.

PLA/chitosan-MNP (4:1) with naproxen was investigated by using confocal Raman. Figure 6 shows, the spectra show the pattern of naproxen on PLA/Chitosan-MNP at approximately 2490 cm<sup>-1</sup>. Depth profile does not clearly show the increasing of naproxen's intensity while increasing of percent penetration as y-axis. Similarly, chitosan intensity does not decrease as increasing the penetration into the samples. This may confirm the idea that naproxen works as co-surfactant for the nanoparticles. It reveals that PLA/Chitosan copolymer and naproxen drug cum together as one phase mixing. Moreover, a model picture for these magnetic nanoparticles as showed in Figure 7.

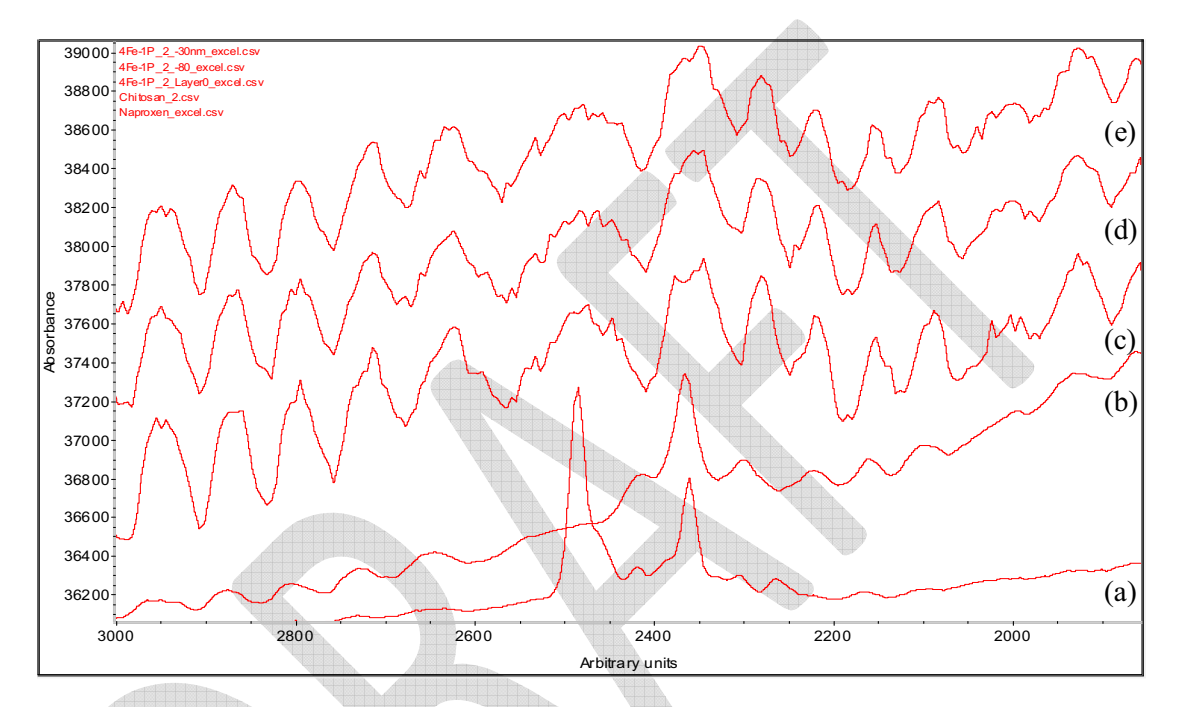


Figure 6. Raman spectra of MNP: Chitosan (4:1) showed: (a) naproxen, (b) chitosan, and confocal spectra of (c) 80 nm, (d)30 nm, and (e) at the surface

Figure 7(a), shows practical spherical core shell as PLA/Chitosan-MNP with loaded naproxen (co-surfactant), one phase mixing of PLA/chitosan and naproxen is observed. However, ideally bilayer outer shell of naproxen in between Fe3O4 and PLA/Chitosan copolymer is not observed.

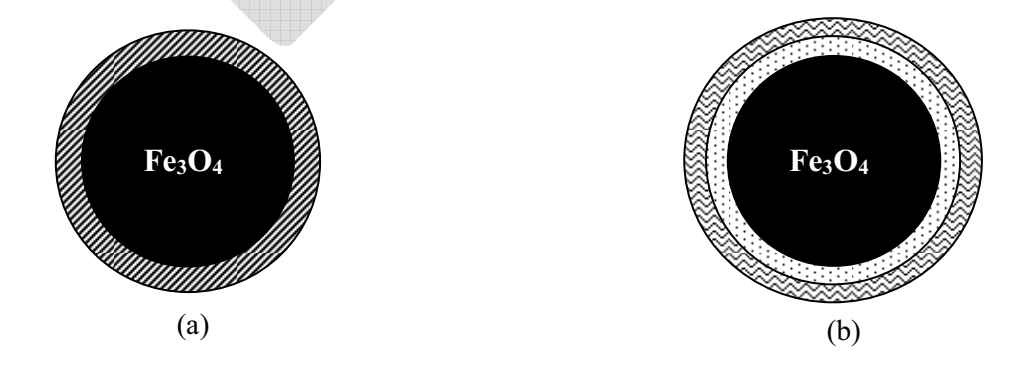


Figure 7. Model for PLA/Chitosan-MNP with loaded naproxen, (a) one phase mixing, (b) bilayer outer shell.

# 3.4. Confirmation of unchanged naproxen drug properties by using Fourier transform infrared spectroscopy (FT-IR).

There is not much changed in the spectra of the mixing of PLA/Chitosan and naproxen together as shown in Figure 8(a). However, small shift to the lower wavelength of carbonyl (C=O) peak of PLA/Chitosan at 1750 cm<sup>-1</sup> was observed. This probably represents the interaction between OH- group of naproxen and the C=O group of PLA/Chitosan copolymer. Therefore, this can be concluded that the properties of naproxen drug are not

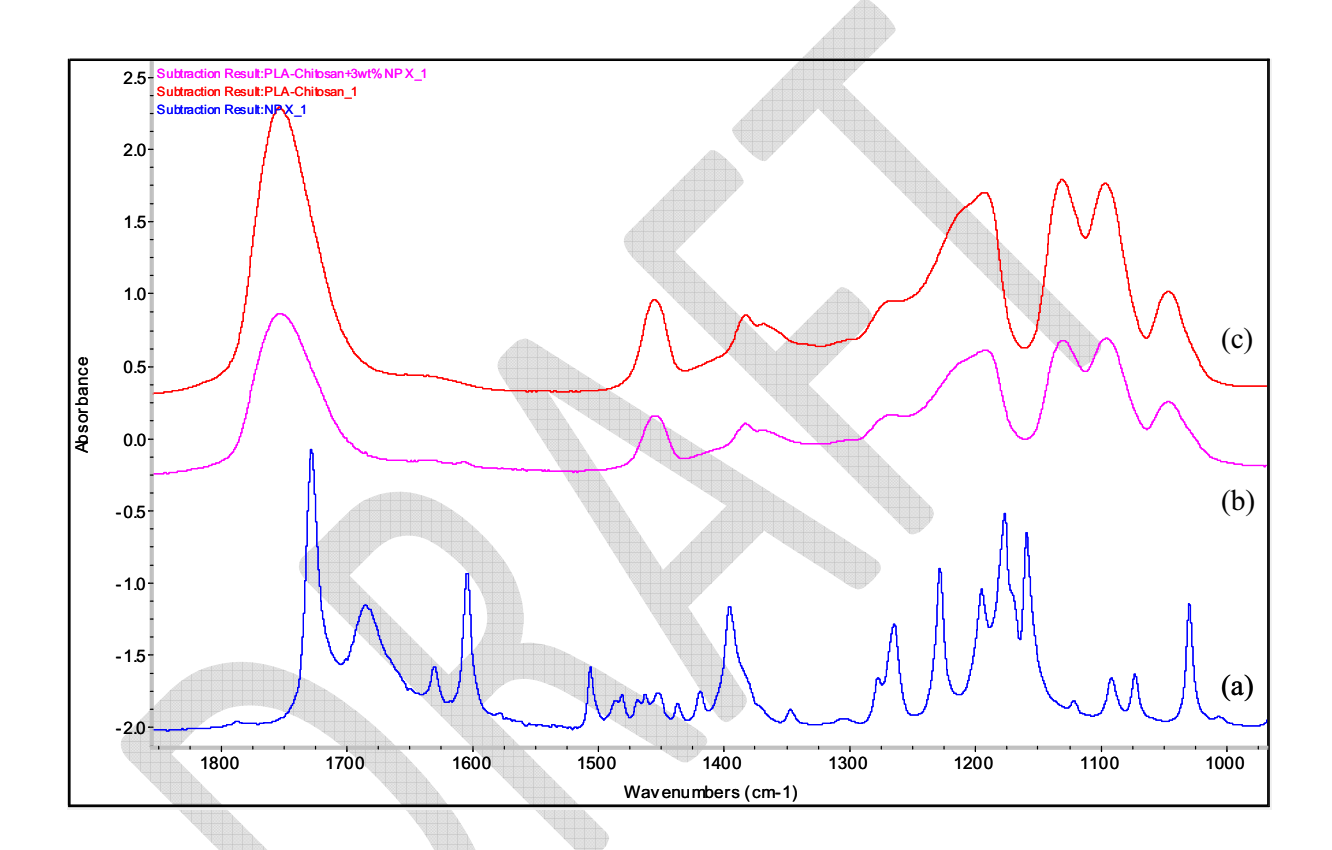


Figure 8. FT-IR spectra of: (a) naproxen, (b) PLA/Chitosan copolymer, and (c) PLA/Chitosan mixed with naproxen drug

## 3.5. X-ray diffraction

XRD spectra of the resulting nanoparticles are examined. Naproxen-loaded PLA/Chitosan-MNP prepared at a 4:1 ratio clearly shows similar crystallinity characteristics to that of the origin  $Fe_3O_4$  magnetite material, as shown in Figure 9. This reveals that modified MNP with PLA/Chitosan and drug does not changed the form of the magnetite.

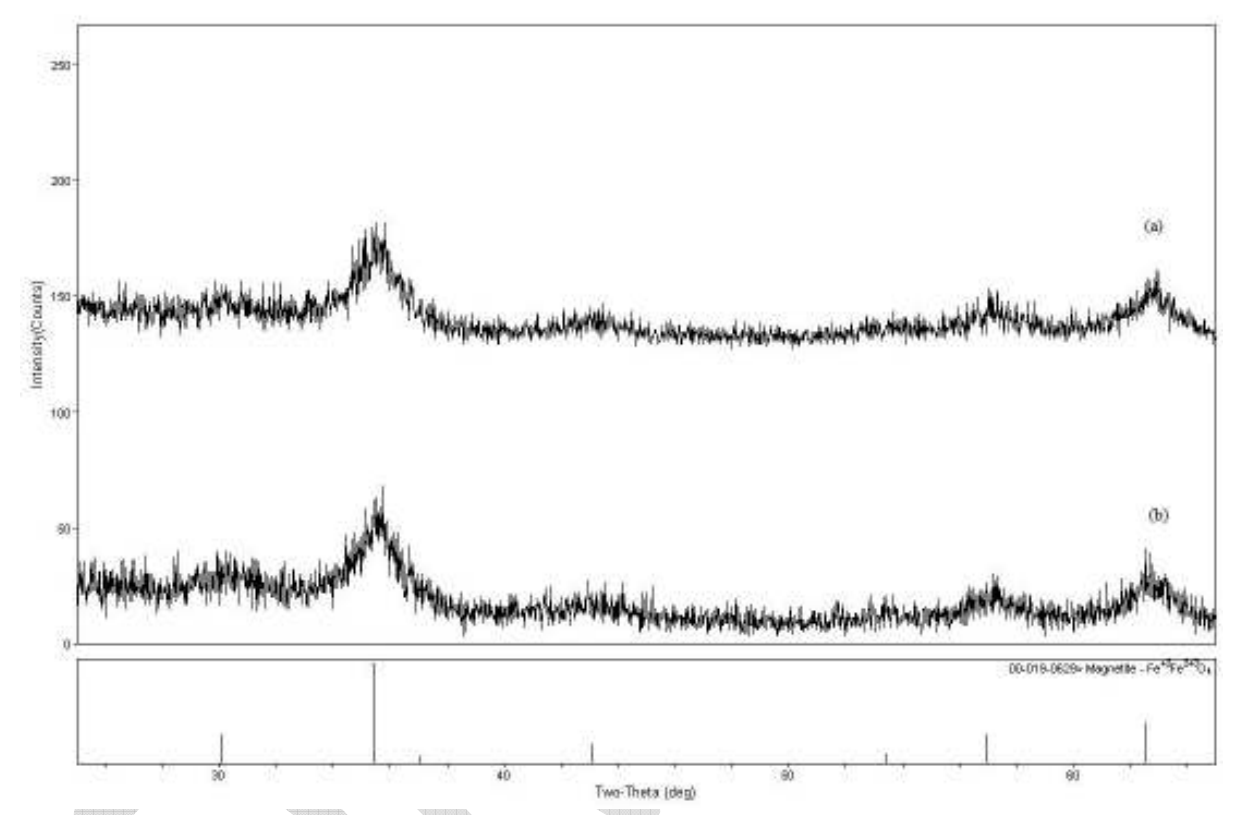


Figure 9. XRD pattern of magnetic nanoparticles of (a) Fe3O4 without coating PLA/Chitosan copolymer and (b) Fe3O4 with coating PLA/Chitosan copolymer and naproxen

### 3.6. Magnetic properties of PLA/Chitosan-MNP with naproxen.

The magnetization curve of naproxen-loaded Fe<sub>3</sub>O<sub>4</sub> nanoparticles is shown in Figure 10. The magnetization curve of 4:1 ratio of PLA/Chitosan-MNP with naproxen is to be without hysteresis, coercivity field and remnant magnetization can be found from the curve. This confirms that PLA/Chitosan-Fe<sub>3</sub>O<sub>4</sub> with loaded naproxen shows superparamagnetic properties. The magnetization curve indicates that the saturation magnetization (Ms) of the prepared magnetic nanoparticles is 0.88 emu/g, which is much lower than that of the oleic acid coated MNP (MS of OA-MNP = 32 emu/g), reported in the literature [13]. This probably due to the highly coating thickness by copolymer, this leads to stronger shield effect on the magnetic properties of the nanoparticles. Nonetheless, this material is suitable for use in biomedical applications, as this is conveniently prepared in a one-step process without the use of external surfactant, in which the copolymer acts as both surfactant and biocompatible coating materials.

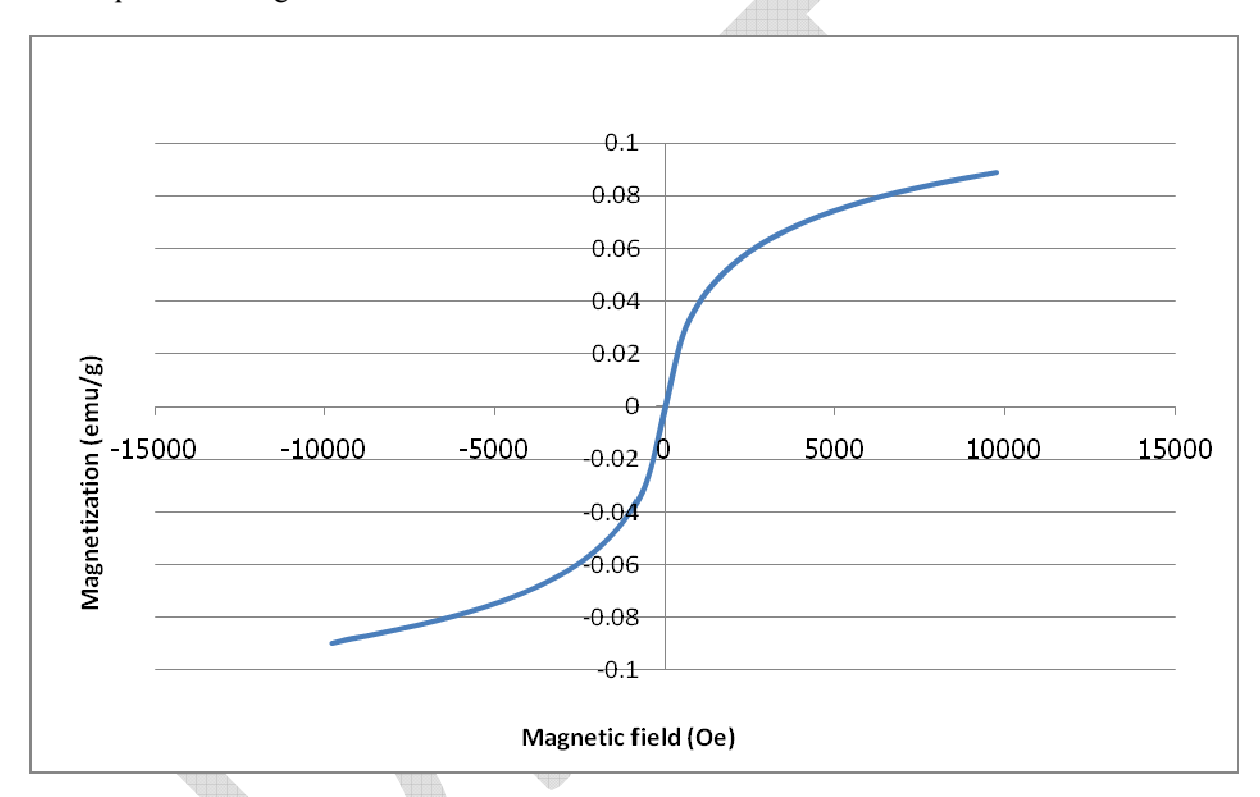


Figure 10. Magnetization curve of 4:1 PLA/Chitosan-MNP with

์ เมธิวิจัยอาวุโส สกว. ศาสตราจารย์ ดร. ประมวล ตั้งบริบูรณ์รัตน์ (ณวันที่ 20 มิย. 2554) รายชื่อกลุ่มวิจัย

-		เริ่มเข้าร่วมโครงการ			ปัจจุบัน	
ชื่อ-นามสกุล	ตำแหน่งวิชาการ	สังก็ด	ตำแหน่ง ในโครงการ	ตำแหน่งวิชาการ	สังกิต	สถานภาพปัจจุบัน
1. ดร.รัชนีย์ อุดมแสงเพีชร	ศาสตราจารย์	ภาควิชาพยาธิชีววิทยา	ที่ปรึกษา	ศาสตราจารย์	ภาควิชาพยาธิชีววิทยา	ยังอยู่ในโครงการ
		คณะวิทยาศาสตร์			คณะวิทยาศาสตร์	
		มหาวิทยาลัยมหิดล			มหาวิทยาลัยมหิดล	
2. ดร.เมธา รัตนากรพิทักษ์	ผู้ช่วยศาสตราจารย์	ภาควิชาเคมี	ที่ปรึกษา	รองศาสตราจารย์	ภาควิชาเคมี	ยังอยู่ในโครงการ
		คณะวิทยาศาสตร์			คณะวิทยาศาสตร์	
		มหาวิทยาลัยนเรศาร			มหาวิทยาลัยนเรศวร	
3. นพ.สุรเดช หงส์อิง	รองศาสตราจารย์	ภาควิชากุมารเวชศาสตร์	ที่ปรึกษา	รองศาสตราจารย์	ภาควิชากุมารเวชศาสตร์	ยังอยู่ในโครงการ
		คณะแพทยศาสตร์ รามาธิบดี			คณะแพทยศาสตร์ รามาธิบดี	
		มหาวิทยาลัยมหิดล			มหาวิทยาลัยมหิดล	
4. Dr.Paul E. Orndorff	Professor	Public Health and Pathobiology, ที่ปรึกษา College of Veterinary Medicine	ที่ปรึกษา	Professor	Public Health and Pathobiology College of	ยังอยู่ในโครงการ
		North Carolina State University			Veterinary Medicine, North Carolina State University	
5. Dr.Masaaki Kai	Professor	Faculty of	ที่ปรึกษา	Professor	Faculty of	ยังอยู่ในโครงการ
		Pharmaceutical Sciences, Nagasaki University			Pharmaceutical Sciences, Nagasaki University	,
6. ดร.นพวรรณ ชนัญพานิช	รองศาสตราจารย์	ภาควิชาเคมีเทคนิค	ที่ปรึกษา	รองศาสตราจารย์	ภาควิชาเคมีเทคนิค	ยังอยู่ในโครงการ
		คณะวิทยาศาสตร์และเทคโนโลยี			คณะวิทยาศาสตร์และเทคโนโลยี	
		สถาบันเทคโนโลยีพระจอมเกล้า			สถาบันเทคโนโลยีพระจอมเกล้า	
		พระนครเหนือ			พระนครเหนือ	

1. ตร.ประมวล ตั้งบริบูรณ์รัตน์ ศาสตราจารย์ มหาวิทยาดี 2. ตร.ปกรณ์ โอภาประกาสิต ผู้ช่วยศาสตราจารย์ ภาควิทยาก มหาวิทยาที่ สินม์เห	วิทยาศาสตร์และเทคโนโลยี มหาวิทยาลัยมหิดล ภาควิชาเคมี มหาวิทยาลัยมหิดล ภาควิชาวิศวกรรมและเทคโนโลยีเคมี ชีวภาพ สถาบันเทคโนโลยี นานาชาติสิรินธร (SIIT)	หัวหน้า กลุ่มกิจัย		คณะวิทยาศาสตร์ _ ั ๊	
้าน์ คาสตราจารย์ ผู้ช่วยศาสตราจารย์ -	เละเทคโนโลยีเคมี คโนโลยี	หวหน้า กลุ่มกิจัย		6	
น์ ผู้ช่วยศาสตราจารย์ -	ล มและเทคโนโลยีเคมี ทคโนโลยี (SIIT)	หัวหน้า กล่มกิจัย		มหาวทยาลยมหดล	
นี้ช่วยศาสตราจารย์	ล มเละเทคโนโลซีเคมี ทคโนโลซี (SIIT)	กลุ่มกิจะเ	ศาสตราจารย์	ภาควิชาเคมี	ยังอยู่ในโครงการ
นี้ช่วยศาสตราจารย์	เละเทคโนโลยีเคมี คโนโลยี SIIT)			คณะวิทยาศาสตร์	
นี้ช่วยศาสตราจารย์				มหาวิทยาลัยมหิดล	
I	กาพ สถาบันเทคโนโลยี นาชาติสิรินธร (SIIT)	นักวิจัย	รองศาสตราจารย์	ภาควิชาวิศวกรรมและ	ยังอยู่ในโครงการ
1	นาชาติสิรินธร (SIIT)			เทคโนโลยีเคมีชีวภาพ สถาบัน	
1				เทคโนโลยีนานาชาติสิรินธร	
1	มหาวิทยาลัยธรรมศาสตร์			มหาวิทยาลัยธรรมศาสตร์	
ให้งชา การแล้ง	ศูนย์เทคโนโลยีโลหะและวัสดุ	นักวิจัย	ı	ศูนย์เทคโนโลยีโลหะและวัสดุ	ยังอยู่ในโครงการ
วิทยา	แห่งชาติ สำนักงานพัฒนา			แห่งชาติ สำนักงานพัฒนา	
	วิทยาศาสตร์และเทคโนโลยี			วิทยาศาสตร์และเทคโนโลยี	
	แห่งชาติ			แห่งชาติ	
4. ดร.มัณทนา โอภาประกาสิต อาจารย์ ภาคริท	ภาควิชาวัสดุศาสตร์	ນັກວີຈັຍ	ผู้ช่วยศาสตราจารย์	ภาควิชาวัสดุศาสตร์	ยังอยู่ในโครงการ
P01823	คณะวิทยาศาสตร์			คณะวิทยาศาสตร์	
์ จุฬาลง	จุฬาลงกรณ์มหาวิทยาลัย			จุฬาลงกรณ์มหาวิทยาลัย	
5. ตร.ไพบูลย์ ศรีอรุโณทัย อาจารย์ ภาควิเ	ภาควิชาวิศวกรรมและเทคโนโลยี	นักวิจัย	อาจารซ์	ภาควิชาวิศวกรรมและ	ชังอยู่ในโครงการ
leater le	เคมีชีวภาพ สถาบันเทคโนโลยี			เทคโนโลยีเคมีชีวภาพ สถาบัน	
unun	นานาชาติสิรินธร			เทคโนโลยีนานาชาติสิรินธร	
มหาวิ	มหาวิทยาลัยธรรมศาสตร์			มหาวิทยาลัยธรรมศาสตร์	
6. ดร.สรวง สมานหมู่ - คูนย์พ้	ศูนย์พันธุวิศวกรรมและ	นักวิจัย	นักวิจัย 1	ศูนย์พันธุวิศวกรรมและ	ยังอยู่ในโครงการ
กุ เมษา	เทคโนโลฮีซีวภาพแห่งชาติ			เทคโนโลฮีชีวภาพแห่งชาติ	
สำนักง	สำนักงานพัฒนาวิทยาศาสตร์			สำนักงานพัฒนาวิทยาศาสตร์	
uizen	และเทคโนโลยีแห่งชาติ			และเทคโนโลยีแห่งชาติ	

7. ตร.สอาด ริยะจันทร์	ผู้ช่วยศาสตราจารย์	ภาควิชาวิทยาศาสตร์และ	นักวิจัย	ผู้ช่วยศาสตราจารย์	ภาควิชาวิทยาศาสตร์และ	ยังอยู่ในโครงการ
	1	เทคโนโลยีวัสดุ			เทคโนโลยีวัสดุ	,
		คณะวิทยาศาสตร์			คณะวิทยาศาสตร์	
		มหาวิทยาลัยสงขลานครินทร์			มหาวิทยาลัยสงขลานครินทร์	
8. ดร.รัฐพร ทองกุม	อาจารซ์	ภาควิชาเคมี	นักวิจัย	ผู้ช่วยศาสตราจารย์	ภาควิชาเคมี	ยังอยู่ในโครงการ
		คณะวิทยาศาสตร์			คณะวิทยาศาสตร์	
		มหาวิทยาลัยมหิดล			มหาวิทยาลัยมหิดล	
9. ดร.สุภา วิรเศรษฐ์	อาจารซ์	ภาควิชาเคมี	นักวิจัย	อาจารซ์	ภาควิชาเคมี	ยังอยู่ในโครงการ
		คณะวิทยาศาสตร์			คณะวิทยาศาสตร์	
		มหาวิทยาลัยมหิดล			มหาวิทยาลัยมหิดล	
10. ตร.ตวงพร พลพานิช	ı	ศูนย์นาโนเทคโนโลยีแห่งชาติ	นักวิจัย	นักวิจัย 1	ศูนย์นาโนเทคโนโลยีแห่งชาติ	ยังอยู่ในโครงการ
		สำนักงานพัฒนาวิทยาศาสตร์			สำนักงานพัฒนาวิทยาศาสตร์	
		และเทคโนโลยีแห่งชาติ			และเทคโนโลยีแห่งชาติ	
11. ตร.กุลชาติ จังภัทรพงศา	อาจารซ์	ภาควิชาจุลชีววิทยาคลินิก	นักวิจัย	ผู้ช่วยศาสตราจารย์	ศูนย์วิจัยพัฒนานวัตกรรม	ยังอยู่ในโครงการ
		คณะเทคนิคการแพทย์			และถ่ายทอดเทคโนโลฮี	
		มหาวิทยาลัยมหิดล			คณะเทคนิคการแพทย์	
					มหาวิทยาลัยมหิดล	
12. ดร.วิชนันท์ แย้มกมล	อาจารซ์	ภาควิชาจุลทรรศนศาสตร์คลินิก	นักวิจัย	อาจารซ์	ศูนย์วิจัยพัฒนานวัตกรรม	ยังอยู่ในโครงการ
		คณะเทคนิคการแพทย์			และถ่ายทอดเทคโนโลฮี	
		มหาวิทยาลัยมหิดล			คณะเทคนิคการแพทย์	
					มหาวิทยาลัยมหิดล	
13. นางสาวรวิวรรณ ถิรมนัส	ı	์ สูนย์นาโนเทคโนโลยีแห่งชาติ	ผู้ช่วยนักวิจัย	ผู้ช่วยนักวิจัย 2	ศูนย์นาโนเทคโนโลยีแห่งชาติ	ยังอยู่ในโครงการ
		สำนักงานพัฒนาวิทยาศาสตร์			สำนักงานพัฒนาวิทยาศาสตร์	
		และเทคโนโลยีแห่งชาติ			และเทคโนโลยีแห่งชาติ	

กณะวิทยาตาสตร์ มหาวิทยาตับสสงขานดรินทร์ มหาวิทยาตับสสงขานดรินทร์ มหาวิทยาตับสสงขานดรินทร์ มหาวิทยาตับสมาติกายาตาสตร์และ นักศึกษา - เทคโนโลยีพอลิเมอร์) ปริญญาโท คณะวิทยาตาสตร์ มหาวิทยาตับสงร์ มหาวิทยาตับสงร์และเทคโนโลยี นักศึกษา - ภาตวิชาวิทยาตาสตร์และเทคโนโลยี นักศึกษา - ภาตวิชาวิทยาตาสตร์และเทคโนโลยี นักศึกษา - ภาตวิชาวิตวารรมและเทคโนโลยี นักศึกษา -	14. ตร.วิรัช ทวีปรีดา	อาจารซึ่	สาขาวิชาวิทยาศาสตร์พอลิเมอร์	นักวิจัย	อาจารซ์	สาขาวิชาวิทยาศาสตร์พอลิเมอร์	ไม่อยู่ในโครงการ
- ภาควิชาเคมี (สาขาวิทยาศาสตร์และ นักศึกษา - เทคโนโลยีพอลิเมอร์) ปริญญาโท คณะวิทยาศาสตร์ มหาวิทยาศาสตร์และ นักศึกษา - เทคโนโลยีพอลิเมอร์) ปริญญาโท คณะวิทยาศาสตร์ มหาวิทยาศาสตร์และ นักศึกษา - เทคโนโลยีพอลิเมอร์) ปริญญาโท คณะวิทยาศาสตร์ มหาวิทยาศาสตร์และ นักศึกษา - เทคโนโลยีพอลิเมอร์) ปริญญาโท คณะวิทยาศาสตร์ มหาวิทยาศาสตร์ นักศึกษา - เทคโนโลยีพอลิเมอร์) (ใต้รับทุน มหาวิทยาสัยมหิดล สาทณ-) กาควิชาวิทยาศาสตร์ นักศึกษา - สาทณ-) กาควิชาวิทยาศาสตร์และเทคโนโลยี นักศึกษา - กาควิชาวิทยาศาสตร์และเทคโนโลยี นักศึกษา - เพลิเริกมากริมและเทคโนโลยี นักศึกษา - เพลิเริกมาพ สถานันพอโนโลยี นักศึกษา - เผลิรีภภาพ สถานันพอโนโลยี นักสิริภภาพ สถานันพอโนโลยี นักสิริภภาพ สถานันพอโนโลยี นักสิริภภาพ สถานันพอโนโลยี นักสิริภภาพ - เผลิรีภภาพ สถานันพอโนโลยี นักสิริภภาพ - เผลิรีภภาพ สถานันพอโนโลยี นักสิริภภาพ - เมลิริภภาพ - เมลิริภิภ			คณะวิทยาศาสตร์			คณะวิทยาศาสตร์	,
- ภาควิชาเคมี (สาขาวิทยาศาสตร์และ นักศึกษา - เทคโนโลยีพอลิเมอร์)			มหาวิทยาลัยสงขลานครินทร์			มหาวิทยาลัยสงขลานครินทร์	
		_	ภาควิชาเคมี (สาขาวิทยาศาสตร์และ	นักศึกษา	1	ตูนย์เทคโนโลยีโลหะและวัสดุ	เสนผูรเบษฐาเษ
- ภาควิชาเคมี สาขาวิทยาสตร์และ นักศึกษา - เทคโนโลยีพอลิเมอร์)  - กาควิชาเคมี (สาขาวิทยาศาสตร์และ นักศึกษา - เทคโนโลยีพอลิเมอร์)  - กาควิชาเคมี (สาขาวิทยาศาสตร์และ นักศึกษา - เทคโนโลยีพอลิเมอร์)  - ภาควิชาเคมี (สาขาวิทยาศาสตร์และ นักศึกษา - เทคโนโลยีพอลิเมอร์)  - กาควิชาเทมี (สาขาวิทยาศาสตร์และ นักศึกษา - เทคโนโลยีพอลิเมอร์)  - กาควิชาวิทยาศาสตร์และเทคโนโลยี นักศึกษา - สวทร.)  - กาควิชาวิทยาศาสตร์และเทคโนโลยี นักศึกษา - เกลิชาวิทยาศาสตร์และเทคโนโลยี นักศึกษา - เกลิชาวิทยาสัยมหาร์  - กาควิชาวิทยาสัยมหาร์ เมื่อกฤษา - เกลิชาวิทยาสัยมหาร์ เมื่อกฤษา - เกลิชาวิทยาสัยมหาร์ เมิกศึกษา - เกลิชาวิทยาสัยมหาร์ เมิกศึกษา - เกลิชาวิทยาสัยมหาร์ เมิกศึกษา - เกลิชาวิทยาสัยมหาร์ เมิกศึกษา - เกลิชาวิทยาสัยสรมผละเทคโนโลยี นักศึกษา - เกลิชาวิทยาสัยสรมยามละเทคโนโลยี นักศึกษา - เกลิชาวิทยาสัยสรมยามละเทคโนโลยี นักศึกษา - เกลิชาวิทยาสัยสรมยามละเทคโนโลยี นักศึกษา - เกลิชาวิทยาสัยสรมยามละเทคโนโลยี นักศึกษา - เกลิชาวิทยาสาขาริทยาสัยสรมยามละเทคโนโลยี นักสิทยาสิทยาสิทยาสิทยาสิทยาสิทยาสิทยาสิทยา	อมรชัยยาพิทักษ์		เทคโนโลยีพอลิเมอร์)	ปริญญาโท		แห่งชาติ สำนักงานพัฒนา	
- ภาควิชาเคมี (สาขาวิทยาศาสตร์และ นักศึกษา - เทคโนโลยีพอลิเมอร์) ปริญญาโท คณะวิทยาศาสตร์ มหาวิทยาศาสตร์และ นักศึกษา - มหาวิทยาศาสตร์ มหาวิทยาศาสตร์และ นักศึกษา - มหาวิทยาศาสตร์ มหาวิทยาศาสตร์และ นักศึกษา - เทคโนโลยีพอลิเมอร์) ปริญญาโท คณะวิทยาศาสตร์ (ได้รับทุน มหาวิทยาศาสตร์ สวทช.) - ภาควิชาวิทยาศาสตร์และเทคโนโลยี นักศึกษา - ภาควิชาวิทยาศาสตร์ นักศึกษา - มหาวิทยาลัยสหาลานครินทร์ ปริญญาโท สมหาวิทยาลัยสหาลานครินทร์ เริ่มถูกโท มหาวิทยาลัยสหาลานครินทร์ เริ่มถูกโท เคมีรีวภาพ สถาบันเพคโนโลยี นักศึกษา - เคมีรีวภาพ สถาบันเพคโนโลยี นักศึกษา -			คณะวิทยาศาสตร์			วิทยาศาสตร์และเทคโนโลยี	
- ภาควิชาเคมี (สาขาวิทยาศาสตร์และ นักศึกษา - เทคโนโลยีพอลิเมอร์) - ภาควิชาวิทยาศาสตร์ นักศึกษา - สวาพ.) - ภาควิชาวิทยาศาสตร์ นักศึกษา - สวาพ.) - ภาควิชาวิทยาศาสตร์ นักศึกษา - วัสดุ คณะวิทยาศาสตร์ นักศึกษา - ภาควิชาวิทยาศาสตร์ นักศึกษา - ภาควิชาวิทยาศาสตร์ นักศึกษา - ภาควิชาวิทยาศาสตร์ นักศึกษา - ภาควิชาวิทยาสามรรมและเทคโนโลยี นักศึกษา - ภาควิชาวิทยาสัยสะเทคโนโลยี นักศึกษา - ภาควิชาวิทยาสัตร์ นิทยาวิทยาสัตร์ นิทยาวิทยาสิทยาสิทยาสิทยาสิทยาสิทยาสิทยาสิทยาส			มหาวิทยาลัยมหิดล			แห่งชาติ	
<ul> <li>เทคโนโลยีพอลิเมอร์)</li> <li>กาควิทยาศาสตร์ มหาวิทยาศาสตร์และ นักศึกษา - เทคโนโลยีพอลิเมอร์)</li> <li>มหาวิทยาสาสตร์และ นักศึกษา - เทคโนโลยีพอลิเมอร์)</li> <li>เทคโนโลยีพอลิเมอร์)</li> <li>เทคโนโลยีพอลิเมอร์)</li> <li>เทคโนโลยีพอลิเมอร์)</li> <li>เทคโนโลยีพอลิเมอร์)</li> <li>เทคโนโลยีพอลิเมอร์)</li> <li>เทคโนโลยีพอลิเมอร์)</li> <li>เทคโนโลยีพอลิเมอร์)</li> <li>เกคโนโลยีพอลิเมอร์)</li> <li>เกคโนโลยีพอลิเมอร์)</li> <li>เกคโนโลยีพอลิเมอร์)</li> <li>เกคโนโลยีพอลิเมอร์)</li> <li>เกคโนโลยีพอลิเมอร์)</li> <li>เกคโนโลยีพอลิเมอร์)</li> <li>เกคโนโลยีพอลิเมอร์</li> <li>เกคโนโลยีพอลิเมอร์</li> <li>เกคโนโลยีพอลิเมอร์</li> <li>เกิดีกษา</li> <li>กาควิชาวิทยาลิยสงยลานครินทร์</li> <li>เกิดีกษา</li> <li>เกลีศราภาพ สถาบันเพตโนโลยี</li> <li>เกิดีกษา</li> </ul>		1	ภาควิชาเคมี (สาขาวิทยาศาสตร์และ	นักศึกษา	1	หจก. เหรียญทองการพิมพ์	สำเร็จการศึกษา
- กาควิชาเคมี (สาขาวิทยาสาสตร์และ นักศึกษา - เทคโนโลยีพอลิเมอร์) ปริญญาโท คณะวิทยาศาสตร์และ นักศึกษา - กาควิชาเคมี (สาขาวิทยาศาสตร์และ นักศึกษา - เทคโนโลยีพอลิเมอร์) ปริญญาโท คณะวิทยาศาสตร์และเทคโนโลยี นักศึกษา - ภาควิชาวิทยาศาสตร์และเทคโนโลยี นักศึกษา - วิสตุ คณะวิทยาศาสตร์และเทคโนโลยี นักศึกษา - วิสตุ คณะวิทยาศาสตร์และเทคโนโลยี นักศึกษา - กาควิชาวิศวกรรมและเทคโนโลยี นักศึกษา - เคมีรีวภพ สถากันเทคโนโลยี เล็กศึกษา - เคมีรีวภพ สถากันเทคโนโลยี เล็กสามราย เคมีรีวภพ สถากันเทคโนโลยี เล็กสีกษา - เคมีรีวภพ สถากันเทคโนโลยี เล็กสีกษา - เคมีรีวภพ สถากันเทคโนโลยี เล็กสีกษา - เคมีรีวภพ สถากันเทคโนโลยี เม็กสีกษา - เล็กสีกษา -	อนันต์จรุงสุข		เทคโนโลยีพอลิเมอร์)	ปริญญาโท			
- ภาควิชาวิทยาศาสตร์และ นักศึกษา - เทคโนโลยีพอลิเมอร์) ปริญญาโท คณะวิทยาศาสตร์และ นักศึกษา - ภาควิชาวิทยาศาสตร์และ นักศึกษา - เทคโนโลยีพอลิเมอร์) ปริญญาโท คณะวิทยาศาสตร์ (ได้รับทุน มหาวิทยาลัยมหิดล สวทช.) สวทร.) - ภาควิชาวิทยาศาสตร์และเทคโนโลยี นักศึกษา - วิสตุ คณะวิทยาศาสตร์ ปริญญาโท มหาวิทยาลัยสงขลานครินทร์ เปริญญาโท มหาวิทยาลัยสงขลานครินทร์ เวิลถูกโท มหาวิทยาลัยสงขลานครินทร์ เวิลถูกโท มหาวิทยาลัยสงขลานครินทร์ เวิลถูกโท มหาวิทยาลัยสงขลานครินทร์ เวิลถูกโท มหาวิทยาลัยสงขลานครินทร์ เวิลถูกโท มหาวิทยาลัยสงขลานครินทร์ เวิลถูกโท			คณะวิทยาศาสตร์ มหาวิทยาลัยมหิดล				
<ul> <li>เทคโนโลยีพอลิเมอร์)</li> <li>- มหาวิทยาสัยมหิตล</li> <li>- มหาวิทยาสัยมหิตล</li> <li>- เทคโนโลยีพอลิเมอร์)</li> <li>- เกควิชาวิทยาศาสตร์และเทคโนโลยี</li> <li>- มหาวิทยาลัยสรขลานครินทร์</li> <li>- ภาควิชาวิศวกรรมและเทคโนโลยี</li> <li>นักศึกษา</li> <li>- เคมีรีวภาพ สถากับเทคโนโลยี</li> <li>นักศึกษา</li> <li>- เคมีรีวภาพ สถากับเทคโนโลยี</li> <li>นักศึกษา</li> </ul>	4. นางสาวเสาวรีย์ ตันพันตรี	1	ภาควิชาเคมี (สาขาวิทยาศาสตร์และ	นักศึกษา	1	บริษัท Siam Modified Starch	สำเร็จการศึกษา
- มหาวิทยาลัยมหิดล  - เทคโนโลซีพอลิเมอร์)  - เทคโนโลซีพอลิเมอร์)  - เทคโนโลซีพอลิเมอร์)  - มหาวิทยาสตร์  - ภาควิชาวิทยาศาสตร์และเทคโนโลซี  มหาวิทยาสตร์และเทคโนโลซี  มหาวิทยาลัยสงขลานครินทร์  - ภาควิชาวิตวกรรมและเทคโนโลซี  นักศึกษา  - ภาควิชาวิตวกรรมและเทคโนโลซี  มักศึกษา  - กาควิชาวิตวกรรมและเทคโนโลซี  มักศึกษา  - กาควิชาวิตวกรรมและเทคโนโลซี  มักศึกษา  - กาควิชาวิตวกรรมและเทคโนโลซี  มักศึกษา  - กาควิชาวิตวกรรมและเทคโนโลซี  มักศึกษา  - กาควิชาวิทยาสตร์  เดมีชีวภาพ สถาทับเทคโนโลซี  มักศึกษา  - กาควิชาวิทยาสัง			เทคโนโลยีพอลิเมอร์)	ปริญญาโท			
- ภาควิทยาลัยมหิดล - กาควิทากสตร์และ นักศึกษา - เหคโนโลยีพอลิเมอร์) ปริญญาโท คณะวิทยาศาสตร์และ เทคโนโลยี นักศึกษา - ภาควิชาวิทยาศาสตร์และเทคโนโลยี นักศึกษา - วัสดุ คณะวิทยาศาสตร์ ปริญญาโท มหาวิทยาลัยลงขลานครินทร์ ปริญญาโท นกศึกษา - กาควิชาวิศวกรรมและเทคโนโลยี นักศึกษา - เคมีสัวภาพ สถาบับเทคโนโลยี นักสิทธ์นาคิน			คณะวิทยาศาสตร์				
- ภาควิชาเคมี (สาขาวิทยาศาสตร์และ นักศึกษา - เทคโนโลยีพอลิเมอร์) ปริญญาโท คณะวิทยาศาสตร์ (ได้รับทุน มหาวิทยาลัยมหิดล สวทช.) - ภาควิชาวิทยาศาสตร์และเทคโนโลยี นักศึกษา - ภาควิชาวิศวกรรมและเทคโนโลยี นักศึกษา - ภาควิชาวิศวกรรมและเทคโนโลยี นักศึกษา - ภาควิชาวิศวกรรมและเทคโนโลยี นักศึกษา - มาควิชาวิศวกรรมและเทคโนโลยี นักศึกษา - มาควิชาวิศวกรรมและเทคโนโลยี นักศึกษา - มาควิชาวิศวกรรมและเทคโนโลยี นักศึกษา - มาควิชาวิศวกรรมและเทคโนโลยี นักศึกษา			มหาวิทยาลัยมหิดล				
<ul> <li>เทคโนโลฮีพอลิเมอร์) ปริญญาโท</li> <li>คณะวิทยาศาสตร์</li> <li>- ภาควิชาวิทยาศาสตร์และเทคโนโลฮี นักศึกษา</li> <li>- มหาวิทยาลัยสงขลานครินทร์</li> <li>- ภาควิชาวิศวกรรมและเทคโนโลฮี นักศึกษา</li> <li>- ภาควิชาวิศวกรรมและเทคโนโลฮี นักศึกษา</li> <li>- กาควิชาวิศวกรรมและเทคโนโลฮี นักศึกษา</li> <li>- กาควิชาวิศวกรรมและเทคโนโลฮี นักศึกษา</li> </ul>	5. นางสาวลลิตา เจริญมาก	1	ภาควิชาเคมี (สาขาวิทยาศาสตร์และ	นักศึกษา	1	อยู่ระหว่างการสมัครงาน	สำเร็จการศึกษา
			เทคโนโลยีพอลิเมอร์)	ปริญญาโท			
- มหาวิทยาลัยมหิดล     - ภาควิชาวิทยาศาสตร์และเทคโนโลยี นักศึกษา     - วัสดุ คณะวิทยาศาสตร์     - มหาวิทยาลัยสงขลานครินทร์     - ภาควิชาวิศวกรรมและเทคโนโลยี นักศึกษา     - กาควิชาวิศวกรรมและเทคโนโลยี นักศึกษา     - กาควิชาวิศวกรรมและเทคโนโลยี นักศึกษา     - กาควิชาวิศวกรรมและเทคโนโลยี นักศึกษา			คณะวิทยาศาสตร์	(ได้รับทุน			
- ภาควิชาวิทยาศาสตร์และเทคโนโลยี นักศึกษา - วัสดุ คณะวิทยาศาสตร์ ปริญญาโท มหาวิทยาลัยสงขลานครินทร์ - ภาควิชาวิศวกรรมและเทคโนโลยี นักศึกษา - เคมีชีวภาพ สถาวันเทคโนโลยี นักศึกษา -			มหาวิทยาลัยมหิดล	TGIST 910			
- ภาควิชาวิทยาศาสตร์และเทคโนโลยี นักศึกษา - วัสดุ คณะวิทยาศาสตร์ ปริญญาโท มหาวิทยาลัยสงขลานครินทร์ - ภาควิชาวิศวกรรมและเทคโนโลยี นักศึกษา - เคมีชีวภาพ สถาวันเทคโนโลยี นักศึกษา				สวทช.)			
วัสดุ คณะวิทยาศาสตร์ ปริญญาโท มหาวิทยาลัยสงขลานครินทร์ - ภาควิชาวิศวกรรมและเทคโนโลยี นักศึกษา -	6. นายอิศรา อินทฤทธิ์	_	ภาควิชาวิทยาศาสตร์และเทคโนโลยี	นักศึกษา	1	ประกอบอาชีพอิสระ	เสนผูรเนษฐาเษ
มหาวิทยาลัยสงขลานครินทร์ - ภาควิชาวิศวกรรมและเทคโนโลยี นักศึกษา - เคมีชีวภาพ สถาวันเทคโนโลยี าโรถถกโพ			วัสดุ คณะวิทยาศาสตร์	ปริญญาโท			
- มาควิชาวิศวกรรมและเทคโนโลฮี นักศึกษา - เดมีชีวภาพ สถาวับเทคโนโลฮี าโรมถกโท			มหาวิทยาลัยสงขลานครินทร์				
าเริ่มเอกโท	7. นางสาวเหงียน ไท เฮียน	_	ภาควิชาวิศวกรรมและเทคโนโลยี	นักศึกษา	1	กลับ	เสนคริกกร
			เคมีชีวภาพ สถาบันเทคโนโลยี	ปริญญาโท		ประเทศเวียดนาม	
นานาชาติสิรินธร (ได้รับทุน			นานาชาติสิรินธร	(ได้รับทุน			

<ul> <li>8. นายอรรถพล กอเดช - เคมีชาภา นานาชาติเ</li> <li>9. นายสิทธิวัฒน์ กิจเสถียรกุล - ภาควิชาวิ</li> <li>10. นางสาวจริยา แก้วเสน่หา - ภาควิชาเค</li> <li>และเทคโน คณะวิทยา</li> <li>มหาวิทยา</li> </ul>	งและเทคโนโลฮี บันเทคโนโลฮี มศาสตร์ งและเทคโนโลฮี	มูลนิธิ SCG) นักศึกษา		
1	<b>₹</b> ₩	4		สำเร็จการศึกษา
1 1	<b>12</b>	บรญญาเท		
1 1	<b>T</b>			
	<b>T</b> a			
I		นักศึกษา –		สำเร็จการศึกษา
ı		ปริญญาโท		
1	นานาชาติสิรินธร			
1	มหาวิทยาลัยธรรมศาสตร์			
และเทคโน คณะวิทยา	ภาควิชาเคมี (สาขาวิทยาศาสตร์	นักศึกษา –	ภาควิชาเคมี (สาขาวิทยาศาสตร์	สำเร็จการศึกษา
คณะวิทยา	และเทคโนโลฮีพอลิเมอร์)	ปริญญาโท	และเทคโนโลฮีพอลิเมอร์)	ปริญญาโท
มหาวิทยาไ	คณะวิทยาศาสตร์		คณะวิทยาศาสตร์	แล้วศึกษาต่อเป็น
	มหาวิทยาลัยมหิดล		มหาวิทยาลัยมหิดล	นักศึกษาปริญญาเอก
				(ได้รับทุน คปก.)
				ยังอยู่ในโครงการ
11. นายวีระชัย นาสัมพันธ์ - ภาควิชาเค	ภาควิชาเคมี (สาขาวิทยาศาสตร์และ	นักศึกษา -	ภาควิชาเคมี (สาขา	นักศึกษา
เทคโนโละ	เทคโนโลยีพอลิเมอร์)	ປຣີຄູຄູກເອກ	วิทยาศาสตร์และเทคโนโลยี	ປຣິญູູນາເອກ
ุ คณะวิทยา	คณะวิทยาศาสตร์	(ได้รับทุน	พอลิเมอร์)	ยังอยู่ในโครงการ
มหาวิทยา	มหาวิทยาลัยมหิดล	พสวท.)	คณะวิทยาศาสตร์	
			มหาวิทยาลัยมหิดล	
12. นางสาวสุกัญญา เหนือแสน   -		นักศึกษา –	ภาควิชาเคมี	นักศึกษา
ุ คณะวิทยา	คณะวิทยาศาสตร์	ປຣີພູຫຼາເອກ	คณะวิทยาศาสตร์	ปริญญาเอก
มหาวิทยา	มหาวิทยาลัยมหิดล		มหาวิทยาลัยมหิดล	จะขอรับทุน คปก.
				ยังอยู่ในโครงการ

13. นายนฤดม ศรีสว่าง	ı	หลักสูตรวิทยาศาสตร์	นักศึกษา	1	หลักสูตรวิทยาศาสตร์	Transfer เป็น
		และวิศวกรรมวัสดุ	ปริญญาโท		และวิศวกรรมวัสดุ	นักศึกษาปริญญาเอก
		คณะวิทยาศาสตร์			คณะวิทยาศาสตร์	ยังอยู่ในโครงการ
		มหาวิทยาลัยมหิดล			มหาวิทยาลัยมหิดล	
14. นางสาวภฤษฎี สุขพ่วง	ı	ภาควิชาวัสดุศาสตร์	นักศึกษา	-	ภาควิชาวัสดุศาสตร์	นักศึกษา
		คณะวิทยาศาสตร์	ປຣີຜູູນາເອກ		คณะวิทยาศาสตร์	ປຣີຜູຜູາເອກ
		จุฬาลงกรณ์มหาวิทยาลัย			จุฬาลงกรณ์มหาวิทยาลัย	ยังอยู่ในโครงการ
15. นางสาวศิริพร บุญพา	ı	ภาควิชาวิศวกรรมและเทคโนโลยี	นักศึกษา	ı	ภาควิชาวิศวกรรมและเทคโนโลยี	นักศึกษา
		เคมีชาภาพ สถาบันเทคโนโลยี	ປຣີຜູູນາເອກ		เคมีชีวภาพ สถาบันเทคโนโลยี	ປຈີພູຫູາເອກ
		นานาชาติสิรินธร	(ได้รับทุน		นานาชาติสิรินธร	ยังอยู่ในโครงการ
		มหาวิทยาลัยธรรมศาสตร์	จาก JGSEE)		มหาวิทยาลัยธรรมศาสตร์	
16. นายทวีศักดิ์ บุญสด	ı	ภาควิชาวิศวกรรมและเทคโนโลยี	นักศึกษา	ı	ภาควิชาวิศวกรรมและเทคโนโลยี	นักศึกษา
		เคมีชีวภาพ สถาบันเทคโนโลยี	ປຣີໝູູກເອກ		เคมีชีวภาพ สถาบันเทคโนโลยี	ປຣີຜູູູໝາເອກ
		นานาชาติสิรินธร	(ได้รับทุน		นานาชาติสิรินธร	ยังอยู่ในโครงการ
		มหาวิทยาลัยธรรมศาสตร์	จาก JGSEE)		มหาวิทยาลัยธรรมศาสตร์	
17. นางการณี ศรีรมร่น	ı	ภาควิชาวิศวกรรมและเทคโนโลยี	นักศึกษา	ı	ภาควิชาวิศวกรรมและเทคโนโลยี	นักศึกษา
		เคมีชวภาพ สถาบันเทคโนโลยี	ปริญญาเอก		เคมีชีวภาพ สถาบันเทคโนโลยี	ປຈີໝູູກາເອກ
		นานาชาติสิรินธร	(ได้รับทุน		นานาชาติสิรินธร	ยังอยู่ในโครงการ
		มหาวิทยาลัยธรรมศาสตร์	จาก สกอ.)		มหาวิทยาลัยธรรมศาสตร์	
18. นายมนตรี นามขจร	ı	สาวสากรรมและเทคโนโลยี	นักศึกษา	-	มหาวิทยาลัยมหิดล	สำเร็จการศึกษา
		เคมีชีวภาพ สถาบันเทคโนโลฮี	ปริญญาโท			ปริญญาโท
		นานาชาติสิรินธร				แล้วศึกษาต่อเป็น
		มหาวิทยาลัยธรรมศาสตร์				นักศึกษาปริญญาเอก
19. นายชาคริต ธรรมวงศ์	ı	ภาควิชาวิศวกรรมและเทคโนโลยี	นักศึกษา	-	ภาควิชาวิศวกรรมและเทคโนโลยี	นักศึกษา
		เคมีชีวภาพ สถาบันเทคโนโลยี	ปริญญาโท		เคมีชีวภาพ สถาบันเทคโนโลยี	ปริญญาโท

	นานาชาติสิรินธร			นานาชาติสิรินธร	ยังอยู่ในโครงการ
	มหาวิทยาลัยธรรมศาสตร์			มหาวิทยาลัยธรรมศาสตร์	
20.นางสาววิไลรัตน์ ทรัพย์มาก	กาควิชาวิศวกรรมและเทคโนโลยี	นักศึกษา	1	ภาควิชาวิศวกรรมและเทคโนโลยี	นักศึกษา
	เคมีชีวภาพ สถาบันเทคโนโลยี	ปริญญาโท		เคมีชีวภาพ สถาบันเทคโนโลยี	ปริญญาโท
	นานาชาติสิรินธร			นานาชาติสิรินธร	ยังอยู่ในโครงการ
	มหาวิทยาลัยธรรมศาสตร์			มหาวิทยาลัยธรรมศาสตร์	
21. นางสาวชมพูนุช โชคบุญเปียม	ภาควิชาเคมี (สาขาวิทยาศาสตร์	นักศึกษา	ı	ภาควิชาเคมี (สาขา	นักศึกษา
	และเทคโนโลยีพอลิเมอร์)	ปริญญาโท		วิทยาศาสตร์ และเทคโนโลยี	ปริญญาโท
	คณะวิทยาศาสตร์			พอลิเมอร์) คณะวิทยาศาสตร์	ยังอยู่ในโครงการ
	มหาวิทยาลัยมหิดล			มหาวิทยาลัยมหิดล	
22. นางสาวณัฐกุล กาญจนถาวร	ภาควิชาเคมี (สาขาวิทยาศาสตร์	นักศึกษา	1	ภาควิชาเคมี (สาขา	นักศึกษา
	และเทคโนโลยีพอลิเมอร์)	ปริญญาโท		วิทยาศาสตร์และเทคโนโลยี	ปริญญาโท
	คณะวิทยาศาสตร์			พอลิเมอร์) คณะวิทยาศาสตร์	ยังอยู่ในโครงการ
	มหาวิทยาลัยมหิดล			มหาวิทยาลัยมหิดล	
23. นางสาวศมน ตรังคธาร -	ภาควิชาเคมี (สาขาวิทยาศาสตร์	นักศึกษา	ı	ภาควิชาเคมี (สาขา	นักศึกษา
	และเทคโนโลยีพอลิเมอร์)	ปริญญาโท		วิทยาศาสตร์และเทคโนโลยี	ปริญญาโท
	คณะวิทยาศาสตร์			พอลิเมอร์)คณะวิทยาศาสตร์	ยังอยู่ในโครงการ
	มหาวิทยาลัยมหิดล			มหาวิทยาลัยมหิดล	
24. นางสาวธนิดา อาภรณ์วิชานพ	กาควิชาเคมี	นักศึกษา	1	ภาควิชาเคมี (สาขา	สำเร็จการศึกษา
	คณะวิทยาศาสตร์	ປຣີญญາตรี		วิทยาศาสตร์และเทคโนโลยี	ປຣີญູູພາທີ່ຮ
	มหาวิทยาลัยมหิดล			พอลิเมอร์) คณะวิทยาศาสตร์	แล้วศึกษาต่อเป็น
				มหาวิทยาลัยมหิดล	นักศึกษาปริญญาโท
					ยังอยู่ในโครงการ
25. นายณัฐพงษ์ หริวงศานุภาพ	กาควิชาเคมี	นักศึกษา	1	ภาควิชาเคมี (สาขา	สำเร็จการศึกษา
	คณะวิทยาศาสตร์	ปริญญาตรี		วิทยาศาสตร์และเทคโนโลยี	ປຣິญญາตรี

		มหาวิทยาลัยมหิดล	(ได้รับทุน	พอดิเม	พอลิเมอร์) คณะวิทยาศาสตร์	แล้วศึกษาต่อเป็น
			YSTP จาก	ุมหาวิท	มหาวิทยาลัยมหิดล	นักศึกษาปริญญาโท
			สวทช.)			ยังอยู่ในโครงการ
26. นายณัฐพงศ์ พรหมะวัน	_	ภาควิชาเคมี	นักศึกษา	. หลักสู่เ	หลักสูตรวิทยาศาสตร์และ	สำเร็จการศึกษา
		คณะวิทยาศาสตร์	ปริญญาตรี	่วิศวกร	วิศวกรรมวัสดุ	ປຣີຜູູູພາຫຣື
		มหาวิทยาลัยมหิดล		คณะวิท	คณะวิทยาศาสตร์	แล้วศึกษาต่อเป็น
				มหาวิท	มหาวิทยาลัยมหิดล	นักศึกษาปริญญาโท
						ยังอยู่ในโครงการ
27. นายเธียรรัตน์ ดังโชยคีรี	_	ภาควิชาจุลชีววิทยาคลินิก	นักศึกษา	. ผู้นญ้า	ศูนย์วิจัยพัฒนานวัตกรรม	สำเร็จการศึกษา
		คณะเทคนิคการแพทฮ์	ปริญญาตรี	เเละถ่า	และถ่ายทอดเทคโนโลฮี	ປຣີຜູູູພາທີ່ຮ
		มหาวิทยาลัยมหิดล		แรกค	คณะเทคนิคการแพทย์	แล้วศึกษาต่อเป็น
				ุมหาวิท	มหาวิทยาลัยมหิดล	นักศึกษาปริญญาโท
						ยังอยู่ในโครงการ
28. นางสาวญาณภัทร	1	ภาควิชาปรสิตวิทยา	นักศึกษา	. ศูนย์วิจ	ศูนย์วิจัยพัฒนานวัตกรรม	สำเร็จการศึกษา
แม้นถาวรศิริ		คณะเทคนิคการแพทย์	ปริญญาตรี	้เครยา	และถ่ายทอดเทคโนโลฮี	ປຣີຜູູູພາຫຣື
		มหาวิทยาลัยมหิดล		แรนค	คณะเทคนิคการแพทย์	แล้วศึกษาต่อเป็น
				มหาวิท	มหาวิทยาลัยมหิดล	นักศึกษาปริญญาโท
						(ได้รับทุน TGIST
						จาก สวทช.)
						ยังอยู่ในโครงการ
29. นายชัชชนก ชูสวัสดิ์	_	ภาควิชาวิศวกรรมและเทคโนโลยี	นักศึกษา		ภาควิชาวิศวกรรมและ	นักศึกษา
		เคมีชั่วภาพ สถาบันเทคโนโลฮี	ปริญญาตรี	้นโคทา	เทคโนโลยีเคมีชีวภาพ สถาบัน	ປຣີຜູູູພາຫຣື
		นานาชาติสิรินธร		เทคโน้	เทคโนโลยีนานาชาติสิรินธร	ยังอยู่ในโครงการ
		มหาวิทยาลัยธรรมศาสตร์		มหาวิท	มหาวิทยาลัยธรรมศาสตร์	

30. นายภวิศ ตั้งวิรุฬห์	1	ภาควิชาวิศวกรรมและเทคโนโลยี	นักศึกษา	ı	ภาควิชาวิศวกรรมและเทคโนโลฮี นักศึกษา	นักศึกษา
		เคมีชวภาพ สถาบันเทคโนโลยี	ປຣີພູພູາທຣີ		เคมีชีวภาพ สถาบันเทคโนโลยี	ປຣີຄູທູາຫຣີ
		นานาชาติสิรินธร			นานาชาติสิรินธร	ยังอยู่ในโครงการ
		มหาวิทยาลัยธรรมศาสตร์			มหาวิทยาลัยธรรมศาสตร์	
31. นายณัฐพล สมานุกูล	I	ภาควิชาวิศวกรรมและเทคโนโลยี	นักศึกษา	1	ภาควิชาวิศวกรรมและเทคโนโลยีเ นักศึกษา	นักศึกษา
		เคมีชีวภาพ สถาบันเทคโนโลยีนานาชา ปริญญาตรี	ปริญญาตรี		ชีวภาพ สถาบันเทคโนโลยีนานาช ปริญญาตรี	ປຣີຄູທູາຫຣີ
		รินธร มหาวิทยาลัยธรรมศาสตร์			รินธร มหาวิทยาลัยธรรมศาสตร์	ยังอยู่ในโครงการ
32. นายปฐมพงศ์ เวศอุไร	1	ภาควิชาปรสิตวิทยา	นักศึกษา	1	ภาควิชาชีวเคมี	สำเร็จการศึกษา
		คณะเทคนิคการแพทฮ์	ปริญญาตรี		คณะวิทยาศาสตร์	ປຣີຍູູູພາສຣີ
		มหาวิทยาลัยมหิดล	(ได้รับทุน		มหาวิทยาลัยมหิดล	แล้วศึกษาต่อเป็น
			ALL ALL			นักศึกษาปริญญาโท
			สวทช.)			(ได้รับทุน TGIST
						จาก สวทช.)
33. นางสาวอัจฉราวลัย พรเจริญ	_	ศูนย์วิจัยพัฒนานวัต	นักศึกษา	_	ศูนย์วิจัยพัฒนานวัด	นักศึกษาปริญญาตรี
		กรรมและการถ่ายทอดเทคโนโลยี	ປຣີຄູຄູາຫຣື		กรรมและการถ่ายทอดเทคโนโลฮี (ได้รับทุน YSTP	(ได้รับทุน YSTP
		คณะเทคนิคการแพทย์			คณะเทคนิคการแพทย์	จาก สวทช.)
		มหาวิทยาลัยมหิดล			มหาวิทยาลัยมหิดล	
34. นายยุรนันท์ ดิษฐโรจน์	-	ภาควิชาจุลชีววิทยาคลินิก	นักศึกษา	1	ภาควิชาจุลทรรศนศาสตร์คลินิก	สำเร็จการศึกษา
		คณะเทคนิคการแพทย์	ປຣີຄູຄູາທຣີ		คณะเทคนิคการแพทฮ์	ປຣິญญາตรี
		มหาวิทยาลัยมหิดล	(ได้รับทุน		มหาวิทยาลัยมหิดล	แล้วศึกษาต่อเป็น
			YSTP จาก			นักศึกษาปริญญาโท
			สวทช.)			
35. นางสาวจุฑารัตน์ เพ็งอัน	-	ภาควิชาจุลชีววิทยาคลินิก	นักศึกษา	1	ภาควิชาจุลทรรศนศาสตร์คลินิก	สำเร็จการศึกษา
		คณะเทคนิคการแพทย์	ปริญญาตรี		คณะเทคนิคการแพทฮ์	ปริญญาตรี
		มหาวิทยาลัยมหิดล			มหาวิทยาลัยมหิดล	แล้วศึกษาต่อเป็น

					นักศึกษาปริญญาโท
					(ได้รับทุน TGIST
					จาก สวทช.)
36. นางสาวศศิธร พรหมวัลย์	1	ภาควิชาจุลชีววิทยาคลินิก	นักศึกษา –	มหาวิทยาลัยศิลปากร	สำเร็จการศึกษา
		คณะเทคนิคการแพทย์	ปริญญาตรี		ປຣີຄູຄູາທຣີ
		มหาวิทยาลัยมหิดล	(ได้รับทุน		แล้วศึกษาต่อเป็น
			YSTP 410		นักศึกษาปริญญาโท
			สวทช.		
37. นายภูเบศร์ นิ่มปุญญกำพงษ์	1	ภาควิชาวิศวกรรมและเทคโนโลยี	นักศึกษา –	ศึกษาต่อปริญญาโท	สำเร็จการศึกษา
		เคมีชีวภาพ สถาบันเทคโนโลฮี	ปริญญาตรี	University of Manchester	ປຣີພູພູາສຣີ
		นานาชาติสิรินธร			แล้วศึกษาต่อเป็น
		มหาวิทยาลัยธรรมศาสตร์			นักศึกษาปริญญาโท
38. นางสาวชลกาญจน์ ศุภสุธีกุล	1	ภาควิชาวิศวกรรมและเทคโนโลยี	นักศึกษา –	ศึกษาต่อปริญูญาโท	สำเร็จการศึกษา
		เคมีชาภาพ สถาบันเทคโนโลยี	ปริญญาตรี	University of Manchester	ປຣີພູພູາສຣີ
		นานาชาติสิรินธร			แล้วศึกษาต่อเป็น
		มหาวิทยาลัยธรรมศาสตร์			นักศึกษาปริญญาโท
39. นางสาวกุลจิรา อิทธิอมรกุล	1	ภาควิชาวิศวกรรมและเทคโนโลยี	นักศึกษา	ศึกษาต่อปริญูญาโท	สำเร็จการศึกษา
		เคมีชิวภาพ สถาบันเทคโนโลยี	ปริญญาตรี	ประเทศอังกฤษ	ປຣີພູພູາສຣີ
		นานาชาติสิรินธร			แล้วศึกษาต่อเป็น
		มหาวิทยาลัยธรรมศาสตร์			นักศึกษาปริญญาโท
40. นายสุพัฒน์ กัมมาระบุตร		ภาควิชาวิศวกรรมและเทคโนโลยี	นักศึกษา	ศึกษาต่อปริญูญาโท	สำเร็จการศึกษา
		เคมีชีวภาพ สถาบันเทคโนโลฮี	ปริญญาตรี	ประเทศอังกฤษ	ປຣິພູທູກສີ
		นานาชาติสิรินธร			แล้วศึกษาต่อเป็น
		มหาวิทยาลัยธรรมศาสตร์			นักศึกษาปริญูญาโท

41. นายปกรณ์ ไตรประเสริฐพงศ์		ภาควิชาวิศวกรรมและเทคโนโลยี	นักศึกษา		บริษัทปูนชิเมนต์ไทย	สำเร็จการศึกษา
		เคมีชาภาพ สถาบันเทคโนโลยี	ปริญญาตรี			
		นานาชาติสิรินธร				
		มหาวิทยาลัยธรรมศาสตร์				
42. นางสาวกิรศิกานท์ ดาบคำ	1	ภาควิชาจุลชีววิทยาคลินิก	นักศึกษา	ı	โรงพยาบาลเปาโล	สำเร็จการศึกษา
		คณะเทคนิคการแพทย์	ປຣີພູພູກສຣີ			
		มหาวิทยาลัยมหิดล				
43. นางสาวภาวิณี โดดเครือ	1	ภาควิชาจุลชีววิทยาคลินิก	นักศึกษา	1	โรงพยาบาลนครธน	สำเร็จการศึกษา
		คณะเทคนิคการแพทย์	ປຣີພູພູກສຣີ			
		มหาวิทยาลัยมหิดล				
44. นายสรยุทธ ฉัตรากาญจน้	1	ภาควิชาปรสิตวิทยา	นักศึกษา	1	สถาบันวิจัยจุฬาภรณ์	สำเร็จการศึกษา
		คณะเทคนิคการแพทย์	ປຣີພູພູກສຣີ		(ในตำแหน่งผู้ช่วยวิจัย)	
		มหาวิทยาลัยมหิดล				
45. นายสุธีรพล ปิงใจ	1	ภาควิชาปรสิตวิทยา	นักศึกษา	1	โรงพยาบาลธนบุรี	สำเร็จการศึกษา
		คณะเทคนิคการแพทย์	ปริญญาตรี			
		มหาวิทยาลัยมหิดล				
46. นางสาวอธิษฐาน ยศสงคราม	1	ภาควิชาจุลทรรศนศาสตร์คลินิก	นักศึกษา	1	ยพาตนหนาน ยพาตนหนาน ยพาตนหนาน	สำเร็จการศึกษา
		คณะเทคนิคการแพทย์	ປຣີຄູຄູກຫຣື		พัฒนาเด็กและครอบครัว	
		มหาวิทยาลัยมหิดล			มหาวิทยาลัยมหิดล	
47. นางสาววราภรณ์ เทียงธรรม	1	ภาควิชาจุลทรรศนศาสตร์คลินิก	นักศึกษา	ı	ประกอบอาชีพอิสระ	สำเร็จการศึกษา
		คณะเทคนิคการแพทย์	ປຣີພູພູກສຣີ			
		มหาวิทยาลัยมหิดล				
48. นายนิติกร อ่อนหวาน	1	ภาควิชาเคมี	นักศึกษา	1	บริษัท ทีโอเอ	สำเร็จการศึกษา
		คณะวิทยาศาสตร์	ປຣີພູພູກສຣີ			
		มหาวิทยาลัยมหิดล				

49. นางสาวชนิตา แสงสุขวาว	1	ภาควิชาเคมี คณะวิทยาศาสตร์	ນັກศึกษา ປຣີພູญາตรี	- เข้าร่วมโคร ประสบการเ	เข้าร่วมโครงการแลกเปลี่ยน ประสบการณ์ที่ต่างประเทศ	สำเร็จการศึกษา
		มหาวิทยาลัยมหิดล				
50. นางสาวอัญชนา	-	ภาควิชาเคมี	นักศึกษา	- ได้รับทุน ส	เด้รับทุน สควค. หลักสูตร	สำเร็จการศึกษา
นิ่มอนุสสรณ์กุล		คณะวิทยาศาสตร์	ปริญญาตรี	ประกาศนีย	ประกาศนียบัตรบัณฑิตวิชาชีพ	
		มหาวิทยาลัยมหิดล		ครู (ป.บัณ	ครู (ป.บัณฑิต) มหาวิทยาลัย	
				ศรีนครินทราิโรฒ	รวิโรฒ	
51. นายดลยา สาบาช	1	ภาควิชาวิทยาศาสตร์และเทคโนโลยี	นักศึกษา	- ทำงานโรงงานยาง	านยาง	สำเร็จการศึกษา
		วัสดุ คณะวิทยาศาสตร์	ปริญญาตรี	จ.สงขลา		
		มหาวิทยาลัยสงขลานครินทร์				

หมายเหตุ

สังกัด

ให้ใส่รายละเอียดที่อยู่ต้นสังกัด เช่น ภาควิชา/คณะ/มหาวิทยาลัย

ส**ถานภาพปัจจุบัน** - ยังอยู่ในโครงการหรือไม่ หากไม่อยู่ในโครงการแล้ว ให้ระบุหน่วยงานใหม่ด้วย

- หากเริ่มเข้าร่วมโครงการเป็นนักศึกษาปริญญาเอก ปริญญาโท หรือปริญญาตรี ให้ระบุว่าปัจจุบันสำเร็จการศึกษาหรือยังไม่สำเร็จการศึกษา